

7/7/95

SANDIA REPORT

SAND95-0488/1 • UC-814

Unlimited Release

Printed May 1995

RECEIVED

JUL 18 1995

OSTI

Yucca Mountain Site Characterization Project

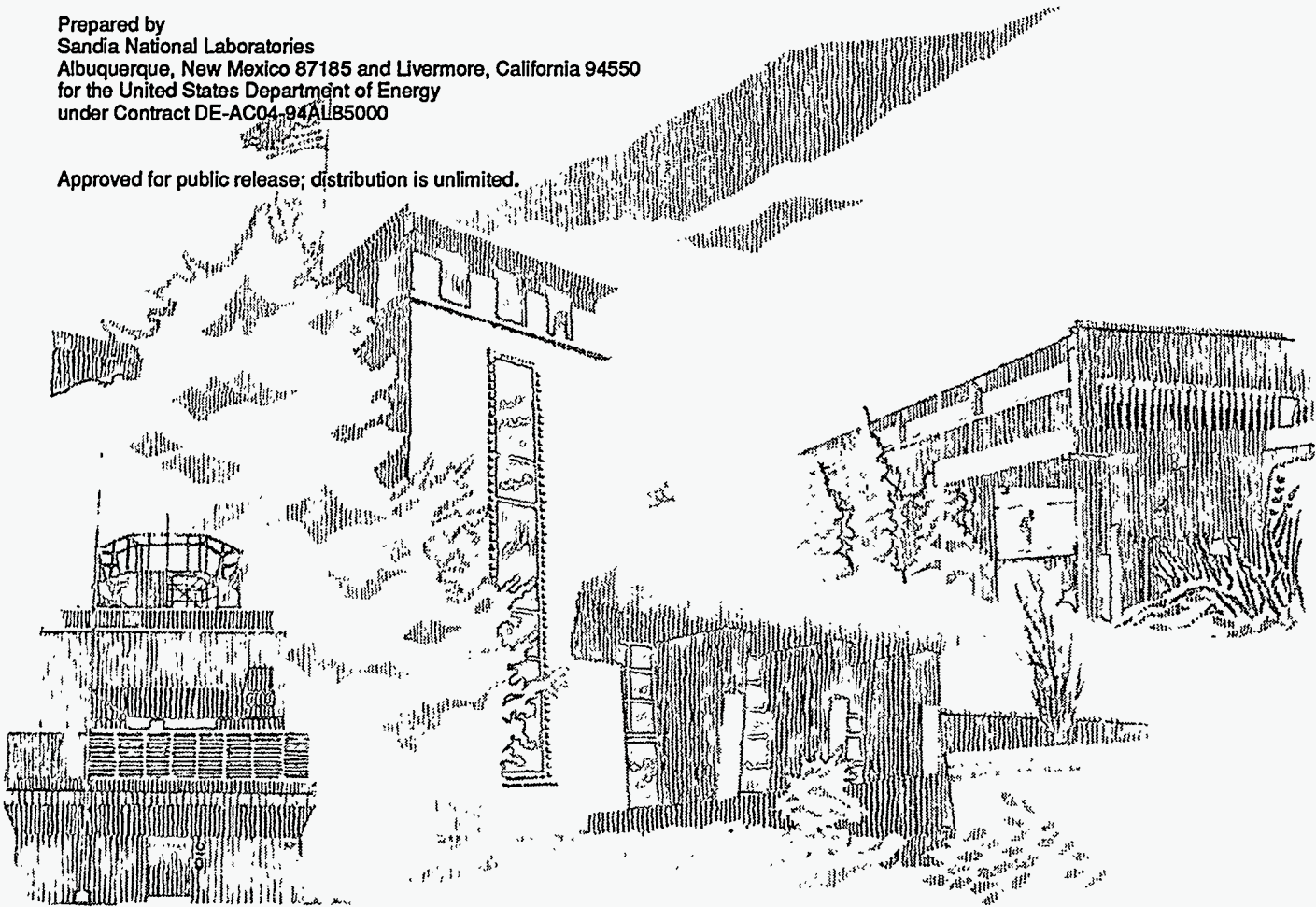
Geotechnical Characterization of the North Ramp of the Exploratory Studies Facility

Volume I of II Data Summary

Carl E. Brechtel, Ming Lin, Eric Martin, David S. Kessel

Prepared by
Sandia National Laboratories
Albuquerque, New Mexico 87185 and Livermore, California 94550
for the United States Department of Energy
under Contract DE-AC04-94AL85000

Approved for public release; distribution is unlimited.



SF2900Q(8-81)

DISTRIBUTION OF THIS DOCUMENT IS UNLIMITED

"Prepared by Yucca Mountain Site Characterization Project (YMSCP) participants as part of the Civilian Radioactive Waste Management Program (CRWM). The YMSCP is managed by the Yucca Mountain Project Office of the U.S. Department of Energy, DOE Field Office, Nevada (DOE/NV). YMSCP work is sponsored by the Office of Geologic Repositories (OGR) of the DOE Office of Civilian Radioactive Waste Management (OCRWM)."

Issued by Sandia National Laboratories, operated for the United States Department of Energy by Sandia Corporation.

NOTICE: This report was prepared as an account of work sponsored by an agency of the United States Government. Neither the United States Government nor any agency thereof, nor any of their employees, nor any of their contractors, subcontractors, or their employees, makes any warranty, express or implied, or assumes any legal liability or responsibility for the accuracy, completeness, or usefulness of any information, apparatus, product, or process disclosed, or represents that its use would not infringe privately owned rights. Reference herein to any specific commercial product, process, or service by trade name, trademark, manufacturer, or otherwise, does not necessarily constitute or imply its endorsement, recommendation, or favoring by the United States Government, any agency thereof or any of their contractors or subcontractors. The views and opinions expressed herein do not necessarily state or reflect those of the United States Government, any agency thereof or any of their contractors.

Printed in the United States of America. This report has been reproduced directly from the best available copy.

Available to DOE and DOE contractors from
Office of Scientific and Technical Information
PO Box 62
Oak Ridge, TN 37831

Prices available from (615) 576-8401, FTS 626-8401

Available to the public from
National Technical Information Service
US Department of Commerce
5285 Port Royal Rd
Springfield, VA 22161

NTIS price codes
Printed copy: A14
Microfiche copy: A01

DISCLAIMER

Portions of this document may be illegible in electronic image products. Images are produced from the best available original document.

SAND95-0488/1
Unlimited Release
Printed May 1995

Distribution
Category UC-814

**GEOTECHNICAL CHARACTERIZATION OF
THE NORTH RAMP OF THE EXPLORATORY STUDIES FACILITY**

**Volume I of II
Data Summary**

by

Carl E. Brechtel
Ming Lin
Eric Martin
Agapito Associates, Inc.
Grand Junction, CO 81506

and

David S. Kessel
Sandia National Laboratories
Albuquerque, NM 87185

ABSTRACT

Geotechnical characterization data were developed in eleven holes, the North Ramp Geotechnical (NRG) boreholes, drilled along the 2800-m route of the North Ramp. The North Ramp is one of two inclined tunnels being excavated to the potential repository horizon for the Yucca Mountain Site Characterization Project. The primary purpose of the drilling program was to produce rock properties data to support subsurface design. Specific data developed included lithologic and rock structural core logs, cross sections with stratigraphic and thermal-mechanical units, rock mechanics laboratory testing, and rock mass quality indices. These data are summarized in this report to address the major topics of geologic setting, geologic features of engineering and construction significance, anticipated ground conditions, and range of required ground support.

Rock structural data and rock mass quality data have been summarized in 3-m (10-ft) intervals and grouped according to the thermal-mechanical units. The distribution of rock mass quality data in all NRG holes within each thermal-mechanical unit has been proposed to be representative of the variability to be encountered by the North Ramp as it cuts across each unit.

MASTER

DISTRIBUTION OF THIS DOCUMENT IS UNLIMITED

et

Document Review and Comment Sheet

This work was supported by the United States Department of Energy under Contract DE-AC04-94AL85000 and was prepared under the Yucca Mountain Site Characterization Project WBS numbers 1.2.3.2.6.2.1, 1.2.3.2.6.2.2, and 1.2.3.2.6.2.3, QA Grading Report #1.2.3.2.6.2.1, Revision 0. The planning document that guided this work activity was Work Agreement #071, Revision 00. The information and data documented in this report were collected under a fully qualified QA Program, except as noted in the report.

This report supports work defined in the Site Characterization Plan Section 8.3.1.14.2 and is discussed in Study Plan SP-8.3.1.14.2, Revision 0, Sections 2.3.1.3 and 2.3.2.3.

ACKNOWLEDGMENTS

Timothy J. Sullivan, Department of Energy (DOE), is the WBS Element Manager responsible for the Soil and Rock Properties studies. David Kessel, Sandia National Laboratories (SNL), is the principal investigator for the Soil and Rock Properties studies and is responsible for management and direction of the activities. Carl E. Brechtel, Agapito Associates, Inc. (AAI), assisted in field coordination and technical direction of the field studies. Ming Lin (AAI) was responsible for development of the rock mass quality indices from core data and estimation of the rock mass mechanical properties. Kimberly Greathouse (AAI) was responsible for data management.

The authors would like to acknowledge the support and contributions of the various organizations involved in conduct of the surface-based site characterization activities. David Buesch, U.S. Geological Survey (USGS), and Jeff Geslin and Tom Moyer of the Science Applications International Corporation (SAIC) provided the geologic logs for the UE25 NRG-2A, -2B, and RF#8* holes. David Buesch provided input to the development and technical review of the North Ramp and Exile Hill cross sections. Robert Elayer, TRW/Morrison Knudsen, provided technical review for some of the NRG geologic logs and the North Ramp and Exile Hill cross sections.

Geologic logs for the North Ramp boreholes were provided by Chris Rautman, Carolyn Coolidge, and Dale Engstrom of SNL. Eric Martin and Richard Lippoth, AAI, performed the quality assurance (QA) rock structural logging. Geologists of TM&SS group were responsible for development of the field rock structural logs and for conducting the Schmidt hammer

* Used as corroborating data, not QA.

measurements. Ron Price, SNL, directed the rock mechanics testing. Rock mechanics testing was performed by New England Research.

Coordination and direction of the field support activities was performed by Arch Girdley, DOE. He was assisted by Kenneth Skipper, Drew Coleman, and Leroy Heath.

TABLE OF CONTENTS

VOLUME I — DATA SUMMARY

<u>Section</u>	<u>Page</u>
1.0 Introduction	1-1
1.1 Purpose	1-1
1.2 Background	1-1
1.3 Scope	1-5
1.4 Quality Assurance	1-8
1.5 Report Organization	1-9
2.0 Geotechnical Summary	2-1
2.1 Introduction	2-1
2.2 Geology and Major Structural Features along the North Ramp	2-2
2.2.1 Known Geologic Features of Engineering and Construction Significance ..	2-3
2.2.2 Potential Geological Features with Engineering and Construction Significance	2-5
2.3 Thermomechanical Stratigraphy	2-6
2.4 Orientations of Joints and Fractures	2-7
2.5 Hydrology	2-7
2.6 Rock Structure Data from the NRG Core	2-8
2.7 Rock Mechanical Properties Tests	2-12
2.8 Rock Mass Quality Indices	2-13
2.8.1 RMR and Q Data	2-13
2.8.2 Projected Range of Ground Support	2-16
2.9 Rock Mass Mechanical Properties Estimates	2-17
3.0 Geologic and Geotechnical Data Development	3-1
3.1 Introduction	3-1
3.2 Lithologic Logging of the Core	3-5
3.3 Rock Structural Logging	3-6
3.4 Rock Mechanical Properties Tests	3-11
3.5 Rock Mass Quality	3-12
3.6 Rock Mass Mechanical Properties	3-15
4.0 Geology of the North Ramp	4-1
4.1 Introduction	4-1
4.2 Stratigraphy	4-1
4.2.1 Ash-Flow Tuffs	4-8
4.2.2 Bedded Tuffs	4-12
4.3 Geologic Cross Sections	4-13
4.3.1 Drilling and Surface Mapping Data	4-14

<u>Section</u>	<u>Page</u>
4.3.2 Seismic Interpretation in Daylight Valley	4-17
4.3.3 Projected Ramp Station Coordinates Stratigraphic Contacts	4-23
4.4 Thermomechanical Stratigraphy	4-23
4.5 Major Structural Features	4-28
4.5.1 Faults Recognized Along North Ramp Alignment	4-28
4.5.2 Recognized Fracture Patterns	4-31
5.0 Rock Structure Data	5-1
5.1 Introduction	5-1
5.2 Core Recovery	5-2
5.3 RQD Data	5-5
5.4 Rock Weathering and Hardness	5-9
5.5 Lithophysae Content	5-12
5.6 Fracture Data	5-15
5.6.1 Feature Type	5-16
5.6.2 Fracture Inclination	5-18
5.6.3 Calculated Fracture Frequencies	5-18
5.6.4 Fracture Infill Mineralization and Thickness	5-23
5.6.5 Fracture Planarity and Roughness	5-27
5.7 Analysis of Rock Structural Character where Boreholes Intersect Faults	5-27
5.8 Correlation of Core Rock Structural Data with Downhole Video Logs	5-33
6.0 Rock Mechanics Laboratory Test Data	6-1
6.1 Introduction	6-1
6.2 Unconfined Compressive Strength	6-2
6.3 Elastic Modulus and Poisson's Ratios	6-5
6.4 Dry Bulk Density, Porosity, and Average Grain Density	6-5
6.5 Indirect Tensile Strength	6-14
6.6 Confined Compressive Strength	6-14
6.7 Schmidt Hammer Rebound Hardness	6-21
7.0 Rock Mass Quality Data	7-1
7.1 Introduction	7-1
7.2 Rock Mass Quality Indices for the Rock Mass Rating System	7-3
7.2.1 Strength Parameter	7-4
7.2.2 Rock Quality Designation Rating	7-7
7.2.3 Spacing of Discontinuity	7-7
7.2.4 Condition of Joint	7-10
7.2.5 Groundwater	7-11
7.2.6 Distribution of Rock Mass Rating Values for the Thermomechanical Units	7-11

<u>Section</u>	<u>Page</u>
7.3 Rock Mass Quality Indices for the Q System	7-15
7.3.1 Rock Quality Designation	7-15
7.3.2 Joint Set Number	7-16
7.3.3 Joint Roughness Number	7-16
7.3.4 Joint Alteration	7-18
7.3.5 Joint Water Reduction Factor	7-20
7.3.6 Stress Reduction Factor	7-20
7.3.7 Distribution of Q Values for the Thermomechanical Units	7-25
7.4 Evaluation of RMR and Q Results	7-25
7.4.1 Correlation of RMR and Q Results	7-27
7.4.2 Comparison of Q and RMR Determined in the NRST to NRG Core-Based Data	7-33
7.5 Comparison of Lithophysae-Rich and Nonlithophysal Portions of the Welded Units	7-35
7.6 Indicated Ground Conditions	7-36
8.0 Rock Mass Mechanical Properties	8-1
8.1 Introduction	8-1
8.2 Rock Mass Strengths	8-1
8.2.1 Yudhbir Criterion	8-4
8.2.2 Hoek and Brown Criterion	8-6
8.2.3 Design Rock Mass Strengths	8-7
8.2.4 Rock Mass Mohr-Coulomb Strength Parameters and Dilation Angles	8-7
8.3 Rock Mass Elastic Modulus	8-15
8.4 Rock Mass Poisson's Ratios	8-16
9.0 References	9-1
Appendix A. Technical Procedure	
Appendix B. Development of Rock Mass Quality Estimates from Core Data	
Appendix C. Ranked Frequency of Occurrence Tables for Q, RMR, and RQD by Thermomechanical Unit	
Appendix D. Rock Mass Quality Indices for the Lithophysae-Rich and Nonlithophysal Tuff Rock in TCw and TS _{w1} Units	

VOLUME II — NRG COREHOLE DATA APPENDICES

<u>Section</u>	<u>Page</u>
1.0 Introduction	1-1
Appendix A. UE25 NRG-1	
Appendix B. UE25 NRG-2	
Appendix C. UE25 NRG-2A	
Appendix D. UE25 NRG-2B	
Appendix E. UE25 NRG-3	
Appendix F. UE25 NRG-4	
Appendix G. UE25 NRG-5	
Appendix H. USW NRG-6	
Appendix I. USW NRG-7/7A	
Appendix J. RF #8	

LIST OF TABLES

<u>Table</u>	<u>Page</u>
1-1	Studies, Objectives, and Activities of the Soil and Rock Properties Study Plan — <i>Studies to Provide Soil and Rock Properties of Potential Locations of Surface and Subsurface Access Facilities</i> 1-7
1-2	Correlation of Study Areas and Activities with Specific Investigations Conducted in the Nonlithified Tuffs 1-7
1-3	Nonqualified and Preliminary Data and Assumptions 1-9
2-1	Projected Ramp Station Coordinates at Stratigraphic Contacts Along North Ramp Alignment Tunnel Centerline 2-2
2-2	Projection of Ramp Station Coordinates at Thermomechanical Unit Contacts 2-6
2-3	Comparison of RQD Data and <i>Enhanced-RQD</i> Data for the Thermomechanical Units — NRG Holes 2-9
2-4	Summary of Mean Values for Rock Mechanical and Physical Properties Testing — NRG Holes 2-12
2-5	Mean Value and Standard Deviation of Schmidt Rebound Hardness 2-12
2-6	RMR Ratings for the Five Rock Mass Quality Categories 2-14
2-7	Q Values for the Five Rock Mass Quality Categories 2-14
2-8	Comparison of Rock Mass Strength Estimates to Intact Strength Data—Rock Mass Category 5 2-18
2-9	Strength Parameters and Dilation Angles for the Mohr-Coulomb Failure Criterion for Rock Mass Classes 1–5 in Each Thermomechanical Unit 2-18
2-10	Estimated Rock Mass Elastic Modulus 2-19
2-11	Estimated Rock Mass Poisson’s Ratio 2-19
3-1	Summary of NRG Drilling Program 3-4
3-2	Numbers of Rock Mechanics Tests Performed on NRG Core for Each Thermomechanical Unit 3-11
4-1	Lithostratigraphic Nomenclature of the Paintbrush Group at Yucca Mountain Nevada Lithostratigraphic Nomenclature of the Paintbrush Tuff at Yucca Mountain Nevada 4-4
4-2	Unit Thickness of NRG-Series Boreholes 4-7
4-3	Projected Ramp Station Coordinates at Stratigraphic Contacts Along North Ramp Alignment Centerline 4-17
4-4	Projection of Ramp Station Coordinates at Thermomechanical Unit Contacts 4-28
4-5	Known Faults Projected to Encounter the North Ramp and Approximate Ramp Station 4-29
4-6	Fracture Orientations as Estimated for Oriented Core and Borehole Television Surveys 4-32

<u>Table</u>	<u>Page</u>
5-1 Summary of Core Recovery, Lost Core, and Rubble by Thermomechanical Unit — NRG Holes	5-3
5-2 Comparison of RQD Data and <i>Enhanced-RQD</i> Data for the Thermomechanical Units — NRG Holes	5-6
5-3 Explanation of Weathering Descriptions and Log Abbreviation	5-9
5-4 Explanation of Estimated Hardness and Log Abbreviation	5-10
5-5 Comparison of Mean, Median, and Standard Deviation of Estimated Lithophysae and Other Void Content in the Thermomechanical Units — NRG Holes	5-15
5-6 Distribution of Core Structural Features by Type and Thermomechanical Unit—NRG Holes	5-16
5-7 Summary of Uncorrected Linear Fracture Frequency	5-20
5-8 Corrected Fracture Frequency by Fracture Inclination	5-21
5-9 Volumetric Fracture Frequency in a Unit Volume of Rock	5-22
5-10 Comparison of Median RQD from Core to RQD Values Calculated Using Fracture Frequency	5-23
5-11 Criteria for Categorizing Borehole Wall Condition	5-34
6-1 Comparison of Mean and Standard Deviation of Unconfined Compressive Strength — NRG Holes	6-3
6-2 Comparison of Mean and Standard Deviation of Elastic Modulus Measurements — NRG Holes	6-6
6-3 Comparison of Mean and Standard Deviation of Poisson's Ratio — NRG Holes	6-7
6-4 Comparison of Mean and Standard Deviation of Dry Bulk Density — NRG Holes ..	6-9
6-5 Comparison of Mean and Standard Deviation of Porosity — NRG Holes	6-10
6-6 Comparison of Mean and Standard Deviation of Average Grain Density — NRG Holes	6-11
6-7 Comparison of Mean and Standard Deviations of Brazilian Tensile Strength — NRG Holes	6-15
6-8 Confined Compressive Strength Test Results	6-17
6-9 Best-Fit Linear Failure Criteria and Mohr-Coulomb Parameters for 25.4-mm Samples from NRG Holes	6-21
6-10 Summary of Statistical Data for Schmidt Hammer Tests in Thermomechanical Units — NRG Holes	6-22
7-1 Summary of Average Intact Strength Values	7-5
7-2 Comparison of Corrected Spacings of Vertical Joints and the Corresponding JS Rating to Median JS Ratings Used in RMR Calculations	7-10
7-3 Factors a, b, and c for JC Rating Calculation	7-11
7-4 RMR Ratings for the Five Rock Mass Quality Categories	7-13
7-5 Algorithm Relating Jr Values to Planarity and Roughness Described in the Geology and Rock Structure Log	7-18
7-6 Algorithm to Determine Ja Values from Log Data	7-20

<u>Table</u>	<u>Page</u>
7-7 Percentage of Occurrence for Relative Rock Mass Quality Estimated using the Q System — NRG Holes	7-27
7-8 Q Values for the Five Rock Mass Quality Categories	7-27
7-9 Comparison of the Range and Mean of Individual parameters Used to Calculate Q at the NRST and in NRG-1	7-34
7-10 Comparison of the Range and Mean of Individual parameters Used to Calculate RMR at the NRST and in NRG-1	7-34
7-11 Comparison of Rock Mass Quality Data for Lithophysae-Rich and Nonlithophysal Portions of the TCw and TSw1	7-36
7-12 Range of Ground Support Indicated by Rock Support Categories in Each Thermomechanical Unit — NRG Holes	7-44
8-1 Tabulation of Q, RMR_{79} , and Design RMR_D Values for Rock Mass Classes 1–5 in Each Thermomechanical Unit	8-3
8-2 Comparison of RMR_D Values Determined Using RMR_{79} and RMR_{74} for Rock Mass Classes 1–5 in Each Thermomechanical Unit	8-4
8-3 Intact Rock Constants for the Rock Mass Strength Criteria	8-6
8-4 Power Law Constants for Rock Mass Strength	8-13
8-5 Strength Parameters and Dilation Angles for the Mohr-Coulomb Failure Criterion for Rock Mass Classes 1–5 in Each Thermomechanical Unit	8-14
8-6 Comparison of Range of Rock Mass Cohesion Using RMR_{79} and RMR_{74} Approaches	8-15
8-7 Estimated Rock Mass Elastic Modulus	8-16
8-8 Estimated Rock Mass Poisson's Ratio	8-16

LIST OF FIGURES

<u>Figure</u>	<u>Page</u>
1-1	Plan Map of Conceptual Repository and Locations of the North Ramp, Main Drift, and South Ramp 1-2
1-2	Topographic Contour Map Showing the North Ramp Alignment and Locations of Geologic Cross Sections and Surface Map 1-4
3-1	Schematic of the Process to Assemble NRG Data for Design of the North Ramp 3-3
3-2	Example of the Geology and Rock Structure Log 3-7
3-3a	Example of the Rock Structural Summary Log 3-9
3-3b	Example of the Rock Structural Summary Log 3-10
3-4	Example of the Q and RMR Estimate Log 3-14
4-1	Lithostratigraphic and Thermomechanical Units Sampled by Cored Intervals of NRG Boreholes 4-6
4-2	North Ramp Cross Section 4-15
4-3	Exile Hill Cross Section 4-16
4-4	Plan View Showing Seismic Lines in Relation to North Ramp Alignment and Exploratory Boreholes in the Vicinity of Exile Hill 4-18
4-5	Alternative Interpretation of Exile Hill Geology Based on Seismic Reflection Data 4-20
4-6	Correlation of Stratigraphic and Thermomechanical Units along the North Ramp Alignment 4-25
4-7	North Ramp Thermomechanical Unit Cross Section 4-26
4-8	Recognized Fracture Sets, ESF North Ramp Starter Tunnel 4-33
5-1	Pie Charts Showing Core Recovery, Lost Core and Rubble Zones as a Percentage of Total Drilling in Thermomechanical Units—NRG Holes 5-4
5-2	Histograms Showing RQD Frequency in the Thermomechanical Units—NRG Holes 5-7
5-3	Histograms Showing <i>Enhanced-RQD</i> Frequency in the Thermomechanical Units—NRG Holes 5-8
5-4	Distribution of the Weathering Parameters in Rock for Thermomechanical Units—NRG Holes 5-11
5-5	Pie Charts Showing Distribution of Estimated Hardness Ratings as a Percentage of Total Drilling in Thermomechanical Units—NRG Holes 5-13
5-6	Histograms of the Distribution of the Percent Lithophysae and Other Cavities in Each Thermomechanical Unit—NRG Holes 5-14
5-7	Bar Charts Showing the Distribution of Structural Features in Each Thermomechanical Unit—NRG Holes 5-17
5-8	Bar Charts Showing the Distribution of Fracture Inclinations in the Thermomechanical Units—NRG-1, -2A, -2B, -4, -5, -6, -7/7A 5-19

<u>Figure</u>	<u>Page</u>
5-9	Bar Charts Showing the Distribution of Fracture Mineral Infillings in the Thermomechanical Units—NRG Holes 5-25
5-10	Bar Charts Showing the Distribution of Fracture Infill Thickness in the Thermomechanical Units—NRG Holes 5-26
5-11	Bar Charts Showing the Distribution of Fracture Planarity in the Thermomechanical Units—NRG Holes 5-28
5-12	Bar Charts Showing the Distribution of Fracture Roughness in the Thermomechanical Units—NRG Holes 5-29
5-13	Fracture Frequency and RQD Data in the Vicinity of Fault Zones Encountered in Holes NRG-2, -2B, and -3 5-31
5-14	USW NRG-6, 342-ft Depth, Class C1 Borehole 5-35
5-15	USW NRG-6, 460.7-ft Depth, Class C2 Borehole 5-35
5-16	USW NRG-6, 973.4-ft Depth, Class C1 Borehole Showing Probable Cavernous Lithophysae in Bottom of Frame 5-36
5-17	USW NRG-6, 1033.4-ft Depth, Class C4 Borehole Showing Large Breakout on Left Side of Frame 5-36
5-18	Correlation of 3-m RQD with Borehole Wall Conditions as Indicated by Downhole Video Logs—NRG-4 5-38
6-1	Summary of Unconfined Compressive Strength Data — NRG Holes 6-4
6-2	Summary of Elastic Modulus — NRG Holes 6-8
6-3	Summary of Poisson's Ratio — NRG Holes 6-8
6-4	Summary of Dry Bulk Densities — NRG Holes 6-12
6-5	Summary of Porosities — NRG Holes 6-12
6-6	Summary of Average Grain Density — NRG Holes 6-13
6-7	Summary of Indirect Tensile Strength — NRG Holes 6-16
6-8	Confined Compressive Strength Results for TCw Unit — NRG Holes 6-18
6-9	Confined Compressive Strength Results for TSw1 Unit — NRG Holes 6-19
6-10	Confined Compressive Strength Results for TSw2 Unit — NRG Holes 6-20
6-11	Summary of Schmidt Hammer Rebound Number — NRG Holes 6-23
7-1	Histograms Showing the Distribution of the Strength Parameter for the RMR System in the Thermomechanical Units—NRG Holes 7-6
7-2	Histograms Showing the Distribution of the RQD Rating for the RMR System in the Thermomechanical Units—NRG Holes 7-8
7-3	Histograms Showing the Distribution of the JS Rating for the RMR System in the Thermomechanical Units—NRG Holes 7-9
7-4	Histograms Showing the Distribution of the JC Rating for the RMR System in the Thermomechanical Units—NRG Holes 7-12
7-5	Distribution of Estimated RMR in Each Thermomechanical Unit—NRG Holes ... 7-14
7-6	Histograms Showing the Distribution of Jn for the Q System in the Thermomechanical Units—NRG Holes 7-17

<u>Figure</u>	<u>Page</u>
7-7	Histograms Showing the Distribution of Jr for the Q System in the Thermomechanical Units—NRG Holes 7-19
7-8	Histograms Showing the Distribution of Ja for the Q System in the Thermomechanical Units—NRG Holes 7-21
7-9	Histograms Showing the Distribution of SRF for the Q System in the Thermomechanical Units—NRG Holes 7-24
7-10	Distribution of Estimated Q in Each Thermomechanical Unit—NRG Holes 7-26
7-11	Correlation of Q and RMR Results for the UO Unit—NRG Holes 7-28
7-12	Correlation of Q and RMR Results for the TCw Unit—NRG Holes 7-29
7-13	Correlation of Q and RMR Results for the PTn Unit—NRG Holes 7-30
7-14	Correlation of Q and RMR Results for the TSw1 Unit—NRG Holes 7-31
7-15	Correlation of Q and RMR Results for the TSw2 Unit—NRG Holes 7-32
7-16	Design Chart Used to Correlate Rock Mass Quality Q with Tunneling Case History Data 7-37
7-17	Cumulative Frequency of Occurrence of Q in UO Compared to Ground Support Design Chart 7-39
7-18	Cumulative Frequency of Occurrence of Q in TCw Compared to Ground Support Design Chart 7-40
7-19	Cumulative Frequency of Occurrence of Q in PTn Compared to Ground Support Design Charts 7-41
7-20	Cumulative Frequency of Occurrence of Q in TSw1 Compared to Ground Support Design Charts 7-42
7-21	Cumulative Frequency of Occurrence of Q in TSw2 Compared to Ground Support Design Charts 7-43
8-1	Design Rock Mass Strength Enveloped for Tuff “X” Unit—NRG Holes 8-8
8-2	Design Rock Mass Strength Enveloped for TCw Unit—NRG Holes 8-9
8-3	Design Rock Mass Strength Enveloped for PTn Unit—NRG Holes 8-10
8-4	Design Rock Mass Strength Enveloped for TSw1 Unit—NRG Holes 8-11
8-5	Design Rock Mass Strength Enveloped for TSw2 Unit—NRG Holes 8-12

1.0 INTRODUCTION

1.1 Purpose

This report presents the results of geological and geotechnical characterization of the Miocene volcanic tuff rocks of the Timber Mountain and Paintbrush groups that the tunnel boring machine (TBM) will encounter during excavation of the Exploratory Studies Facility (ESF) North Ramp. The information in this report was developed to support the design of the ESF North Ramp. The ESF is being constructed by the U.S. Department of Energy (DOE) as part of the Yucca Mountain Project site characterization activities. The purpose of these activities is to evaluate the feasibility of locating a potential high-level nuclear waste repository on lands within and adjacent to the Nevada Test Site (NTS), Nye County, Nevada. This report was prepared as part of the Soil and Rock Properties Studies, W.B.S. 1.2.3.2.6.2 in accordance with Study Plan 8.3.1.14.2, *Studies to Provide Soil and Rock Properties of Potential Locations of Surface and Subsurface Access Facilities* (DOE, 1991).

1.2 Background

The North Ramp is one of two inclined tunnels currently planned to provide access to the potential repository horizon for the Yucca Mountain Site Characterization Project (YMP). In the current configuration (DOE, 1994a), the North Ramp will be excavated 2,800 m (9,186 ft) at a grade of -2.05% using a 7.6-m (25-ft) diameter TBM. Beyond this point, the Topopah Spring level (TSL) Main Drift will be excavated 3,150 m (10,334 ft) across the proposed repository block by the TBM. The South Ramp will then be excavated 1,830 m (6,004 ft) at a slope of 2.63% to connect to the surface. Figure 1-1 shows a map of the conceptual controlled area of the YMP, the conceptual repository area, and the locations of the North Ramp, Main Drift, and South Ramp.

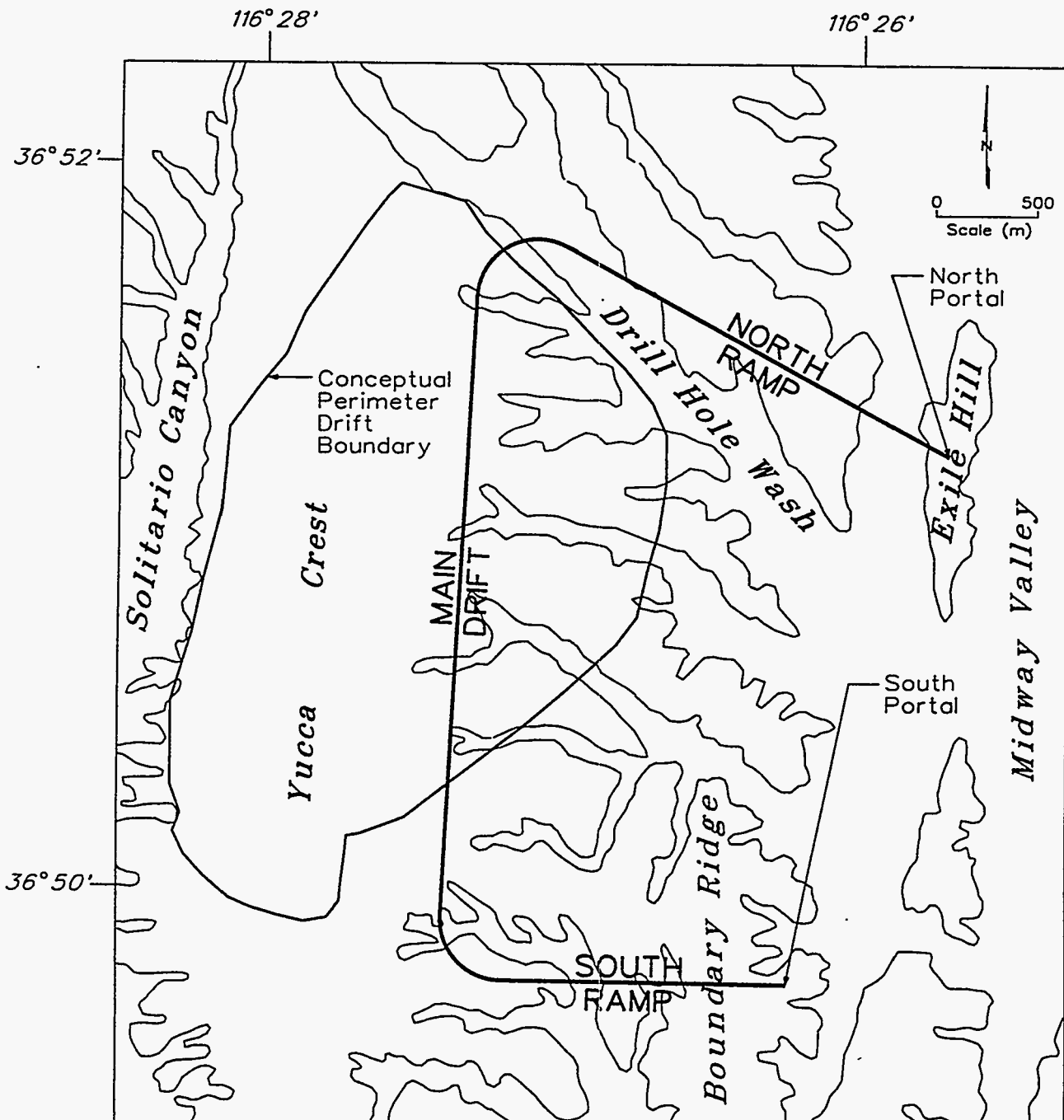


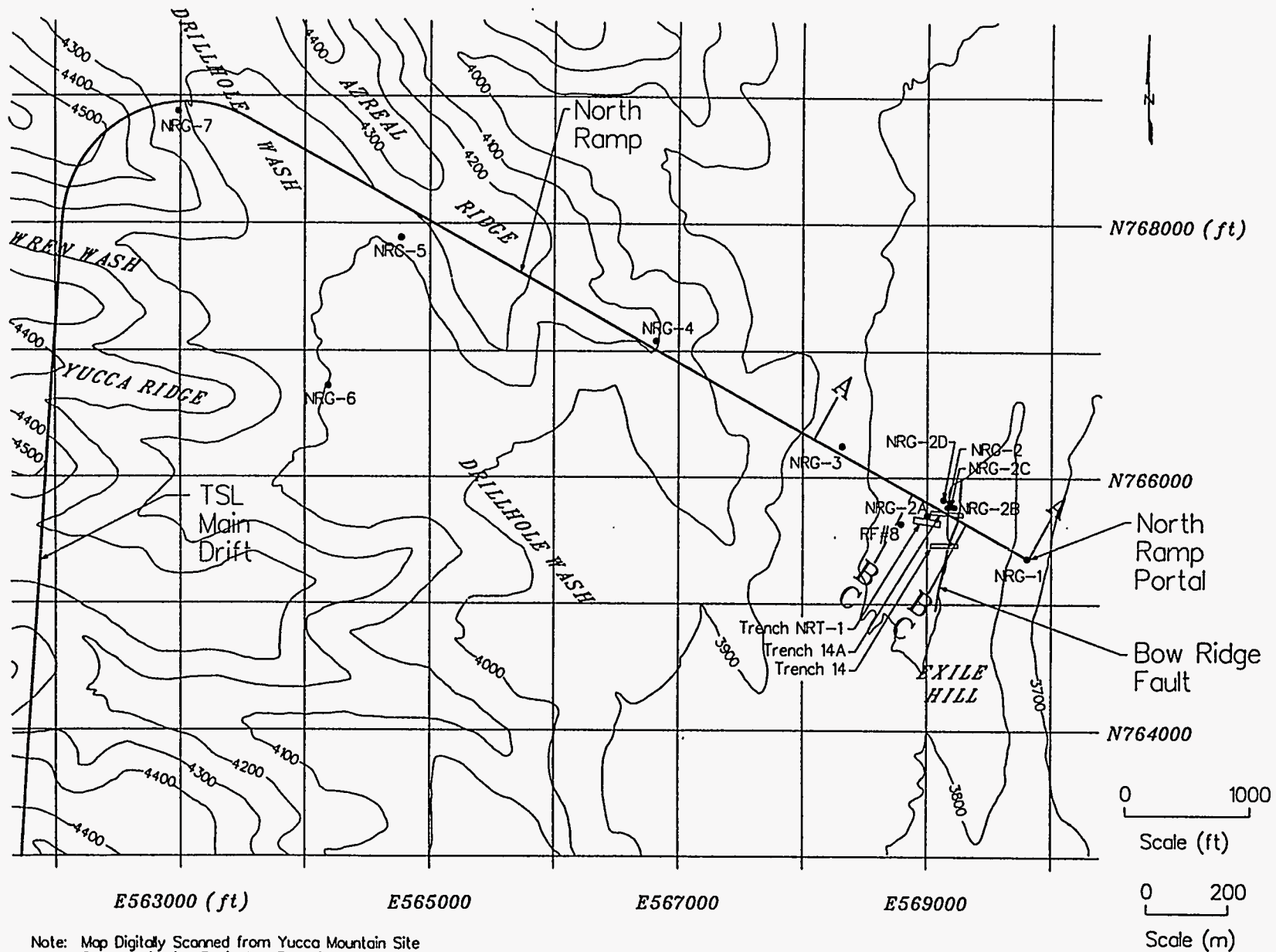
Figure 1-1. Plan Map of Conceptual Repository and Locations of the North Ramp, Main Drift, and South Ramp

The first phase of ESF construction, construction of the North Ramp portal and surface pad, was completed in 1994. To support the second phase, design and construction of the North Ramp to the potential repository horizon, 11 exploratory boreholes, the North Ramp Geologic (NRG) holes, were drilled to characterize the geology and rock engineering properties along the ramp alignment in accordance with the requirements of Study Plan 8.3.1.14.2.

The holes were drilled using down-the-hole hammers in some intervals and the dry compressed-air coring technology developed for the YMP. Two inclined holes were drilled to penetrate fault structures, and 9 holes were drilled vertically. The depth of the holes varied, but was generally planned to penetrate just beyond the depth of the adjacent ramp. Holes were located next to the planned ramp alignment but were required to be a minimum of 15 m (49.2 ft) from the ramp centerline, as per the ESF Design Requirements, Rev. 0, DCN008 3.2.4L7 (DOE, 1994b).

Geologic cross sections showing the subsurface distribution of the welded and nonwelded tuffs and the thermomechanical (thermal-mechanical) units were prepared. Geologic cross sections for the eastern portion of the North Ramp (ramp stations 0+00 m to 6+00 m) and of the full ramp are presented in this report. Figure 1-2 shows the location of the North Ramp, location of the boreholes, and positions of the cross sections.

Geologic, geotechnical, and geophysical logs were generated on each hole, and rock mechanics testing was performed on core samples selected throughout each hole. Geologic logging consisted of detailed lithologic descriptions and stratigraphic identifications based on the nomenclature of Scott and Bonk (1984) and nomenclature revised for subsurface



Note: Map Digitally Scanned from Yucca Mountain Site
 Characterization Project - Repository Base Map - Sheet A

Contour Interval 100'

Figure 1-2. Topographic Contour Map Showing the North Ramp Alignment and Locations of Geologic Cross Sections and Surface Map

identification by the USGS¹. A detailed log of rock structural features, including feature types, fracture characteristics, Rock Quality Designation (RQD), core recovery, weathering, hardness, and lithophysae and other void content was generated. Geophysics, including gamma, density, resistivity, and neutron logs were generated on each hole. In addition, borehole televiewer logs of the hole were run. Rock mechanics testing included measurements of density, porosity, uniaxial compressive strength (UCS), triaxial compressive strength, and Brazilian tensile strength. Schmidt hammer rebound hardness measurements were also generated on nominal 3-m (10-ft) intervals.

The core logging data was used to develop estimates of rock mass quality using the "Q" (Barton et al., 1974) and "RMR" systems (Bieniawski, 1979). Rock mass quality estimates were generated on even 3-m (10-ft) intervals throughout each hole. The estimates were presented in a log format for each hole so that they could be correlated with stratigraphy and thermomechanical (thermal-mechanical) units, and were also grouped by thermomechanical unit for use in design.

The rock mass quality data and rock mechanics testing data were used to derive estimates of rock mass mechanical properties required for design analysis. The methodology proposed by Hardy and Bauer (1991) was utilized in generation of the rock mass mechanical properties.

1.3 Scope

This report presents the results of the geological and geotechnical investigations to support the design and construction of the ESF North Ramp between stations 0+00 and 28+00 m. The primary focus of this report is the rock mass quality and rock mass mechanical properties

¹ Jeffrey K. Geslin, Thomas C. Moyer, and David C. Buesch, 1994 in press. *Summary of Lithologic Logging of New and Existing Boreholes at Yucca Mountain, Nevada, August 1993 to February 1994*, U.S. Geological Survey Open-File Report 94-342, U.S. Department of the Interior, Denver, Colorado.

along the North Ramp. Geologic cross sections are presented to provide the stratigraphic context for the rock properties data. A brief section describing the geology along the North Ramp is included.

As the North Ramp exploration was conducted, nonwelded, volcanic ash flows and falls of the Rainier Mesa formation were identified in the hanging wall of the Bow Ridge fault, as anticipated from earlier mapping (Scott and Bonk, 1984, and Gibson et al., 1992). Some of these tuffs were nonlithified (soil-like) and, since these intervals would be intersected by the North Ramp, additional detailed investigations were planned and conducted in FY 94. The results of these detailed investigations are presented in a separate report.²

A surface seismic survey was also conducted to support the detailed investigations of the nonlithified tuffs. The results of this work which support the North Ramp stratigraphic cross sections in the area of Exile Hill and Daylight Valley are included in this report. The complete results of the seismic study was presented in a separate report.³

The soil and rock study plan includes site characterization studies and activities required for siting and designing the ESF, including both surface structures and subsurface access structures. Table 1-1 lists the individual studies within the study plan, their objectives, and the activities included in each study. The investigation activities conducted during the North Ramp geotechnical drilling program supported all three of the studies in Table 1-1.

² D.S. Kessel, C.E. Brechtel, G.M. Norris, M.M. Angell, and M. Riggins, 1994. "Geoengineering Characterization of Nonlithified Tuffs to be Encountered by the North Ramp West of the Bow Ridge Fault," SLTR94-0001 Rev. 7, Yucca Mountain Site Characterization Project, Sandia National Laboratories, Albuquerque, New Mexico.

³ G.J. Elbring, 1994. *High Resolution Shallow Seismic Reflection and Refraction Studies at Exile Hill, Nye County, Nevada*, SAND94-2374 (in preparation), Sandia National Laboratories, Albuquerque, New Mexico.

Table 1-1. Studies, Objectives, and Activities of the Soil and Rock Properties Study Plan (8.3.1.14.2) — Studies to Provide Soil and Rock Properties of Potential Locations of Surface and Subsurface Access Facilities (DOE, 1991)

SCP Activity No.	Study	Objectives	Activities
8.3.1.14.2.1	Exploration Program	Characterize soil and rock conditions that influence ESF construction.	Site Reconnaissance Preliminary and Detailed Exploration
8.3.1.14.2.2	Laboratory Tests and Material Property Measurements	Conduct laboratory tests and material property measurements on representative samples of soil and rock.	Physical Properties and Index Laboratory Tests Mechanical and Dynamic Laboratory Property Tests
8.3.1.14.2.3	Field Tests and Characterization Measurements Study	Conduct field tests and characterization measurements to determine in situ physical, mechanical, and dynamic properties of soil and rock.	Physical Property Field Tests and Characterization Measurements Mechanical Property Field Tests Geophysical Field Measurements

Table 1-2 correlates study activities with specific investigations conducted during geotechnical characterization for the North Ramp. The objectives of each study are also summarized in the table.

Table 1-2. Correlation of Study Areas and Activities with Specific Investigations Conducted in the Nonlithified Tuffs

Study	Activity	Investigation	Objective
Exploration Program	Preliminary and Detailed Exploration	Drill NRG-1, -2A, -2B, -3, -4, -5, -6, and -7/7A.	Determine depth, thickness, and continuity of strata and thermomechanical (thermal-mechanical) units intersected by North Ramp cross section.
		Perform Schmidt Hammer measurements.	Preliminary estimates of rock strength and boreability.
		Perform down-hole video logs.	Provide visual estimate of rock quality, fracturing density, detect free water.
		Perform geophysical logging.	Stratigraphic correlations in new holes.
Laboratory Tests and Materials Property Measurements	Physical Property and Index Laboratory Tests	Laboratory Measurements of Physical Properties— density, porosity, grain density.	Characterize bulk properties of rock for engineering designs of materials handling facilities; verify geophysical tool functions.
	Mechanical and Dynamic Laboratory Property Tests	Laboratory Mechanical Property tests—uniaxial compressive strength, triaxial strength, elastic modulus, Poisson's ratio, Brazilian tensile strength.	Measure intact rock properties to provide basis for rock mass quality assessment and rock mass mechanical properties.

Table 1-2. *continued*

Study	Activity	Investigation	Objective
Field Tests and Characterization of Measurements	Physical Property Field Tests and Characterization Measurements	Rock Structural Logging	Describe rock structural features to support development of rock mass quality indices.
		Generate Rock Mass Classification—Q and RMR	Provide basis for empirical design of tunnel support, provide basis for developing rock mass mechanical properties.
	Mechanical Property Field Tests	Generate Rock Mass Mechanical Property Estimates—Strength and Modulus	Provide design parameters for numerical analysis of thermal and seismic loading.
	Geophysical Field Measurements	Seismic Reflection and Refraction in Daylight Valley	Locate faults covered by alluvium; constrain fault displacements.

1.4 Quality Assurance

All core logging and rock testing data from the NRG boreholes were generated under Quality Assurance (QA) procedures governing the various technical organizations involved in the activities. Data collection and collation, supporting preparation of this report, was documented in scientific notebooks and analysis files in accordance with SNL Quality Assurance Implementing Procedures 20-2 and 2-4. These notebooks will be entered into the SNL participant data archive. All data presented in this report were generated under QA procedures unless otherwise noted.

Nonqualified existing data and preliminary data been utilized in this report where qualified data do not exist or are not currently available. Table 1-3 has been developed to document these occurrences and to meet requirements of the DOE's Quality Assurance Requirements and Description for maintenance of traceability. Throughout the text, some footnotes have been utilized to refer to information relevant to the North Ramp which is in preparation and represents preliminary data. Other footnotes refer to qualified data submitted to the project by Technical Data Information Form but not assigned accession numbers required for listing in the references.

Table 1-3. Nonqualified and Preliminary Data and Assumptions

Data or Assumptions	Data Status*	Application	Data Reference	Effects
Geologic Cross Section along North Ramp	N	Presentation of lithostratigraphic units along North Ramp— Figure 4-2	Basis of development is footnote 17 pg. 4-13, nonqualified geologic model of the North Ramp with NRG boreholes.	Projection of geologic contacts between NRG holes, fault displacements, Tables 2-1, 2-2, 4-3, 4-4, and 4-5.
Borehole RF#8	N	Corroborating data in Figure 4-3, Exile Hill Cross Section	Geology and Rock Structure Log RF #8	Projection of Tuff Unit "X" contact in Figure 4-3.
High Resolution Seismic Survey over Daylight Valley	N	Development of Alternate Geologic Cross Section in Figure 4-5	Elbring (1994) in footnote 3, pg. 1-6	Projection of strata and faults under Daylight Valley, Figure 4-5. Tables 2-1, 2-2, 4-3, 4-4, and 4-5.
Thermomechanical (Thermal-Mechanical) Units Cross Section Figure 4-7	N	Presentation of thermomechanical units along North Ramp	Basis for development is Figure 4-2.	Table 4-4
Recognized Fracture Patterns, Section 4.5.2	P	Interaction of predominant joint orientations with North Ramp orientation	Lin et al. (1993b) and footnote 6, pg. 2-7—preliminary mapping data, North Ramp Starter Tunnel	Section 2.4, Table 4-6 and Figure 4-8
Estimates of Range of Jn Parameter, pg. 7-16	P	Monte Carlo simulation of rock mass quality parameter Jn	Lin et al. (1993b) and footnote 6, pg. 2-7—preliminary mapping data North Ramp Starter Tunnel	Determination of Q indices
Estimates of Distribution of SRF Parameter, pg. 7-20	P	Monte Carlo simulation of rock mass quality parameter SRF	Footnote 6, pg. 2-7—preliminary mapping data North Ramp Starter Tunnel	Determination of Q indices
Confining Pressure Effects on TSw1 and TSw2 Rock Mechanics Lab Samples	N	Develop estimates of rock mass strength	Used material constants derived from nonqualified lab test data described in Lin et al. (1993b).	Tables 2-8, 2-9, 8-3, 8-4, 8-5, and 8-6, Figures 8-4 and 8-5

*N—Nonqualified existing data.

P—Preliminary data taken under approved QA program.

1.5 Report Organization

This report is presented in two volumes:

- ♦ Volume I — Data Summary
- ♦ Volume II — NRG Corehole Data Appendices

Volume I presents the collation and analysis of the data for the thermomechanical (thermal-mechanical) units and discusses the resulting rock mass quality and rock mass mechanical properties. The geotechnical data and logs for individual NRG holes are presented in Volume II.

Following this introduction in Volume I, Section 2.0 of the report presents the summary and conclusions. Section 3.0 discusses the methodology of development of the geotechnical data. A brief description of the geology along the North Ramp is presented in Section 4.0 to facilitate correlation of the data presented with the stratigraphic and thermomechanical (thermal-mechanical) units.

The rock structural data is presented in Section 5.0. Rock mass quality estimates for each thermomechanical (thermal-mechanical) unit, derived from the data in Sections 5.0 and 6.0, are described in Section 7.0. Section 8.0 presents estimates of the rock mass mechanical properties. References are presented in Section 9.0.

Four appendices are included in Volume I to provide a detailed description of the structural logging methodology (Appendix A) and the methodology used in developing the core-based estimates of Q and RMR (Appendix B). Appendix C contains rank-ordered tables of rock mass quality and Appendix D contains a comparison of rock mass quality indices from nonlithophysal and lithophysae-rich portions of the TCw and TSw1 thermomechanical (thermal-mechanical) units.

2.0 GEOTECHNICAL SUMMARY

2.1 Introduction

The purpose of this section is to summarize the subsurface rock conditions anticipated in the North Ramp and the projected impact that these conditions may have on design. Since the method of excavation has been previously chosen to be mechanical excavation by tunnel boring machine (TBM), this report focuses on the prediction of the rock mass characteristics and properties, and identification of the required range of ground support. The North Ramp will be excavated at -2.05% grade for a distance of 2800 m (9,186 ft) using a 7.6-m (25-ft) diameter TBM. Portal and starter tunnel facilities were completed in 1994 and the TBM was assembled by August 1994. Initial start-up and shakedown of the TBM began in October 1994.

Data in this report include previously existing studies at Yucca Mountain, including both surface mapping and drilling, but are primarily based upon information produced during drilling of the NRG-series boreholes along the ramp. Data collected in the NRG holes included lithologic and stratigraphic identification, rock structural logging, determination of rock quality indices RQD, Q and RMR, rock mechanics testing, and geophysical logs. Cross sections of the stratigraphic units along the ramp have been generated and faults have been projected to the ramp based upon surface mapping. The thermomechanical (thermal-mechanical) stratigraphy, proposed by Ortiz et al. (1984), was used to organize the rock mass properties into units with similar mechanical characteristics.

2.2 Geology and Major Structural Features along the North Ramp

The North Ramp will be constructed through a sequence of welded and nonwelded volcanic tuffs of the Miocene Paintbrush and Timber Mountain groups. These rocks include six different formation level ash-flow tuffs which were deposited in the sequence of the Topopah

Spring, Pah Canyon, Yucca Mountain, Tiva Canyon, and Rainier Mesa Formations. These ash-flow formations are separated by thin bedded tuffs. The two thickest formations, the Topopah Spring and Tiva Canyon, are predominantly welded and have relatively high intact-rock strengths. The Pah Canyon, Yucca Mountain, and Rainier Mesa Formations are nonwelded tuffs of relatively low intact strengths. The bedded tuffs lying between the ash-flow units are characteristically thin units of nonwelded, relatively low strength rocks. A nonlithified (soil-like) sequence of bedded tuffs occurs between the Tiva Canyon and Rainier Mesa Formations. Site geology is discussed in Section 4.0 of the report and a cross section along the North Ramp showing the stratigraphic units is presented in Figure 4-2. Ramp stations at the projected intersections of stratigraphic units are listed in Table 2-1.

Table 2-1. Projected Ramp Station Coordinates at Stratigraphic Contacts Along North Ramp Alignment Tunnel Centerline

Stratigraphic Unit	Projected Ramp Station (m)**	Projected Distance in Unit (m)**
Tiva Canyon Tuff (Tpc)	0+00	196
Rainier Mesa Tuff (Tmr)	1+96	13
Tuff Unit "X" (Tpki)	2+09	136 to 226
Tiva Canyon Tuff (Tpc)*	3+45 to 4+35	455 to 545
Pre-Tiva Canyon Tuff Bedded Tuff (Tpbt4)	8+90	<10
Yucca Mountain Tuff (Tpy)	9+00	20
Pre-Yucca Mountain Tuff Bedded Tuff (Tpbt3)	9+20	25
Pah Canyon Bedded Tuff (Tpbt)	9+45	83
Pre-Pah Canyon Tuff Bedded Tuff	10+28	34
Topopah Spring Tuff (Tpt):		
Crystal-rich nonlithophysal zone, crystal-rich vitric zone (Tptm)	10+62	754
Crystal-rich upper nonlithophysal and crystal-poor upper lithophysal zones (Tpul)	18+16	947
Crystal-poor middle nonlithophysal zone (Ttpmn)	27+63	37

*Range reflects uncertainty due to possible faults under Daylight Valley. Range given is where tunnel roof intersects contact.

**Inclined distance along ramp, along centerline.

There are three known major geological features with proven and potential engineering and construction significance that are projected to be intersected by the North Ramp:

- ♦ The Bow Ridge Fault (1+96 m);
- A section of nonwelded, nonlithified (soil-like) tuffs immediately west of the Bow Ridge Fault (1+96 m to 2+71 m); and
- ♦ The Drill Hole Wash Fault (approximately 21+04 m).

Another geologic feature with potential engineering and construction significance is currently suspected underneath surface alluvium in Daylight Valley on the basis of geophysical data. These features are discussed separately in the following material.

2.2.1 Known Geologic Features of Engineering and Construction Significance

The Bow Ridge Fault is a N-S striking, steeply dipping, down-on-the-west fault that is projected to intersect the North Ramp at station 1+96 m. The location and character of this fault has been well characterized by both surface trenching and by boreholes drilled in the area of the North Ramp. The dip separation on the fault is approximately 130±5 m and has juxtaposed very hard, welded rocks of the Tiva Canyon Formation in the footwall against very soft, nonlithified tuffs of the Rainier Mesa Formation and pre-Rainier Mesa Bedded Tuffs in the hanging wall. The gouge zone of broken and intermingled welded tuffs, nonwelded, and nonlithified tuffs is projected to be approximately 2–4 m wide in the ramp excavation. Although a zone with potential to conduct water from the surface exists, the presence of water in volumes large enough to impact construction was not detected. Figure 4-3, Section 4.0, shows a detailed cross section through the Bow Ridge Fault.

Immediately west of the Bow Ridge Fault, the ramp will enter a section of very weak, nonlithified tuffs that has been locally preserved for a distance of 75 m. This feature was initially identified by drilling holes NRG-2, NRG-2A, and NRG-2B. Very detailed exploration and soil characterization was then conducted to support ramp design and the results are presented in a report.⁴ Although the nonlithified tuffs were projected to be cohesive, moisture contents in one portion were high and the potential for running or sloughing ground conditions was indicated. This section of the ramp will require heavier support in the form of steel ring beams or other equivalent systems. A series of inspections of the nonlithified tuffs exposed in trench NRT-1 and meetings with the TRW Management and Operations (M&O) and the constructor were held to directly communicate these observations.

The ramp is projected to encounter the N-W trending Drill Hole Wash Fault at station 21+04 m, a structure inferred to be of substantial width. No direct characterization data are available at the depth or at the location that the North Ramp will penetrate the fault. This fault exhibits right-lateral strike-slip movements of unknown magnitude that produce a dip separation estimated to be 10 m. The ramp is projected to penetrate the Topopah Spring, upper lithophysal zone in both hanging wall and footwall; thus, no major discontinuity in rock type is expected across the fault. Strike-slip faults in this area have been described as having breccia zones 20 m or greater in width (Scott et al., 1984). In other parts of Drill Hole Wash this structure is mapped as two splays up to 150 m (500 ft) apart. Buesch et al.⁵ conclude that the Drill Hole Wash Fault

⁴ Kessel et al.

⁵ D.C. Buesch, R.W. Spengler, T.C. Moyer, and J.K. Geslin, 1994 in press. *Revised Stratigraphic Nomenclature and Macroscopic Identification of Lithostratigraphic Units of the Paintbrush Group Exposed at Yucca Mountain, Nevada*, U.S. Geological Survey, Department of Interior.

is most likely a complex of interconnected faults in a zone 120–180 m (400–600 ft) wide. Although no data exist on the fault zone at depth and the fault is generally covered by alluvium at the surface, borehole sampling is not currently planned. Review of core recovery in the stratigraphic unit indicates an average 35% lost core and 16% rubble. It is therefore not certain that coring through the fault would produce data showing a detectable difference with the surrounding rocks. The fault zone is expected to require heavier ground support, at least locally, in zones where the strike-slip movement has been concentrated.

2.2.2 Potential Geological Features with Engineering and Construction Significance

Seismic reflection data collected in Daylight Valley suggest the presence of at least two buried faults that may occur between ramp stations 3+50 m and 4+00 m. The seismic data indicate a small graben that drops the Tuff Unit “X” down to the ramp elevation along the ramp to station 4+40 m. The resulting alternate geologic interpretation (presented in Figure 4-5, Section 4.0) projects the ramp encountering two additional normal fault zones with the tunnel roof continuously in Tuff Unit “X” and pre-Tuff Unit “X” Bedded Tuff. The floor of the tunnel encounters two blocks of Tiva Canyon Formation at each fault zone. This mixed face geometry will be further complicated by the nonlithified pre-Tuff Unit “X” Bedded Tuff which will constitute a very soft layer 1.7 to 4.3 m thick between the Tuff Unit “X” and Tiva Canyon. Heavy ground support similar to that required in the nonlithified tuffs just west of the Bow Ridge Fault may be required in this zone.

Eight additional normal faults are anticipated along the ramp alignment (see Table 4-5, Section 4.0, for projected ramp stations) based upon surface mapping by Scott and Bonk (1984). Displacements are relatively small and gouge zones are expected to be small. Core data from

holes NRG-2 and -3, angle holes that penetrate the Bow Ridge normal fault and a normal fault shown on the Scott and Bonk (1984) surface map, respectively, did not indicate discernible rock disturbance outside of the immediate fault zone. The Bow Ridge Fault zone was observed to be 2–4 m wide in trenches at Exile Hill. The fault zone was penetrated by NRG-3, based on surface mapping, but could not be identified in the core.

2.3 Thermomechanical (Thermal-Mechanical) Stratigraphy

The rocks at Yucca Mountain have been grouped into thermomechanical (thermal-mechanical) units that exhibit generally similar physical and mechanical properties that are important to design. The North Ramp will pass through five thermomechanical (thermal-mechanical) units, as defined by Ortiz et al. (1984), which are illustrated in the cross section in Figure 4-7 and correlated with stratigraphy in Figure 4-6, Section 4.0. Table 2-2 lists the thermomechanical (thermal-mechanical) units of Ortiz et al. (1984) and the projected ramp station where each unit will be intersected. These thermomechanical (thermal-mechanical) units have been used as the basis to perform the geotechnical characterization to support design. The TCw and TSw1 units have been further subdivided into lithophysae-rich and nonlithophysal portions to investigate whether further structural differences exist.

Table 2-2. Projection of Ramp Station Coordinates at Thermomechanical (Thermal-Mechanical) Unit Contacts

Thermomechanical (Thermal-Mechanical) Unit	Projected Ramp Station (m)**	Projected Length of Tunnel in Unit (m)**
Tiva Canyon Welded (TCw)	0+00	196
Undifferentiated Overburden (UO)*	1+96	149 to 239
Tiva Canyon Welded (TCw)*	3+45 to 4+35	455 to 545
Upper Paintbrush Nonwelded (PTn)	8+90	172
Topopah Welded Unit, Lithophysae-rich, nonlithophysal subzones (TSw1n)	10+62	754
Topopah Welded Unit, Lithophysae-rich, lithophysal-bearing subzones (TSw1l)	18+16	947
Topopah Welded Unit, Lithophysae-poor (TSw2)	27+63	37

*Range reflects uncertainty due to projected faults under Daylight Valley.

**Horizontal distance along centerline.

2.4 Orientations of Joints and Fractures

Existing data from previously reported oriented coring (Lin et al., 1993b) and underground mapping data (preliminary non-QA) from the North Ramp Starter Tunnel (NRST)⁶ indicate that the predominant joint orientations consist of two relatively orthogonal joint sets with dips ranging generally from 70° to 90°. The predominant joints trend N17°W to N-E with steep dips generally to the west. This set intersects the North Ramp alignment at angles of 44° to 60° which, combined with its steep dip, tends to reduce its structural impact. The other orthogonal set strikes N77°E to due east, but occurs much less frequently. A N42°W set is more nearly parallel to the North Ramp alignment, but it occurs relatively infrequently which minimizes its structural impact.

A subhorizontal joint set is also identified in the data and may be associated with the horizontal foliation of the tuff beds. This set was observed in both the drilling data and tunnel mapping data. It was also observed to contribute to one localized roof instability in the NRST. A stereonet comparing the joint orientations to the North Ramp alignment is shown in Figure 4-8, Section 4.0.

No additional fracture orientation data was developed in the NRG drilling program.

2.5 Hydrology

The NRG drilling indicated generally dry conditions along the North Ramp alignment. Although little data exist on the fault intersections along the North Ramp, those sampled by holes NRG-2 and -3 did not indicate water in volumes large enough to impact construction at the fault

⁶ M.F. Fahy and F.C. Beason, 1995 in press. "Geotechnical analysis for the Exploratory Studies Facility North Ramp Boxcut and Starter Tunnel," preliminary report prepared for the Department of Energy and Management and Operating Contractor Architect/Engineer by the Bureau of Reclamation/U.S. Geological Survey, Volumes 1 and 2.

intersections in the holes. Conditions in the other faults at depth along the North Ramp alignment are not known. Review of video logs of the NRG boreholes did not indicate any water inflow through the entire depth penetrated by the ramp.

2.6 Rock Structure Data from the NRG Core

Analysis of the condition of the core from the NRG drilling was performed to quantify the character of the rock. In general, the rock quality as indicated by RQD was low in the welded units due to extensive fracturing of the core and content of large cavities in the high lithophysal zones. Between the fractures, the intact welded rocks have generally high strength (57–179 MPa). In portions of the TSw1, the lithophysae and associated alteration produce lower strengths in the welded rocks. Rock quality as indicated by RQD was generally better in the weaker, nonwelded tuffs with less indicated fracturing.

The amount of lost core and rubble in the NRG holes is high and increases with depth to the base of the Topopah Spring. This is attributed to the fracturing and the occurrence of lithophysae in same zones. Core condition within the nonwelded tuffs of the PTn unit and in the deeper nonwelded Calico Hills was generally better than the welded tuffs, even though the rocks were much weaker.

Extensive lost core and rubble zones occurred in the NRG holes. Rubble zones, as a percent of total drilled length, ranged from 10.0% in the PTn to 16.6% in TSw2. The percent of lost core ranged from 13.3% of the total drilled length in the TCw to 32.6% in TSw2. The percentage of lost core and rubble increased with increased depth. Lithophysae-rich portions of the TCw and TSw2 had higher percentages of lost core (partly due to cavities larger than the

core) and rubble zones (partly due to inhomogeneity of the core) than the nonlithophysal portions.

The RQD was low for each of the thermomechanical (thermal-mechanical) units; mean, median, and standard deviations are compared in Table 2-3. The median values ranged from 39% in the PTn to 8% in the TSw2. A conservative value of RQD was calculated by considering all types of breaks (natural, indeterminate, and coring induced), and these values were used in all calculations for rock mass quality. An *enhanced-RQD* was also calculated by filtering the effects of coring induced fractures and is compared to the RQD in Table 2-3. Some difference in median RQD occurred in the TSw1 unit between the lithophysae-rich and nonlithophysal portions, with the nonlithophysal portion having the higher RQD. A similar, but smaller difference, occurred in the TCw unit.

Table 2-3. Comparison of RQD Data and *Enhanced-RQD* Data for the Thermo-mechanical (Thermal-Mechanical) Units — NRG Holes

		TCw NL	TCw LR	PTn	TSw1 NL	TSw1 LR	TSw2	Relative Rating	
		RQD (%)						Rating	
RQD	Mean	29	26	39	32	18	13	91–100	Excellent
	Median	26	22	39	30	14	8	76–90	Good
	Std. Dev.	20	21	28	26	18	17	51–75	Fair
<i>Enhanced RQD</i>	Mean	49	46	59	58	40	31	26–50	Poor
	Median	51	49	66	65	38	26	1–25	Very Poor
	Std. Dev.	24	24	29	30	26	23	0–1	Extremely Poor
<i>Enhanced RQD</i> <u>RQD</u>	Mean	1.7	1.8	1.5	1.8	2.2	2.4		
	Median	2.0	2.2	1.7	2.2	2.7	3.3		

NL—Nonlithophysal; LR—Lithophysae Rich

Fractures, identified during logging as coring induced, were a substantial part of the total and impacted the value of the RQD. The impact was assessed by calculating an *enhanced-RQD*, where coring-induced fractures were filtered from the piece length calculation. Mean

enhanced-RQD values ranged from 1.51 (PTn) to 2.38 (TSw2) times greater than mean RQD values and are listed in Table 2-3.

Between fractures, most of the rock exposed by the NRG holes was described as fresh (F) or slightly weathered (S) in the welded units. Twenty percent of the PTn core was described as moderately weathered. Estimations of rock hardness rated most of the core in the welded units as very hard to moderately hard. PTn was rated as soft to very soft rock.

The majority of fractures logged in the NRG core were identified as coring induced, probably forming along subhorizontal planes of incipient weakness, with dip angles from 0–10°. Coring-induced fractures ranged from 42% of the total in the TCw nonlithophysal portion to 73% in the TSw1 lithophysae-rich portion.

When the coring-induced (type C) fractures were removed from the data and the density of fracturing was corrected for sampling bias, the steeply dipping fractures dominate the population. The fracture frequency was estimated by applying the Terzaghi (1965) correction to account for the sampling bias due to the orientation of the borehole with respect to the fracture orientation. The resulting estimates of average fracture frequency indicate predominantly near-vertical fractures (70–90°) with frequencies that range from 7.9 m⁻¹ in the TCw to 22.6 m⁻¹ in the TSw2 (see Table 5-8, Section 5.0). This suggests that rock quality would be dominated by the near-vertical fractures and generates questions regarding the adequacy of using vertical boreholes which might not effectively sample the near-vertical structure. These questions were investigated by calculating RQD based on the total, corrected fracture frequency, and comparing those values to the median RQD determined by the core logging approach. This comparison, shown in Table 5-10, Section 5.0, showed that RQD determined by the core logging was in all

cases less than the RQD calculated using vertical fracture frequency and assuming 100% fracture continuity. RQD presented in this report was therefore judged to be a conservative indicator of rock conditions along the ramp alignment.

The fractures identified as natural or indeterminate in origin were predominantly clean ranging between 53% and 85% of the fractures for the different thermomechanical (thermal-mechanical) units. Most infills were classed as surface sheens or thin coatings. The predominant infills were white crystalline or white non-crystalline materials. Very few clay infillings were observed. Fracture surfaces were generally described as planar or irregular with moderate roughness.

In the three holes which penetrated normal faults, rock quality as indicated by RQD and fracture frequency did not appear to be a function of fault-related fracturing outside of the immediate zone of breccia and gouge development. Variations that were observed in core adjacent to the fault zones were more likely due to changes in lithology and welding. Two of these holes (NRG-2 and NRG-2B) penetrated the Bow Ridge Fault, the third (NRG-3) penetrated a possible normal fault, with no offset indicated by the stratigraphic units.

Lithophysal and other void contents averaged 1.74% and 0.3% for the lithophysae-rich and non-lithophysal portions of the TCw, respectively. In the TSw1 unit, the lithophysae-rich portion averaged 5.4% and the nonlithophysal portion averaged 0.29%. These determinations are based on intact core and do not include lithophysae that exceed the core diameter.

2.7 Rock Mechanical Properties Tests

Results of rock mechanics testing of NRG core indicated properties similar to previous test results at YMP (DOE, 1991). Mean values of the rock mechanical and physical properties are listed in Table 2-4.

Table 2-4. Summary of Mean Values for Rock Mechanical and Physical Properties Testing — NRG Holes

	UO (Tuff "X")	TCw	PTn	TSw1	TSw2
Uniaxial Compressive Strength (MPa)	6.8	125.1	8.0	56.9	178.5
Elastic Modulus (GPa)	4.3	28.4	2.5	18.9	32.3
Cohesion (MPa)	ND*	55.4	ND*	14.1	42.8
Angle of Internal Friction	ND*	48.0	ND*	46.0	50.0
Poisson's Ratio	0.14	0.21	0.20	0.26	0.21
Dry Bulk Density (g/cc)	1.23	2.14	1.30	2.16	2.27
Porosity (%)	46.8	13.7	45.5	15.8	10.9
Average Grain Density (g/cc)	2.34	2.53	2.38	2.58	2.55

*No Data

Schmidt hammer rebound hardness was measured on the NRG core in an attempt to supplement the uniaxial compression data. Table 2-5 compares the mean and standard deviation of the rebound number for each thermomechanical (thermal-mechanical) unit. Estimates of uniaxial compressive strength based upon a correlation with Schmidt hammer data gave reasonable predictions for the TCw and TSw2 unit, but overestimated strength in the PTn and TSw1 units.

Table 2-5. Mean Value and Standard Deviation of Schmidt Rebound Hardness*

	UO (Tuff "X")	TCw	PTn	TSw1	TSw2
Mean	ND**	41.0	27.2	46.5	47.2
Standard Deviation	ND**	10.1	11.5	7.2	7.5

*L-type Schmidt hammer, impact energy of 0.74 Nm.

**No data.

2.8 Rock Mass Quality Indices

Rock mass quality indices Q and RMR were estimated for each 3-m (10-ft) interval of the NRG core logging data based upon the described condition of the core, the rock mechanics data, and structural features observed in surface mapping. The 3-m (10-ft) interval data were then grouped by thermomechanical (thermal-mechanical) unit and the statistical distribution of the data utilized to estimate the variation of ground conditions and the required ground support to be expected along the North Ramp. Certain parameters used to calculate the rock mass quality could not be generated directly for each interval and were therefore generated by Monte Carlo simulation based on the observed distribution of the parameter. Because of this simulation and because the drilling density along the ramp is low, no spatial correlation was assumed for the individual Q and RMR values derived from the drilling data. The distribution of the Q and RMR data within each thermomechanical (thermal-mechanical) unit was, however, projected to represent the variability that will be encountered as the North Ramp is excavated through the full vertical extent of each unit. Fault zones are not specifically represented in the rock quality estimates, but may be covered by the extreme lower range of the Q and RMR. The methodology used to produce the estimates is discussed in Section 7.0.

2.8.1 RMR and Q Data

The rock mass quality index RMR was estimated for 3-m (10-ft) intervals in all holes and was grouped by thermomechanical (thermal-mechanical) unit. The distribution of RMR⁷ in each thermomechanical (thermal-mechanical) unit was summarized by generating values corresponding to five rock mass classes defined by frequencies of occurrence of 5%, 20%, 40%, 70%, and 90%. Table 2-6 lists the range of values for each thermomechanical

⁷ No adjustments made for joint orientation.

(thermal-mechanical) unit. Appendix C contains rank-ordered tables of the RMR data correlated with discrete values of the frequency of occurrence.

Table 2-6. RMR Ratings for the Five Rock Mass Quality Categories

Rock Mass Quality Category*	Frequency of Occurrence (%)	UO (Tuff "X")	TCw	PTn	TSw1	TSw2	Relative Rating	
1	5	50	51	45	49	51	very good	81-100
2	20	53	56	52	53	56	good	61-80
3	40	56	59	55	57	58	fair	41-60
4	70	59	67	65	62	63	poor	21-40
5	90	60	72	70	70	67	very poor	<20

*Corresponds to category ranges proposed by Hardy and Bauer, 1991.

The range of RMR between all thermomechanical (thermal-mechanical) units is small with the rock classed as fair to good. This predilection of RMR for the fair rock category has been observed in other data (Kirsten, 1988), and it has therefore only been used here to estimate rock mass properties.

The rock mass quality index Q, generated for 3-m (10-ft) intervals, is summarized for the five frequency of occurrences in Table 2-7 for each thermomechanical (thermal-mechanical) unit. Rank-ordered data is presented in Appendix C.

Table 2-7. Q Values for the Five Rock Mass Quality Categories

Rock Mass Quality Category*	Frequency of Occurrence (%)	Old UO (Tuff "X")	TCw	PTn	TSw1	TSw2
1	5	2.23	0.38	0.15	0.24	0.30
2	20	7.50	0.68	0.28	0.87	0.65
3	40	10.98	2.08	0.66	1.73	1.91
4	70	14.49	5.66	1.62	5.09	3.75
5	90	24.29	9.14	3.74	12.00	8.44

*Corresponds to category ranges proposed by Hardy and Bauer, 1991.

The range of Q values for the welded thermomechanical units indicate very poor to good rock mass quality. The nonwelded thermomechanical (thermal-mechanical) units, UO and PTn, range from extremely poor to good rock mass quality.

The correlation of Q versus RMR values in the NRG holes were generally within the range suggested by Bieniawski (1976). However, at Q values below 1.0, the corresponding RMR values diverge from the published correlation with the corresponding values of RMR being higher than expected. This may be due to the fact that adjustment for joint orientation was not performed on the RMR because it is only used here to estimate rock mass properties.

Q and RMR data from hole NRG-1 were compared to data generated from observations in the NRST (Section 7.4.2). Described intervals within the NRST were characterized by a range of Q and RMR (minimum–maximum). The NRG-1 data compared very well with the maximum range of the data. The minimum values in the NRST were affected by intermediate-scale vertical structures/broken zones containing weathered, crushed rock. These features were not sampled by the vertical borehole and did not allow characterization of the joint surface condition. In general, however, the minimum range of the NRST data was covered by the distribution of all borehole data for the welded units.

The differences between rock mass quality indices in the lithophysae-rich and nonlithophysal portions of the TCw and TSw1 were small in the lower rock mass categories 1–4. The observed differences were not judged sufficient to impact the North Ramp design and the lithophysae-rich and nonlithophysal portions of the TCw and TSw1 were therefore grouped together.

2.8.2 Projected Range of Ground Support

Specific design of the ground support for the North Ramp must be based upon the capabilities of the TBM equipment and must take the excavation and support installation features/limitations into account. The ground support indicated by the distribution of the core-based Q data and the ground support categories associated with the Q-based empirical design system (Barton et al., 1974) have been tabulated in Section 7.6, Table 7-12 to describe the range of support indicated and the projected proportion of the North Ramp requiring each level of support. The major conclusions derived are listed below in order of increasing support requirements:

- Very little of the North Ramp excavation in any of the thermomechanical (thermal-mechanical) units would qualify for “no support required.” A maximum of 5% of the Q data had values above the no-support-required boundary in any thermomechanical (thermal-mechanical) unit.
- The majority of the North Ramp can be supported with combinations of rockbolts on spacings down to 1 m (3.28 ft) with wire mesh and up to 5 cm (2 in.) of shotcrete. Within the nonwelded UO unit, the Q data projects this to be the heaviest support required. In the welded units and PTn unit, the Q data projects this range of support to be suitable for all but 49% of the North Ramp.
- ♦ The remaining 21–26% of the Q data project bolts, wire mesh, and shotcrete up to 12.5 cm (5 in.) thick. The indicated ground support categories also contain recommendations for cast-in-place concrete up to 50 cm (20 in.) thick; however,

these very heavy support systems would be in response to squeezing ground conditions which are not anticipated.

- The lower 21–26% of the Q data indicate ground support consistent with that utilized in the NRST.

Exceptions to these general ground support requirements are known to occur within the nonlithified tuff interval west of the Bow Ridge Fault and are anticipated to occur within the Drill Hole Wash Fault zone. However, within these zones, the capability of the TBM to install steel ring beams is projected to meet the requirements for heavier support.

It is also anticipated that heavier support may be required in the UO (Tuff Unit “X”) interval underneath Daylight Valley (stations 3+50 m to 4+40 m). In this section of the North Ramp, nonlithified tuff of the pre-Tuff Unit “X” Bedded Tuff may be encountered three different times, if fault structures inferred from surface seismic data occur underneath the alluvium.

There is currently no data available which indicates that the support capabilities of the TBM, as currently configured, are not sufficient to cover the full spectrum of requirements.

2.9 Rock Mass Mechanical Properties Estimates

Rock mass mechanical properties have been estimated based upon the methodology proposed by Hardy and Bauer (1991) which utilizes published empirical correlations with RMR. These estimates are developed to support numerical modeling to assess thermomechanical (thermal-mechanical) and seismic loading impacts on the North Ramp.

The estimated rock mass strengths represent substantial reductions from the laboratory measurements of intact rock compressive strength. Table 2-8 compares the estimated rock mass

strength for the highest rock mass category (90% frequency of occurrence) to laboratory strengths and lists the ratio of rock mass strength to that measured in the lab.

Table 2-8. Comparison of Rock Mass Strength Estimates to Intact Strength Data—Rock Mass Category 5 (90% frequency of occurrence)

Thermo-Mechanical Unit	Estimated Rock Mass Strength (MPa)	Intact Strength		Ratio* of Rock Mass to Intact Strength (%)
		Mean (MPa)	Standard Deviation (MPa)	
TCw	15.89	125.1	94.9	12.7
PTn	0.97	8.0	13.0	12.1
TSw1	7.23	56.9	30.1	12.7
TSw2	18.88	178.5	78.3	10.6

*Rock Mass Strength ÷ Intact Strength

Rock mass strength based on the Mohr-Coulomb failure criteria were determined for the five rock mass categories and are listed in Table 2-9 for each thermomechanical (thermal-mechanical) unit.

Table 2-9. Strength Parameters and Dilation Angles for the Mohr-Coulomb Failure Criterion for Rock Mass Classes 1–5 in Each Thermomechanical (Thermal-Mechanical) Unit

		Rock Mass Class*				
		1	2	3	4	5
		Frequency of Occurrence (%)				
		5	20	40	70	90
UO (Tuff "X")	cohesion (MPa)	0.4	0.5	0.5	0.5	0.5
	friction angle (degrees)	50	51	51	52	52
	dilation angle (degrees)	25	25	26	26	26
TCw	cohesion (MPa)	1.2	1.3	1.7	2.4	3.0
	friction angle (degrees)	53	53	54	55	55
	dilation angle (degrees)	26	27	27	27	27
PTn	cohesion (MPa)	0.3	0.3	0.3	0.4	0.5
	friction angle (degrees)	40	41	42	43	44
	dilation angle (degrees)	20	20	21	21	22
TSw1**	cohesion (MPa)	0.7	0.9	1	1.3	1.9
	friction angle (degrees)	41	42	42	43	43
	dilation angle (degrees)	20	21	21	21	22
TSw2**	cohesion (MPa)	1.3	1.6	2.2	2.8	3.8
	friction angle (degrees)	49	49	50	50	50
	dilation angle (degrees)	25	25	25	25	25

* Corresponds to category ranges proposed by Hardy and Bauer (1991).

**Based on nonqualified data reported by Lin et al. (1993b).

Rock mass elastic modulus, determined for each of the five rock mass classes, are listed in Table 2-10.

Table 2-10. Estimated Rock Mass Elastic Modulus (GPa)

Thermomechanical (Thermal-Mechanical) Unit	Rock Mass Class				
	1	2	3	4	5
UO (Tuff "X")	4.30	4.30	4.30	4.30	4.30
TCw	6.70	8.92	13.33	21.20	27.71
PTn	2.50	2.50	2.50	2.50	2.50
TSw1	5.66	8.78	11.71	17.86	18.90
TSw2	6.37	8.96	12.55	17.11	23.51

Recommended values of Poisson's ratio for the each thermomechanical (thermal-mechanical) unit are listed in Table 2-11.

Table 2-11. Estimated Rock Mass Poisson's Ratio

UO (Tuff "X")	TCw	PTn	TSw1	TSw2
0.14	0.20	0.20	0.30	0.21

This page left intentionally blank.

3.0 GEOLOGIC AND GEOTECHNICAL DATA DEVELOPMENT

3.1 Introduction

This section of the report describes the types of data collected in the North Ramp characterization program and the process used to produce the rock mass data used for design. Because the excavation method and route have been previously selected, design requirements focus primarily on the prediction of ground conditions for identification of the required ground support. Empirical design methods (Barton et al., 1974, and Bieniawski, 1979) based on rock mass quality were the basis of design support.

A YMP repository drift design methodology (DDM) has been proposed previously by Hardy and Bauer (1991). This methodology includes the definition of the required design data to support both empirical design methods based on rock mass quality (for ambient rock temperature) and analytical/numerical design methods based on rock mass mechanical properties (for thermal- and seismic-induced loading). The geotechnical data collection system implemented for the NRG holes was designed to produce rock structural data, the rock mass properties estimates data, and rock mass quality identified in the DDM. The data collection system was also structured to allow the flexibility to implement other design approaches if deemed appropriate by the Management and Operations (M&O) designers.

Specific types of data collected on each of the NRG holes were:

- ♦ Detailed description of the rock structural characteristics in core;
- ♦ Detailed lithologic logs of the core with identification of stratigraphic and thermomechanical (thermal-mechanical) units;

- ♦ Rock mechanical properties testing consisting of both laboratory measurements and Schmidt hammer rebound hardness logs; and
- ♦ Geophysical and borehole video logs.

The core logs were assembled in a system to produce estimates of rock mass quality using both the Q (Barton et al., 1974) and RMR (Bieniawski, 1979) systems. Figure 3-1 presents a schematic showing the process used to develop the rock mass quality data from core data. Core logging data, core testing data, and field mapping observations were used to develop rock mass quality. The rock mass quality (Q and RMR) data and the rock mechanics testing data were then used to produce estimates of the rock mass mechanical properties based on empirical correlations. The rock mass quality would be utilized directly in empirical design of rock support systems for the North Ramp construction. Rock mass mechanical properties based on RMR and rock mechanics testing would be used in numerical analyses for projecting the impacts of seismic and thermal loads.

Eleven boreholes (NRG-1, -2, -2A, -2B, -2C, -2D, -3, -4, -5, -6, and -7) were drilled along the North Ramp. The average spacing was 400 m (see Figure 1-2, Section 1.0); four of the holes were drilled at the Bow Ridge fault. Drilling depths along the ramp grade varied and not all strata units were sampled by each hole. The North Ramp will be excavated at a -2.05% grade and cross cuts the subhorizontal stratigraphic units at a very low angle. The holes provide a sampling of the vertical variability in rock quality, and to a lesser extent, the horizontal variability. Variability has been characterized by grouping data from all holes for each of the thermomechanical (thermal-mechanical) units. This grouping⁸ was done because previous studies

⁸ See Section 4.0 for discussion of thermomechanical (thermal-mechanical) stratigraphy.

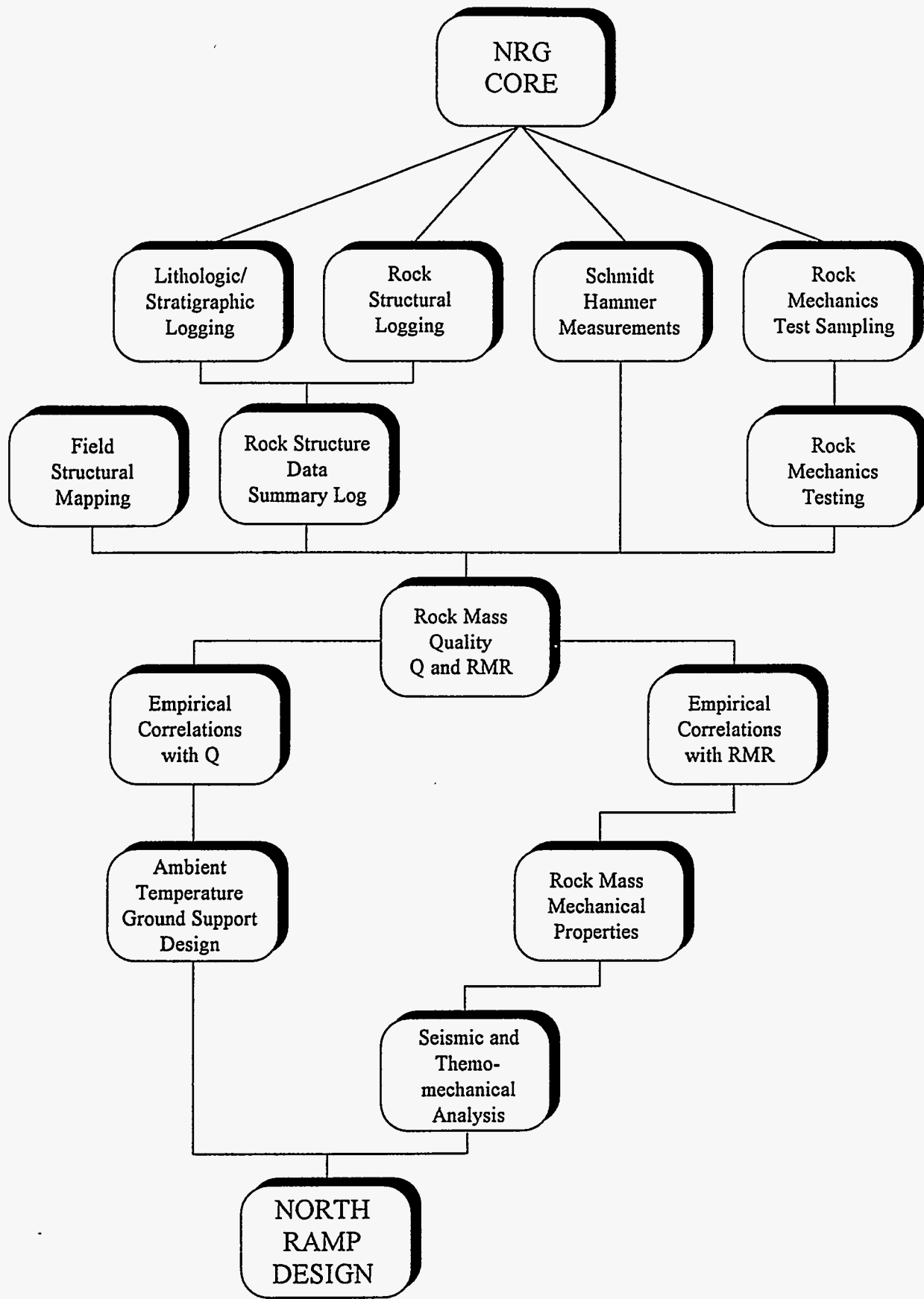


Figure 3-1. Schematic of the Process to Assemble NRG Data for Design of the North Ramp

(Ortiz et al., 1984) at Yucca Mountain have concluded that the degree of welding and porosity of the tuff rocks is the aspect that most affects the physical and mechanical properties. Table 3-1 lists the individual holes, their location, drill depths, and the thermomechanical (thermal-mechanical) units penetrated. The holes are listed with their full title in Table 3-1; however, they will be referred to by their NRG designation throughout the report. Two additional NRG holes, NRG-2C and -2D, were drilled in the North Ramp exploration, but were drilled to sample the nonlithified tuffs of the Rainier Mesa and pre-Rainier Mesa bedded tuffs locally preserved in the hanging wall of the Bow Ridge Fault. NRG-2C and -2D are not discussed here since no intact core was recovered.

Table 3-1. Summary of NRG Drilling Program

Hole	Locations (m)		Total Depth (m)	Cored Interval (m)	Stratigraphic Member Penetrated	Thermomechanical (Thermal-Mechanical) Units Penetrated
	North	East				
UE25 NRG-1	233, 284.14	173, 678.08	46.06	3.32-46.06	Tiva Canyon	TCw
UE25 NRG-2*	233, 407.64	173, 482.71	89.61	0-89.61	Rainier Mesa, Tiva Canyon	UO, TCw
UE25 NRG-2A	233, 388.18	173, 433.64	80.99	24.57-80.99	Tuff "X", Tiva Canyon	UO, TCw
UE25 NRG-2B	233, 408.08	173, 498.70	100.43	0.67-100.43	Rainier Mesa, Tuff "X", Pah Canyon	UO, PTn
UE25 NRG-3**	233, 556.02	173, 224.85	100.58	0-100.58	Tiva Canyon	TCw
UE25 NRG-4	233, 808.89	172, 768.83	221.29	114.3-221.29	Tiva Canyon, Yucca Mtn., Pah Canyon, Topopah Spring	TCw, PTn, TSw1
UE25 NRG-5	234, 055.60	172, 143.95	411.48	210.22-303.55	Tiva Canyon, Yucca Mtn., Pah Canyon, Topopah Spring	TCw, PTn, TSw1, TSw2
USW NRG-6	233, 701.07	171, 966.29	335.28	0-335.28	Tiva Canyon, Yucca Mtn., Pah Canyon, Topopah Spring	TCw, PTn, TSw1, TSw2
USW NRG-7/7A	234, 357.51	171, 599.61	461.29	0-461.29	Tiva Canyon, Yucca Mtn., Pah Canyon, Topopah Spring	TCw, PTn, TSw1, TSw2, TSw3, CHn1

*Azimuth 100.5°, inclined 60.4° down from horizontal.

**Azimuth 98.7°, inclined 59.8° down from horizontal

Drilling records and core marking use units of feet and all rock structural and lithologic logging of the core was therefore performed using the units of feet. The presentations of the NRG Geologic and Rock Structural Logs, Rock Structure Data Summary Logs, Schmidt Hammer Rebound Hardness Logs, and Q and RMR Estimate Logs are therefore in the units of feet in Volume II. In this data summary report, SI units are used.

The types of data that have been generated for the NRG core holes are described here to indicate the scope and variety of information that is available. All core produced in the NRG holes were either HQ or PQ in size and meet ASTM suggestion for the size of core used for determination of RQD (Kirkaldie, 1988). Although the primary objective of the data development was to support North Ramp design, there may be other potential uses for the information for site characterization or performance assessments. The information collected during lithologic logging is described in Section 3.2 and structural logging data is discussed in Section 3.3. The different forms of graphical presentation of the core log data are also described. Rock mechanics testing is discussed in Section 3.4. The process of combining the core log and rock testing data is presented in Section 3.5 and rock mass properties estimation is discussed in Section 3.6.

3.2 Lithologic Logging of the Core

Detailed lithologic logging of the core was performed to describe the character of the tuff rocks penetrated. Observations recorded include:

- mineralogic characteristics,
- degree of welding,
- ♦ lithophysal content,

- ♦ extent of vapor-phase alteration,
- ♦ degree of argillization,
- ♦ degree of devitrification,
- ♦ color, and
- ♦ physical characteristics.

These data are presented in a composite log with the rock structural data. An example of the composite log, Geology and Rock Structure (G&RS) Log, is presented as Figure 3-2.

Stratigraphic identifications are also recorded in the G&RS Log. The borehole logging primarily used the nomenclature of Scott and Bonk (1984), which was based on extensive geologic mapping of Yucca Mountain and outcrop characteristics of the various units. The NRG drilling has proceeded in parallel with work by the USGS to develop a detailed nomenclature based on compositional and other lithologic distinctions that are identified in core.⁹ This report incorporates the new nomenclature, and both the Scott and Bonk (1984) and new USGS nomenclature are provided in the stratigraphic summaries for the individual NRG logs in Volume II. Geology and stratigraphy of the rocks along the ramp are discussed in Section 4.0.

3.3 Rock Structural Logging

A detailed logging system was developed and employed to describe the structural condition of the core. Field logging was performed at the drill site by T&MSS Drilling Management Group personnel using Procedure YLP-SII.2Q-SMF. The field log was then checked in detail against both video records of the core and the core using the instructions presented as Appendix A of this report. Data recorded in this log included:

⁹ Geslin et al.

GEOLOGY AND ROCK STRUCTURE LOG

DEPTH (FT)	CORE			FRACTURES								ROCK QUALITY DESIGNATION-RQD (%)				FRACTURES (PER 10 FT)			HARDNESS	WEATHERING	ESTIMATED % LITHOPHYSAL AND OTHER CAVITIES	Aspiclic Lithoph. Vapor Ph. Devitrification Welding	Geology	LITHOLOGIC DESCRIPTION AND STRATIGRAPHY												
	INTERVAL	% RECOVERY (RUN ROD-%)	LOST CORE & RUBBLE	FRACTURE TYPE	PLANARITY/ROUGHNESS	INFILL THICKNESS AND MINERALS	DIP	INDUCED	PEECE LENGTH	VERY POOR 25	POOR 50	FAIR 75	GOOD 80	EXCELLENT	10	20	30	10							20	30										
	100	(51)			PS	TEN	90							37%	2	(40)				0%																Topopah Spring—Crystal-Rich Nonlithophysal Zone (rounded): (continued)
480.0	RUN 99		X.15																															478.2-489.5 ft, Topopah Spring— Crystal-Rich Upper Lithophysal Zone: Light red-brown, densely welded, devitrified, 12-15% 8:1 flat light-gray pumice, 10% sanidine, plagioclase and biotite phenocrysts, 5% light red-brown lithics to 10 mm, 15% lithophysae in contorted texture that signals top of upper lithophysal zone.		
485.0	69	(36)	X.06											58%	0	(31)					4%													482.0 - 485.0 ft, Transition, quartz latite to rhyolitic composition with dramatic increase in lithophysae and disturbed texture. 485.0-490.0 ft, 10-15% void 488.0 ft, Dark very flattened quartz latite blobs in rhyolitic host - lithics flow with disturbed texture.		
490.0	RUN 100		X.08																															489.5-518.4 ft, Topopah Spring— Crystal Transition Subzones: Light mottled red-gray (10R 8/2), densely welded, devitrified, going from crystal-rich at 489.5 ft with 8-10% phenocrysts to crystal-poor at 518.4 ft with 2-3% phenocrysts. Medium to very large lithophysae with four levels of vapor-phase mineralization haloed: (1) vapor-phase minerals (0.5-2 mm long) coat the interior of lithophysal cavities and have euhedral terminations that project into the cavity; (2) light gray to light pink vapor-phase alteration rims on lithophysae up to 30-mm diameter; (3) light gray rims typically have a thin 1-2 mm reddish purple border (5RP/4-5); (4) very fine-grained blue-hued vapor-phase recrystallization of the groundmass (5RP6/2), up to 10% is pumice with 8:1 flattening; zones of most intense vapor-phase mineralization contain microcrystals of bladed specularite.		
495.0	67	(34)	X.10											41%	0	(17)					9%													499.0 - 506.6 ft, 35-45% is void due to lithophysae		
500.0			X.12																																	

Structure file: NRG7RV6A.STR Lithology file: Data: 06/16/94

WPlog v 4.60

Figure 3-2. Example of the Geology and Rock Structure Log

- ♦ core run interval, run recovery, lost core and rubble zones;
- ♦ location of individual structural features—fractures and vugs;
- ♦ fracture characteristics—type of fracture, inclination, roughness, planarity, mineral infill type, infill thickness, moisture condition and healing;
- ♦ estimated rock hardness and weathering for the run interval;
- ♦ piece lengths greater than or equal to 100 mm (4 inches) in length;
- ♦ rock quality designation (RQD) calculated on the run interval; and
- ♦ percent lithophysal and any other void content for the run interval.

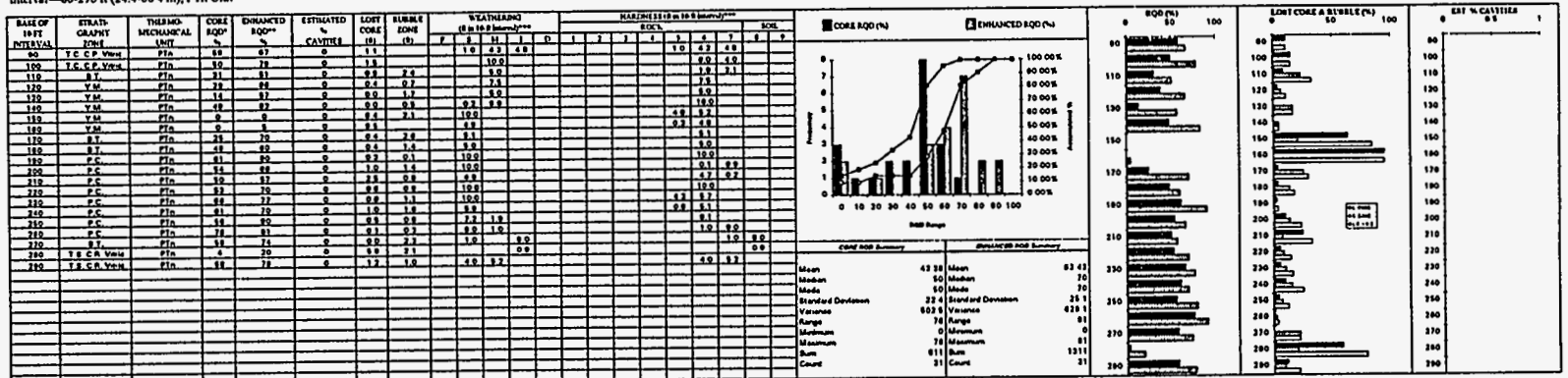
These data were entered into computer files for input to the program WPLOG Version 4.60 which produced the graphical display of the information (G&RS Log). WPLOG is a Windows™ application generated to display core logging data produced for the NRG holes. Copies of the G&RS Log for each NRG hole are presented in Volume II.

The graphical display of the rock structural data is illustrated by Figure 3-2, which shows one page of the G&RS Log for hole NRG-7/7A. In this log, individual data are displayed with abbreviated notation versus depth in the hole. RQD is calculated on an even 3-m (10-ft) interval in addition to the run RQD. Total fractures and natural plus indeterminate fracture are summed for each interval and displayed in the log. The lithophysal content determined on the run intervals are used to calculate length-weighted averages for 3-m (10-ft) intervals.

The rock structural data were summarized on 3-m (10-ft) intervals in a second log called the Rock Structural Data Summary Log, an example of which is shown in Figure 3-3. Individual logs are presented in Volume II. In this log, data on weathering, hardness, and fracture characteristics are sorted within each interval and displayed. The intervals are correlated with

Figure 3-3a. Example of the Rock Structural Summary Log
 Note: Normally Presented in 11" x 17" format.

YUCCA MOUNTAIN SITE CHARACTERIZATION PROJECT
 Core Hole Structural Data Summary
 Hole USW NRG-77A
 Interval—80-290 ft (24.4-88.4 m), Ptn Unit



* CORE RQD - Determined from piece lengths formed by all types of fractures (C, L, N and V)
 ** ENHANCED RQD - Determined by filtering the effects of fractures identified as zoning indicators (Type C) from the piece lengths.
 *** Percentages in bins may not equal 100% because of lost core, rubble, or comminution during logging.

both stratigraphic members and thermomechanical (thermal-mechanical) units. Summary statistics are generated for the RQD parameter.

The sorted data in the Rock Structure Summary Log for 3-m (10-ft) intervals were used to summarize the structural characteristics of the different thermomechanical (thermal-mechanical) units. The distributions of the different parameters are discussed in Section 5.0.

3.4 Rock Mechanical Properties Tests

Rock mechanical properties were measured on NRG core samples selected throughout each hole on approximately 3-m (10-ft) intervals where core conditions allowed. The frequency of sampling was controlled by lost core and rubble zones, which were extensive in some parts of the holes. Sample selection was biased toward the better quality core because of the core condition, however, a conscious attempt was made to include samples containing discrete structural flaws (healed fractures, vapor phase alteration, lithophysae). Results of the individual tests are presented in log form for each NRG hole in Volume II. Table 3-2 lists the number of tests by thermomechanical (thermal-mechanical) unit.

Table 3-2. Numbers of Rock Mechanics Tests Performed on NRG Core for Each Thermomechanical (Thermal-Mechanical) Unit

Test Type	Number of Samples				
	UO (Tuff "X")	TCw	PTn	TSw1	TSw2
Uniaxial Compression	6	56	24	54	53
Triaxial Compression	0	16	0	23	8
Brazilian Tensile	6	44	25	82	51
Elastic Modulus	6	62	24	55	33
Poisson's Ratio	6	62	24	55	33
Dry Bulk Density	12	125	57	136	117
Porosity	15	123	66	190	132
Average Grain Density	11	88	54	100	86

The laboratory tests included measurements of :

- ♦ uniaxial compressive strength;
- ♦ elastic modulus and Poisson's ratio;
- ♦ Brazilian tensile strength;
- ♦ triaxial compressive strength (confining pressures 5, 10 MPa); and
- ♦ dry bulk density, porosity and average grain density.

Experimental procedures utilized in the laboratory tests are described by Martin et al. (1994).

In addition to the laboratory tests, Schmidt Hammer Rebound Hardness was measured on nominal 3-m (10-ft) intervals in each hole. The Schmidt Hammer measurements were used to estimate uniaxial compressive strength using a correlation presented in Stacey and Page (1986).

Mechanical properties data are organized by thermomechanical (thermal-mechanical) unit in Section 6.0.

3.5 Rock Mass Quality

Rock mass quality was determined for the 3-m (10-foot) intervals using both the Q system developed by Barton et al. (1974) and the RMR system developed by Bieniawski (1979). The rock mass quality indices were calculated from data summarized in the Rock Structure Data Summary Log and the rock mechanics testing data. Q and RMR values were displayed in a log format for each 3-m (10-ft) interval and are presented in Volume II. The methodology used to calculate Q and RMR from core log data is described in Appendix B of this report.

The variability of rock mass quality indices are associated with the general rock conditions, excluding the fault zones. Fault zones have not been discretely sampled by the NRG holes, with the exception of NRG-2 and -2B which penetrated the Bow Ridge fault. Characteristics of the fault zones will be variable depending on the amount of displacement and

proximity to surface weathering. Although the range of Q and RMR data may cover fault conditions at the lower end, the data presented describes the rock between the faults. Figure 3-4 presents an example of the Q and RMR estimates presented in spreadsheet format. In the calculation process, any spatial correlation that exists for the rock mass quality parameter may have been preserved in the RMR index because there was generally a direct association between the data in the 3-m (10-ft) interval and the resulting index. Two of the parameters used to calculate Q were not determined from the logging data, they were estimated based on surface mapping and underground mapping in the North Ramp Starter tunnel. For the Q index, the parameters J_n and SRF were generated for each interval by Monte Carlo simulation based on the observed frequency of occurrence in the mapping data or in rock strength in the case of the PTn and UO units. This approach was used to incorporate the observed variability into the Q index; however, it eliminated any spatial correlation of the Q estimate.

The Q and RMR data from all NRG holes were grouped by thermomechanical (thermal-mechanical) unit to characterize the variability in Section 7.0. All data within each thermomechanical (thermal-mechanical) unit were rank ordered and the cumulative frequency of occurrence was calculated to define the distribution of rock mass quality within the unit. Five rock mass quality classes were then defined to characterize the credible variability using frequency of occurrences of 5%, 20%, 40%, 70%, and 90%. Other levels of confidence can be defined depending on the requirements of the design process by using the ranked frequency of occurrence tables in Appendix C.

3.6 Rock Mass Mechanical Properties

Estimates of the rock mass mechanical properties were calculated based on the rock mass quality and laboratory testing data and are presented in Section 8.0. The estimates correspond to the five rock mass quality classes defined by the frequency of occurrence of rock mass quality data and were developed for each thermomechanical (thermal-mechanical) unit. Published correlations between the RMR index and rock mass mechanical properties were utilized according to the approach proposed by Hardy and Bauer (1991). The rock mass properties determined support the application of equivalent-continuum type analysis based upon Mohr-Coulomb failure criteria. The rock mass mechanical properties estimated are:

- ♦ Cohesion,
- ♦ Angle of internal friction,
- ♦ Dilation angle,
- ♦ Elastic modulus,
- ♦ Poisson's ratio, and
- ♦ Power law rock mass strength criteria.

This page left intentionally blank.

4.0 GEOLOGY OF THE NORTH RAMP

4.1 Introduction

The purpose of this section is to provide the geologic and stratigraphic framework for the rocks encountered along the ESF North Ramp alignment. Geologic investigation of the alignment included lithologic analysis of core from NRG-series boreholes and analysis of geologic mapping done by Scott and Bonk (1984). Additionally, extensive work was done to characterize the nonlithified tuffs to be encountered by the ramp in the hanging wall of the Bow Ridge fault and is presented in a separate report.¹⁰

The objective of the geologic investigation of the North Ramp alignment, using the NRG-series boreholes, was to generate data to:

- ♦ Develop geologic and thermomechanical (thermal-mechanical) cross sections along the ramp alignment;
- ♦ Confirm or modify the existing interpretations of major fault blocks; and
- Correlate rock structure data, rock mass quality data, and rock mass properties data with the thermomechanical (thermal-mechanical) and stratigraphic units.

No additional surface mapping has been performed west of ramp station 6+00 m and surface mapping by Scott and Bonk (1984) has not been verified by this study.

4.2 Stratigraphy

The ESF North Ramp alignment passes through rocks of the Miocene Paintbrush and Timber Mountain Groups. The stratigraphic units found along the alignment are part of a thick sequence of bedded and ash-flow tuffs which originated in eruptions of the Timber

¹⁰ Kessel et al.

Mountain-Oasis Valley Caldera Complex to the north of Yucca Mountain between 11 and 14 million years ago (Byers et al., 1976). The Paintbrush Group consists of five distinct ash-flow tuffs separated by thin bedded tuffs. These ash-flow tuffs are, from oldest to youngest, the Topopah Spring Tuff, the Pah Canyon Tuff, the Yucca Mountain Tuff, the Tiva Canyon Tuff, and Tuff Unit "X." Of the Timber Mountain Group, the Rainier Mesa Tuff and a sequence of Pre-Rainier Mesa Tuff bedded tuffs are present along the alignment.

This report uses recently developed stratigraphic nomenclature of the USGS.¹¹ A detailed stratigraphy of the Paintbrush Group has been evolving continuously since the inception of the project, and a variety of nomenclature has been used. Previously, the most widely used nomenclature was that of Scott and Bonk (1984), who based their scheme on extensive geologic mapping of Yucca Mountain and outcrop characteristics of the various units. Recent work by the USGS has modified the stratigraphy by raising the Paintbrush and Timber Mountain Tuffs to group status and by assigning the Tuff Unit "X" of Carr (1992) to the Paintbrush Group (Sawyer et al., 1994). Additionally, a detailed nomenclature based on compositional and other lithologic distinctions identified in core and less on outcrop data has been developed by the USGS.¹²

Core logging by SNL personnel, as part of this study, has used a nomenclature based primarily on that of Scott and Bonk (1984), but has adopted some of the descriptive nomenclature of the USGS as it has developed. Additionally, SNL personnel have used nomenclature for the sequence of locally preserved nonwelded tuffs between the Tiva Canyon and Rainier Mesa Tuffs developed by Carr (1992) and Angell (1994). Because of the greater

¹¹ Geslin et al.

¹² Ibid.

consistency of the recently developed USGS stratigraphy,¹³ it has been adopted for this report and is used in the cross sections. However, the NRG borehole logs, presented in Volume II of this report, include a stratigraphic and thermomechanical (thermal-mechanical) units summary that correlates both the Scott and Bonk (1984) and the new USGS nomenclatures.

A generalized correlation of the schemes of the USGS¹⁴ and of Scott and Bonk (1984) is shown in Table 4-1. Major stratigraphic divisions are shown in bold type, and can be correlated across the columns. Subdivisions within the individual tuff units, however, cannot be directly correlated for all cases. Therefore, the various stratigraphic zones are simply listed side by side for this report.

Stratigraphic and thermomechanical (thermal-mechanical) units that were sampled within the NRG-series boreholes by coring are summarized in Figure 4-1. This chart shows only which units were sampled and contains gaps where units were missing due to fault displacement or were not present. Thickness of the stratigraphic units encountered is given separately in Table 4-2.

Description of the stratigraphic units is presented first for the ash-flow tuffs from oldest to youngest in Section 4.2.1. For ease of description, the intervening bedded tuffs are described separately, in Section 4.2.2.

¹³ Ibid.

¹⁴ Ibid.

Table 4-1.

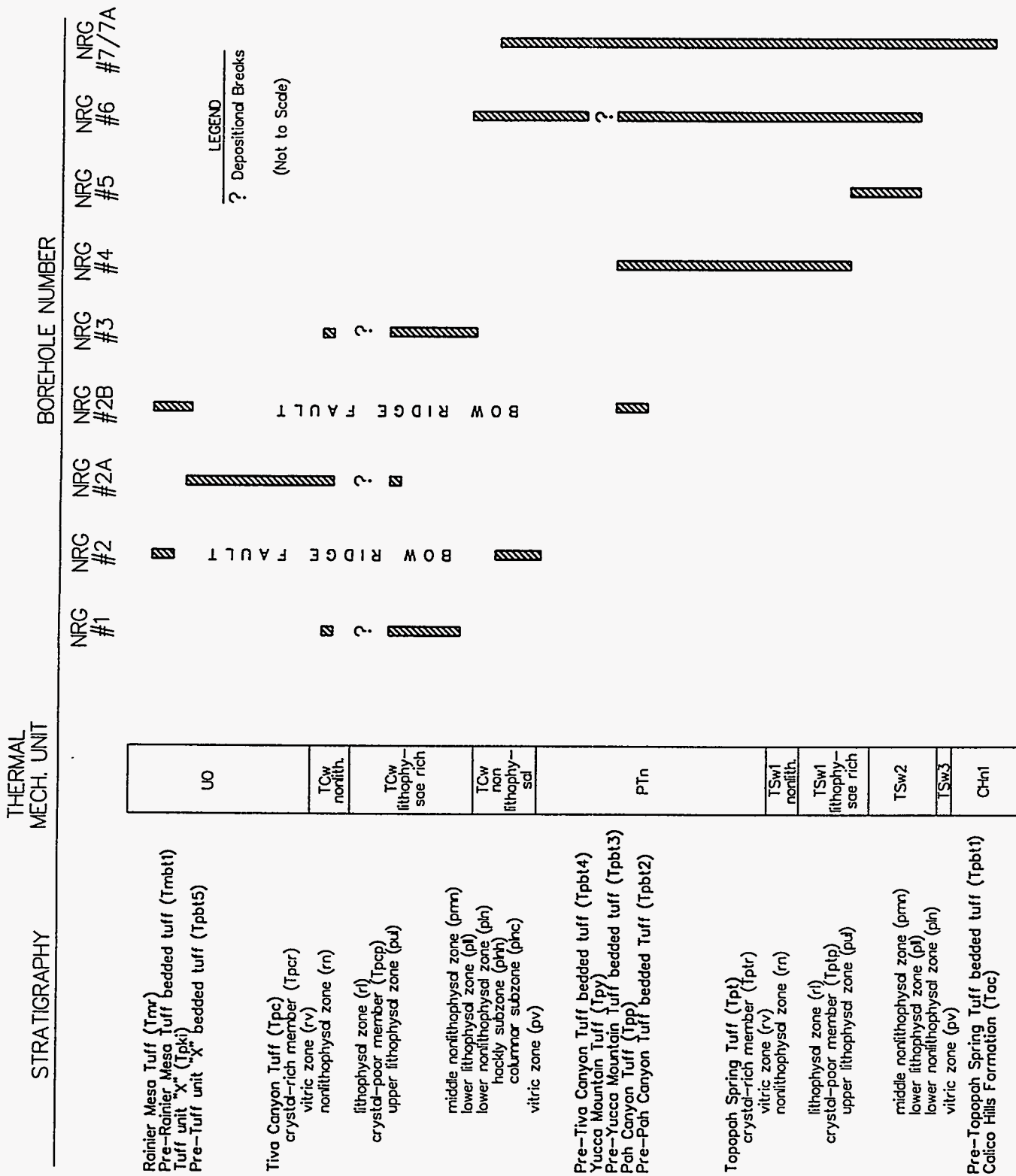
Lithostratigraphic Nomenclature of the Paintbrush Group at Yucca Mountain Nevada (USGS)*		Lithostratigraphic Nomenclature of the Paintbrush Tuff at Yucca Mountain Nevada (Scott and Bonk, 1984)	
Paintbrush Group		Paintbrush Tuff	
Tuff Unit "X"	Tpki		
Pre-Tuff Unit "X" Bedded Tuff	Tpbt5		
Tiva Canyon Tuff	Tpc-	Tiva Canyon Member	
crystal-rich member (quartz latite)	Tpcr	undifferentiated	cu
vitric zone	Tpcrv	caprock zone	ccr
non- to partially welded subzone	Tpcrv3	upper cliff zone	cuc
moderately welded subzone	Tpcrv2	upper lithophysal zone	cul
vitrophyre subzone	Tpcrv1	clinkstone zone	cks
nonlithophysal zone	Tpcrn	lower cliff zone	clc
subvitrophyre transition subzone	Tpcrn4	gray clinkstone zone	cgks
pumice-poor subzone	Tpcrn3	red clinkstone zone	crks
mixed pumice subzone	Tpcrn2	upper clinkstone zone	cuks
crystal transition subzone	Tpcrn1	lower clinkstone zone	cml
lithophysal zone	Tpcrl	middle lithophysal zone	clks
crystal transition subzone	Tpcrl1	rounded step zone	crs
crystal-poor member (high-silica rhyolite)	Tpcp	lower lithophysal zone	cil
upper lithophysal zone	Tpcpul	lower lithophysal & hackly zones undifferentiated	chl
spherulite-rich subzone	Tpcpul1	hackly zone	ch
middle nonlithophysal zone	Tpcpmn	columnar zone	cc
upper subzone	Tpcpmn3		
lithophysae-bearing subzone	Tpcpmn2		
lower subzone	Tpcpmn1		
lower lithophysal zone	Tpcpl1		
lower nonlithophysal zone	Tpcpln		
hackly subzone	Tpcplnh		
columnar subzone	Tpcplnc		
spherulitic pumice interval	Tpcplnc3		
argillic pumice interval	Tpcplnc2		
vitric pumice interval	Tpcplnc1		
vitric zone	Tpcpv		
vitrophyre subzone	Tpcpv3		
moderately welded subzone	Tpcpv2		
non- to partially welded subzone	Tpcpv1		
Pre-Tiva Canyon Tuff Bedded Tuff	Tpbt4	Bedded Tuff	bt

* Jeffrey K. Geslin, Thomas C. Moyer, and David C. Buesch, 1994 in press. *Summary of Lithologic Logging of New and Existing Boreholes at Yucca Mountain, Nevada, August 1993 to February 1994*, U.S. Geological Survey Open-File Report 94-342, U.S. Department of the Interior, Denver, Colorado.

Table 4-1. *continued*

Lithostratigraphic Nomenclature of the Paintbrush Group at Yucca Mountain Nevada (USGS)*		Lithostratigraphic Nomenclature of the Paintbrush Tuff at Yucca Mountain Nevada (Scott and Bonk, 1984)	
Yucca Mountain Tuff	Tpy	Yucca Mountain Member	ym
		undifferentiated ash-flow tuff	ym
		upper zone	ymu
		middle zone	ymm
		lower zone	yml
Pre-Yucca Mountain Tuff Bedded Tuff	Tpbt3	Bedded Tuff	bt
Pah Canyon Tuff	Tpp	Pah Canyon Member	pc
		undifferentiated ash-flow tuff	pc
		upper zone	pcu
		middle zone	pcm
		lower zone	pcl
Pre-Pah Canyon Tuff Bedded Tuff	Tpbt2	Bedded Tuff	bt
Topopah Spring Tuff	Tpt-	Topopah Spring Member	
crystal-rich member (quartz latite)	Tptr	undifferentiated	tu
vitric zone	Tptrv	caprock zone	tc
non- to partially welded subzone	Tptrv3	rounded zone	tr
moderately welded subzone	Tptrv2	thin lithophysal zone	ttl
vitrophyre subzone	Tptrv3	red lithophysal zone	trl
nonlithophysal zone	Tptrn	upper lithophysal zone	tul
lithophysal zone	Tptrl	lower lithophysal zone	tll
crystal-rich lithophysal subzone	Tptrl2	lithophysal zone	tl
crystal transition subzone	Tptrl1	nonlithophysal zone	tnl
crystal-poor member (high-silica rhyolite)	Tptp	gray nonlithophysal zone	tgnl
upper lithophysal zone	Tptpul	orange zone	to
cavernous lithophysae subzone	Tptpul2	brick zone	tb
small lithophysae subzone	Tptpul1	orange brick zone	tob
middle nonlithophysal zone	Tptpmn	orange brick lithophysal zone	tobl
upper subzone	Tptpmn3	brownish-orange brick zone	tbob
lithophysae-bearing subzone	Tptpmn2	grayish-red lithophysal zone	tgrl
lower subzone	Tptpmn1	orangish-red lithophysal zone	torl
lower lithophysal zone	Tptpll	mottled lithophysal zone	tml
lower nonlithophysal zone	Tptpln	purplish-brown lithophysal	tpbl
vitric zone	Tptpv	reddish brown brick zone	trbb
vitrophyre subzone	Tptpv3	brownish-orange lithophysal zone	tbol
moderately welded subzone	Tptpv2	mottled zone	tm
non- to partially welded subzone	Tptpv1	vitrophyre zone	tv
		partially welded zone	tpw
Pre-Topopah Spring Bedded Tuff	Tpbt1	Bedded Tuff	bt

* Ibid.



LEGEND
? Depositional Breaks
(Not to Scale)

BOW RIDGE FAULT

Figure 4-1. Lithostratigraphic and Thermomechanical Units Sampled by Cored Intervals of NRG Boreholes (See Figure 4-2 for the Borehole Locations)

Table 4-2. Unit Thickness of NRG-Series Boreholes (meters)

Stratigraphic Unit	Symbol	NRG-1	NRG-2	NRG-2A	NRG-2B	NRG-3	NRG-4	NRG-5	NRG-6	NRG-7/7A
Timber Mountain Group:										
Rainier Mesa Tuff	Tmr		36.6*		35.7*					
Pre-Rainier Mesa Bedded Tuff	Tmbt1		6.9*		11.6					
Paintbrush Group:										
Tuff Unit "X"	Tpki		F	21.5*	22.9					
Pre-Tuff Unit "X" Bedded Tuff	Tpbt5		F	4.5	F					
Tiva Canyon Tuff	Tpc-									
crystal-rich member (quartz latite)	Tpcr-									
vitric zone	Tpcrv		F	1.9	F					
nonlithophysal zone	Tpcrn	6.4*	F	27.3	F	26.4*				
lithophysal zone	Tpcrl	NP	F	NP	F	NP				
crystal-poor member (high-silica rhyolite)	Tpcp-									
upper lithophysal zone	Tpcpul	23.6	F	1.3*	F	28.2				
middle nonlithophysal zone	Tpcpmn	12.8*	F		F	16.2				
lower lithophysal zone	Tpcpll		F		F	16.3*			16.8*	
lower nonlithophysal zone	Tpcpln		28.1*		F				24.5	21.2*
vitric zone	Tpcpv		4.7*		F				7.1	10.1
Pre-Tiva Canyon Tuff Bedded Tuff	Tpbt4				F				1.3	1.1
Yucca Mountain Tuff	Tpy				F				NP	15.7
Pre-Yucca Mountain Tuff Bedded Tuff	Tpbt3				7.7*		1.8*		3.7	5.5
Pah Canyon Tuff	Tpp				11.8		23.5		14	25.2
Pre-Pah Canyon Tuff Bedded Tuff	Tpbt2				1.7*		3.1		7.9	6.5
Topopah Spring Tuff	Tpt-									
crystal-rich member (quartz latite)	Tptr-									
vitric zone	Tptrv						6.3		5	6.2
nonlithophysal zone	Tptrn						52.3		50.5	54.2
lithophysal zone	Tptrl						15.1		11.1	12.3
crystal-poor member (high-silica rhyolite)	Tptp-									
upper lithophysal zone	Tptpul						4.9*	21.4	75.4	76.2
middle nonlithophysal zone	Tptpmn							32.2	29.6	33.3
lower lithophysal zone	Tptpll							28.8*	88.4	107
lower nonlithophysal zone	Tptpln									56.8
vitric zone	Tptpv									23.8
Pre-Topopah Spring Bedded Tuff	Tpbt1									1.5

*Denotes thickness of unit penetrated by borehole where both contacts are not present.
 NP = Unit not present.
 F = Unit not present due to fault displacement.

Boreholes NRG-2 and NRG-3 drilled at 30° from vertical. Thicknesses given are adjusted to vertical. Remainder of boreholes drilled vertically. Boreholes not adjusted for strike and dip of stratigraphic units.

4.2.1 Ash-flow Tuffs

Calico Hills Formation — 4.69 m (15.4 ft) of this unit was penetrated by one of the NRG-series boreholes, NRG-7/7A. At this location the unit is characterized by an upper pyroclastic flow deposit underlain by a fallout deposit. Both deposits are nonwelded and contain zeolitic alteration.

Paintbrush Group

- Topopah Spring Tuff — The Topopah Spring Tuff is a multiple-flow, compound cooling unit, ash-flow tuff consisting of three eruptive pulses (Lipman et al., 1966). This unit has been divided into a lower crystal-poor unit (high-silica rhyolite) and an upper crystal-rich unit (quartz latite).¹⁵ Thickness for the unit is 390.1 m (1280 ft) at NRG-7/7A. The unit is characterized by thin zones at the top and bottom where the nonwelded tuffs grade into moderately to densely welded vitrophyre zones. The thick middle portion of the flow is moderately to densely welded, devitrified, and commonly altered by vapor phase mineralization.

Lithophysal cavities vary throughout and break the unit into a number of distinct zones which help define the thermomechanical (thermal-mechanical) stratigraphy for this unit and are discussed further in Section 4.4. The basal vitric zone is nonlithophysal, forming the lowermost zone. This is overlain by a sequence of mixed nonlithophysal and lithophysal zones, including the lower lithophysal zone and a lithophysal bearing subzone in the middle nonlithophysal zone. The proposed repository horizon is within the middle nonlithophysal zone which typically contains less than 2% lithophysal cavities by volume. The next

¹⁵ Ibid.

distinct lithophysal horizon includes the crystal-poor upper lithophysal zone and the crystal-rich lithophysal zone with cavities up to 10%–25% by volume. Within this interval, a lithophysae subzone occurs which is characterized by rubblized core and large oblate lithophysae which are commonly larger than the core diameter. Finally, the top portion of the unit contains the crystal-rich nonlithophysal zone and the crystal-rich vitric zone, which is largely nonlithophysal.

Colors for the Topopah Spring Tuff matrix are highly variable and typically includes hues of very light gray, grayish orange-pink, light reddish gray, and grayish pink for the devitrified zones, and dark reddish-brown to grayish black for the vitrophyres. Phenocrysts range from less than 3% for the lower crystal-poor member and up to 10%–12% phenocrysts of feldspars, quartz and biotite in the crystal-rich member.

- Pah Canyon and Yucca Mountain Tuffs — The Pah Canyon and Yucca Mountain Tuffs are both nonwelded ash flows that form a significant break in the otherwise moderately to densely welded Paintbrush Group. The Pah Canyon ranges in thickness from 0 to about 23 m (75.5 ft), and in color from grayish orange-pink to grayish orange. It generally contains several percent up to 15% phenocrysts of feldspar, biotite and clinopyroxene, up to 30% pumice clasts, and traces of volcanic lithics. The Yucca Mountain Tuff is from 0 to 16 m (52.5 ft) in thickness and is characteristically a uniform, shard-rich tuff with very low percentages of phenocrysts and a medium light gray to grayish orange-pink color.

- ◆ Tiva Canyon Tuff — The Tiva Canyon Tuff is a compound cooling unit, ash-flow tuff which forms the vast majority of surface outcrops at Yucca Mountain. None of the NRG-series boreholes penetrates the entire unit; however, a combination of the logs from NRG-2A and NRG-6 indicate a thickness of greater than 60 m (196.8 ft) along the ramp alignment. The Tiva Canyon Tuff is similar to the Topopah Spring Tuff in compositional zoning and post-emplacement alteration. With the exception of non- to partially welded tuffs found along the chilled margins, the unit is almost entirely densely welded and devitrified, and exhibits poorly to well developed eutaxitic foliation. The Tiva Canyon Tuff does have glass-shard-rich vitric zones along the margins, but does not exhibit the well developed vitrophyres found within the Topopah Spring Tuff.

Colors for the Tiva Canyon Tuff matrix are variable and typically include hues of very light gray, grayish orange-pink, light reddish gray, and grayish pink. This unit contains a lower, crystal-poor, high-silica rhyolite zone characterized by less than 5% pumice clasts and less than 2% phenocrysts. Above this is an upper, crystal-rich, quartz latite zone with pumice clasts typically 10%–15% and phenocrysts of feldspar, clinopyroxene and biotite 10%–12%. Lithophysae and spherulites are common within certain portions of the unit, particularly within an interval in the center of the flow including the lower lithophysal, middle nonlithophysal, and upper lithophysal zones of the crystal-poor member and the lithophysal zone of the crystal-rich member.

- ♦ Tuff Unit "X" — Tuff Unit "X" is a nonwelded ash flow preserved locally in the hanging wall block of the Bow Ridge fault and buried beneath alluvium in Midway Valley (Carr, 1992). Exposures of this unit in excavations for the North Portal Duct Bank were examined by Angell (1994). This unit is generally well lithified, nonwelded, massively bedded, and poorly sorted. Color is typically very light yellowish gray, with vitric pumice comprising 30%–50% of the rock, and volcanic lithics 7%–10%. Accessory minerals include quartz, biotite, hornblende, and sphene. Zeolitic alteration is common and gives the rock its characteristic yellow hue, but is not found everywhere within the unit.

Timber Mountain Group

- ♦ Rainier Mesa Tuff — The Rainier Mesa Tuff is a nonwelded ash-flow tuff locally preserved within the hanging wall block of the Bow Ridge fault along the ramp alignment. Limited surface outcrops of this unit are found along the west side of Exile Hill.

An upper lithified and a lower nonlithified (soil-like) zone are distinguished largely by the degree of cementation. Unweathered color ranges from very light pinkish orange and grayish orange pink to very light gray, with the lighter tones predominating in the nonlithified zone. Lithologically, the zones are similar, with pumice fragments ranging from <1 to 20 mm, and phenocrysts of feldspars, quartz, and bronze biotite forming 15%–20% of the rock. A more detailed description of this unit is given by Angell (1994).

4.2.2 Bedded Tuffs

Bedded tuffs are found separating all of the ash-flow units of the Paintbrush and Timber Mountain Groups. These tuffs are typically nonwelded and are nonlithified to moderately lithified. They range from 0–10 m (32.8 ft) in thickness and contain a variety of ash-flow and ash-fall deposits, with minor reworked tuffaceous sandstones. Five of these bedded tuffs are recognized within the Paintbrush Group, and an additional one is found at the base of the Rainier Mesa Tuff. The convention used in naming these units is to assign them to the overlying major ash-flow unit. For example, the lowermost Paintbrush Group bedded tuff underlies the Topopah Spring Tuff and is named the Pre-Topopah Spring Tuff Bedded Tuff (Tpbt1). The remainder of the units are, in ascending order, the Pre-Pah Canyon Tuff Bedded Tuff (Tpbt2), the Pre-Yucca Mountain Tuff Bedded Tuff (Tpbt3), the Pre-Tiva Canyon Tuff Bedded Tuff (Tpbt4), the Pre-Tuff Unit “X” Bedded Tuff (Tpbt5), and within the Timber Mountain Group, the Pre-Rainier Mesa Tuff Bedded Tuff (Tmbt1).

In composition, the bedded tuffs vary considerably, ranging from very light gray to grayish orange in color, and having variable amounts and types of phenocrysts and volcanic lithics. Weakly-developed paleosol horizons are found in some areas, and a variety of ash-flow, ash-fall, and reworked subunits are observed to vary considerably over short lateral distances. Detailed descriptions of the nonlithified Pre-Tuff Unit “X” Bedded Tuffs and Pre-Rainier Mesa Tuff Bedded Tuffs is given by Angell (1994) and engineering characteristics of the nonlithified tuffs are reported¹⁶ to support design of the North Ramp. Further detailed research for these units on an area-wide basis is provided by Diehl and Chornack (1990).

¹⁶ Kessel et al.

4.3 Geologic Cross Sections

Geologic cross sections were developed to project the stratigraphic and thermo-mechanical (thermal-mechanical) contacts along the ramp alignment. The cross sections were based on previous (Scott and Bonk, 1984) and on-going¹⁷ site geologic studies by the USGS. NRG drilling was performed to verify stratigraphic depths in some, but not all, of the blocks between the identified faults. The holes were projected into the North Ramp cross sections along the strike of the stratigraphic units. Adjustments were made where the previous projections did not agree with the local drilling data.

The geologic cross sections, based on drilling and surface mapping data, are presented in Section 4.3.1. In general, surface mapping was available to help constrain the fault locations and the amount of dip separation across faults. Some uncertainty was apparent in the area of Daylight Valley, immediately west of the Bow Ridge fault, where the alluvial cover masked potential, undetected faults whose presence was inferred by surface gravity data. A high resolution surface seismic study¹⁸ was therefore performed in an attempt to define the depth of alluvium and/or nonlithified tuffs and to detect any fault offsets. The interpretation of the seismic data suggests two additional faults with displacements sufficient to increase the distance that the North Ramp will be constructed through the nonwelded Tuff Unit "X" and the nonlithified Pre-Tuff Unit "X" Bedded Tuff. The seismic interpretation is discussed in Section 4.3.2. Projected stations where the North Ramp will intersect the various tuff units are discussed in Section 4.3.3.

¹⁷ L.R. Hayes, 1993. Letter to J. Russell Dryer, Acting Project Manager, U.S. Department of Energy, re: 2-D Geologic Model of North Ramp, U.S. Geological Survey.

¹⁸ Elbring.

4.3.1 Drilling and Surface Mapping Data

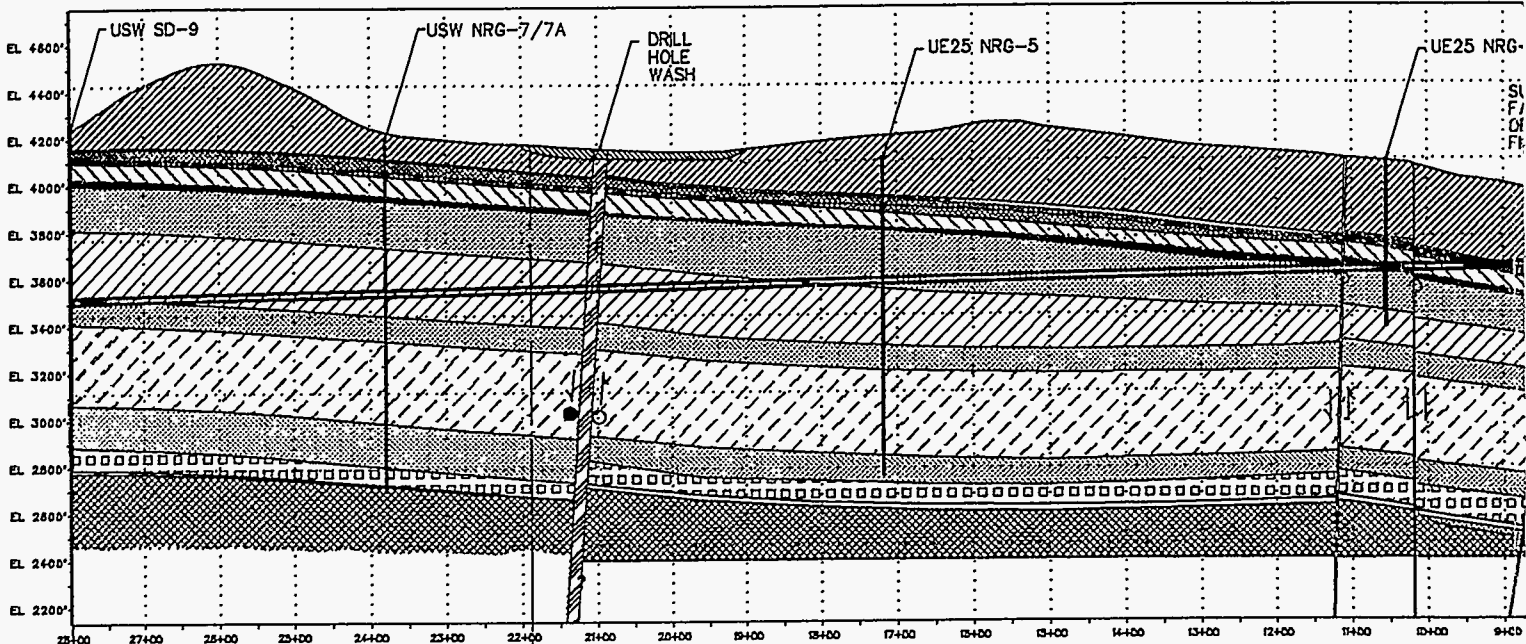
The North Ramp of the Exploratory Studies Facility (ESF) at Yucca Mountain will descend from the east side of the mountain through most of the Miocene Paintbrush Group. The location of the North Ramp and the NRG-series boreholes is shown in Figure 1-2, Section 1.0. A geologic cross section based on borehole and surface mapping data showing the rocks to be penetrated is presented in Figure 4-2. Additionally, a geologic cross section through Exile Hill (ramp station 0+00 to 6+00 m) is presented in Figure 4-3 which shows the area around the Bow Ridge fault zone and the North Portal at an enlarged scale. An alternative interpretation based on the seismic data is discussed in Section 4.3.2.

The start of the ramp can be seen most clearly in Figure 4-3. The North Portal has been constructed in welded rock of the Tiva Canyon Tuff. The ramp will proceed through welded rocks of the Tiva Canyon Tuff for 196 m where it will intersect the Bow Ridge fault zone. Based on the projection of borehole data, the ramp will then penetrate the lowermost nonwelded portion of the Rainier Mesa Tuff and continue down-section through a sequence of Pre-Rainier Mesa Bedded Tuffs. These tuffs are nonlithified and present an off-normal condition for ramp construction. Geologic and engineering characterization of the nonlithified tuff interval for ramp design is presented by Kessel et al.¹⁹ The ramp then intersects Tuff Unit "X," and the nonlithified Pre-Tuff Unit "X" Bedded Tuffs before re-entering the Tiva Canyon Tuff. Uncertainty about the length of the Tuff Unit "X" and Pre-Tuff Unit "X" in the section is discussed in Section 4.3.2.

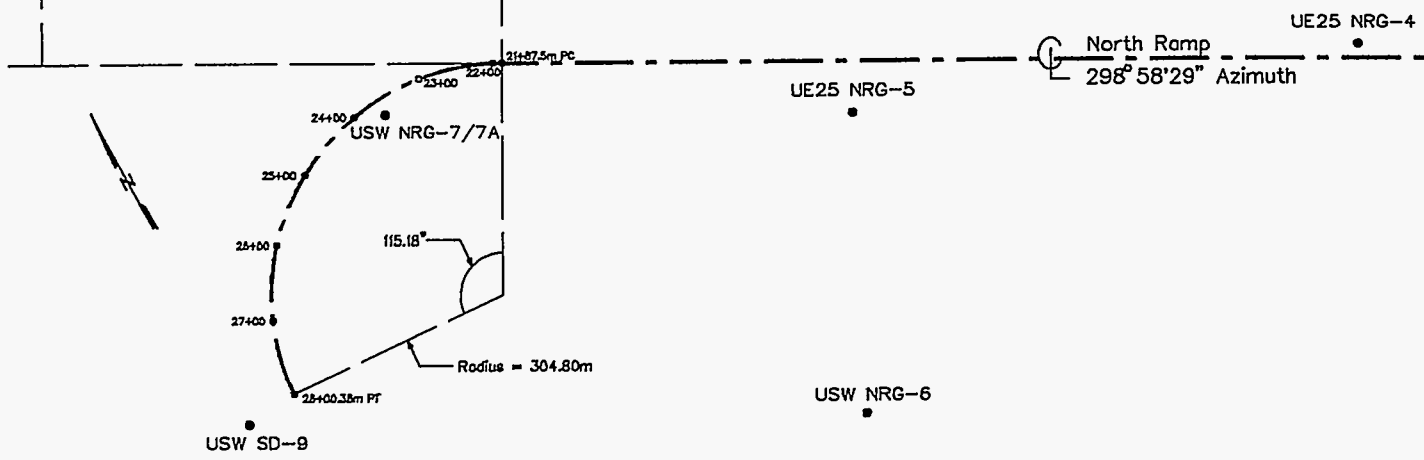
The continuation of the ramp can be seen in Figure 4-2. As the tunnel proceeds to the west, it will then continue down-section through most of the Paintbrush Group, encountering the

¹⁹ Kessel et al.

SECTION VIEW



PLAN VIEW



E:171280
 E:171804
 N:234394
 E:171909
 E:172214
 N:234089
 E:172519
 N:233784
 E:172823

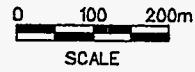
PRELIMINARY RAMP DATA QA:NA

Station (m)	Grade	State Plane Coord. (m) Northing	State Plane Coord. (m) Easting	Elevation (m)
0+00 (Partial)	-2.06%	233280.0	173078.0	1122.55
21+87.5 (PC)		234338.4	171788.8	1079.79
22+00		234315.2	171755.5	1079.53
23+00		234374.7	171860.5	1077.48
24+00		234372.0	171881.0	1075.43
25+00		234337.3	171487.7	1073.38
26+00		234274.5	171380.8	1071.33
27+00		234190.2	171357.7	1069.28
28+00.38 (PT)		234092.9	171314.8	1067.22

2 Reference Drwg. SS-N-SK028.DGN and verbal communication from N-K; December, 1993.

BOREHOLE

Borehole	Project Section Azim
UE25 NRG-1	N
UE25 NRG-2	181
UE25 NRG-2A	181
UE25 NRG-2B	181
UE25 NRG-2C	181
UE25 NRG-2D	181
UE25 NRG-3	21
UE25 NRG-4	21
UE25 NRG-5	3
USW NRG-7/7A	0.1
RF#8	
USW SD-9 ³	84

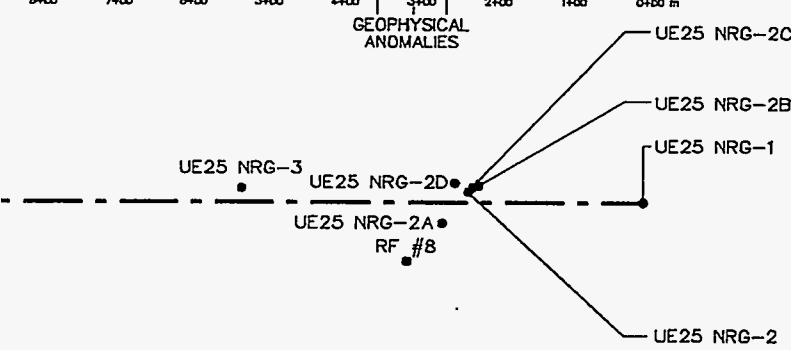
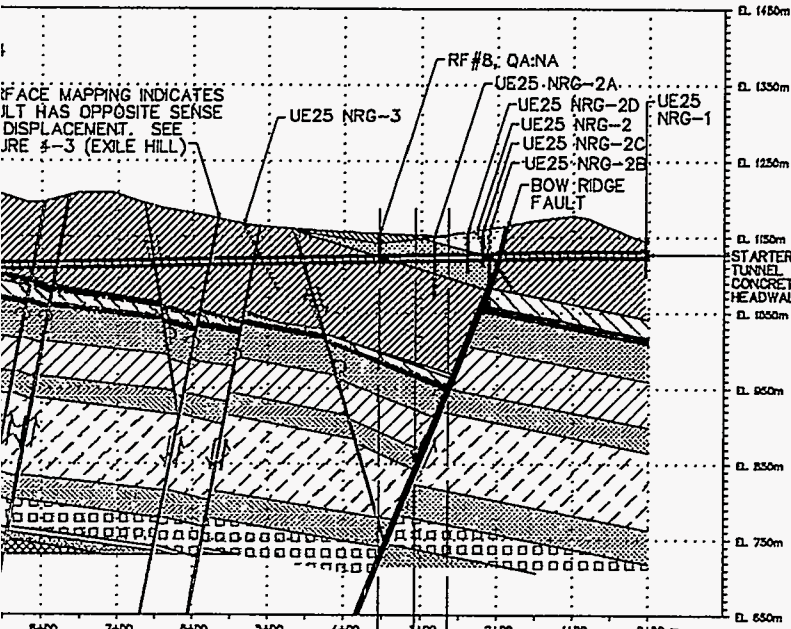


SYMBOLS

GROUP	FORMATION	INFORMAL UNITS	THERMO-MECHANICAL UNITS
TIMBER MOUNTAIN TUFF	RAINIER MESA	Qac: Alluvium	UO
	?	Tmr: Rainier Mesa Tuff	
		Tmbt1: pre-Rainier Mesa Tuff bedded tuff	
		Tpki: tuff unit "X"	
		Tpbt5: pre-tuff unit "X" bedded tuff	
TIVA CANYON		Tpc: Tiva Canyon Tuff	TCw
		Tpbt4: pre-Tiva Canyon Tuff bedded tuff	
YUCCA MTN		Tpy: Yucca Mountain Tuff	PTn
		Tpbt3: pre-Yucca Mountain Tuff bedded tuff	
PAH CANYON		Tpp: Pah Canyon Tuff	TSw1
		Tpbt2: pre-Pah Canyon Tuff bedded tuff	
		Tptrc: Crystal-rich nonlithophysal crystal-rich vitric zone	
TOPOPAH SPRING		Tptpl: Lower Lithophysal crystal-poor	TSw2
		Tptprn: Middle Nonlithophysal crystal-poor	
		Tptpv: Vitric vitrophyre and non welded subzones	
		Tpbt1: pre-Topopah Spring Tuff bedded tuff	
CALICO HILLS		Tact: Calico Hills lava flow	TSw3
		Tacb: Calico Hills bedded tuff	

STRATIGRAPHIC NOMENCLATURE DEVELOPED BY USGS

- DRILL HOLE WASH FAULT ZONE, LOCATION AND ATTITUDE UNCERTAIN
- BOW RIDGE FAULT ZONE
- MINOR FAULT, ? - ATTITUDE UNCERTAIN
- PROPOSED NORTH RAMP ALIGNMENT
- APPROXIMATE
- STRIKE-SLIP SEPARATION INTO PAGE
- STRIKE-SLIP SEPARATION OUT OF PAGE



PROJECTIONS QA:L

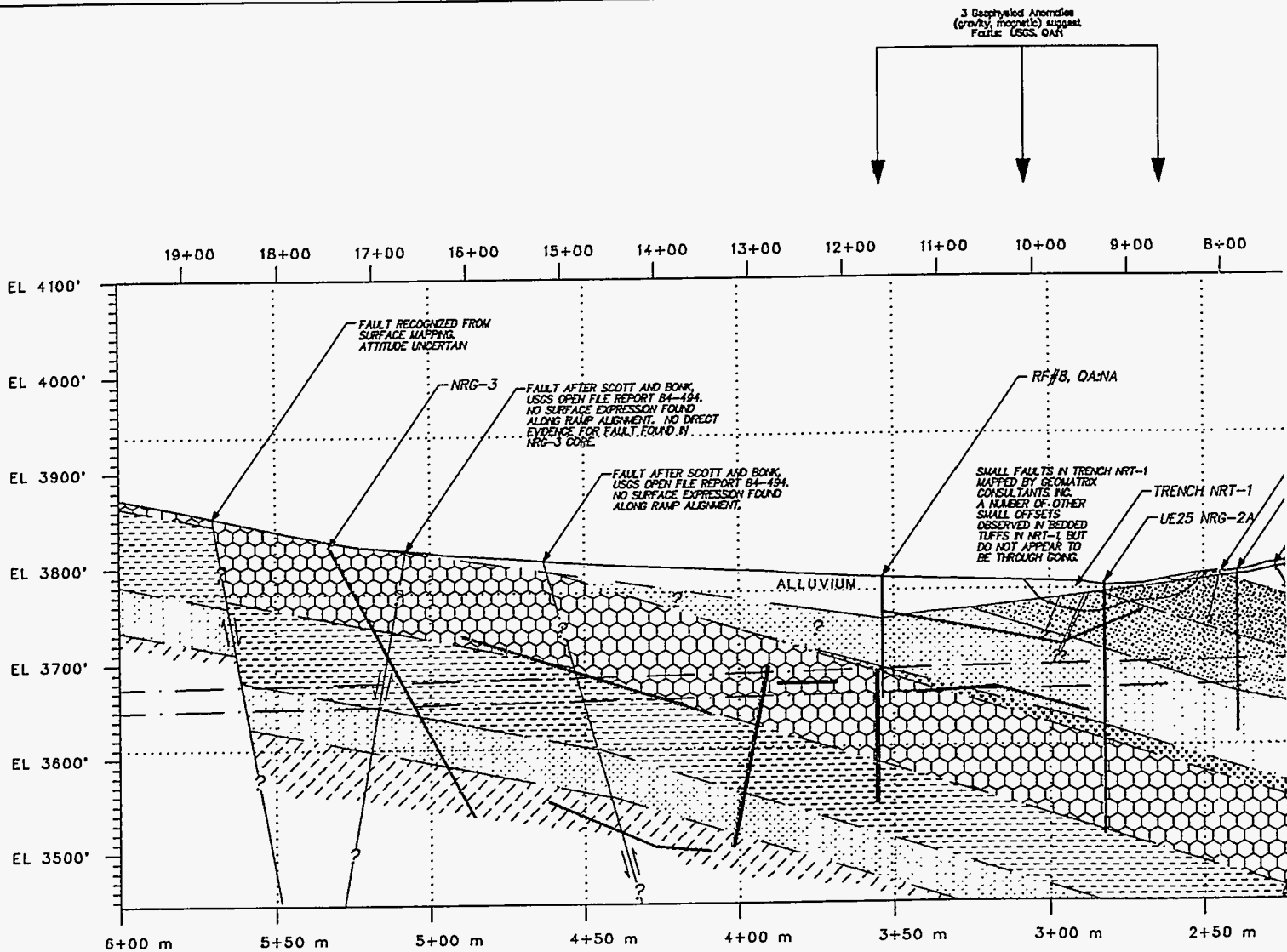
to	Ground Elevation (m)	Distance to Section (m)
ong	1144.05	0.0
	1157.23	15.20
	1152.31	30.85
	1158.87	24.05
	1158.80	22.34
	1155.82	28.86
	1185.35	20.20
	1249.82	18.52
	1251.71	68.44
	1282.78	22.05
	1154.55	86.52
	1302.28	72.60

Note: Boreholes projected into cross section along strike of rock units
 NP - Not projected
³ USW SD-9 Projected approximately down-dip to nearest point on cross section

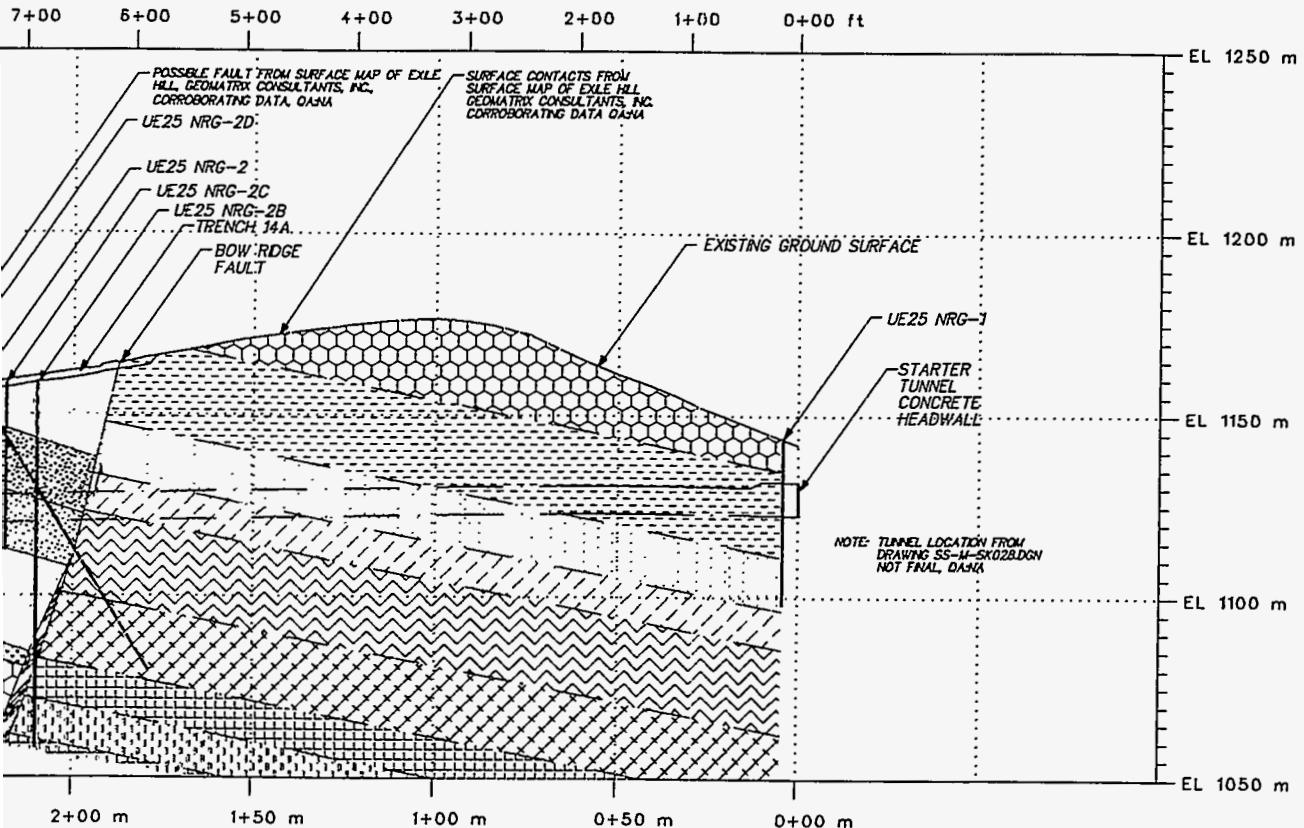
REFERENCE:
 DRAWING NO. 88-60-09
 VERSION QA:L7

QA:L

Figure 4-2. North Ramp Cross Section



GROUP	FORMATION	MAJOR ZONES	FURTHER DESCRIPTION	
TIMBER MOUNTAIN GROUP	RAINIER MESA TUFF		LITHIFIED, NONWELDED	
			NONLITHIFIED, TUFF AND FALLOUT	
	?		PRE-RAINIER MESA TUFF BEDDED TUFF	NONLITHIFIED, TUFF AND FALLOUT
			TUFF UNIT "X"	NONWELDED PYROCLASTIC FLOW AND FALLOUT
			PRE-TUFF UNIT "X" BEDDED TUFF	NONLITHIFIED, REWORKED PYROCLASTIC FLOW AND FALLOUT
PAINTBRUSH GROUP	TIVA CANYON TUFF		CRYSTAL-RICH VITRIC AND NONLITHOPHYSAL ZONES	NONWELDED TO DENSELY WELDED
			CRYSTAL-POOR UPPER LITHOPHYSAL ZONE	DENSELY WELDED
			CRYSTAL-POOR MIDDLE NONLITHOPHYSAL ZONE	DENSELY WELDED
			CRYSTAL-POOR LOWER LITHOPHYSAL ZONE	DENSELY WELDED
			CRYSTAL-POOR LOWER NONLITHOPHYSAL ZONE	DENSELY WELDED
			CRYSTAL-POOR VITRIC ZONE	DENSELY WELDED
			PRE-TIVA CANYON TUFF BEDDED TUFF	NONWELDED
	PAH CANYON TUFF		NONWELDED	NONWELDED
		PRE-PAH CANYON TUFF BEDDED TUFF	NONWELDED	



LEGEND

- LITHOLOGIC CONTACT, SOLID LINE WHERE APPROXIMATE, DASHED LINE WHERE INFERRED
- FAULT ZONE
- FAULT, ?-ATTITUDE UNCERTAIN
- PROPOSED TUNNEL OUTLINE
- POSSIBLE FAULTS IDENTIFIED BY REFLECTION SEISMIC TECHNIQUES, SAND94-2374
- IDENTIFIED SEISMIC REFLECTORS, SAND94-2374

Borehole	Projected to Section along Azimuth	Ground Elevation (m)	Distances to Section (m)
UE25 NRG-1	NP	1144.05	0.0
UE25 NRG-2	182°	1157.23	15.20
UE25 NRG-2A	2°	1152.31	30.85
UE25 NRG-2B	182°	1158.87	24.05
UE25 NRG-2C	182°	1158.60	22.34
UE25 NRG-2D	182°	1155.82	28.86
UE25 NRG-3	211°	1165.35	20.20
RF #8	2°	1154.55	86.52

Note: Boreholes projected into cross section along strike of rock units

NP - Not projected

REFERENCE:
DRAWING NO. 88-60-08
VERSION QA1.5
QA:L

CROSS SECTION CONSTRUCTED ALONG RAMP ALIGNMENT - AZIMUTH 299°

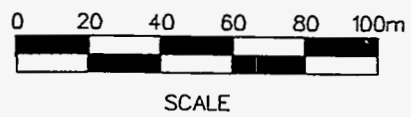


Figure 4-3. Exile Hill Cross Section

Tiva Canyon, Yucca Mountain and Pah Canyon Tuffs, and ending in the crystal-poor middle nonlithophysal unit of the Topopah Spring Tuff where it intersects the Topopah Spring level main drift. The approximate ramp station coordinates at which the stratigraphic contacts are projected are listed in Table 4-3. The coordinates listed are where the contact crosses the ramp centerline and are not necessarily the first point of contact by the TBM bore.

Table 4-3. Projected Ramp Station Coordinates at Stratigraphic Contacts Along North Ramp Alignment Tunnel Centerline

Stratigraphic Unit	Projected Ramp Station (m)**	Projected Distance in Unit (m)**
Tiva Canyon Tuff (Tpc)	0+00	196
Rainier Mesa Tuff (Tmr)	1+96	13
Tuff Unit "X" (Tpki)	2+09	136 to 226
Tiva Canyon Tuff (Tpc)*	3+45 to 4+35	455 to 545
Pre-Tiva Canyon Tuff Bedded Tuff (Tpbt4)	8+90	<10
Yucca Mountain Tuff (Tpy)	9+00	20
Pre-Yucca Mountain Tuff Bedded Tuff (Tpbt3)	9+20	25
Pah Canyon Bedded Tuff (Tpbt)	9+45	83
Pre-Pah Canyon Tuff Bedded Tuff	10+28	34
Topopah Spring Tuff (Tpt):		
Crystal-rich nonlithophysal zone, crystal-rich vitric zone (Tptm)	10+62	754
Crystal-rich upper nonlithophysal and crystal-poor upper lithophysal zones (Tpul)	18+16	947
Crystal-poor middle nonlithophysal zone (Tptpmn)	27+63	37

*Range reflects uncertainty due to possible faults under Daylight Valley. Range given is where tunnel roof intersects contact. All other values listed are where ramp centerline intersects contact.

**Horizontal distance along centerline.

4.3.2 Seismic Interpretation in Daylight Valley

Seismic refraction and reflection lines were run in Daylight Valley to investigate uncertainties in the stratigraphy in the hanging wall block of the Bow Ridge fault and the potential for undetected structures beneath the alluvial cover. Description of the seismic work is presented by Elbring.²⁰ Three high-resolution seismic lines were run in close proximity to the ramp alignment as shown in Figure 4-4. The first line used both reflection and refraction

²⁰ Elbring.

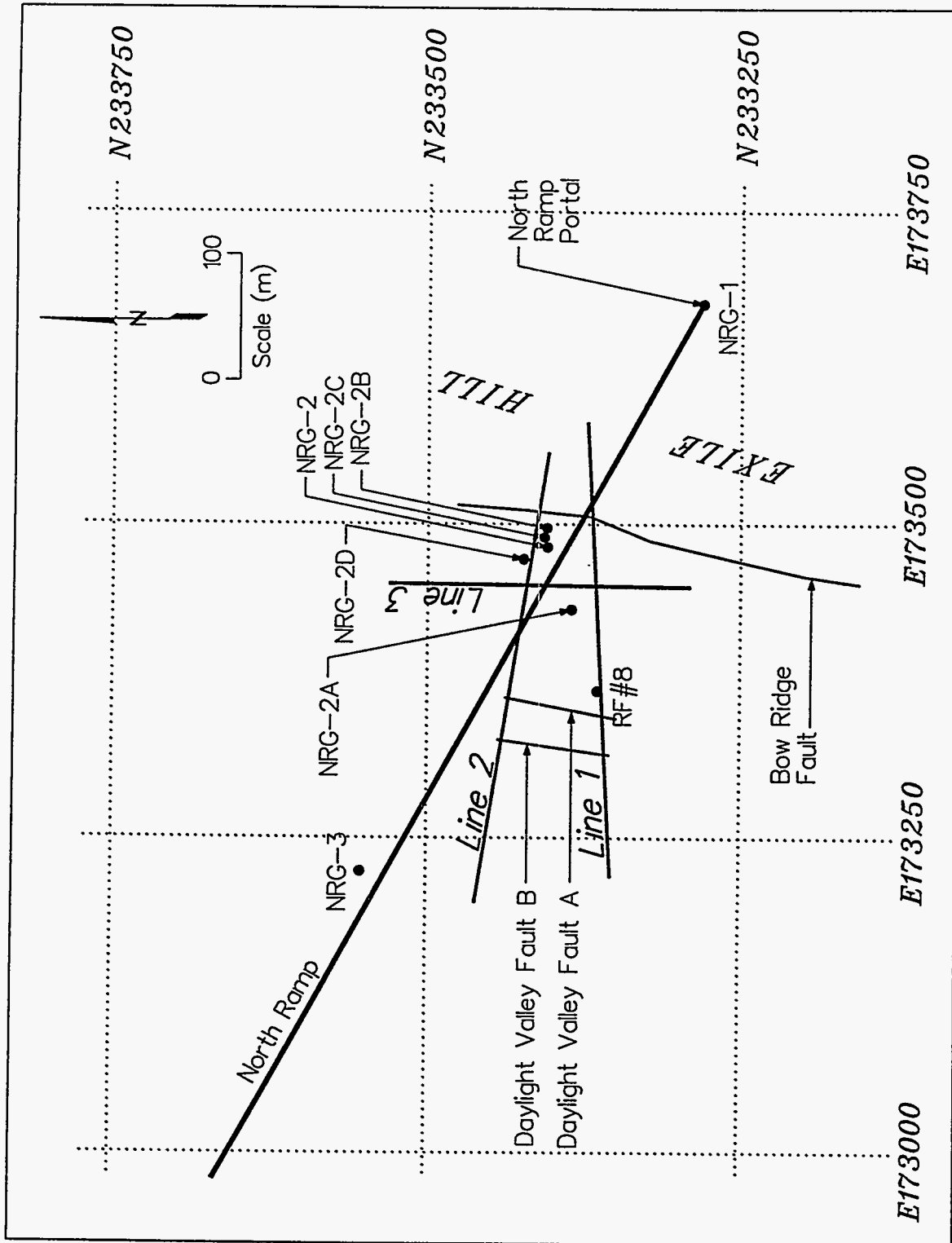


Figure 4-4. Plan View showing Seismic Lines* in Relation to North Ramp Alignment and Exploratory Boreholes in the Vicinity of Exile Hill

*Elbring.

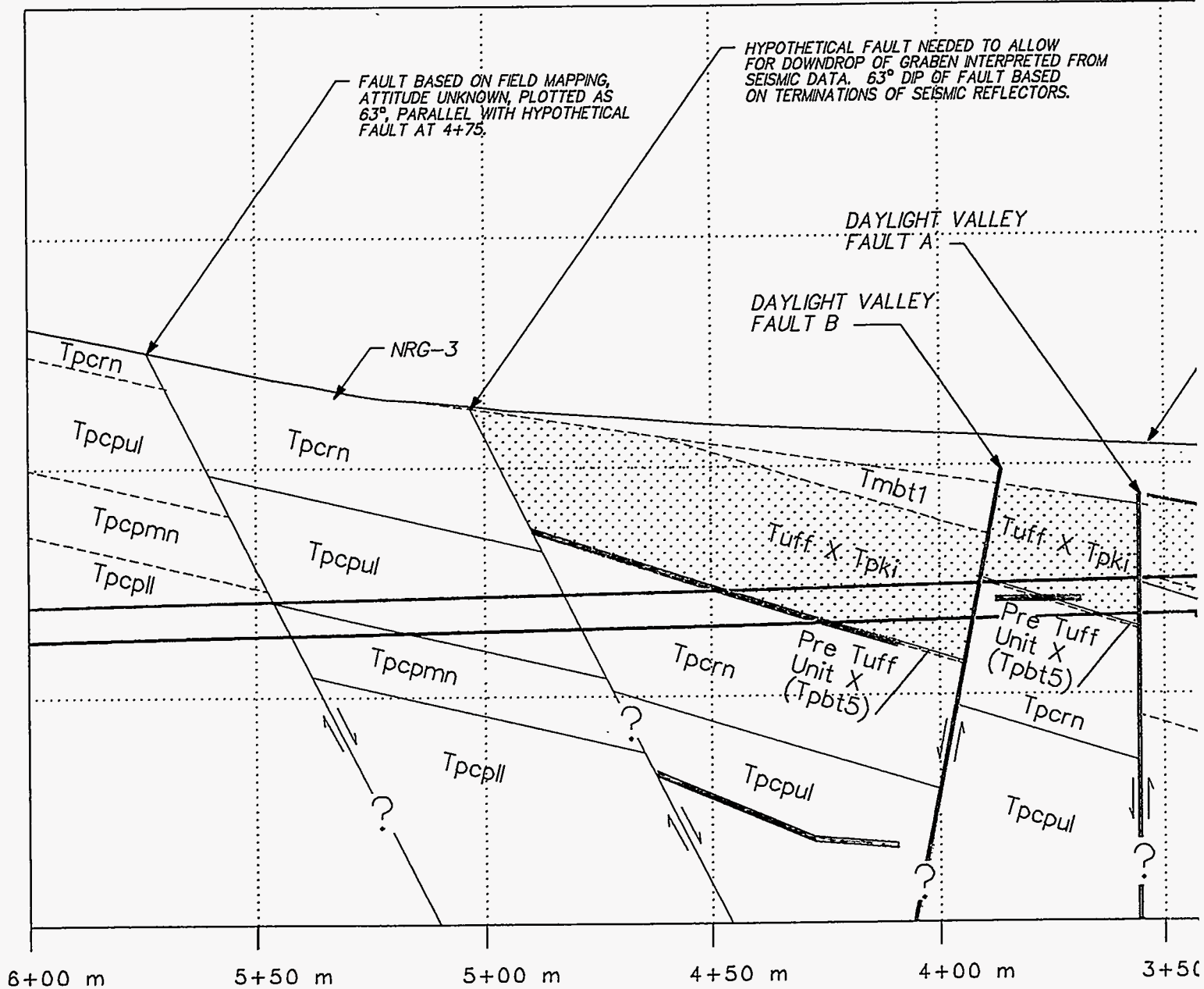
techniques while the other two used reflection only. Lines one and two were perpendicular to the axis of the valley while the third was parallel. The refraction data could not be processed to show structure but was used to determine seismic velocities. The reflection data, on the other hand, showed a number of prominent features in lines one and two, including two interpreted faults and several east-dipping reflectors that parallel the strata.

Line two of the study was located closest to the ramp alignment, crossing it near ramp station 3+00 m. The features identified²¹ in the processed reflection section have been projected into Figure 4-3 for comparison to the geology. The two interpreted faults are located between stations 3+50 m and 4+00 m. The westernmost fault is interpreted to have down-to-the-west movement based on the offset of the middle reflector, while the other less prominent fault is interpreted to have a smaller amount of down-to-the-east displacement. The highest elevation reflector shown between stations 2+50 m and 3+50 m was interpreted to be the base of the alluvium. A middle reflector, broken by the faults, was interpreted to be the contact of the nonwelded Tuff Unit "X" and the welded Tiva Canyon upper nonlithophysal zone, and a third reflector was interpreted as the base of the upper nonlithophysal zone based on the mapped thickness of this unit.






These seismic features cause some significant divergences from the interpretation of the geology between stations 3+50 and 5+00 m shown in Figure 4-3. An alternative cross section based on the seismic interpretation is shown in Figure 4-5 to illustrate these differences. The base of the alluvium and the base of Tuff Unit "X" are matched with core data from borehole RF #8 in line one. In the data from line two plotted onto Figure 4-3, however, the alluvium is shown to be nearly 15 m deeper from the seismic data than from what was observed in Trench

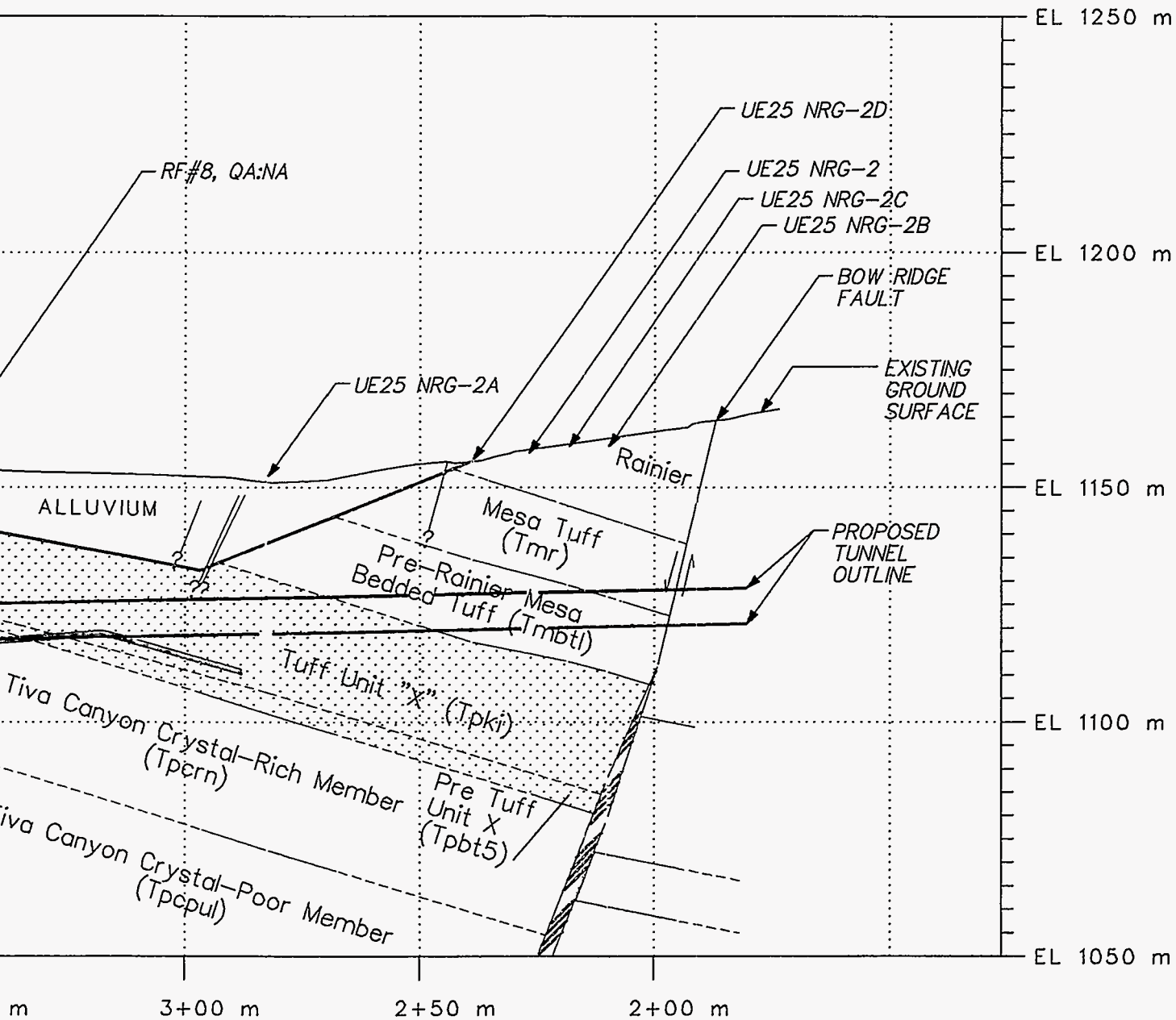
²¹ Ibid.

This page left intentionally blank.

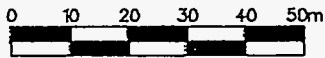


LEGEND

-  LITHOLOGIC CONTACT, SOLID LINE WHERE APPROXIMATE, DASHED LINE WHERE INFERRED
-  FAULT ZONE
-  FAULT, ?-ATTITUDE UNCERTAIN
-  POSSIBLE FAULTS IDENTIFIED FROM REFLECTION SEISMIC SAND94-2374
-  IDENTIFIED SEISMIC REFLECTORS SAND94-2374



CROSS SECTION CONSTRUCTED
ALONG RAMP ALIGNMENT - AZIMUTH 299°



REFERENCE:
DRAWING NO. SLTREXS2
VERSION 0

QA:NA

Figure 4-5. Alternative Interpretation of Exile Hill Geology Based on Seismic Reflection Data*

*Elbring, 1994.

NRT-1, and the base of Tuff Unit "X" is several meters higher than projected from borehole NRG-2A. Although it is possible that the alluvium could be thickened locally by channeling, it is more likely that this reflector is due at least in part to something other than this contact. As for the Tuff Unit "X" contact in this part of the section, the seismic data is unable to differentiate between the Tuff Unit "X"/bedded tuff contact and the bedded tuff/Tiva Canyon Tuff contact, a margin of error of approximately ± 5.2 m (17 ft).

The interpretation of the faults and reflectors to the west of station 3+50 m is even more problematic. Elbring²² postulates approximately 12 to 15 m (40 to 50 ft) of down-to-the-west offset on the fault at 4+00 m, and approximately 1.5 m (5 ft) of down-to-the-east offset on the fault projected to 3+50 m, based on the disruption of this reflector. Figure 4-5 assumes the attitude of all three reflector segments to approximate that of the surrounding mapped units (approximately 15° to the east) and suggests that both faults are down to the west.

The interpretation of the two reflector segments between 4+00 and 5+00 m as being the base of Tuff Unit "X" and the base of the Tiva Canyon Tuff upper nonlithophysal zone, respectively, runs into problems as well. Both of these horizons continue without apparent interruption across the small fault mapped by Scott and Bonk (1984) at 4+50 m shown in Figure 4-3. No surficial evidence for this fault was found while mapping the NRG-3 vicinity as part of this study. Therefore, the fault required to explain the downdrop of Tuff Unit "X" is plotted along the terminations of the reflectors in Figure 4-5 and would require approximately 25 m (80 ft) of down-to-the-east stratigraphic throw. No surface evidence for such a fault was found either, as the hill slope is covered by colluvium in this vicinity.

²² Ibid.

Projection of the base of the Tiva Canyon crystal-rich member to the fault at 4+50 m lines up with the westernmost reflector shown in Figure 4-3. A change in vapor phase alteration and lithophysal content can be observed across this contact, but it is unknown if this has an effect on seismic velocities.

The existence of the faults as interpreted from the seismic lines is plausible based on models of deformation within the hanging wall blocks of listric normal faults. Notably, the existence of small faults and grabens is predicted as a mechanism to accommodate differential extension along curved fault surfaces by the models of Cloos (1968) and Hamblin (1965). The series of small displacement normal faults mapped within the Tiva Canyon Tuff to the west of Exile Hill (Scott and Bonk, 1984) and the small faults observed within Trench NRT-1 (Angell, 1994) fall into this pattern. The position of the reflectors to the west of 4+00 m raise the possibility of a small graben dropping additional sections of Tuff Unit "X" down to the level of the North Ramp. The North Ramp would re-enter Tuff Unit "X" via fault contacts at stations 3+55 and 3+90 m after brief exposures of the depositional top of the Tiva Canyon Tuff in the tunnel walls. Using this scenario, the tunnel roof could possibly be within Tuff Unit "X" or the nonlithified Pre-Tuff Unit "X" bedded tuffs continuously from station 2+70 to 4+40 m. This alternative would place the ramp in nonwelded rocks where the current interpretation places it in welded rocks of the Tiva Canyon Tuff. However, the nonlithified rocks of the Pre-Rainier Mesa Bedded Tuff, characterized by soil-like engineering properties, would not be encountered beyond station 4+40 m as previously projected.

In general, both the seismic data and models of hanging wall deformation in listric normal fault zones suggest that the North Ramp will encounter additional faults and possibly small

grabens beneath the alluvium to the west of Exile Hill. Projection of borehole and surface data suggests that any displacement present is small, but does not provide a complete picture of the section of Daylight Valley covered by alluvium.

4.3.3 Projected Ramp Station Coordinates at Stratigraphic Contacts

The NRG drilling program has generally verified the existing stratigraphic interpretations long the North Ramp with minor local corrections required. Exceptions uncovered in the hanging wall of the Bow Ridge fault were primarily due to the character of the nonlithified portions of the Rainier Mesa and Pre-Rainier Mesa Bedded Tuff which have required alteration in ground support design. Some uncertainty exists in the stratigraphic interpretation under Daylight Valley, where the geophysical data suggests the presence of two undetected, normal faults with dip separations of up to 35 m. Table 4-3 lists the range in distance that the tunnel must be excavated in Tuff Unit "X" and the nonlithified Pre-Tuff Unit "X" Bedded Tuff based on the different geologic interpretations in Figures 4-3 and 4-5. This uncertainty may impact the ground support requirements in that the North Ramp may encounter the relatively thin nonlithified materials in the Pre-Tuff "X" Bedded Tuff at additional locations.

4.4 Thermomechanical (Thermal-Mechanical) Stratigraphy

The volcanic rocks at Yucca Mountain display a relatively narrow variance in composition. The aspects which most affect the physical and mechanical properties are the degree to which the individual particles in the deposits have been fused together or "welded" by post-emplacement heat and pressure and the degree of porosity. Repository design efforts are based on thermomechanical (thermal-mechanical) units that are defined by similarities in rock

mass thermal and mechanical properties, which are largely a function of the degree of welding and porosity.

The North Ramp will pass through five previously defined thermomechanical (thermal-mechanical) units (Ortiz et al., 1984) and NRG-series drill holes have penetrated seven. A chart correlating Yucca Mountain stratigraphy with the thermomechanical (thermal-mechanical) units is included in Figure 4-6, and a version of the full ramp cross section showing only thermomechanical (thermal-mechanical) units is presented in Figure 4-7. Within the welded units the variable which most affects the thermomechanical (thermal-mechanical) properties is the amount of lithophysal cavities and the effect this has on total porosity values. In this report, the high lithophysal and nonlithophysal subunits within the TCw and TSw1 units are examined to assess whether rock structure and rock mass quality are different within these subunits.

The thermomechanical (thermal-mechanical) units are based primarily on welded versus nonwelded rocks and secondarily, on the presence of lithophysal cavities. The degree of welding present within the rocks of the Paintbrush and Timber Mountain Groups ranges from nonwelded bedded tuffs that can be crumbled by hand to densely welded ash-flow tuffs. As the degree of welding may vary both vertically and laterally within an ash-flow unit, the thermomechanical (thermal-mechanical) unit boundaries reflect the boundaries between welded and nonwelded zones. Although the thermomechanical (thermal-mechanical) units generally correspond to the stratigraphic units, some variances do occur. For instance, the Upper Paintbrush nonwelded unit (PTn) was created to group the nonwelded ash-flows of the Yucca Mountain and Pah Canyon Tuffs together. However, this unit also contains nonwelded portions of the Topopah Spring and

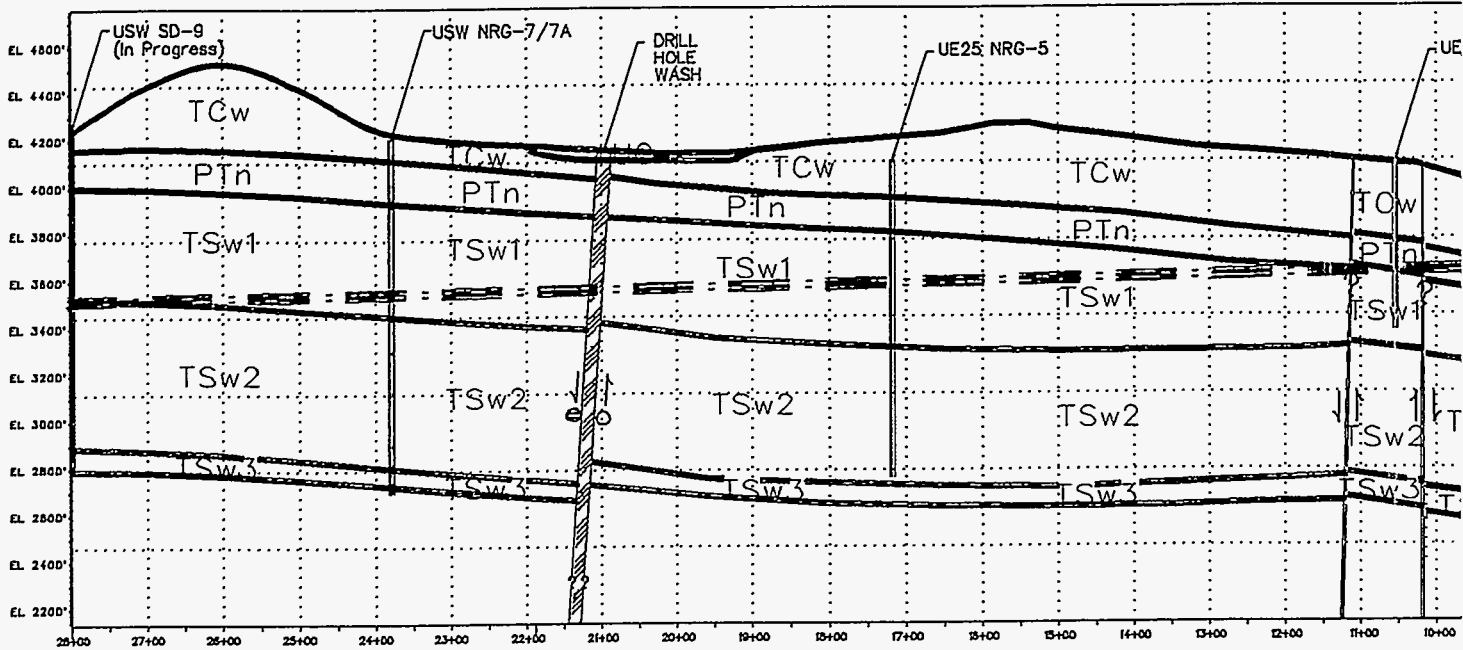
Geologic Stratigraphy		Thermal Mech. Unit	Lithologic Description	Stratigraphic Units ¹
Paintbrush Group	Alluvium	U0	Alluvium, nonwelded ashflows and bedded tuffs	QTac, Tmr, Tmbt1, Tпки, Tplot5, Tpcrv3, Tpcrv2
	Rainier Mesa Tuff			
	Tuff Unit "X"			
	Tiva Canyon Tuff	TCw	Nonlithophysal subzone	Tpcrv3, Tpcrn
			Lithophysae-bearing subzone	Tpcrl, Tpcpul, Tpcpmn, Tpcpl
			Nonlithophysal subzone	Tpcplh, Tpcpv3
	Yucca Mtn. Tuff	PTn	Vitric nonwelded	Tpcpv2, Tpcpul, Tpb4, Tpy, Tpb3, Tpp, Tpb2, Tptrv3, Tptrv2
	Pah Canyon Tuff			
	Topopah Spring Tuff	TSw1	Nonlithophysal subzone welded devitrified tuff lithophysae poor	Tptrv1, Tptrn
			Lithophysae bearing subzone welded devitrified tuff up to 25% lithophysal cavities by volume	Tptr1, Tptpul
		TSw2	"Nonlithophysal" (contains sparse lithophysae); potential subzone repository horizon	Tptpmn, Tptpl, Tptpln
		TSw3	Virtophyre	Tptpv3
Calico Hills Formation	CHn1	Ashflows and bedded units may be vitric or zeolitized	Tptpv2, Tptpul, Tpb1, Tac	

¹ New USGS nomenclature, Geslin et al., (1994)

Figure 4-6. Correlation of Stratigraphic and Thermomechanical (Thermal-Mechanical) Units along the North Ramp Alignment (modified from Ortiz et al., 1984)

This page left intentionally blank.

SECTION VIEW



Reference Stratigraphy Unit Name (Designation)	Description	UNIT SYMBOL
Undifferentiated Overburden (UO)	Alluvium; colluvium; nonwelded, vitric ash-flow tuff of the Tiva Canyon Tuff of the Paintbrush Group; any other tuff units that stratigraphically overlie the welded devitrified Tiva Canyon Tuff.	UO
Tiva Canyon welded unit (TCw)	Moderately to densely welded, devitrified ash-flow tuff of the Tiva Canyon Tuff of the Paintbrush Group. Contains lithophysal and nonlithophysal subunits.	TC
Upper Paintbrush nonwelded unit (PTn)	Partially welded to nonwelded, vitric and occasionally devitrified tuffs of the lower Tiva Canyon, Yucca Mountain, Pah Canyon, and Topopah Spring Tuffs of the Paintbrush Group.	PT
Topopah Spring welded unit, lithophysae-rich (TSw1)	Moderately to densely welded, devitrified ash flows of the Topopah Spring Tuff of the Paintbrush Group that locally contains more than approximately 10% by volume lithophysal cavities. Subdivided in this report into an upper nonlithophysal subunit and a lower lithophysal subunit.	TS
Topopah Spring welded unit, lithophysae-poor (TSw2)	Moderately to densely welded, devitrified ash flows of the Topopah Spring Tuff of the Paintbrush Group that contains less than approximately 10% by volume lithophysal cavities. This is the proposed repository host rock.	TS
Topopah Spring welded unit, vitrophyre (TSw3)	Vitrophyre near the base of the Topopah Spring Tuff of the Paintbrush Group.	TS

STATE PLANE COORDINATES
ALONG RAMP ALIGNMENT (m)

E171289

E171604

N234584

E171909

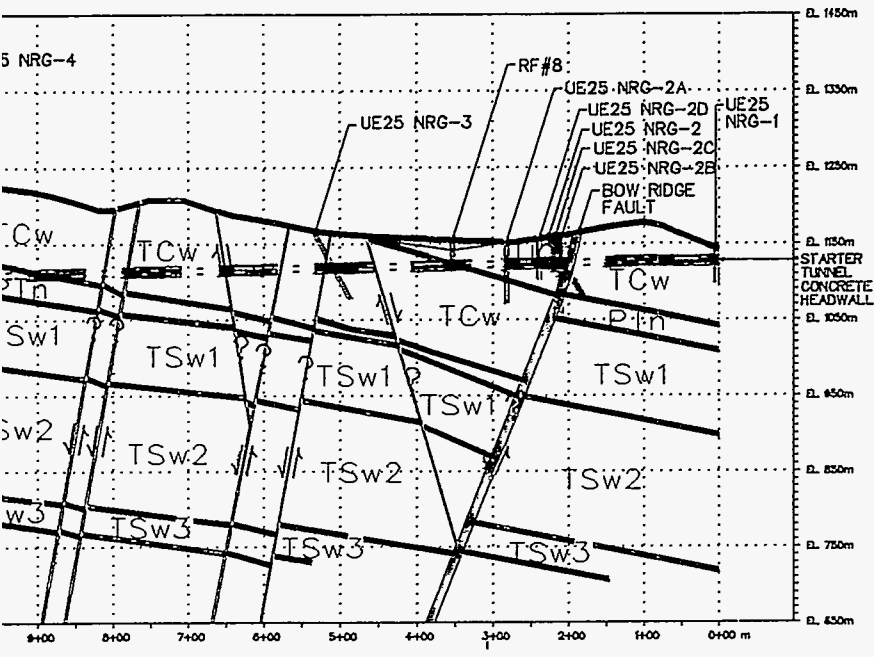
E172214

N234089

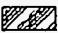



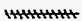


E172519

N233784

E172523



SYMBOLS

-  DRILL HOLE WASH FAULT ZONE, LOCATION AND ATTITUDE UNCERTAIN
-  BOW RIDGE FAULT ZONE
-  MINOR FAULT, ? -ATTITUDE UNCERTAIN
-  PROPOSED NORTH RAMP ALIGNMENT
-  APPROXIMATE
-  STRIKE-SLIP SEPARATION INTO PAGE
-  STRIKE-SLIP SEPARATION OUT OF PAGE

B178128

N255479

B178433

Figure 4-7. North Ramp Thermomechanical (Thermal-Mechanical) Unit Cross Section

Tiva Canyon Tuffs, units which are otherwise moderately to densely welded. Likewise, the uppermost nonwelded portions of the otherwise welded Tiva Canyon Tuff are assigned to the Undifferentiated Overburden unit (UO), as opposed to the Tiva Canyon welded unit (TCw).

Of note to the design of the ESF is the distinction between the upper two Topopah Spring welded units, TSw1 and TSw2. These units are both within the densely welded, devitrified Topopah Spring Tuff, but reported to differ in that TSw1 contains zones where void space from lithophysal cavities exceeds 10% by volume. TSw2, which contains the proposed repository horizon, also contains lithophysae bearing units.

The stations where the North Ramp is projected to intersect the various thermomechanical (thermal-mechanical) units are listed as Table 4-4. Ramp stations listed are where the contact of the thermomechanical (thermal-mechanical) unit intersects the centerline of the TBM bore. The North Portal has been constructed in welded rocks of the Tiva Canyon Tuff (TCw). The North Ramp will proceed through the Bow Ridge fault, where it will encounter nonwelded tuffs of unit UO where uncertainty due to projected faults under Daylight Valley is indicated both in the length of UO in the tunnel and in the contact with TCw. The ramp will then continue to descend to progressively deeper levels back through the TCw into the PTn, TSw1, and finally TSw2 units.

Table 4-4. Projection of Ramp Station Coordinates at Thermomechanical (Thermal-Mechanical) Unit Contacts

Thermomechanical (Thermal-Mechanical) Unit	Projected Ramp Station (m) ²	Projected Length of Tunnel in Unit (m) ²
Tiva Canyon Welded (TCw)	0+00	196
Undifferentiated Overburden (UO) ¹	1+96	149 to 239
Tiva Canyon Welded (TCw) ¹	3+45 to 4+35	455 to 545
Upper Paintbrush Nonwelded (PTn)	8+90	172
Topopah Welded Unit, Lithophysae-rich, nonlithophysal subzones (TSw1n)	10+62	754
Topopah Welded Unit, Lithophysae-rich, lithophysal-bearing subzones (TSw1l)	18+16	947
Topopah Welded Unit, Lithophysae-poor (TSw2)	27+63	37

¹Range reflects uncertainty due to projected faults under Daylight Valley.

²Horizontal distance along centerline.

4.5 Major Structural Features

4.5.1 Faults Recognized Along North Ramp Alignment

Surface mapping by Scott and Bonk (1984) indicates the North Ramp will pass through two prominent fault zones, the Bow Ridge and Drill Hole Wash faults, and eight minor faults. Additionally, geophysical data suggests that minor faults may be present beneath the alluvium of Daylight Valley. The Bow Ridge fault is one of a number of north to north-northeast trending, high angle, west-dipping, normal faults that break Yucca Mountain into gently east-dipping blocks 1–4 km across. The Drill Hole Wash fault, on the other hand, is a northwest trending, right-lateral, down-to-the-west, oblique-slip fault. The structural block containing the ESF is 3–4 km wide and is bounded on the west and east by the Solitario Canyon and Bow Ridge faults, respectively. Displacement on the Solitario Canyon fault, which is not crossed by the North Ramp alignment, reaches more than 400 m (Carr, 1984).

Faults along the west sides of the major structural blocks at Yucca Mountain typically show highly brecciated zones as wide as 500 m, while the east margins of the blocks are characterized by abundant, sub-parallel, west-side-down, west-dipping normal faults described as

imbricate normal fault zones (Scott and Rosenbaum, 1986). Individual faults within these zones typically displace strata by only a few meters and the dip of strata between the faults progressively steepens eastward toward the margins of the broken zones. These fault zones increase in width toward the southern end of Yucca Mountain, which paleomagnetic and field mapping evidence shows to have rotated about 30° in a clockwise direction relative to the north end of the mountain (Spengler and Fox, 1989). A number of northwest-trending, right-lateral, strike-slip faults exist in the northern portions of Yucca Mountain, but the amount of displacement is probably minor as inferred from little or no offset of stratigraphic units (Carr, 1984).

The known and suspected faults to be encountered by the North Ramp are summarized in Table 4-5. With the exception of the Bow Ridge fault, attitudes are derived from surface mapping or geophysics and the ramp station intersections are, therefore, approximate.

Table 4-5. Known Faults Projected to Encounter the North Ramp and Approximate Ramp Station

Ramp Station (m)*	Strike (degrees)	Dip (degrees)	Fault Type	Projected Dip-Slip Displacement	Name
1+96	N14E	67W	normal	122 m	Bow Ridge Fault
3+55	N12E	90W	normal	10 m	Daylight Valley Fault A**
3+92	N08E	80W	normal	27 m	Daylight Valley Fault B**
4+52	N15E	79E	normal	0 m to >25 m***	Fault #1
5+18	N15E	79W	normal	0 m	Fault #2
5+60	N18E	80E	normal	25 m	Fault #3
6+48	N17E	81E	normal	5 m	Fault #4
7+77	N07E	80W	normal	3 m	Fault #5
8+08	N16E	80W	normal	1 m	Fault #6
10+14	N27E	90	normal	7 m	Fault #7
11+09	N22E	88W	normal	5 m	Fault #8
20+98	N43W	86W	oblique slip	<10 m	Drill Hole Wash Fault

*Along centerline.

**Faults interpreted from seismic data.

***Upper values given for alternate interpretation based on seismic data as shown in Figure 4-5.

The Bow Ridge fault, shown in Figure 4-3, is found on the west side of Exile Hill and shows normal, down-to-the-west dip slip movement estimated at 130 ± 5 m at the base of the Tiva Canyon Tuff. A sequence of nonwelded ash flows and bedded tuffs including Tuff Unit "X" and Rainier Mesa Tuff have been down-faulted against welded tuffs of the Tiva Canyon Tuff at the level of the ramp. Boreholes NRG-2 and NRG-2B indicate that the dip on the Bow Ridge fault shallows with depth, supporting the interpretation of a curved or listric geometry. Reverse drag (a gradual steepening of stratal dips toward the fault plane) and a number of small synthetic and antithetic faults are observed in the nonlithified tuffs adjacent to the fault zone in Trench NRT-1. Furthermore, the gradual steepening of stratal dips towards the Bow Ridge fault is observed within the imbricate fault zone immediately to the west, and a pair of small faults are interpreted from seismic reflection data beneath the alluvium west of the Bow Ridge fault. These features are characteristic of hanging wall deformation near listric normal faults (Cloos, 1968; Hamblin, 1965).

Faults numbered 1 through 8 in Table 4-5 and shown in Figure 4-2 west of the Bow Ridge fault are part of the imbricate fault zone described above. Displacement on these faults ranges from 1–12 m. Faults 1, 3, and 4 are east-dipping with down-to-the-east displacement and an antithetic orientation to the Bow Ridge fault. The remainder of the faults are west-dipping with down-to-the-west displacement and progressively steepening dips with distance from the Bow Ridge fault. The faults labeled A and B in Table 4-5 are those interpreted from seismic reflection data and, if present, would fall into the same structural framework as the faults mentioned above. These faults may, at depth, terminate against the Bow Ridge fault, as predicted by the models of Cloos (1968) and Hamblin (1965).

Surface mapping of the NRG-3 vicinity as part of this study resulted in a different interpretation of this area from that of the USGS²³ based on the mapping of Scott and Bonk (1984). In particular, faults 1 and 2 were not found here due to colluvial cover, and fault 3 was found to have an opposite sense of displacement, as shown in Figure 4-3. Although no exposure of the fault plane was found, outcrops were found that placed rocks of the Tiva Canyon crystal-rich, crystal transition subzone (Tpcrn1) on the west against rocks of the Tiva Canyon crystal-rich, pumice-poor subzone (Tpcrn3) on the east. Based on unit thicknesses derived from NRG-3 core, this accounts for approximately 25 m (80 ft) of stratigraphic throw.

The Drill Hole Wash fault is projected to cross the North Ramp at station 21+04. This fault exhibits right-lateral strike-slip movement of an unknown displacement. However, the strike-slip component is likely small, as evidenced by little offset of stratigraphic units. Dip-slip displacement is estimated at less than 10 m down to the west from Figure 4-2.

4.5.2 Recognized Fracture Patterns

Analysis of fracture patterns has been performed on oriented core data from boreholes USW G-3, GU-3, and G-4 (Lin et al., 1993b) and on preliminary (non-QA) mapping data from the ESF North Ramp Starter Tunnel and related excavations.²⁴

The oriented core data is summarized in Table 4-6, and is presented on the basis of geologic formation. Additionally, average fracture set data for the ESF North Ramp Starter Tunnel is presented in a stereonet plot in Figure 4-8. The following similarities in interpretation of the data are noted by the above authors. Both sources of data suggest up to three fracture sets dominated by a high-angle north-trending set. All of the recognized sets are characterized by

²³ Hayes.

²⁴ Fahy and Beason.

high-angle dips. In addition to the high-angle sets, both sources of data show a handful of low-angle east-dipping fractures consistent with rock foliation.

Table 4-6. Fracture Orientations as Estimated for Oriented Core and Borehole Television Surveys*

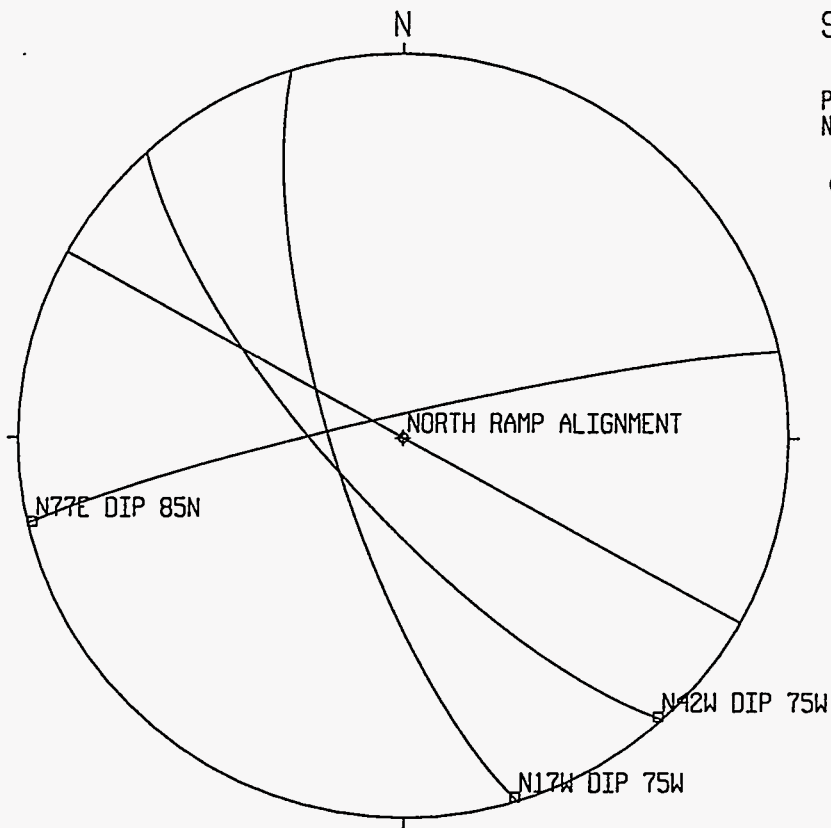
Geologic Formation	USW GU-3		USW G-4	
	Strike	Dip	Strike	Dip
Tiva Canyon Tuff	N18°W-N36°E	85°-90° SW/NE	N-N22°E	65°-90°NW
	N50°W	12°NE	—	—
	—	—	E-W	70°-90°N/S
	—	—	N50°W	70°-90°NE/SW
Topopah Spring Tuff	N10°W	75°-90°NE/SW	N12°W	80°-90°NE/SW
	N25°E	10°SE	—	—
	N45°E	80°-90°SE/NW	N-N40°E	NM

NM Not measured by borehole television system.

— No corresponding joint was observed.

* From Lin et al., 1993a.

The trend of the ESF North Ramp is plotted for comparative purposes on Figure 4-8. Note that the tunnel alignment will intersect the dominant north-trending fracture set and the subsidiary northeast-trending set at angles of approximately 45° or greater to the axis of the tunnel. The minor fracture set at N40°W to N50°W, however, will intersect the tunnel at angles of less than 20°. Although this fracture set could conceivably cause some stability problems from fractures that are nearly parallel to the tunnel walls, the number of fractures in this subset are minor and the vast majority of fractures to be encountered by the North Ramp will be at angles greater than 45° to the axis of the tunnel.



SANDIA NORTH RAMP STRUCTURE

Projection Schmidt
 Number of Sample Points 8

QA:NA; Preliminary

Figure 4-8. Recognized Fracture Sets, ESF North Ramp Starter Tunnel*

*Fahy and Beason.

This page left intentionally blank.

5.0 ROCK STRUCTURE DATA

5.1 Introduction

This section of the report presents rock structural data developed from core logs of the NRG holes and other data sources that relate to North Ramp construction. All data summarized in this section for the NRG boreholes were qualified. Data from the NRG holes were summarized by grouping the 3-m (10-ft) intervals from the Rock Structural Data Summary Logs by thermomechanical (thermal-mechanical) unit. Further subdivision was introduced within the TCw and TSw1 units because both of these units include sections of lithophysae-rich (LR) and nonlithophysal (NL) tuffs. The lithophysae-rich sections have been isolated to test whether the structural characteristics indicate the need for subdivision.

The rock structure data from the NRG holes are discussed under the subheadings of:

- ♦ Lost Core and Rubble Zones,
- ♦ Rock Quality Designation (RQD),
- ♦ Rock Weathering and Hardness,
- ♦ Fracture Type,
- ♦ Fracture Mineral Infill and Thickness,
- ♦ Fracture Surface Roughness and Planarity, and
- ♦ Fracture Frequency.

Orientations of the identified fracture sets from surface mapping and previous oriented coring at Yucca Mountain are compared to the NRG data to project impacts during tunneling. The rock structure characteristics in the vicinity of fault zones penetrated by NRG-2 and NRG-3

are examined to evaluate the extent to which fault occurrence may impact rock quality in their vicinity.

The core hole data for individual NRG holes are presented in Volume II. Detailed instructions for describing the structural data during the core logging process are presented in Appendix A of Volume I.

5.2 Core Recovery

The quantity of core recovered as both whole core and rubble, and the quantity of lost core are general indicators of both the quality of the rock and drilling technique. At the YMP, requirements to limit the introduction of water and chemical additives typical in core drilling have led to the development of compressed-air core drilling technology. The circulating media was high velocity, dry compressed air in all of the NRG holes with the exception of NRG-2C and -2D which were auger drilled. The impact of this new drilling technique on core quality is difficult to establish because of limited data for comparison.

The proportions of whole core, lost core, and rubble are compared in Table 5-1 which lists total drilled length, whole core recovered, rubble zones, and lost core recovered for each thermomechanical (thermal-mechanical) unit. The percentages of each category normalized to the total cored length are also listed in Table 5-1 and are compared in Figure 5-1. The proportion of whole core in the TCw and PTn units was similar at around 70%, but decreased in the deeper TSw1 and TSw2 units to 62.3% and 48.7%, respectively. The amount of lost core increases with increasing depth for all of the units, reaching 34.8% for the TSw2. The quantity of rubble is similar for all zones, ranging from 10% in the PTn to 16.5% in the TSw2.

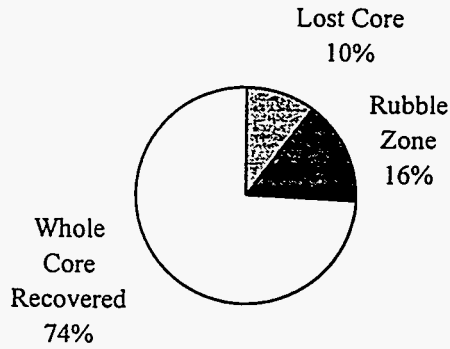
Table 5-1. Summary of Core Recovery, Lost Core, and Rubble by Thermomechanical (Thermal-Mechanical) Unit — NRG Holes

Thermomechanical (Thermal-Mechanical) Units	Total Drilled (m)	Whole Core Recovered (m)	% of Total	Lost Core (m)	% of Total	Rubble Zones (m)	% of Total	Lost Core & Rubble (m)	% of Total
TCw—total drilled	274.3	196.3	71.6	36.4	13.3	41.6	15.2	78.0	28.4
nonlithophysal	170.7	126.4	74.1	17.3	10.1	26.9	15.8	44.3	25.9
lithophysae rich	103.6	69.9	67.4	19.1	18.4	14.7	14.2	33.7	32.6
PTn	161.5	114.5	70.8	30.9	19.1	16.2	10.0	47.1	29.2
TSw1—total drilled	387.1	241.0	62.3	96.7	25.0	49.4	12.8	146.1	37.7
nonlithophysal	170.7	135.3	79.3	21.1	12.4	14.3	8.4	35.4	20.7
lithophysae rich	216.4	105.7	48.8	75.7	35.0	35.1	16.2	110.7	51.2
TSw2	402.4	204.3	50.7	131.3	32.6	66.9	16.6	198.2	49.2

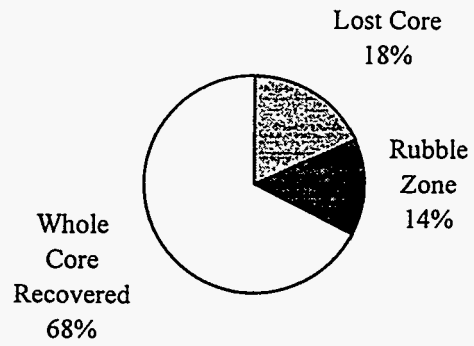
Comparison of the lithophysae-rich and nonlithophysal portions of the TCw and TSw1 units indicate greater portions of lost core and rubble are associated with the lithophysae occurrence.

In general, it appears that the compressed-air coring technique is not responsible for the large proportion of lost core and rubble observed in the welded tuffs. The higher proportions of rubble and lost core observed in the TSw1 and TSw2 units are attributed to their fractured nature and the presence of lithophysal voids. This is somewhat confirmed by the increase in rubble and lost core associated with the lithophysae-rich portions of the TCw and TSw1, and the fact that lost core in the weaker nonwelded rock of the PTn is lower than TSw1 or TSw2. Core condition in the nonwelded rocks of the Calico Hills (CHn1) that underlie TSw2 is also much better than in the overlying welded units.

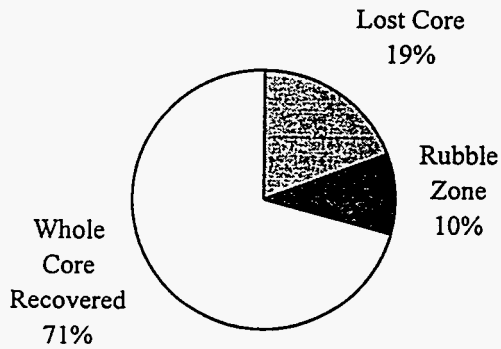
TCw Nonlithophysae Unit



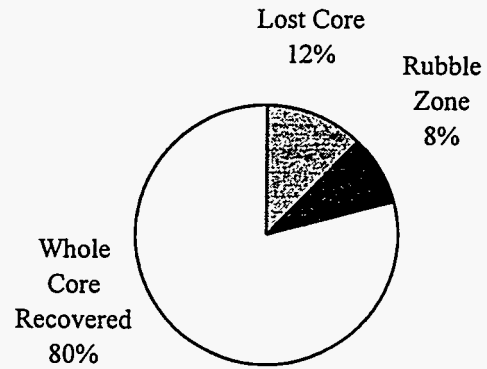
TCw Lithophysae-Rich Unit



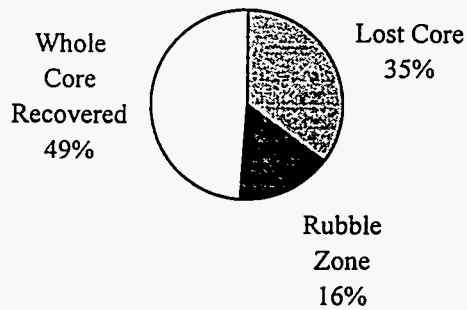
PTn Unit



TSw1 Nonlithophysae Unit



TSw1 Lithophysae-Rich Unit



TSw2 Unit

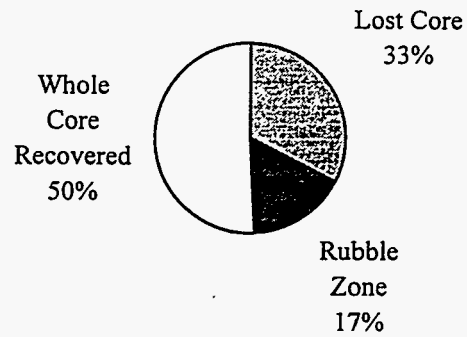


Figure 5-1. Pie Charts Showing Core Recovery, Lost Core and Rubble Zones as a Percentage of Total Drilling in Thermomechanical (Thermal-Mechanical) Units—NRG Holes

5.3 RQD Data

The rock quality designation index—RQD (Deere, 1963)—was determined based on ASTM STP 984 (Kirkaldie, 1988) which specifies its application on core, ranging from HQ to PQ (36.5 mm–85 mm) in diameter. All NRG core was either HQ or PQ size and meets the size requirements in ASTM STD 984. The highly fractured nature of much of the core from the NRG holes and the fact that fracturing is predominantly vertical and sampled by vertical boreholes has prompted a conservative approach to the calculation of the rock quality designation. The lack of mineral infillings and the existence of a subhorizontal fabric in some of the tuff rocks, similar to a foliation, makes identification of drilling induced features difficult. RQD was therefore calculated using equation 5-1:

$$\text{RQD (\%)} = 100 \times \left[\frac{\sum \text{Piece lengths} \geq 10.2 \text{ cm (4 inches)}}{\text{Interval length}} \right] \quad (5-1)$$

where all through-going structural features that were observed in the core were considered. Lost core and rubble zones do not contribute any piece lengths, but are included in the interval length. This approach is sanctioned by the ASTM STP 984 and by ISRM procedures (Brown, 1981) when difficulty in identification of natural features warrants a conservative approach. RQD was calculated both on the core run interval and on even 3.0-m (10-ft) intervals.

The detailed logging approach employed in this work also allowed the calculation of RQD where the effects of fractures, which were judged by the core loggers to be drilling induced, could be filtered out. This parameter is labeled “*enhanced*”-RQD, where the term “enhanced” indicates that the value has been made greater than the core condition by the filtering all type C (drilling induced) fractures from the piece length determination. Type C fractures were generally subhorizontal, rough, and clean fractures. The *enhanced-RQD* was calculated to provide an estimate of the degree of conservatism that may have been incorporated in the RQD parameter.

Enhanced-RQD was not used in any of the subsequent estimation of rock mass quality using the core data.

The mean, median, and standard deviation of RQD and *enhanced-RQD* and the ratio of *enhanced-RQD*:RQD are compared in Table 5-2. Figures 5-2 and 5-3 show frequency histograms and cumulative percent occurrence for RQD and *enhanced-RQD*, respectively.

Table 5-2. Comparison of RQD Data and *Enhanced-RQD* Data for the Thermomechanical (Thermal-Mechanical) Units — NRG Holes

		TCw NL	TCw LR	PTn	TSw1 NL	TSw1 LR	TSw2	Relative Rating RQD (%) Rating	
RQD	Mean	29	26	39	32	18	13	91–100	Excellent
	Median	26	22	39	30	14	8	76–90	Good
	Std. Dev.	20	21	28	26	18	17	51–75	Fair
<i>Enhanced RQD</i>	Mean	49	46	59	58	40	31	26–50	Poor
	Median	51	49	66	65	38	26	1–25	Very Poor
	Std. Dev.	24	24	29	30	26	23	0–1	Extremely Poor
<i>Enhanced RQD</i> RQD	Mean	1.7	1.8	1.5	1.8	2.2	2.4		
	Median	2.0	2.2	1.7	2.2	2.7	3.3		

NL—Nonlithophysal; LR—Lithophysae Rich

The relative rock quality indicated by the numerical values, based upon the RQD system (Deere, 1968), can be judged in the small table listing the relative rating in Table 5-2. On the basis of the RQD, the TCw and PTn units are poor quality rock and the TSw1 and TSw2 are very poor quality rock. Locally, the nonlithophysal portion of the TSw1 has higher quality and would be ranked as poor quality rock. The relative ratings are similar for both the mean and median values of RQD.

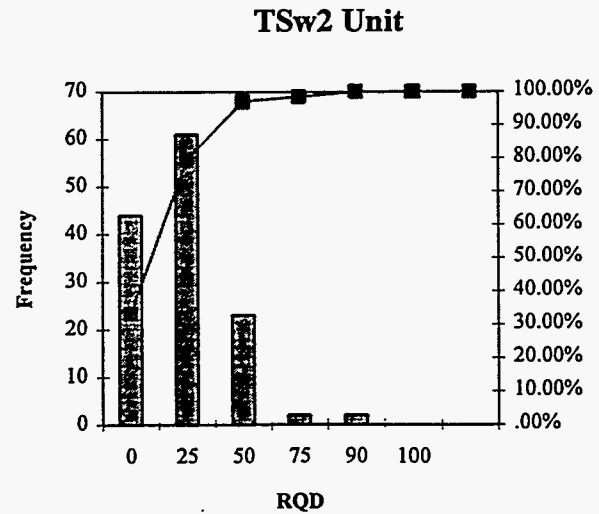
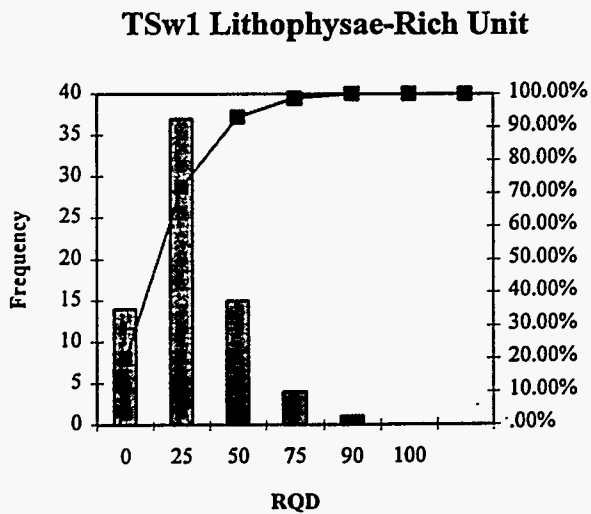
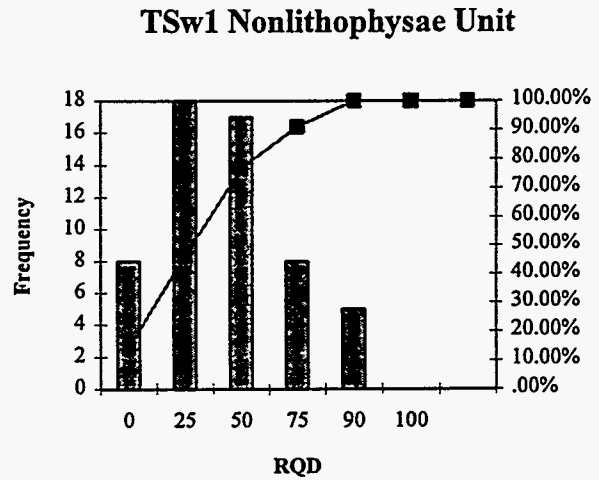
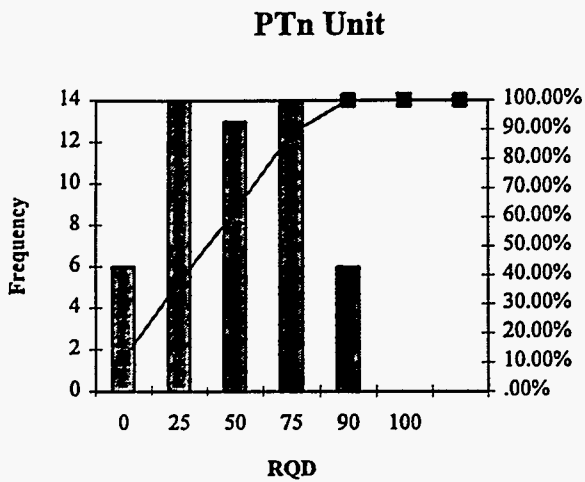
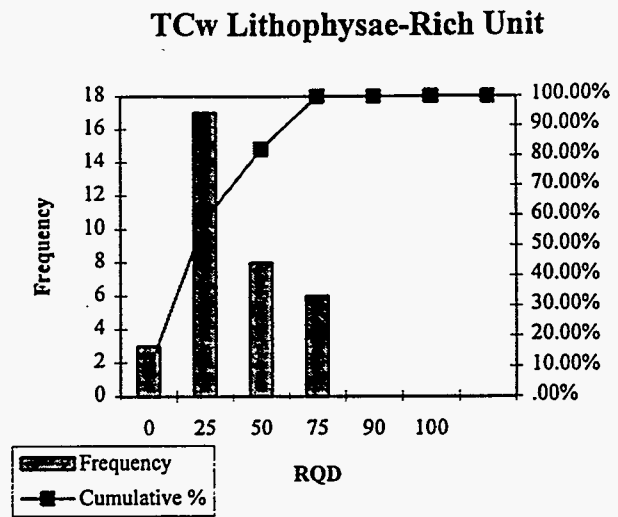
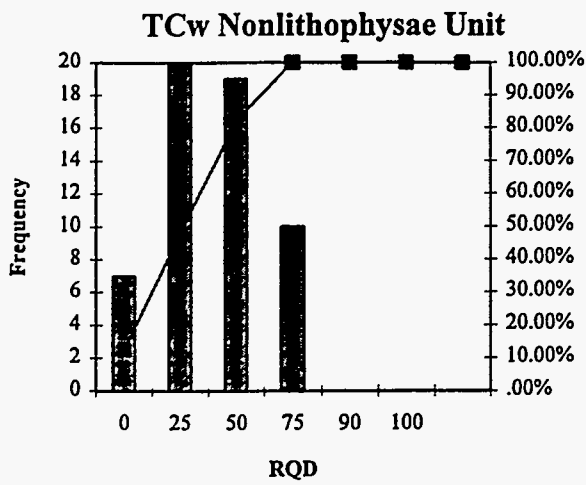
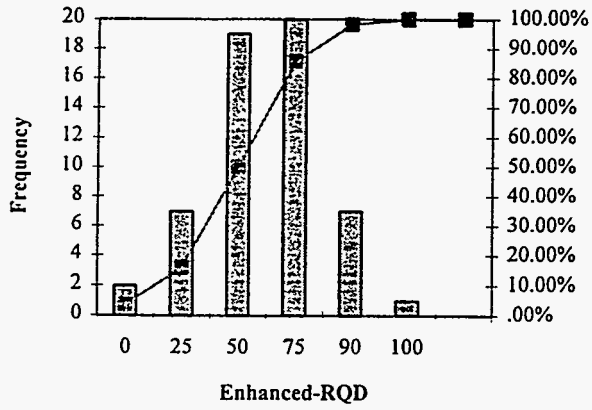
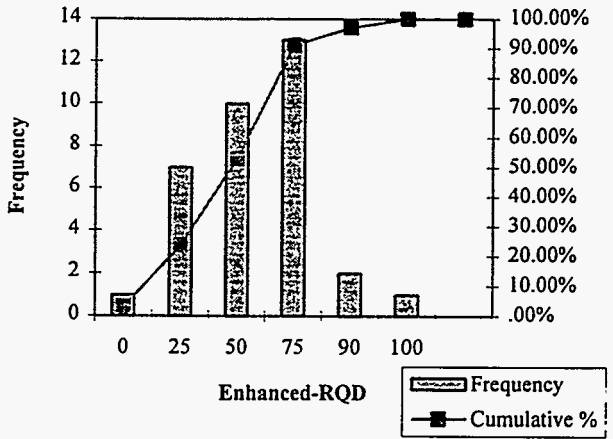


Figure 5-2. Histograms Showing RQD Frequency in the Thermomechanical (Thermal-Mechanical) Units — NRG Holes

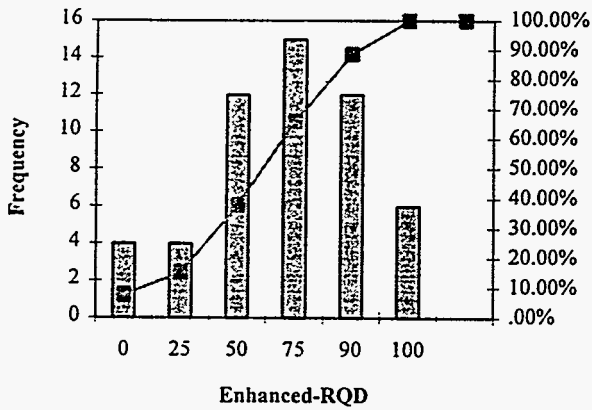
TCw Nonlithophysae Unit



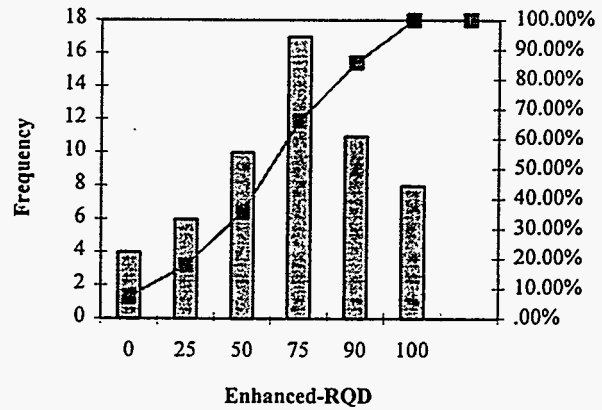
TCw Lithophysae-Rich Unit



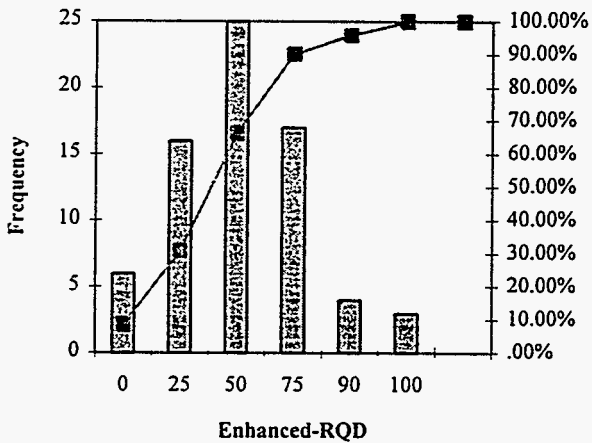
PTn Unit



TSw1 Nonlithophysae Unit



TSw1 Lithophysae-Rich Unit



TSw2 Unit

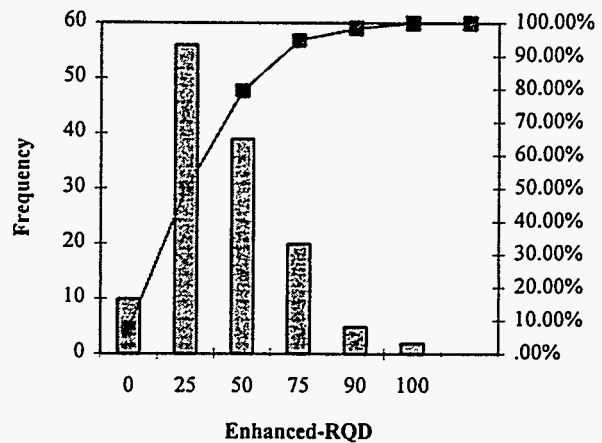


Figure 5-3. Histograms Showing *Enhanced-RQD* Frequency in the Thermomechanical (Thermal-Mechanical) Units—NRG Holes

The ratio of mean *enhanced-RQD* to RQD ranges from 1.51 to 2.38, with the largest numerical impact associated with the units with lowest RQD. The effect of filtering the “drilling-induced” features is varied in the relative sense, producing no change in the poor rating of the TCw, but an increase of one class in both the PTn (fair from poor) and TSw1, TSw2 (poor from very poor).

5.4 Rock Weathering and Hardness

Rock weathering and estimated hardness were described using the five and nine categories, listed in Tables 5-3 and 5-4, respectively. The parameters were described on a per-run basis; however, run intervals were not logged when the volume of lost core or condition of the rubble did not allow description.

Table 5-3. Explanation of Weathering Descriptions and Log Abbreviation

Weathering Class	Log Abbreviation	Further Explanation
fresh	F	Rock and fractures not oxidized or discolored, no separation of grains, change of texture or solutioning.
slightly weathered	S	Oxidized or discolored fractures and nearby rock, some dull feldspars, no separation of grains, minor leaching.
moderately weathered	M	Fractures and most of the rock oxidized or discolored, partial separation of grains, rusty or cloudy crystals, moderate leaching of soluble minerals.
intensely weathered	I	Fractures and rock totally oxidized or discolored, extensive clay alteration, leaching complete, extensive grain separation, rock is friable.
decomposed	D	Grain separation and clay alteration complete.

Table 5-4. Explanation of Estimated Hardness and Log Abbreviation

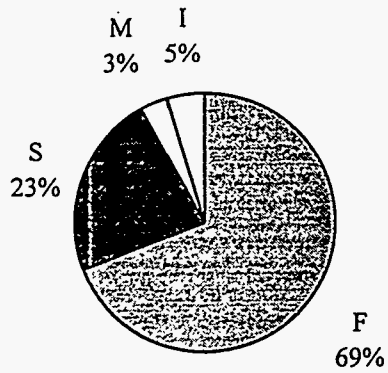
Hardness Class	Log Abbreviation	Further Explanation
extremely hard	1	Cannot be scratched, chipped only with repeated heavy hammer blows.
very hard	2	Cannot be scratched, broken only with repeated heavy hammer blows.
hard	3	Scratched with heavy pressure, breaks with heavy hammer blow.
moderately hard	4	Scratched with light-moderate pressure, breaks with moderate hammer blow.
moderately soft	5	Grooved (1/16th inch) with moderate heavy pressure, breaks with light hammer blow.
soft	6	Grooved easily with light pressure, scratched with fingernail, breaks with light-moderate manual pressure.
very soft	7	Readily gouged with fingernail, breaks with light pressure.
soil-like	8	cohesive
soil-like	9	non-cohesive

The distribution of rock weathering is presented graphically as pie charts in Figure 5-4. Fresh (F) and slightly weathered (S) rock accounts for approximately 60% to 70% of the total length cored in the welded tuff units, TCw, TSw1, and TSw2. The PTn unit had 20% of the core length moderately weathered.

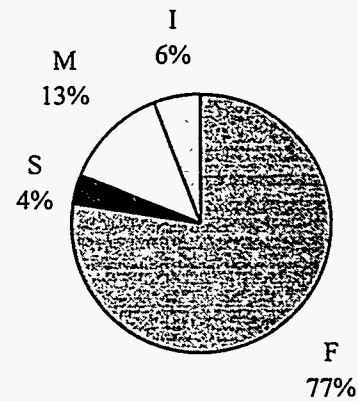
The many competing technical requirements for analysis of the YMP core materials have placed limitations on the activities required to determine core hardness. Actual scratching of the core and further breakage by hammer blows have, therefore, not been performed and the hardness ratings described in Table 5-4 are subjectively estimated values. This estimation process was not judged to adversely impact data quality because extensive rock mechanics lab tests and Schmidt hammer rebound hardness measurements were being performed on the same core.

F=Fresh, S=Slightly Weathered, M=Moderately Weathered, I=Intensely Weathered, D=Decomposed

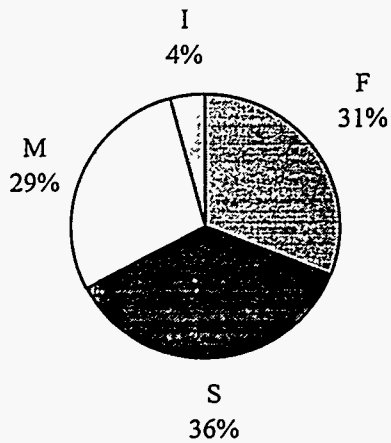
TCw Nonlithophysae Unit



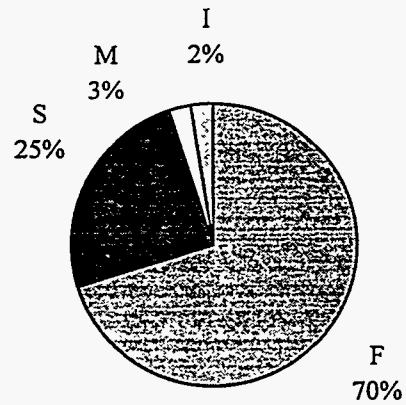
TCw Lithophysae-Rich Unit



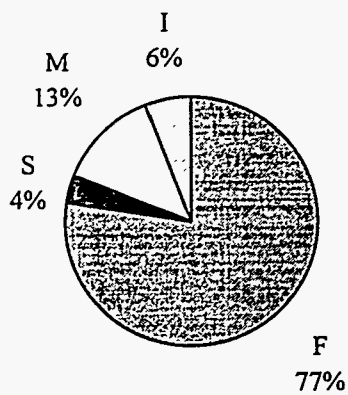
PTn Unit



TSw1 Nonlithophysae Unit



TSw1 Lithophysae-Rich Unit



TSw2 Unit

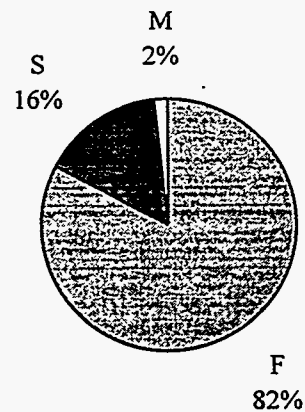


Figure 5-4. Distribution of the Weathering Parameters in Rock for Thermomechanical (Thermal-Mechanical) Units —NRG Holes

The distributions of estimated rock hardness are shown in pie charts presented in Figure 5-5 for the different thermomechanical (thermal-mechanical) units. Most of the rock in the welded tuff units were estimated to be in the very hard (2), hard (3) or moderately hard (4) categories with the highest percentage in the hard (3) category. The PTn unit rock is much softer than the welded tuffs, and approximately half of the core in the PTn unit was estimated to be in the soft (6) and very soft (7) categories.

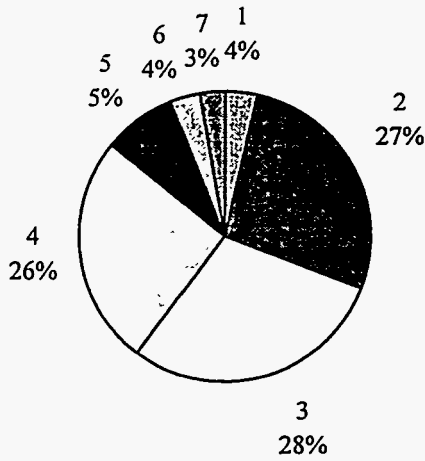
5.5 Lithophysae Content

The surface area percentage of lithophysal and other cavities or voids observed on the surface of the core is estimated for each run interval using standard charts for estimating mineral contents in thin sections. The methodology for the estimation is described in Appendix A. Run interval estimates are then composited by length-weighted average on 3-m (10-ft) intervals in the Geology and Rock Structure Logs and Rock Structure Summary Logs in Volume II. This estimate does not account for lithophysae larger than the core, which are observed in the borehole video logs in some high lithophysal content zones.

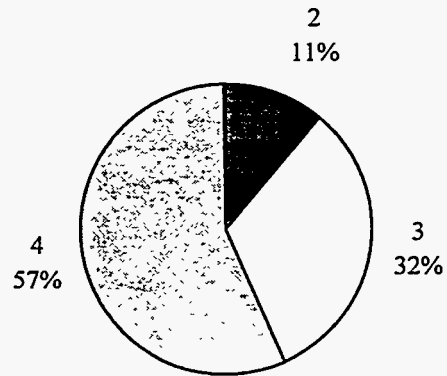
The distribution of estimated lithophysal content is shown as bar charts for each thermomechanical (thermal-mechanical) unit in Figure 5-6. Table 5-5 lists the mean value, median value, and sample standard deviation for each unit.

1=Extremely Hard, 2=Very Hard, 3=Hard, 4=Moderately Hard, 5=Moderately Soft, 6=Soft, 7=Very Soft, 8=Soil-Like, Cohesive, 9=Soil-Like, Non-Cohesive

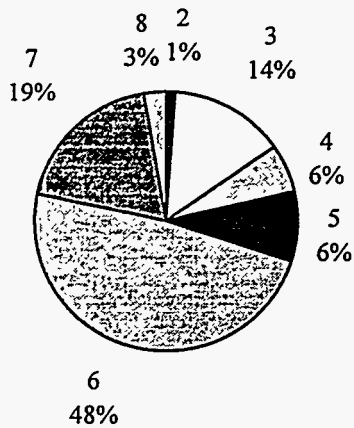
TCw Nonlithophysae Unit



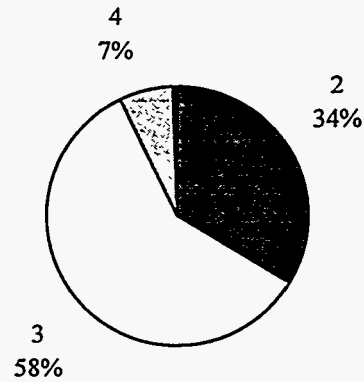
TCw Lithophysae-Rich Unit



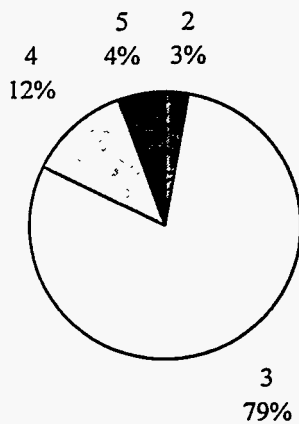
PTn Unit



TSw1 Nonlithophysae Unit



TSw1 Lithophysae-Rich Unit



TSw2 Unit

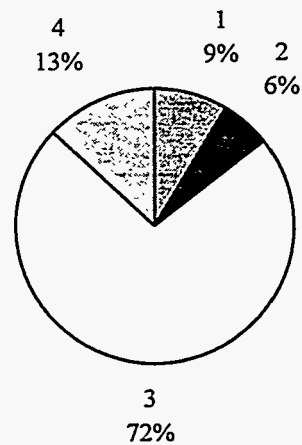


Figure 5-5. Pie Charts Showing Distribution of Estimated Hardness Rating as a Percentage of Total Drilling in Thermomechanical (Thermal-Mechanical) Units—NRG Holes

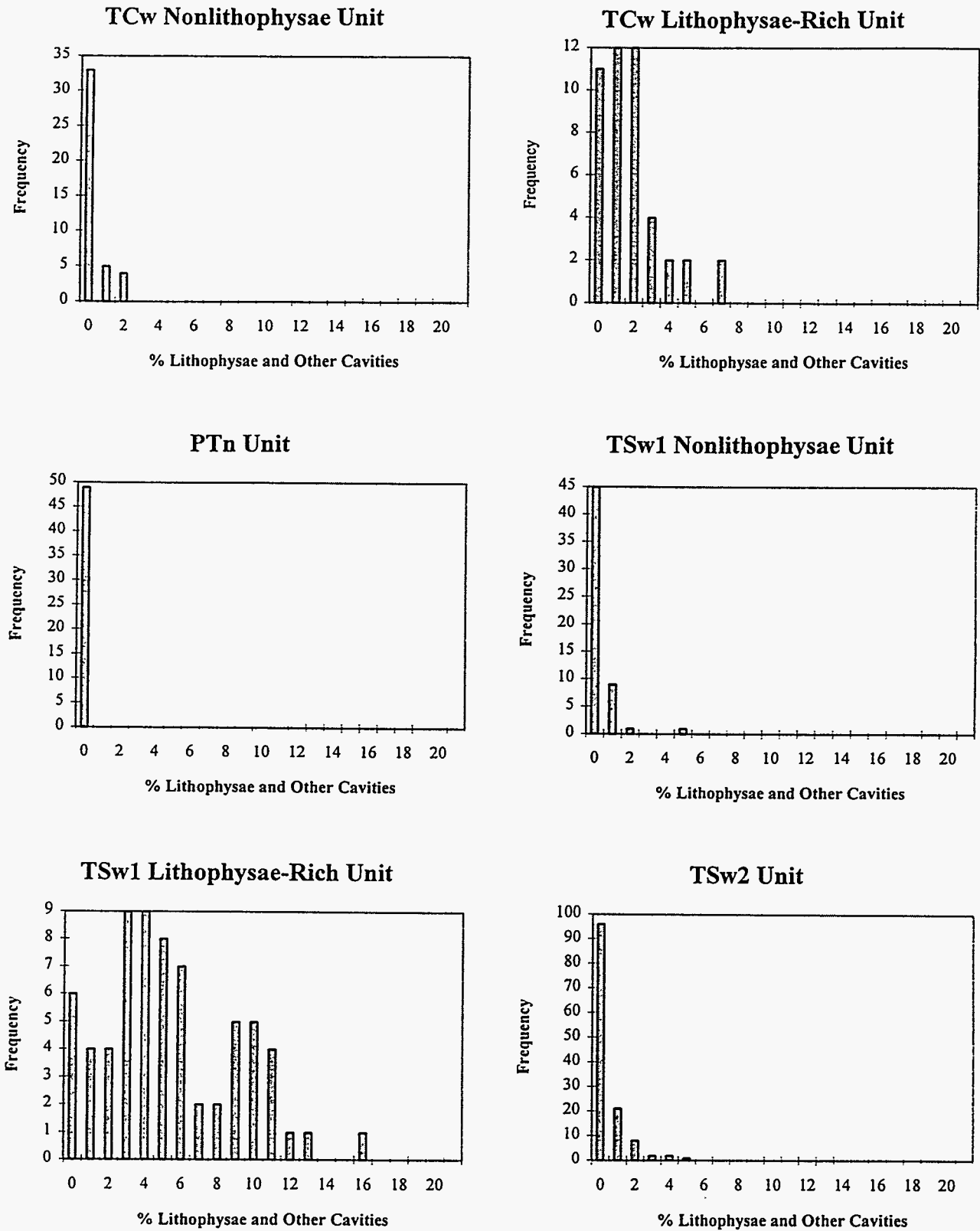


Figure 5-6. Histograms of the Distribution of the Percent Lithophysae and Other Cavities in Each Thermomechanical (Thermal-Mechanical) Unit—NRG Holes

Table 5-5. Comparison of Mean, Median, and Standard Deviation of Estimated Lithophysae and Other Void Content in the Thermomechanical (Thermal-Mechanical) Units — NRG Holes

Thermomechanical (Thermal-Mechanical) Unit	Mean (%)	Median (%)	Standard Deviation (%)
TCw-NL	0.3	0	0.64
TCw-LR	1.7	1	1.74
PTn	0.0	0	—
TSw1-NL	0.3	0	0.78
TSw1-LR	5.4	5	3.67
TSw2	0.4	0	0.90

NL—Nonlithophysal; LR—Lithophysae Rich

5.6 Fracture Data

The structural logging data for the NRG-series core holes contain extensive description of fractures and other structural features that occur in the core. The information recorded for each individual fracture can include:

- ♦ structural feature type,
- ♦ fracture inclination,
- ♦ fracture mineral infilling,
- ♦ fracture infilling thickness,
- ♦ fracture planarity, and
- ♦ fracture roughness.

Detailed instructions for the description of the fracture characteristics are discussed in Appendix A. The distribution of each of these fracture characteristics is described in the following subsections. Prediction of fracture frequencies based on the recorded information is also described.

5.6.1 Feature Type

Four categories of structural features that cross cut the core are described during logging of the core.

- N — natural fractures I — indeterminate (uncertain origin) fractures
 C — coring-induced fractures V — vug or void larger than core

Figure 5-7 presents the distribution of feature types as bar charts with the percentage of total occurrence recorded above the bar. Fractures identified as coring induced have the largest proportion of occurrence in all units. The total number of recorded features and the numbers of natural (N), coring-induced (C), and indeterminate (I) fractures are tabulated in Table 5-6. The coring-induced fractures in the PTn unit and the TSw1 lithophysae-rich portion are 69.8% and 73.0% of the total fractures, respectively.

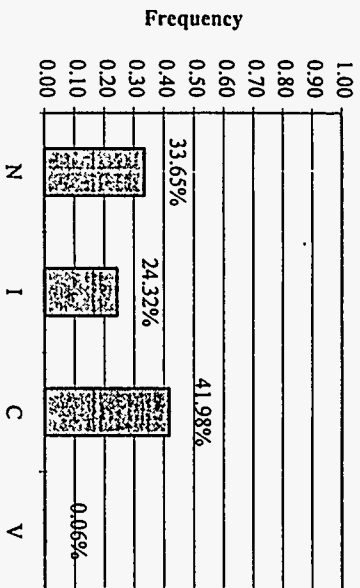
Table 5-6. Distribution of Core Structural Features by Type and Thermomechanical (Thermal-Mechanical) Unit — NRG Holes

Thermomechanical (Thermal-Mechanical) Unit	Total Features	Natural N	Indeterminate I	Coring Induced C	Voids V
TCw—total	2738	812	751	1173	2
nonlithophysal	1801	606	438	756	1
lithophysae rich	937	206	313	417	1
PTn	1109	119	216	774	0
TSw1—total	3108	601	692	1814	1
nonlithophysal	1684	468	441	775	0
lithophysae rich	1424	133	251	1039	1
TSw2	3343	709	561	2071	2

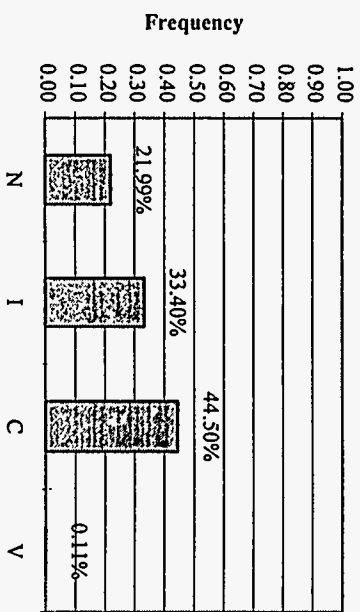
Only the natural (N) and indeterminate (I) features have been considered in the following Sections 5.6.2 through 5.6.5.

N=Natural Fracture, C=Coring-Induced Fracture, I=Indeterminate Fracture, V=Vug or Large Void

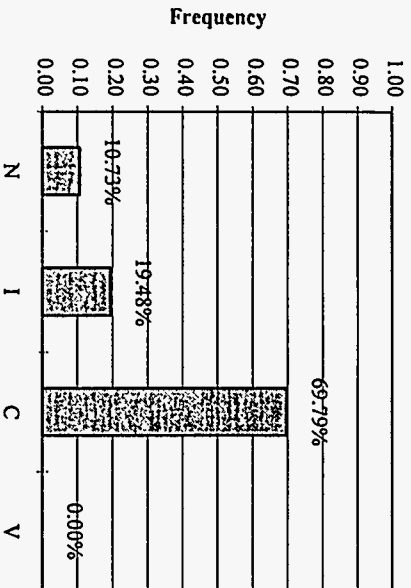
TCw Nonlithophysae Unit



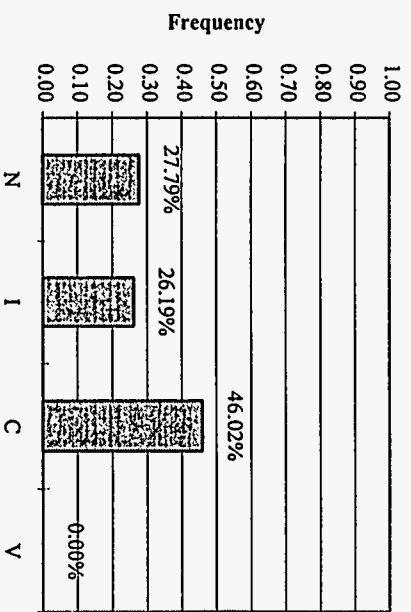
TCw Lithophysae-Rich Unit



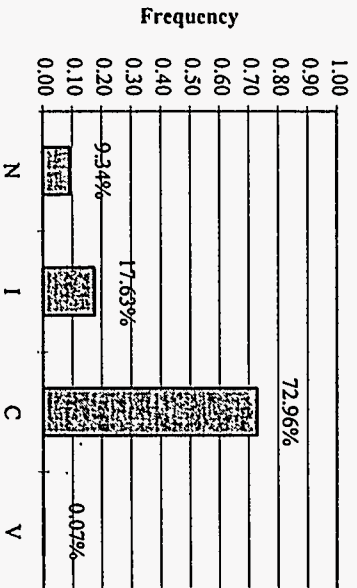
PTn Unit



TSw1 Nonlithophysae Unit



TSw1 Lithophysae-Rich Unit



TSw2 Unit

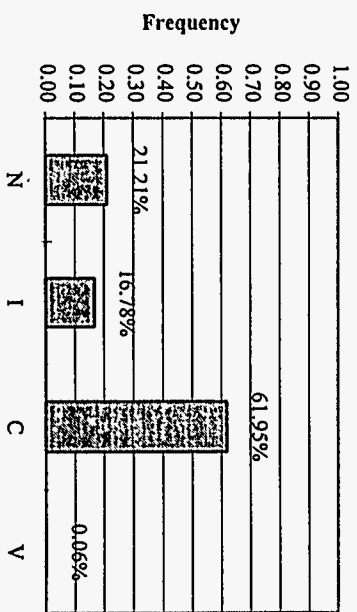


Figure 5-7. Bar Charts Showing the Distribution of Structural Features in Each Thermo-mechanical (Thermal-Mechanical) Unit—NRG Holes

5.6.2 Fracture Inclination

The fracture inclination is measured as the angle between the plane normal to the core axis and the fracture plane (dip angle for vertical holes). All fractures with a non-zero inclinational angle were logged as either "N" or "I" types. Drilling-induced (C) features generally had zero-degree inclinations. The NRG core holes were drilled vertically downward with the exceptions of NRG-2 and NRG-3 which were both inclined approximately 30° from vertical. Figure 5-8 presents the fracture inclination data as bar charts of the frequency of occurrence. Data from NRG-2 and NRG-3 are excluded from the presentation because the hole inclination makes the dip angle indeterminate.

Sampling the inclination of fractures with a core hole introduces a bias in favor of fractures perpendicular to the drill hole axis. Figure 5-8 indicates the fractures with low dip angles occurred most frequently in all the units except TSw2. Terzaghi's (1965) correction procedure was applied to the core hole data to correct for the sampling bias and estimate the true distribution of fracture inclination. The fracture frequencies presented in next subsection were calculated by applying this procedure.

5.6.3 Calculated Fracture Frequencies

The abundance of fractures in the rock mass can be quantitatively represented by the fracture frequency. Three types of fracture frequencies are calculated and presented in this section: the uncorrected linear fracture frequency along the drill hole axis, corrected linear fracture frequency for each joint set inclined in 10-degree intervals, and volumetric fracture frequency in a unit volume of rock. Procedures used for calculating these three types of fracture frequencies has been previously described by Lin et al. (1993a).

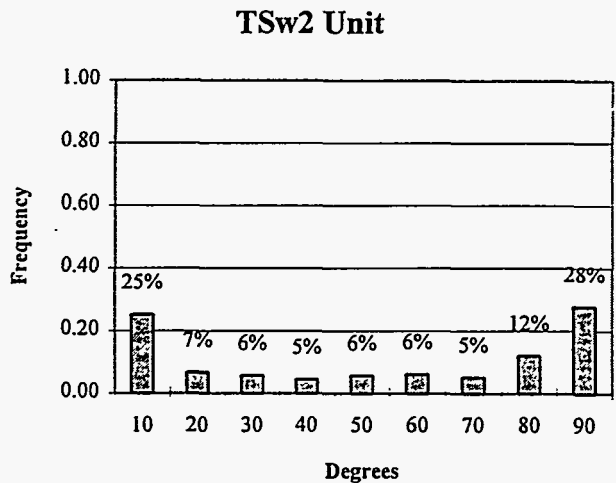
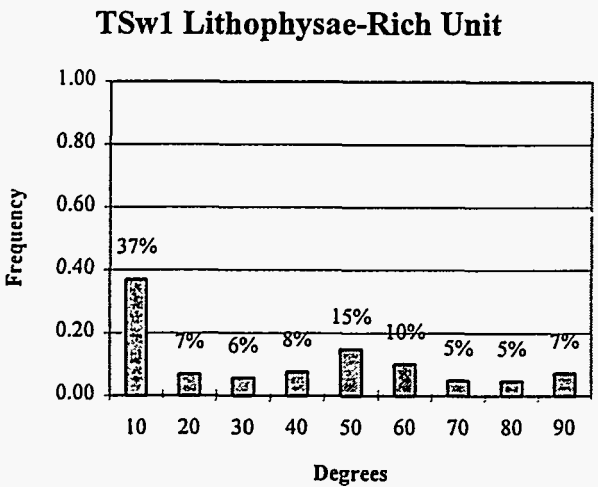
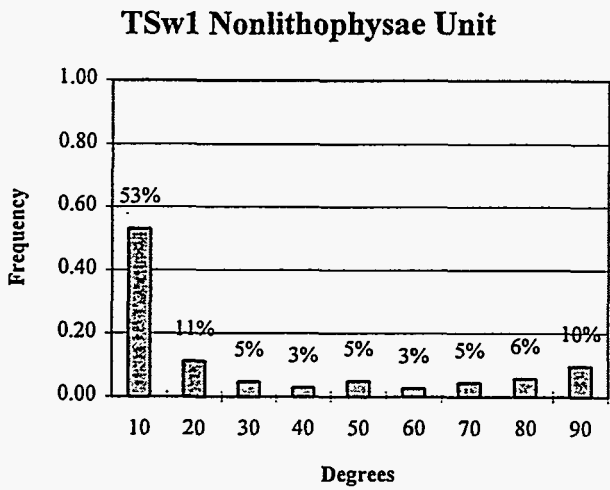
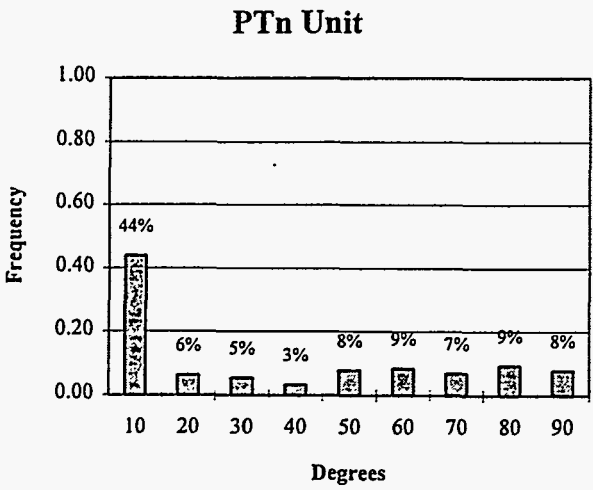
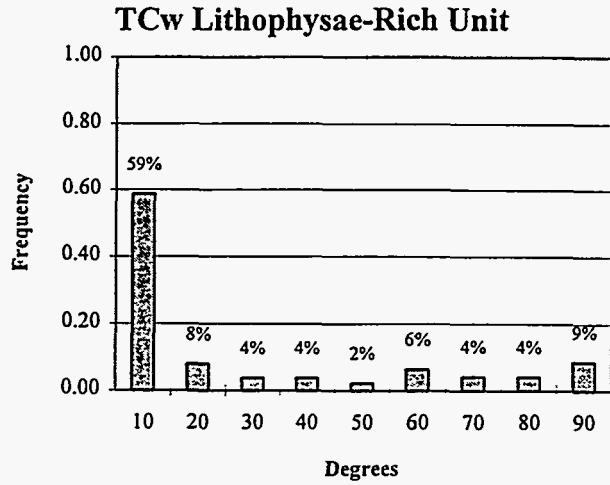
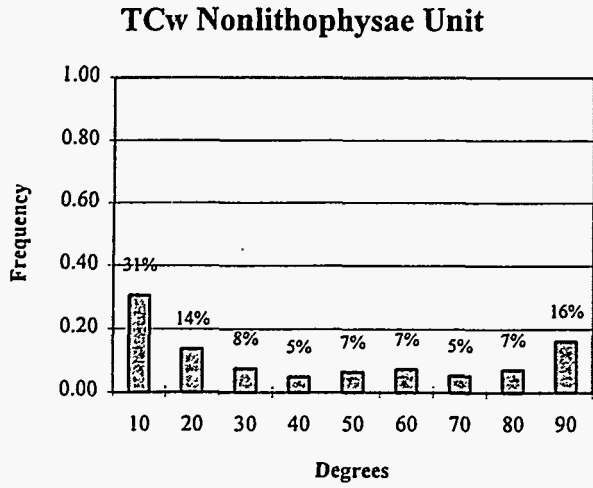


Figure 5-8. Bar Charts Showing the Distribution of Fracture Inclinations (without Terzaghi correction) in the Thermomechanical (Thermal-Mechanical) Units—NRG-1, -2A, -2B, -4, -5, -6, -7/7A

Uncorrected linear fracture frequency along the drill hole axis was computed by dividing the total number of fractures by the length of whole core recovered in the unit (lost core and rubble excluded). Table 5-7 lists the total number of fractures, the length of core in each thermomechanical (thermal-mechanical) unit, and the linear fracture frequency (LFF—per linear foot and per linear meter) along the drill hole axis. The fracture frequency in the welded units is similar, ranging between 6.2 m^{-1} and 8.25 m^{-1} , but decreased with increasing depth. Fracture frequency in the PTn unit is less than 50% of the values in the welded units.

Table 5-7. Summary of Uncorrected Linear Fracture Frequency (LFF)

Thermomechanical (Thermal-Mechanical) Unit	Total Whole Core Recovered* m (ft)	Total No. of Fractures	LFF (ft ⁻¹)	LFF (m ⁻¹)
TCw-NL	126.48 (415.0)	1044	2.5	8.25
TCw-LR	69.83 (229.1)	519	2.3	7.43
PTn	114.34 (375.1)	335	0.9	2.93
TSw1-NL	135.37 (444.1)	909	2.0	6.71
TSw1-LR	105.60 (346.5)	384	1.1	3.64
TSw2	204.42 (670.7)	1270	1.9	6.21

NL—Nonlithophysal; LR—Lithophysae Rich

*less rubble zones and lost core

The corrected linear fracture frequency is defined as the number of fractures that would exist for a unit length along a line perpendicular to the fracture plane. The corrected fracture frequency, Table 5-8, was calculated by summing the total number of fractures in 10° dip increments for the total whole core recovered in all holes and calculating percentage in each dip interval. Terzaghi's (1965) correction procedure, shown in equation 5-2, was then applied to adjust for the sampling bias caused by the angle between the core hole and each fracture plane. The correction factor is cut off at a value of 11.3 for the 80° – 90° dip range. Table 5-8 lists the corrected linear fracture frequency for each thermomechanical (thermal-mechanical) unit, determined by equation 5-2:

Table 5-8. *Corrected Fracture Frequency by Fracture Inclination (m⁻¹)

Thermal-Mechanical Unit	Fracture Dip (degrees)								
	10	20	30	40	50	60	70	80	90
TCw-NL	1.64	0.61	0.61	0.90	2.14	1.95	1.85	1.83	9.89
TCw-LR	4.03	0.56	0.28	0.31	0.22	0.76	0.67	1.09	6.79
PTn	1.29	0.19	0.18	0.12	0.33	0.43	0.48	1.06	2.65
TSw1-NL	3.60	0.78	0.35	0.24	0.47	0.32	0.72	1.52	7.56
TSw1-LR	0.89	0.18	0.24	0.24	0.28	0.30	0.58	1.42	13.40
TSw2	1.57	0.43	0.40	0.35	0.51	0.68	0.77	2.92	19.76

NL—Nonlithophysal; LR—Lithophysae Rich

*Terzaghi's correction applied.

$$\lambda_c = \lambda \left(\frac{P(\phi)}{\cos(90 - \phi)} \right) \quad (5-2)$$

where λ_c = corrected fracture frequency (no. of fractures ÷ whole core interval) for a dip interval (m⁻¹),

λ = total uncorrected linear fracture frequency (m⁻¹),

$P(\phi)$ = measured percentage of total fractures in the sampled dip interval, and

ϕ = angle between the hole axis and the midpoint of the dip interval.

The fracture frequency is based upon the length of core recovered as whole core and excludes lost core and rubble zones.

The corrected fracture frequencies in Table 5-8 are in agreement with similar data from previous YMP drilling (Lin et al., 1993a) and mapping data indicate the predominance of near vertical fractures. The use of the Terzaghi correction has been questioned because of the large correction that occurs for fractures parallel to the hole. Lin et al. (1993a) performed some statistical tests in an attempt to evaluate the use of the correction and reported very good agreement if fracture continuity is 100%. For lower values of fracture continuity, the Terzaghi correction was shown to underestimate the fracture frequency. The drilling data as corrected are therefore judged to accurately portray a relatively high density of near vertical fractures,

especially in the TSw2. However, since joint persistence (length) is not characterized by drilling, the proportion of those fractures whose persistence and continuity will affect the excavation is not known.

Volumetric fracture frequency, a nondirectional parameter without the sampling bias, is estimated from the number of fractures in a sphere with a diameter of 1 m. It is linearly proportional to the total sum of the corrected fracture frequencies for all 10-degree intervals. The computed volumetric fracture frequencies are presented in Table 5-9 and are in agreement with interpretations of previous YMP data (Lin et al., 1993a).

Table 5-9. *Volumetric Fracture Frequency in a Unit Volume of Rock (m⁻³)

Thermomechanical (Thermal-Mechanical) Unit	Volume of Fracture Frequency
TCw-NL	26.56
TCw-LR	18.27
PTn	8.35
TSw1-NL	19.31
TSw1-LR	21.72
TSw2	33.97

NL—Nonlithophysal; LR—Lithophysae Rich

*Terzaghi's correction applied.

RQD values have been calculated using expressions based on fracture frequency to assure that RQD values derived in the core logging are reasonable and have not been distorted by the use of vertical boreholes to sample the predominantly vertical structural fractures. The converted linear fracture frequency was calculated by summing all the dip intervals and used to calculate RQD using equation 5-3 proposed by Hudson and Priest (1979):

$$RQD = 100e^{-0.1\lambda} (0.1\lambda + 1.0) \quad (5-3)$$

where λ = average fracture frequency (m⁻¹).

A second estimate was calculated based upon the volumetric fracture frequency listed in Table 2-9 using an expression proposed by Barton et al. (1974) and presented in equation 5-4.

$$RQD = 115 - 3.3 J_v \quad (5-4)$$

where J_v = joints per unit volume (m^{-3}).

Table 5-10 lists the results of the calculation for each thermomechanical (thermal-mechanical) interval and compares them to the median value of RQD from the core data. The calculated RQD agree well for both equations 5-3 and 5-4 with the exception of the TSw2 unit. At high values of volumetric fracture frequency, the RQD predicted by equation 5-4 can become a negative value. The RQD data from core logging includes the effects of rubble zones and lost core intervals and is generally lower than the values calculated based on fracture frequency. There is no indication that the core-derived RQD data is producing an overestimate of conditions due to the use of vertical boreholes for characterization.

Table 5-10. Comparison of Median RQD from Core to RQD Values Calculated Using Fracture Frequency

Thermomechanical (Thermal-Mechanical) Unit	Calculated RQD (%)		Median RQD (%) from Core Logging
	Corrected Linear Fracture Frequency**	Corrected Volumetric Fracture Frequency***	
TCw—NL*	36.9	29.2	26
TCw—LR*	56.8	54.7	22
PTn	85.4	87.4	39
TSw1—NL*	53.9	51.3	30
TSw1—LR*	47.7	43.3	14
TSw2	24.2	2.9	8

*NL—Nonlithophysal; LR—Lithophysae Rich

**Calculated by linear fracture frequency—Hudson and Priest (1979).

***Calculated by volumetric fracture frequency—Barton et al. (1974).

5.6.4 Fracture Infill Mineralization and Thickness

Fourteen categories of infill mineralization and six categories of infill thickness were used to describe the fracture infill. These categories and their log abbreviations are listed below:

Mineralization

C	— clean,	SI	— silica
WC	— white, crystalline	MN	— manganese
WN	— white, non-crystalline	CA	— calcite
BC	— black crystalline	CL	— clay
BD	— black dendritic	TN	— tan, non-crystalline
TD	— brown dendritic	FE	— iron
TC	— tan crystalline	BN	— brown, non-crystalline

Thickness

C	— clean, no filling	M	— moderately thick (0.1-0.4 inch)
S	— very thin, surface sheen	V	— very thick (0.4-1.0 inch)
T	— thin (up to 0.1 inch)	E	— extremely thick (>1.0 inch)

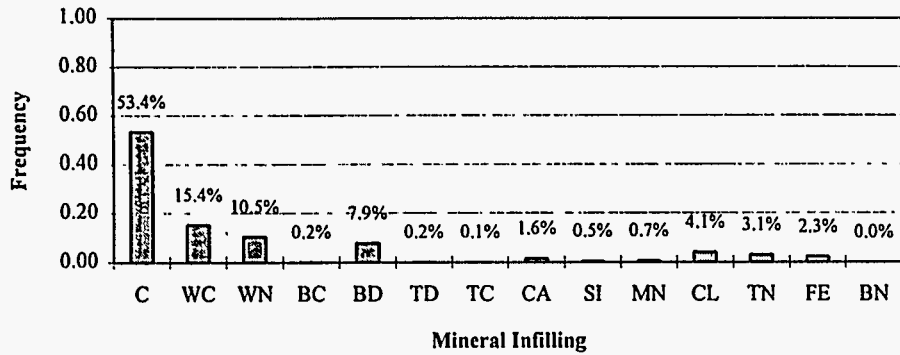
Infill descriptions include both specific mineral types and generic descriptions based on physical characteristics. The generic descriptions are utilized because in many cases, several different minerals have a similar appearance, and often these minerals cannot be identified without laboratory analysis.

Infill thickness, on the fractures not described as clean, were mostly limited to surface sheens or thin coatings. In any thermomechanical (thermal-mechanical) unit, the maximum number of fractures with infill thickness greater than a surface sheen was 16.8% of the total.

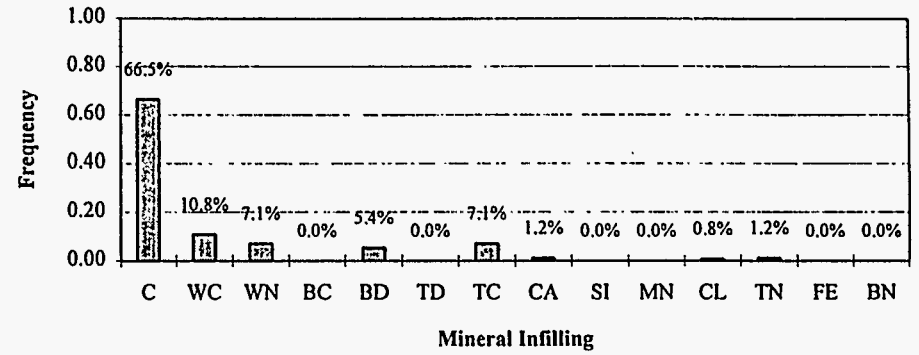
The distribution of infill mineralization and thickness data from the NRG holes are presented in Figures 5-9 and 5-10, respectively. The distributions indicate that clean joint surfaces are predominant, ranging between 53.4% and 84.9% of the occurrences for the different thermomechanical (thermal-mechanical) units. Fractures with white crystalline (WC) and white non-crystalline (WN) infill also appear to be abundant and accounted for approximately 15% to 25% of the total fractures. Clay infilling are scarce for all units. The observed fractures in the nonlithophysal portion of the TCw unit contained the highest percentage of clay infilling at approximately 4% of the total fractures.

C=Clean, WC=White Crystalline, WN=White Noncrystalline, BC=Black Crystalline, BD=Black Dendritic, TD=Brown Dendritic
 TC=Tan Crystalline, TN=Tan Noncrystalline, CA=Calcite, SI=Silica, MN=Manganese, CL=Clay

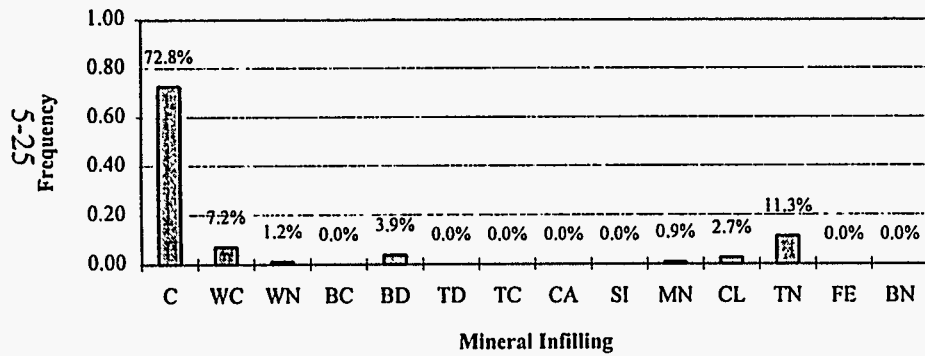
TCw Nonlithophysae Unit



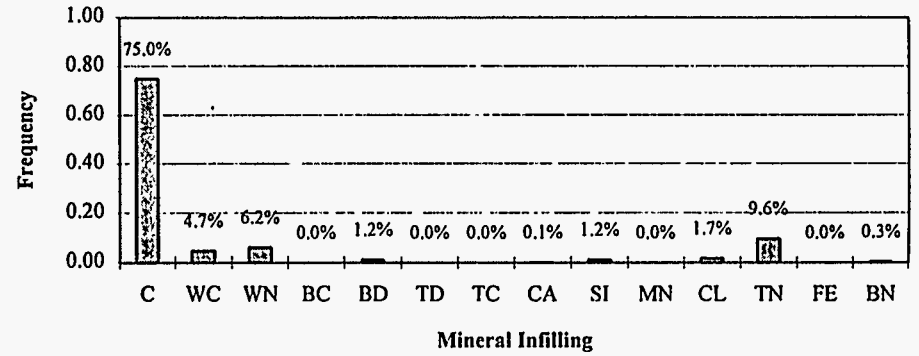
TCw Lithophysae-Rich Unit



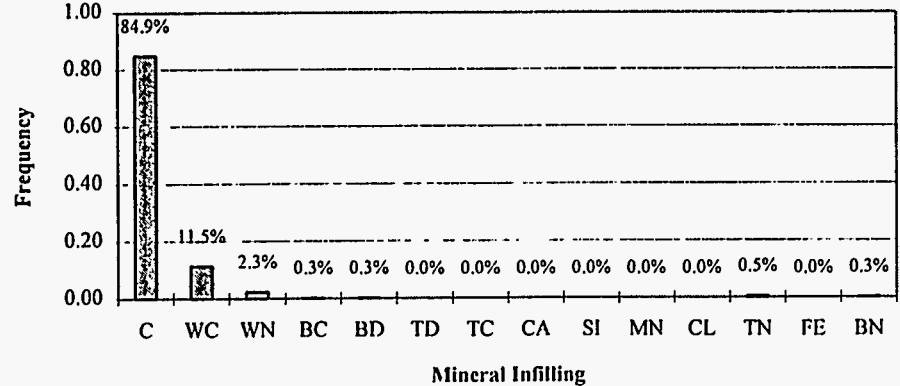
PTn Unit



TSw1 Nonlithophysae Unit



TSw1 Lithophysae-Rich Unit



TSw2 Unit

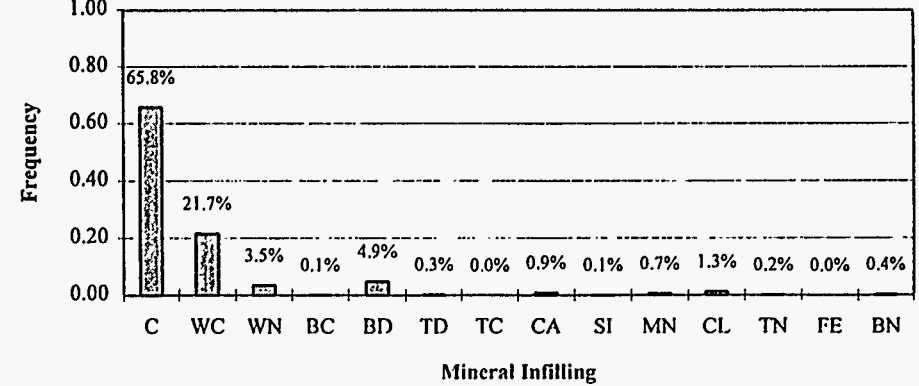


Figure 5-9. Bar Charts Showing the Distribution of Fracture Mineral Infillings in the Thermomechanical (Thermal-Mechanical) Units—NRG Holes

C=Clean; S=Very thin, surface sheen; T=Thin (<0.1"); M=Moderately thick (0.1-0.4");
 V=Very thick (0.4-1.0"); E=Extremely thick (>1")

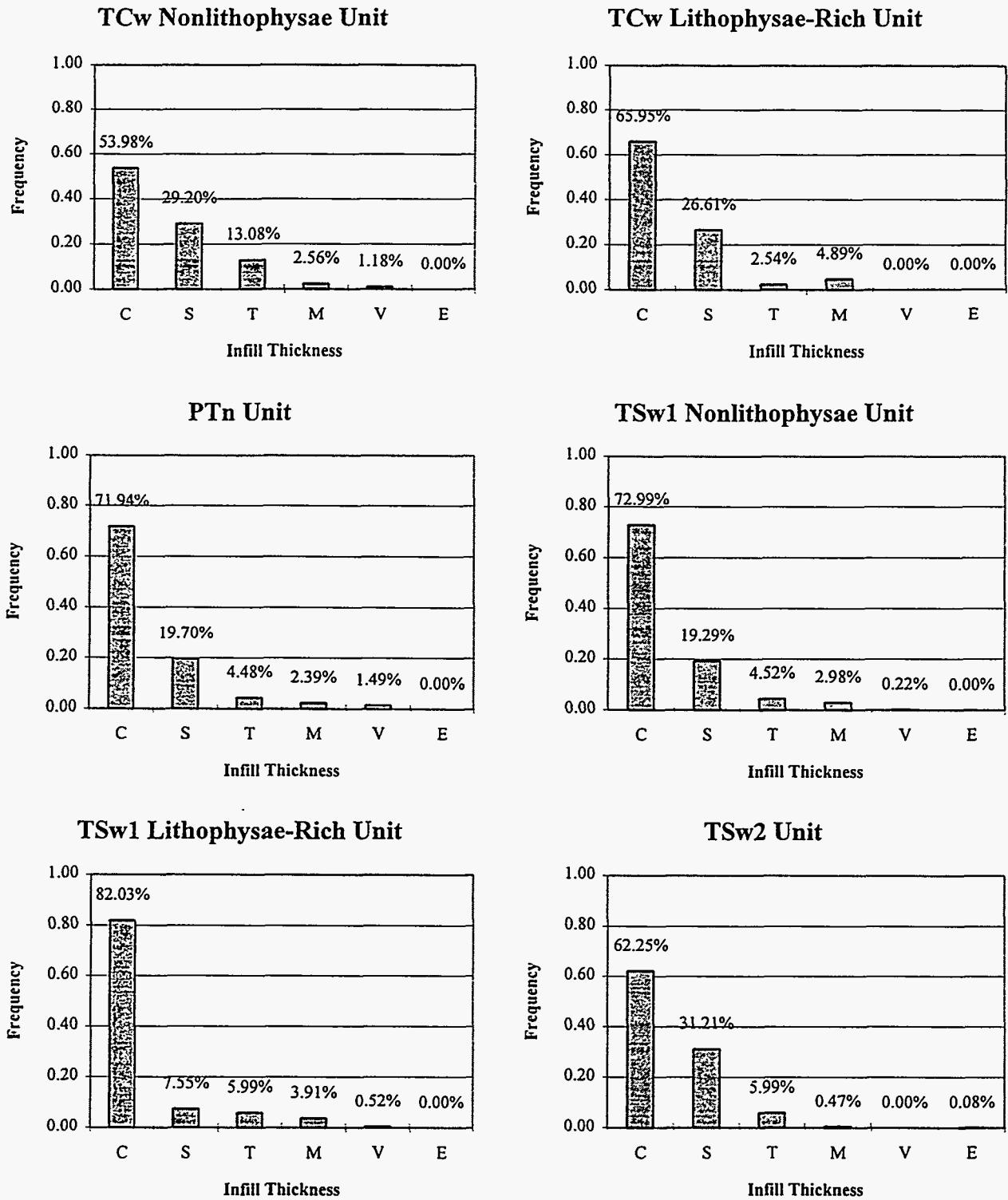


Figure 5-10. Bar Charts Showing the Distribution of Fracture Infill Thickness in the Thermo-mechanical (Thermal-Mechanical) Units—NRG Holes

5.6.5 Fracture Planarity and Roughness

The abbreviations and corresponding descriptions of the fracture planarity and roughness are listed below:

Planarity

P — planar
C — curved

S — stepped
I — irregular

Roughness

V — very rough
R — rough
M — moderately rough

S — smooth
I — polished

The distributions of fracture planarity and roughness are presented in Figures 5-11 and 5-12, respectively. Most of the fractures have either a planar (P) or irregular (I) surface with moderate (M) roughness. This parameter describes the small-scale roughness of the fractures and indicates that the fractures would have generally higher friction factors due to the requirement of fractures to dilate (open) to allow shear movement.

5.7 Analysis of Rock Structural Character where Boreholes Intersect Faults

The character of the core in boreholes that have intersected faults is of interest in defining rock mass quality variation in the area of the fault. Three of the NRG-series boreholes penetrate faults: holes NRG-2 and -2B intersect the Bow Ridge Fault, and NRG-3 intersects a possible minor normal fault.

NRG-2 was inclined 30° from vertical and drilled in the direction S80°E to penetrate nonwelded units of the Timber Mountain Group and welded units of the Tiva Canyon Tuff juxtaposed by the Bow Ridge Fault. At the elevation of the North Ramp, Pre-Rainier Mesa Tuff

P=Planar, C=Curved, S=Stepped, I=Irregular

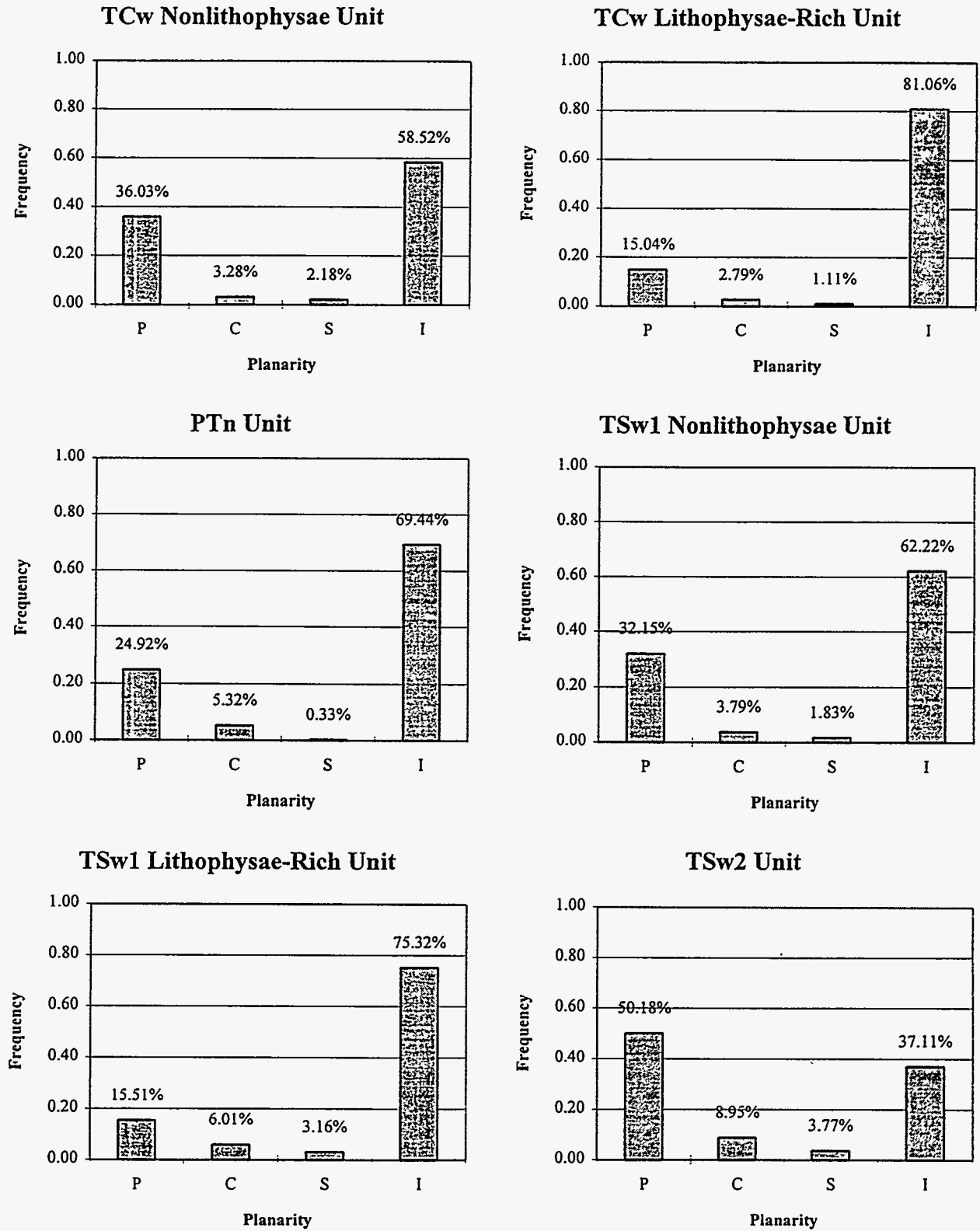


Figure 5-11. Bar Charts Showing the Distribution of Fracture Planarity in the Thermo-mechanical (Thermal-Mechanical) Units—NRG Holes

V=Very Rough, R=Rough, M=Moderately Rough, S=Smooth, P=Polished

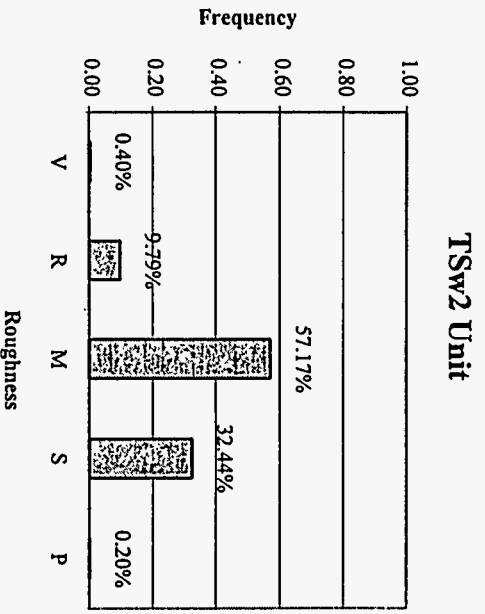
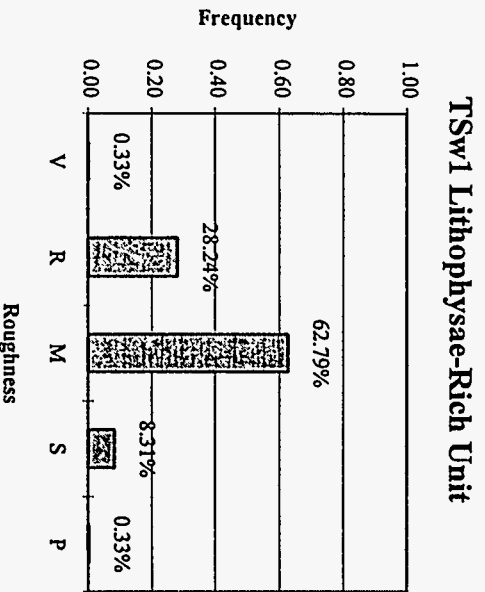
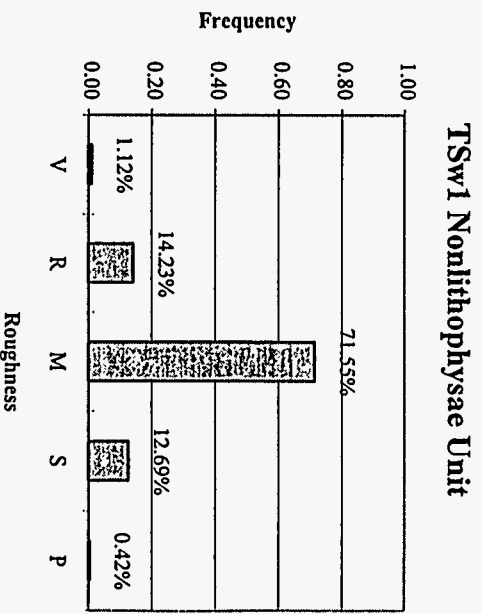
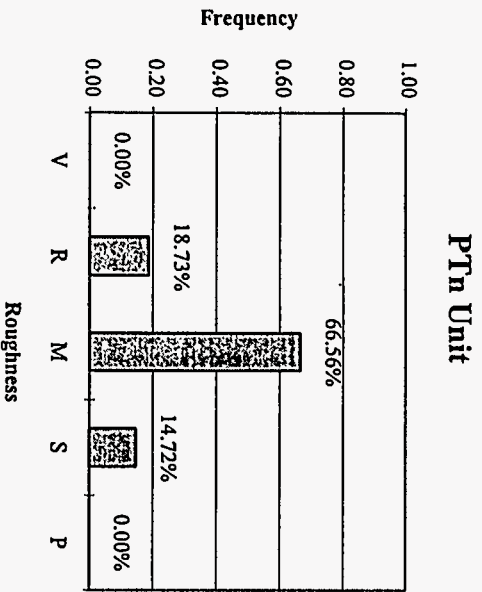
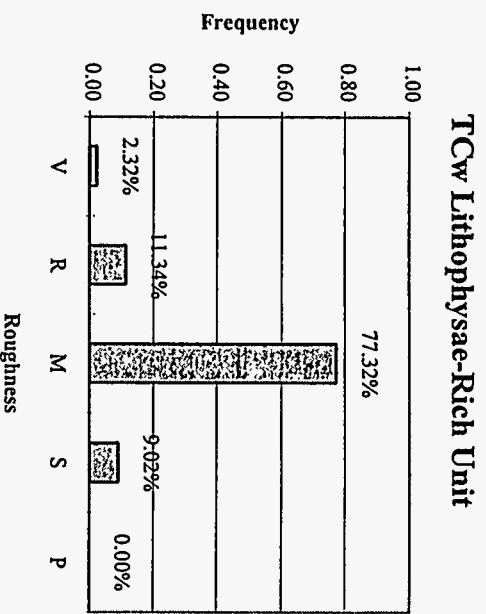
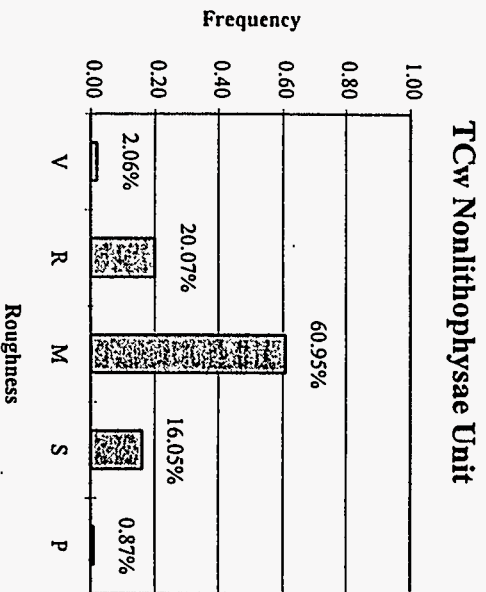


Figure 5-12. Bar Charts Showing the Distribution of Fracture Roughness in the Thermo-mechanical (Thermal-Mechanical) Units—NRG Holes

Bedded Tuff is present in the hanging wall, downfaulted against the crystal-poor lower nonlithophysal zone of the Tiva Canyon Tuff in the footwall.

Fracture frequency and RQD data for NRG-2 over 3-m (10-ft) intervals are summarized in Figure 5-13 for the zones on both sides of the Bow Ridge Fault. Borehole depths of 0–39.63 m (0–130 ft) in the hanging wall are in nonlithified, nonwelded tuffs resulting in poor recoveries and rubblization of the core. Better recoveries, and correspondingly higher RQD and fracture frequency data, were recorded from 39.62 m (130 ft) to the Bow Ridge Fault at 51.76 m (169.8 ft) in lithified, nonwelded tuffs. The interval ending at 51.82 m (170 ft) contains the Bow Ridge Fault Zone and is characterized by lack of recovery and rubble from 50.17 to 51.76 m (164.6 to 169.8 ft). This interval shows a slight decrease in fracture frequency, as would be expected with the unrecovered interval, but a slight increase in RQD. The intervals below the fault are in densely welded rocks of the Tiva Canyon and show a gradual increase in fracture frequency and a decrease in RQD with increasing distance from the fault. These trends are the opposite of what would be expected if fracturing was related to faulting, and suggest that the observed footwall rock quality may be more a function of stratigraphic variability.

Borehole NRG-2B intersects a part of the Bow Ridge Fault that downfaulted the nonwelded Tuff Unit "X" against the Pre-Tiva Canyon Tuff Bedded Tuff of the Upper Paintbrush Nonwelded Unit. The Bow Ridge Fault is identified in this hole as a zone of altered and broken core with significant unrecovered intervals from 70.81-m (232.3-ft) to 79.25-m (260.0-ft) depth. The fracture frequency and RQD values shown in Figure 5-13 are low within the fault zone largely because of the unrecovered intervals. Other trends are an increase of

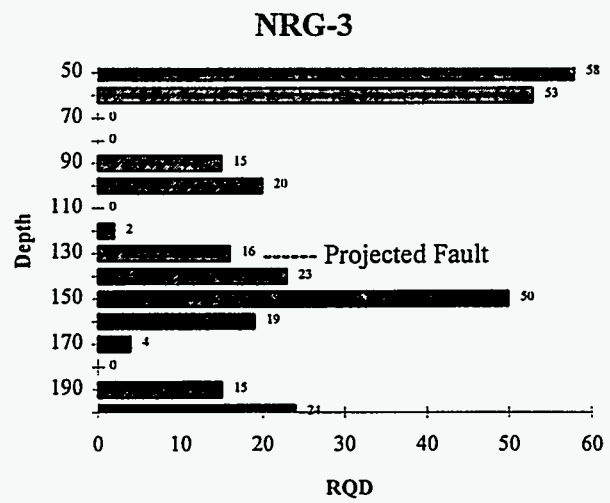
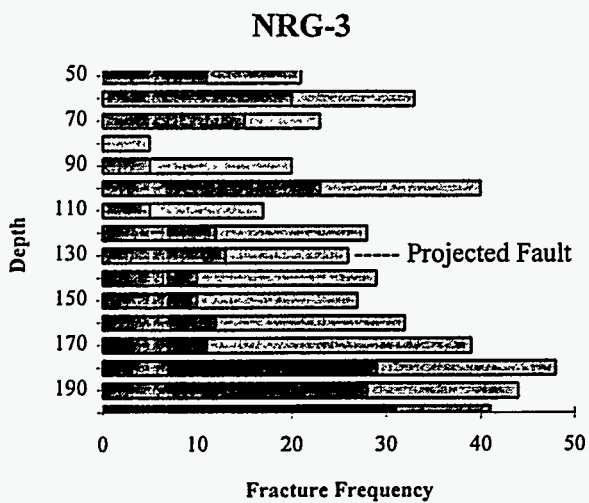
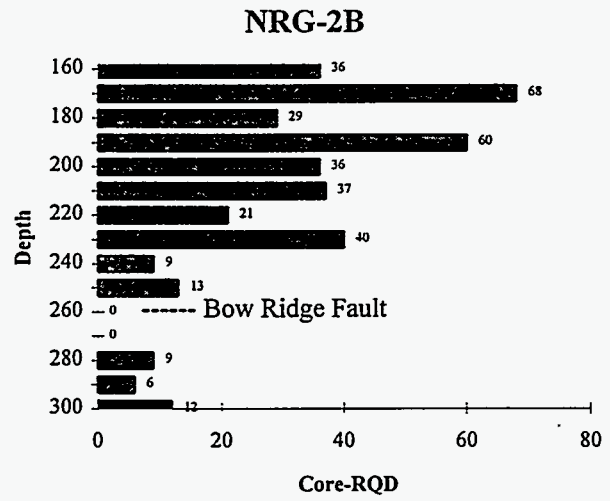
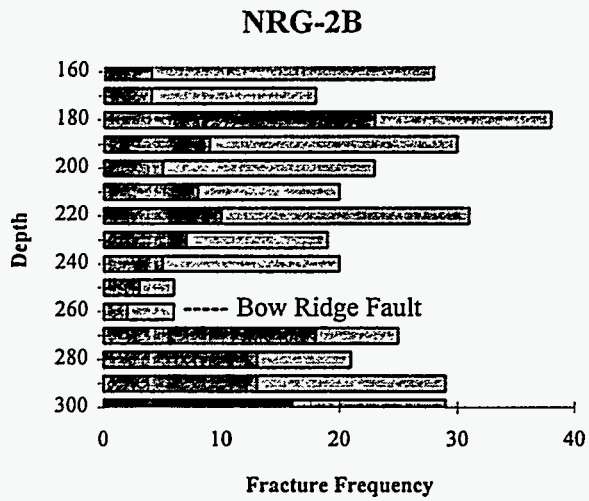
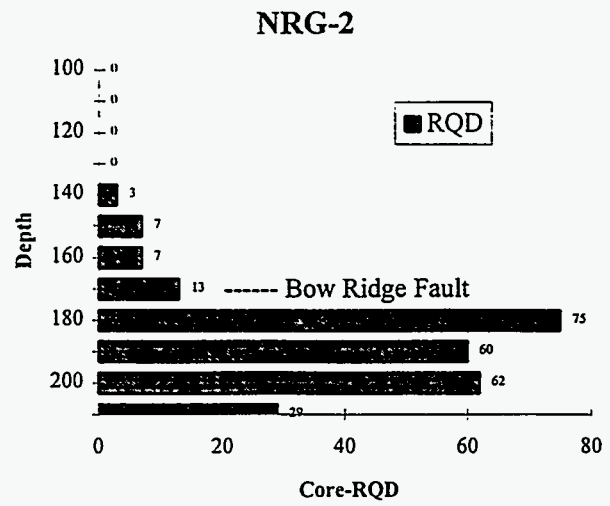
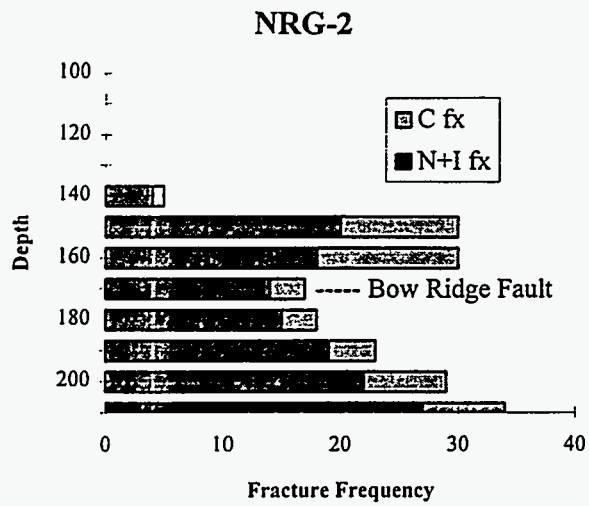


Figure 5-13. Fracture Frequency (uncorrected) and RQD Data in the Vicinity of Fault Zones Encountered in Holes NRG-2, -2B, and -3

natural and indeterminate fractures and a decrease in RQD values in the footwall relative to the hanging wall. These trends are most likely attributed to the contrast in lithology across the fault.

Borehole NRG-3 is another inclined hole at 30° from vertical drilled at N80E, and penetrates a possible normal fault with no apparent offset based on the stratigraphy. The fault was not recognized in lithologic logging, but was projected from surface mapping.

Fracture frequency and RQD data vary throughout the interval as shown in Figure 5-13. The projection of the fault coincides with a zone of relatively little variation in fracture frequency, but with an increase in RQD values with depth. The presence of high RQD values without a decrease in fracturing suggests that these values are not related to fracturing due to faulting. Elsewhere in the hole, zones of low RQD coincide with intervals of rubble and unrecovered core.

No regular trends are visible within the NRG data to indicate a significant increase in fracture frequency or rock damage in proximity to fault zones. Within the normal faults sampled by NRG drilling, modification of rock quality by faulting appears significant only within the faults with larger displacement such as the Bow Ridge Fault, and appears to be restricted to a localized zone of breccia, alteration, and gouge development.

Fracture frequency and RQD data did not show significant changes near the fault penetrated by NRG-2 or the possible fault penetrated by NRG-3, at least within the resolution of the Geology and Rock Structure Log.

The Drill Hole Wash Fault to be encountered at ramp station 21+04 m has not been sampled by NRG-series boreholes. Scott et al. (1984) describe some of the northwest-trending strike-slip faults in this part of Yucca Mountain as having breccia zones 20 or more meters wide.

The Drill Hole Wash Fault is concealed by alluvium along the ramp alignment. Buesch et al. (1994) have mapped the fault as a single surface where it crosses the ramp alignment, but show it as two splays up to 150 m (500 ft) apart over much of Drill Hole Wash. This interpretation is based on numerous faults observed in core from UE25-A and -B series boreholes located within the wash. Such evidence leads Buesch et al.²⁵ to conclude the Drill Hole Wash Fault is most likely a complex of interconnected faults in a fault zone 120 to 180 m (400 to 600 ft) wide over much of Drill Hole Wash.

Consequently, the North Ramp may intersect a significant zone of faulting and brecciation at the Drill Hole Wash Fault.

5.8 Correlation of Core Rock Structural Data with Downhole Video Logs

Downhole color video logs have been generated for the NRG boreholes which show the condition of the borehole walls after drilling has been completed. These provide a visual record of intervals of lost core and rubble that is unavailable from the examination of the core. The logs are obtained by running a cable-mounted video camera at a constant speed to the bottom of the hole and back while continuously recording the image. The camera has a wide-angle lens that is pointed directly down the hole and a shielded light source mounted in front of the lens. A digital readout of depth and orientation is superimposed upon the screen.

The image produced shows borehole features as they approach or recede from the lens as the camera is lowered into or retrieved from the borehole. Perpendicular views of the borehole walls can be obtained by stopping the camera assembly in the hole and switching to a side-mounted black-and-white camera that can then be rotated through 360°. While this

²⁵ Buesch et al.

technique can be used to investigate individual features more closely than is possible with the downhole view, it necessitates that the researcher be present during logging to direct the operator.

A subjective method of rating the condition of the borehole walls has been devised by Fernandez et al. (1994). In this method, the downhole video is viewed and analyzed in regard to borehole symmetry, fracturing, enlargement, and lithophysal content as shown in Table 5-11. The rating scheme used assigns the borehole walls to one of four categories, C1 through C4. C1 is the highest quality hole exhibiting a clean, symmetric bore with few irregularities. C4 is the lowest quality with extensive enlargement and asymmetry.

Table 5-11. Criteria for Categorizing Borehole Wall Condition (after Fernandez et al., 1994)

Category	Criteria
C1	Excellent, typically symmetrical hole with a smooth surface; no hole enlargement; no to few lithophysae; no pronounced fractures; minor "pluckouts."
C2	Good, typically symmetrical hole with a smooth surface; hole enlargement small or intermediate but infrequent; no to few fractures; uniform lithophysae can be present.
C3	Poor—typically a rough surface; hole enlargement is intermediate and frequent, but it is possible for hole to be symmetrical; lithophysae can be prevalent, large, and nonuniformly distributed; fractures are frequent.
C4	Extremely poor, typically a nonsymmetrical hole having an extremely irregular surface; hole enlargement is large; large lithophysae can be present; fractures are frequent and pronounced.

The downhole videos for boreholes NRG-4, -5, -6, and -7/7A were viewed and a category assigned for each 3.05-m (10-ft) interval using the C1 through C4 standards. Images captured from the downhole videos showing examples for each of the four categories as observed in USW NRG-6 are presented in Figures 5-14 to 5-17. In addition to the four categories a number of additional descriptors based on the above categories have been recorded in a spreadsheet format. Six columns giving qualitative ratings of lithophysal content and borehole wall quality have been recorded as follows:

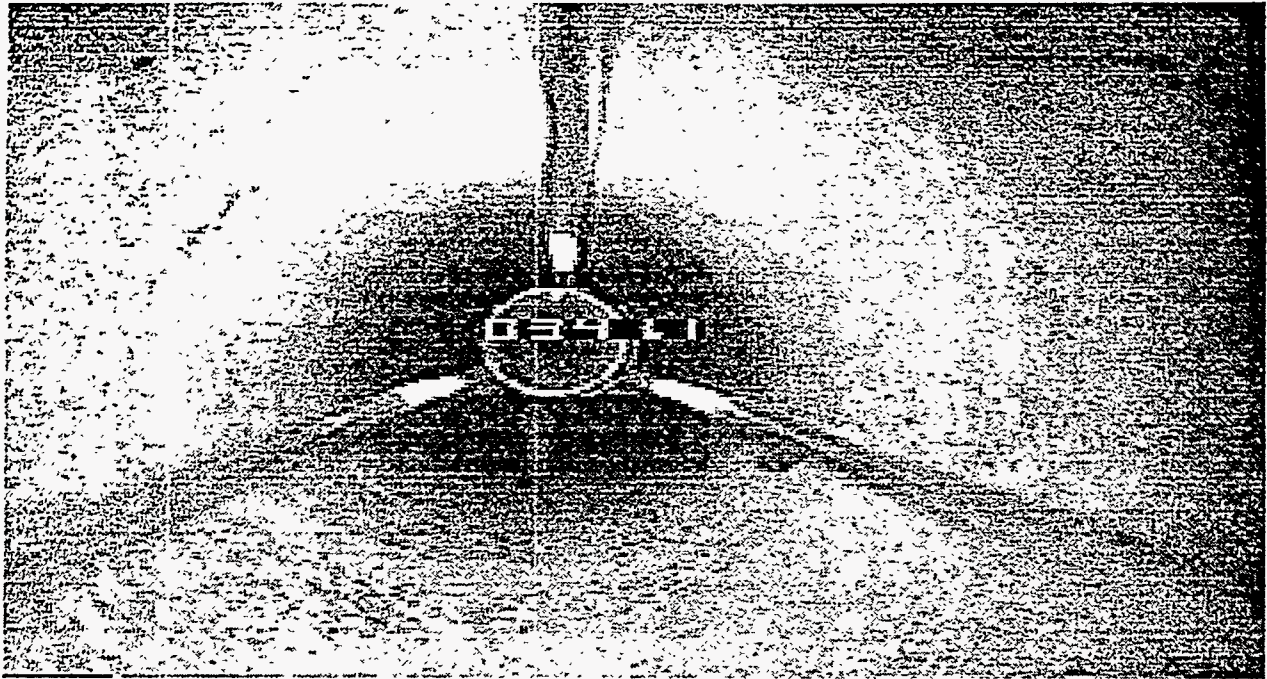


Figure 5-14. USW NRG-6, 342-ft Depth, Class C1 Borehole

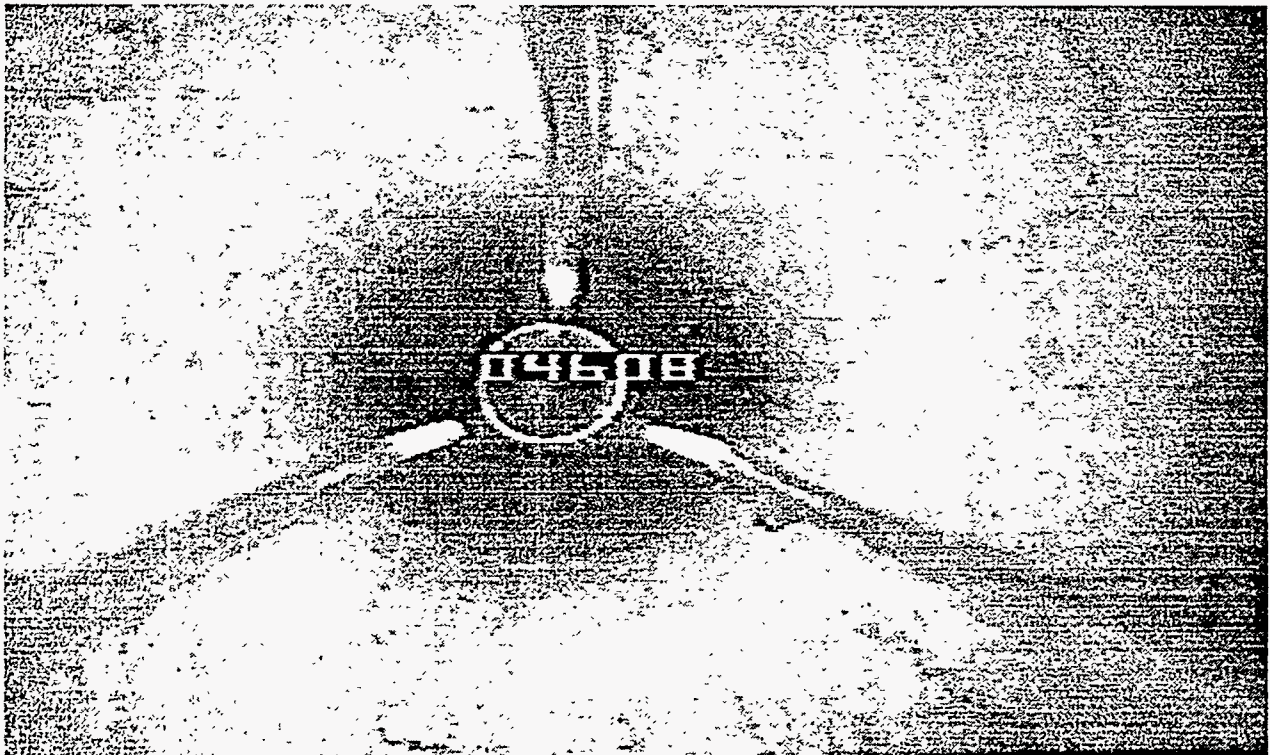


Figure 5-15. USW NRG-6, 460.8-ft Depth, Class C2 Borehole

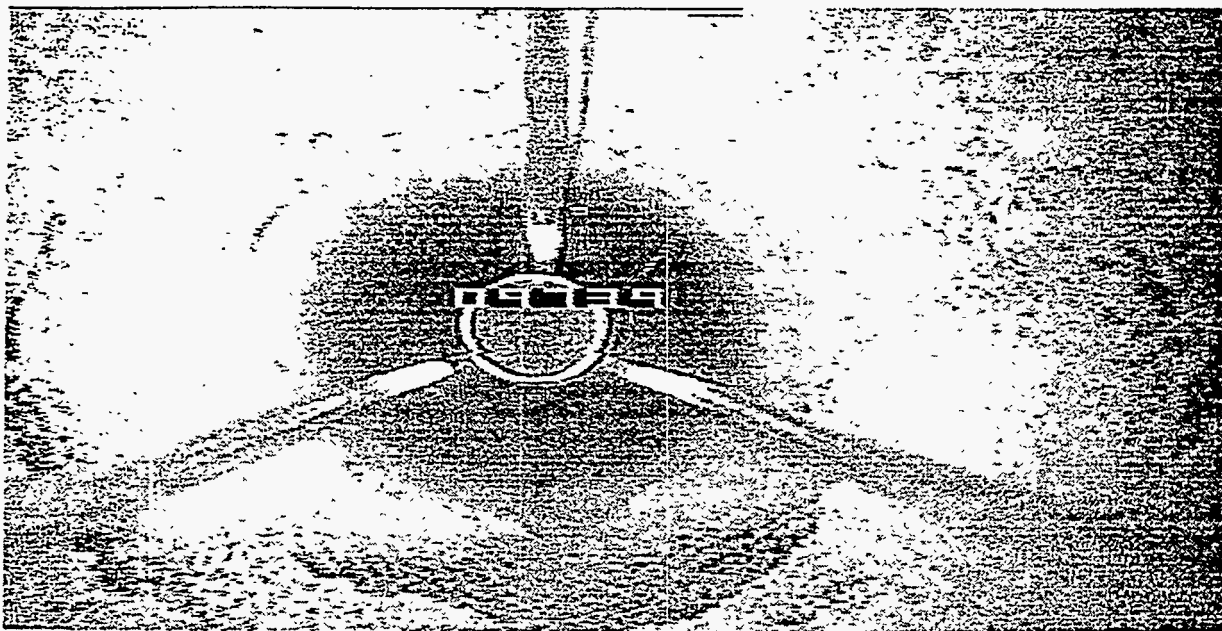


Figure 5-16. USW NRG-6, 973.4-ft Depth, Class C1 Borehole Showing Probable Cavernous Lithophysae in Bottom of Frame

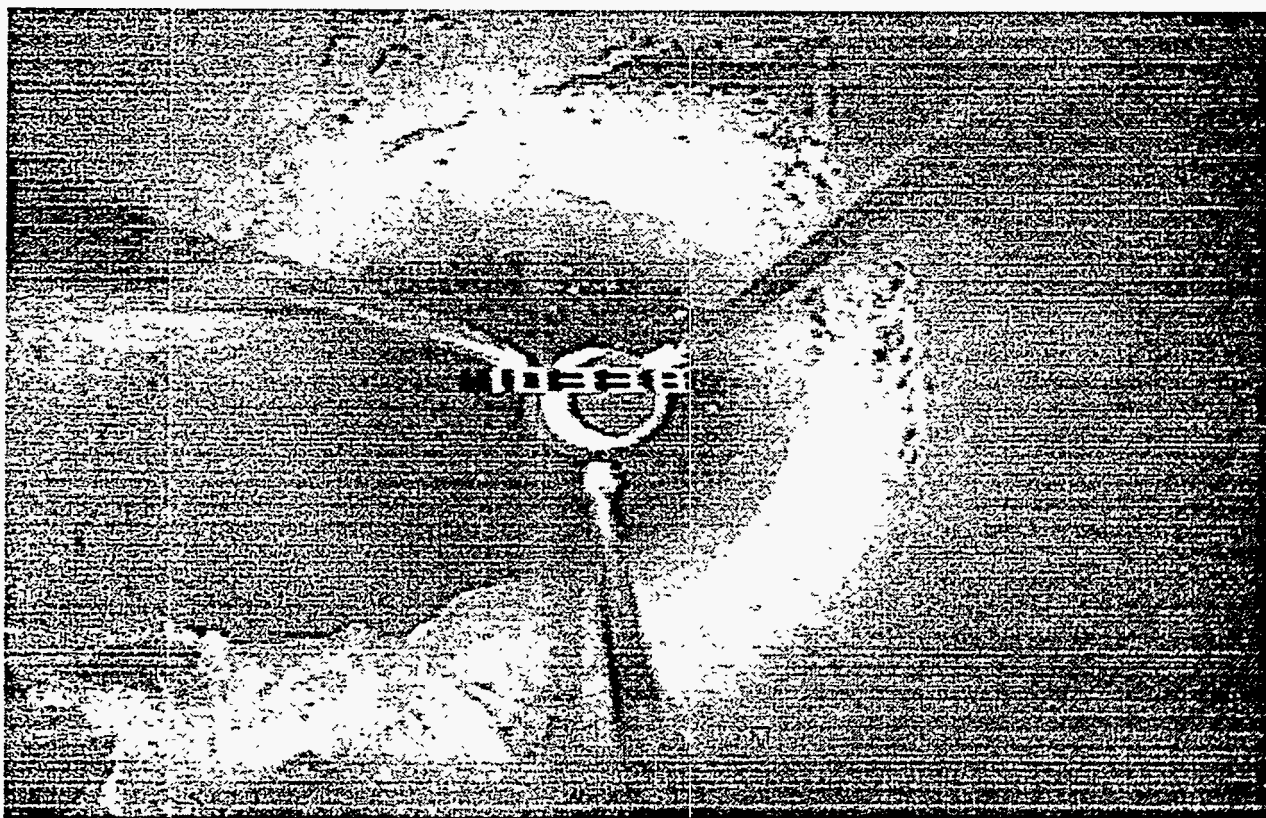


Figure 5-17. USW NRG-6, 1033.8-ft Depth, Class C4 Borehole Showing Large Breakout on Left Side of Frame

Lithophysae:

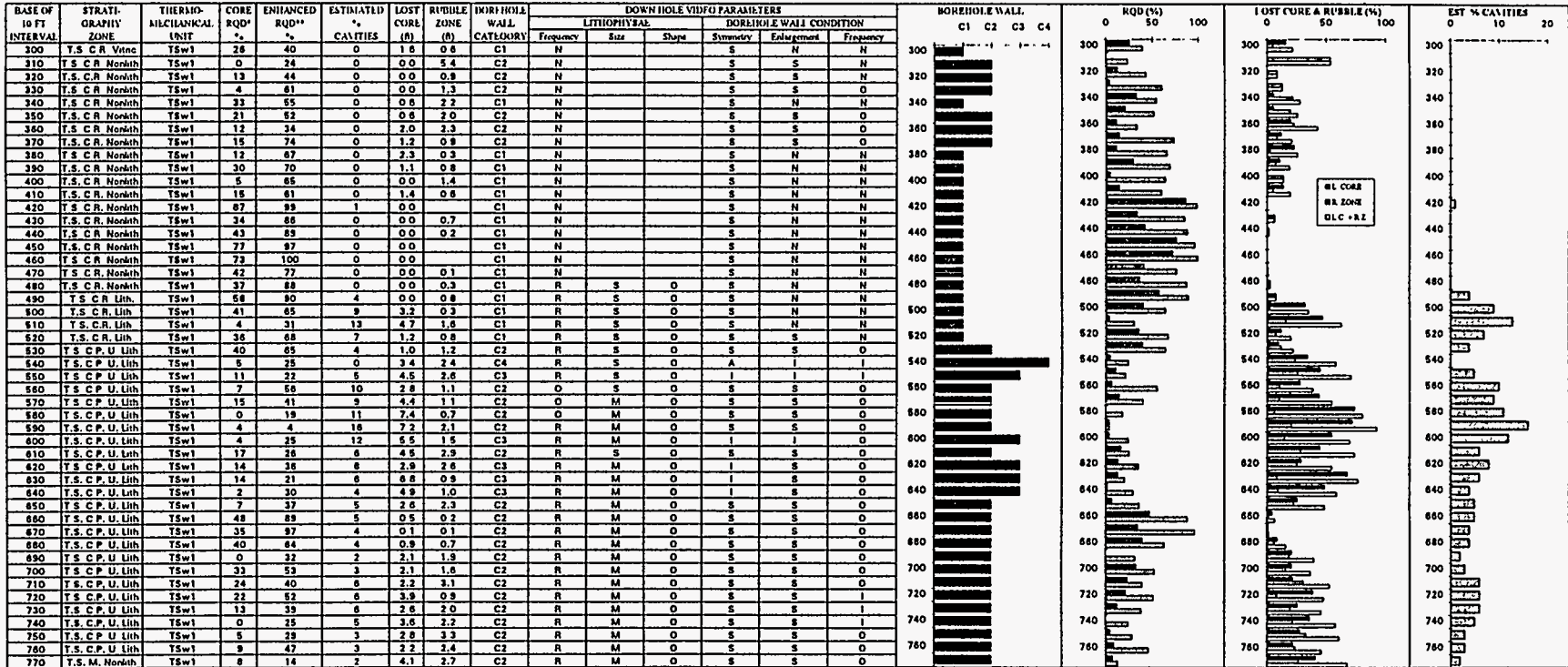
- Frequency — No, not observed or indeterminate
- Rare, several cavities observed over 10 foot interval
- Occasional, several cavities observed per foot
- Moderate, 5 to 10 per foot
- Frequent, greater than 10 per foot
- Size — Small, less than 0.1 foot
- Medium, 0.1 to 0.2 foot
- Large, 0.2 to 0.4 foot
- Cavernous, greater than 0.4 foot
- Shape — Oblate
- Spherical

Borehole Wall Condition:

- Symmetry — Symmetric, displays consistent round bore
- Intermediate, contains a mixture of symmetric and asymmetric segments within interval
- Asymmetric, oval or asymmetric bore generally associated with hole enlargement
- Enlargement — No
- Small, less than 1/4 borehole diameter
- Intermediate, 1/4 to 1/2 borehole diameter
- Large, greater than 1/2 borehole diameter
- Frequency of “pluckouts” — None
- and/or — Occasional, several per 3.05-m (10-ft) interval
- enlarged — Intermediate, numerous small or occasional large features within
- zones 3.05-m (10-ft) interval
- Continuous, entire 3.05-m (10-ft) interval enlarged

An example of the comparison sheet of borehole wall quality ratings and structural data obtained from the core is shown in Figure 5-18 for the TSw1 interval of USW NRG-6. These sheets have been prepared for NRG-4, -5, -6, and -7/7A and are included in Volume II of this report. The format used allows for direct comparison of downhole video data with the core data. For each 3.05-m (10-ft) interval, stratigraphic and thermomechanical (thermal-mechanical) units are given, as well as RQDs, percent (%) cavities, lost core and rubble, plus the video data described above. Charts are presented for visual comparison of borehole wall category with RQD values, lost core and rubble, and percent (%) cavities.

YUCCA MOUNTAIN SITE CHARACTERIZATION PROJECT
 Comparison of Downhole Video Data with Core Data
 Hole USW NRG-77A
 Interval—290-770 ft (88.4-234.7 m), TSw1 Unit



* CORE RQD—Determined from piece lengths formed by all types of fractures (C, I, N and V).
 ** ENHANCED RQD—Determined by filtering the effects of fractures identified as coining induced (Type C) from the piece lengths.
 DOWNHOLE VIDEO PARAMETERS:
 Frequency: No, Rare, Occasional, Moderate, Frequent.
 Size: Small, Medium, Large Caverosus.
 Shape: Oblate, Spherical.
 Symmetry: Symmetric, Intermediate, Asymmetric.
 Enlargement: No, Small, Intermediate, Large.
 Frequency: None, Occasional, Intermediate, Continuous.

Figure 5-18. Correlation of 3-m (10-ft) RQD with Borehole Wall Conditions as Indicated by Downhole Video Logs—NRG-4

The data for USW NRG-6 in Figure 5-18 show characteristics common to the other holes. In general, zones of good borehole quality (C1 or C2 rating) are more common in non- to moderately welded rocks with few or no lithophysal cavities, and zones of poor borehole quality (C3 or C4 rating) are typically found in densely welded rocks containing numerous fractures and lithophysae. Furthermore, zones of low RQD with high lost core and rubble values correlate with poor borehole wall quality, and zones of high RQD with good borehole wall quality. Additionally, intervals of core that are typified by lost core and rubble are observed to coincide in the video logs with sections of poor borehole quality showing large and frequent breakouts and cavities. An exception to this trend is sometimes found in bedded tuffs, where zones of lost core may coincide with good borehole quality. This is probably due to the nonwelded, largely unfractured bedded tuff forming a smooth bore, but the poorly lithified nature of the material resulting in poor recovery.

Lithophysae are often difficult to identify with certainty from the videos, but where identified in abundance, do tend to correlate with zones of poor borehole quality. In general, cavities that lack evidence of controlling fractures and angular breakouts are interpreted as being lithophysae, but coatings of dust and the oblique angle of the lens often make this difficult. Large or cavernous lithophysae can be confused with large breakouts. A cauliflower-like appearance of vapor phase mineralization within the lithophysal cavity can sometimes be seen with the video, and contrasted to angular breakouts that are largely fracture controlled. Overall, the lithophysae data may be useful for comparative purposes, and for identifying cavernous lithophysae in zones of lost core, but is not of sufficient quality for estimating percent volume of cavities.

Hole enlargement is most frequently irregular and related to wall breakouts. Most sections of C3 or C4 rating are typified by large breakouts alternating with sections of little or no enlargement. Sections where the bore is continuously and uniformly enlarged are sometimes found within the bedded tuffs and are characterized by relatively small enlargements and C2 ratings.

Eutaxitic foliation was not positively identified in any of the video logs examined, and it appears unlikely that the logs would be of much use in orienting core. Some of the more prominent fractures, however, could be approximately oriented with the video.

6.0 ROCK MECHANICS LABORATORY TEST DATA

6.1 Introduction

Rock mechanics laboratory test data compiled in this summary report include:

- ♦ unconfined compressive strength,
- ♦ elastic modulus and Poisson's ratio,
- ♦ dry bulk density, porosity, average grain density,
- ♦ indirect tensile strength, and
- ♦ confined compressive strength.

The laboratory test data from all NRG holes were combined and analyzed by thermomechanical (thermal-mechanical) unit. Rock mechanics test samples were selected throughout the length of the NRG boreholes. The sample selection was limited by the condition of the core and the extensive lost core and rubble zones that occurred in some portion of the holes. Uniaxial compression and Brazilian tensile tests of core strength were performed on 50.8-mm (2-inch) diameter samples. Confined compression tests were conducted on 25.4-mm (1.0-inch) diameter samples that were drilled from larger samples. All strength test samples were saturated at a pressure of 10 MPa for one hour minimum. The pressure saturation was then followed by vacuum saturation cycles until the incremental weight gain was less than 0.05%. Samples were then tested at nominal saturation to eliminate variability associated with partial saturation.

More detailed presentations of the rock mechanics laboratory data from the NRG holes are made by Martin et al. (1994), Martin et al. (1995), Boyd et al.^{26 27} These reports contain descriptions of the experimental procedures and more detailed processing of the results.

²⁶ P.J. Boyd, R.H. Price, J.S. Noel, and R.J. Martin III, 1994a. *Bulk and Mechanical Properties of the Paintbrush Tuff Recovered from Boreholes UE25 NRG-2, -2A, -2B, and -3: Data Report*, SAND94-1902, in review, Sandia National Laboratories, Albuquerque, New Mexico.

Schmidt hammer rebound hardness measurements were also conducted on the NRG holes to produce early strength estimates and to supplement the rock mechanics test data. The measurements were performed following ISRM suggested methods (Brown, 1981) and analysis of the results incorporates suggested improvements to the ISRM methods by Goktan and Ayday (1993). Pieces of core were selected on nominal 3-m (10-ft) intervals down hole and clamped in a testing anvil weighing a minimum of 20 kg (44.1 lbs). A group of 20 rebound hardness measurements were then conducted. The data is presented in a log format in Volume II.

6.2 Unconfined Compressive Strength

The results of the unconfined compressive strength tests are presented in Table 6-1 by thermomechanical (thermal-mechanical) unit in the form of mean, standard deviation, and number of the tests. The data are tabulated for individual holes and for all holes. The mean and standard deviation for each thermomechanical (thermal-mechanical) unit are compared graphically in Figure 6-1. Overall the TSw2 unit has the highest mean unconfined compressive strength of 178 MPa while the PTn has the lowest of 8 MPa. The average strength of 169 MPa for lithophysae-rich TCw was increased by including six test results on small samples (average strength of 311 MPa) from a depth of 3.28 m (22.2 ft) of NRG-6 core hole. If these data are excluded, the average strength for the lithophysae-rich portion was reduced to 74 MPa. The strength of rock in the nonlithophysae portion of TCw is, in general, comparable to that of TSw2

²⁷ P.J. Boyd, P.J., R.H. Price, J.S. Noel, and R.J. Martin III, 1994b. *Bulk and Mechanical Properties of the Paintbrush Tuff Recovered from Boreholes UE25 NRG-4 and -5: Data Report*, SAND94-? (being drafted), Sandia National Laboratories, Albuquerque, New Mexico.

Table 6-1. Comparison of Mean and Standard Deviation of Unconfined Compressive Strength (MPa) — NRG Holes

CORE HOLE	UO (Tuff "X")			ALL TCw			TCw-NL			TCw-LR			PTn			ALL TSw1			TSw1-NL			TSw1-LR			TSw2			
	mean	sdev	N	mean	sdev	N	mean	sdev	N	mean	sdev	N	mean	sdev	N	mean	sdev	N	mean	sdev	N	mean	sdev	N	mean	sdev	N	
UE25 NRG-2				163.4	35.6	8	163.4	35.6	8																			
UE25 NRG-2A	6.8	1.8	6	32.6	28.0	11	31.0	29.0	10	53.0		1																
UE25 NRG-2B																												
UE25 NRG-3				92.9	68.2	22	104.0	85.0	13	77.0	33.0	8																
UE25 NRG-4													5.0	3.0	8	48.9	25.3	20	53.0	25.0	17	27.0	9.0	3				
UE25 NRG-5																								173.3	99.4	8		
USW NRG-6				254.4	88.9	10	170.0	87.0	4	311.0	16.0	6	10.0	18.0	10	69.8	31.0	18	69.0	31.0	16	73.0	32.0	2	154.8	72.0	14	
USW NRG-7/7A				150.3	51.9	5	150.0	52.0	5				10.0	9.0	6	53.1	30.5	17	58.0	30.0	13	39.0	30.0	4	190.6	75.1	31	
ALL HOLES																												
— Range	4.1 – 9.8			10.4 – 332.4			10.4 – 245.6			32.5 – 332.4			0.8 – 61.8			15.7 – 149.4			25.7 – 149.4			15.7 – 95.8			31.6 – 312.4			
— Mean	6.8			125.1			110.0			169.0			8.0			56.9			60.0			42.0			178.5			
— Sdev	1.8			94.9			79.0			123.0			13.0			30.1			29.0			29.0			78.3			
— N	6			56			40			15			24			55			46			9			53			

sdev = standard deviation, N = number of samples

NL = Nonlithophysal, LR = Lithophysae Rich

Shaded area = No tests conducted, thermomechanical unit not sampled by borehole.

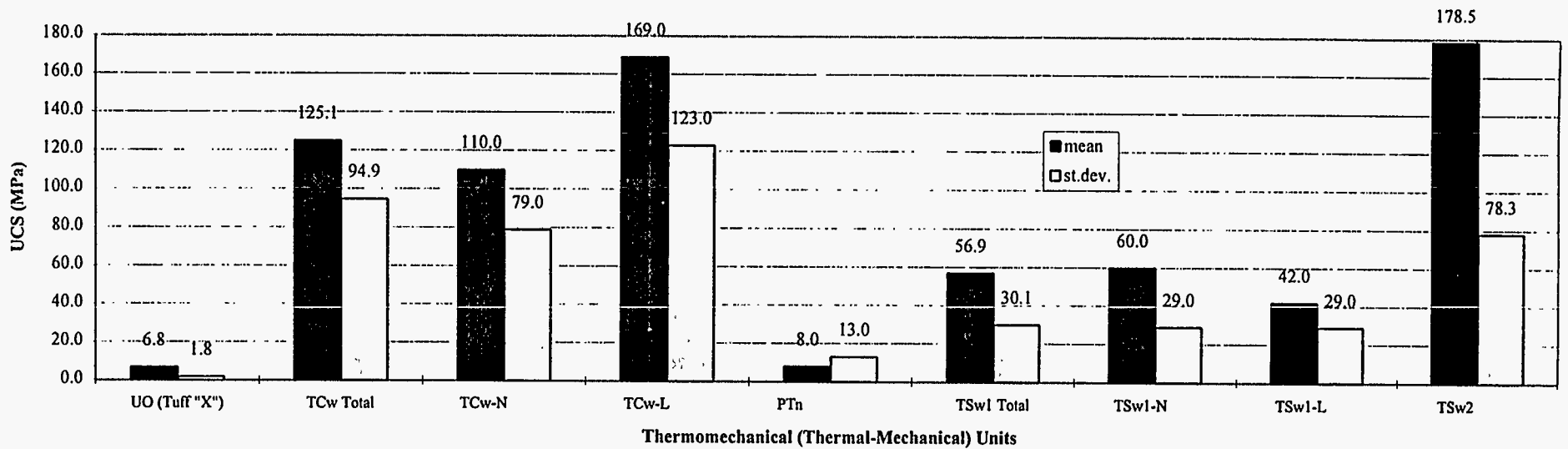


Figure 6-1. Summary of Unconfined Compressive Strength Data—NRG Holes

unit except in core hole NRG-2A where a group of low strength samples occurred. The results from NRG-2A are concentrated in the cap rock zone of TCw where the degree of welding is moderate and contrasts with the more densely welded portions of the TCw. The results for the TSw1 unit are around 50 ± 25 MPa regardless of lithophysae or nonlithophysae portion.

6.3 Elastic Modulus and Poisson's Ratios

The laboratory measurements of elastic modulus and Poisson's ratios are summarized in Tables 6-2 and 6-3 for each thermomechanical (thermal-mechanical) unit. The mean, standard deviation, and number of samples for test results obtained in each NRG hole and for all the NRG holes are presented in these two tables. The mean and standard deviation for elastic modulus and Poisson's ratios are shown graphically in Figures 6-2 and 6-3, respectively, as bar charts. The trend for the elastic modulus results is similar to that of the unconfined compressive strengths. The average elastic modulus of 32.3 GPa in unit TSw2 is the highest, while average elastic modulus of 2.5 GPa at unit PTn is the lowest. The average Poisson's ratio are consistently around 0.20 to 0.21 for all units except TSw1.

6.4 Dry Bulk Density, Porosity, and Average Grain Density

The mean, standard deviation, and number of samples for bulk density, porosity, and average grain density are listed in Tables 6-4 to 6-6 for each thermomechanical (thermal-mechanical) unit. The mean, standard deviation, and number of samples obtained in each NRG hole and for all NRG holes are included in the tables. The mean and standard deviation are presented graphically in Figures 6-4 to 6-6, for dry density, porosity, and average grain density.

Table 6-2. Comparison of Mean and Standard Deviation of Elastic Modulus (GPa) Measurements — NRG Holes

CORE HOLE	UO (Tuff "X")			ALL TCw			TCw-NL			TCw-LR			PTn			ALL TSw1			TSw1-NL			TSw1-LR			TSw2			
	mean	sdev	N	mean	sdev	N	mean	sdev	N	mean	sdev	N	mean	sdev	N	mean	sdev	N	mean	sdev	N	mean	sdev	N	mean	sdev	N	
UE25 NRG-2				38.9	1.4	8	38.9	1.4	8																			
UE25 NRG-2A	4.3	0.8	6	13.9	8.6	11	13.6	8.9	10	17.5		1																
UE25 NRG-2B																												
UE25 NRG-3				26.3	10.2	20	27.3	12.8	11	25.2	6.4	9																
UE25 NRG-4													1.2	0.7	8	16.9	7.2	20	18.3	6.9	17	9.1	2.4	3				
UE25 NRG-5																								32.5	10.8	8		
USW NRG-6				34.9	4.5	18	27.2	3.1	4	37.1	0.9	14	3.2	4.4	10	22.3	5.9	18	21.7	5.9	16	26.9	3.3	2	30.0	6.1	14	
USW NRG-7/7A				28.9	5.0	5	28.9	5.0	5				3.3	2.5	6	17.5	6.3	17	18.9	6.0	13	13.0	5.6	4	34.9	6.0	11	
ALL HOLES																												
— Range	3.1 – 5.1			6.5 – 41.4			6.5 – 41.4			14.8 – 39.0			0.2 – 14.8			6.0 – 34.3			9.2 – 34.3			6.0 – 29.2			13.4 – 41.8			
— Mean	4.3			28.4			26.3			31.8			2.5			18.9			19.6			14.8			32.3			
— Sdev	0.8			10.9			12.1			7.6			3.2			6.8			6.4			8.0			7.5			
— N	6			62			38			24			24			55			46			9			33			

sdev = standard deviation, N = number of samples

NL = Nonlithophysal, LR = Lithophysae Rich

Shaded area = No tests conducted, thermomechanical unit not sampled by borehole.

Table 6-3. Comparison of Mean and Standard Deviation of Poisson's Ratio — NRG Holes

CORE HOLE	UO (Tuff "X")			ALL TCw			TCw-NL			TCw-LR			PTn			ALL TSw1			TSw1-NL			TSw1-LR			TSw2		
	mean	sdev	N	mean	sdev	N	mean	sdev	N	mean	sdev	N	mean	sdev	N	mean	sdev	N	mean	sdev	N	mean	sdev	N	mean	sdev	N
UE25 NRG-2				0.21	0.01	8	0.21	0.01	8																		
UE25 NRG-2A	0.14	0.05	6	0.21	0.04	11	0.21	0.04	10	0.22		1															
UE25 NRG-2B																											
UE25 NRG-3				0.20	0.04	20	0.20	0.02	11	0.21	0.05	9															
UE25 NRG-4													0.24	0.14	8	0.28	0.09	20	0.26	0.06	17	0.40	0.18	3			
UE25 NRG-5																								0.20	0.06	8	
USW NRG-6				0.22	0.01	18	0.23	0.02	4	0.21	0.01	14	0.21	0.07	10	0.24	0.06	18	0.24	0.05	16	0.25	0.18	2	0.20	0.05	14
USW NRG-7/7A				0.19	0.01	5	0.19	0.01	5				0.14	0.10	6	0.25	0.10	17	0.24	0.08	13	0.28	0.16	4	0.22	0.06	11
ALL HOLES																											
— Range	0.05 – 0.20			0.15 – 0.32			0.15 – 0.29			0.15 – 0.32			0.06 – 0.53			0.09 – 0.60			0.15 – 0.43			0.09 – 0.60			0.10 – 0.40		
— Mean	0.14			0.21			0.21			0.21			0.20			0.26			0.25			0.31			0.21		
— Sdev	0.05			0.03			0.03			0.03			0.11			0.09			0.06			0.16			0.06		
— N	6			62			38			24			24			55			46			9			33		

sdev = standard deviation, N = number of samples

NL = Nonlithophysal, LR = Lithophysae Rich

Shaded area = No tests conducted, thermomechanical unit not sampled by borehole.

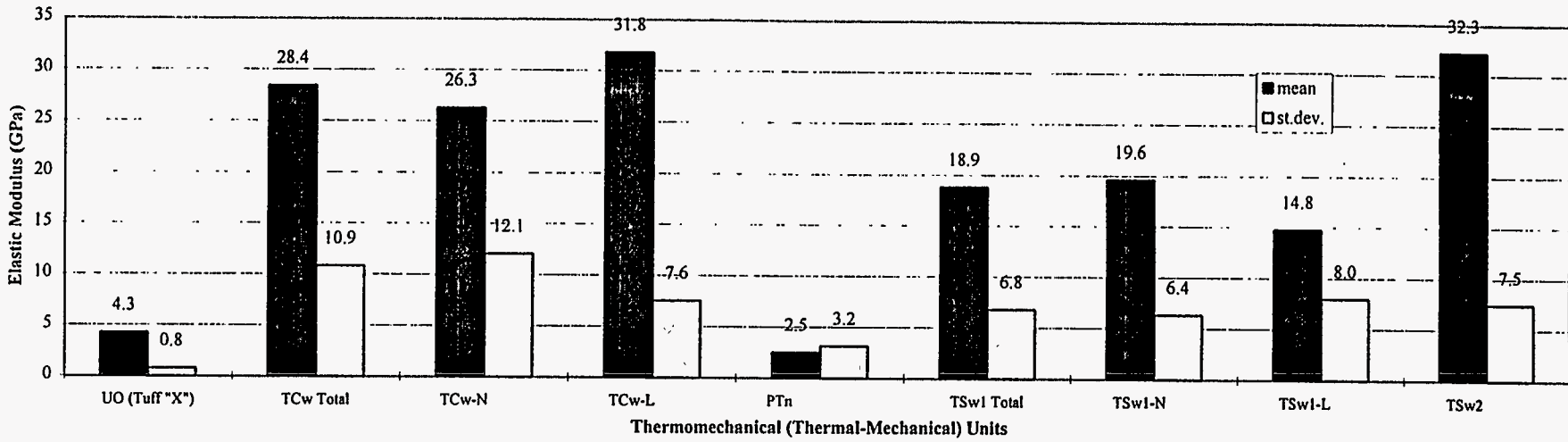


Figure 6-2. Summary of Elastic Modulus—NRG Holes

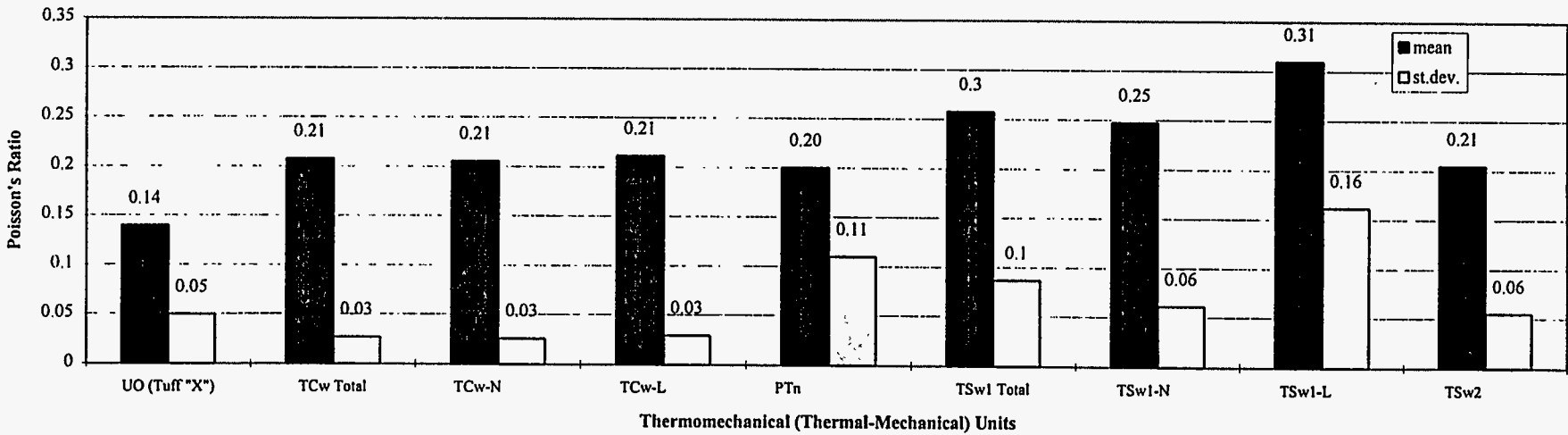


Figure 6-3. Summary of Poisson's Ratio—NRG Holes

Table 6-4. Comparison of Mean and Standard Deviation of Dry Bulk Density (g/cc) — NRG Holes

CORE HOLE	UO (Tuff "X")		ALL TCW		TCW-NL		TCW-LR		PTn		ALL TSWI		TSWI-NL		TSWI-LR		TSW2	
	mean	sdev	N	mean	sdev	N	mean	sdev	N	mean	sdev	N	mean	sdev	N	mean	sdev	N
UE25 NRG-2	1.23	0.06	12	1.85	0.23	27	1.84	0.23	26	2.08	—	1						
UE25 NRG-2A	1.23	0.06	12	2.34	0.01	17	2.34	0.01	17									
UE25 NRG-2B				2.13	0.19	45	2.13	0.21	32	2.14	0.10	13						
UE25 NRG-3																		
UE25 NRG-4																		
UE25 NRG-5																		
UE25 NRG-6				2.33	0.05	24	2.27	0.04	8	2.36	0.01	16	1.29	0.28	16	2.22	0.04	40
USW NRG-77A				2.22	0.13	12	2.22	0.13	12				1.31	0.23	33	2.14	0.10	84
ALL HOLES																		
— Range	1.13 - 1.31	1.45 - 2.37	1.45 - 2.36	1.95 - 2.37	1.00 - 1.90	1.81 - 2.33	1.98 - 2.33	1.81 - 2.28	1.84 - 2.42									
— Mean	1.23	2.14	2.11	2.25	1.30	2.16	2.19	2.11	2.27									
— Sdev	0.06	0.24	0.25	0.13	0.23	0.09	0.07	0.11	0.08									
— N	12	125	95	30	57	136	93	43	117									

sdev = standard deviation, N = number of samples
 NL = Nonlithophysal, LR = Lithophysae Rich
 Shaded area = No tests conducted, thermomechanical unit not sampled by borehole.

Table 6-5. Comparison of Mean and Standard Deviation of Porosity (%) — NRG Holes

CORE HOLE	UO (Tuff "X")			ALL TCw			TCw-NL			TCw-LR			PTn			ALL TSw1			TSw1-NL			TSw1-LR			TSw2		
	mean	sdev	N	mean	sdev	N	mean	sdev	N	mean	sdev	N	mean	sdev	N	mean	sdev	N	mean	sdev	N	mean	sdev	N	mean	sdev	N
UE25 NRG-2				7.5	0.7	17	7.5	0.7	17																		
UE25 NRG-2A	46.8	2.1	15	27.5	9.2	19	28.0	9.1	18	18.0	—	1															
UE25 NRG-2B																											
UE25 NRG-3				15.6	8.1	45	15.9	9.3	32	15.0	4.0	13															
UE25 NRG-4													48.0	6.0	15	16.7	2.9	51	16.4	2.7	46	19.9	2.0	5			
UE25 NRG-5															19.2		1				19.2		1	11.0	2.2	24	
USW NRG-6				6.8	2.1	30	8.8	1.9	12	5.4	0.5	18	44.9	12.7	18	15.1	6.2	54	13.0	2.0	40	21.2	9.6	14	11.7	2.6	31
USW NRG-7/7A				11.1	5.1	12	11.1	5.1	12				44.6	9.3	33	15.8	3.7	84	14.3	2.7	49	17.4	4.3	35	10.5	3.7	77
ALL HOLES																											
— Range	44.5 – 51.0			4.5 – 44.5			5.2 – 44.5			4.5 – 22.6			16.8 – 59.4			6.8 – 32.1			6.8 – 22.8			9.7 – 32.1			0.7 – 27.7		
— Mean	46.8			13.7			15.1			9.7			45.5			15.8			14.6			18.6			10.9		
— Sdev	2.1			9.4			10.1			5.6			9.7			4.4			2.9			6.1			3.2		
— N	15			123			91			32			66			190			135			55			132		

sdev = standard deviation, N = number of samples

NL = Nonlithophysal, LR = Lithophysae Rich

Shaded area = No tests conducted, thermomechanical unit not sampled by borehole.

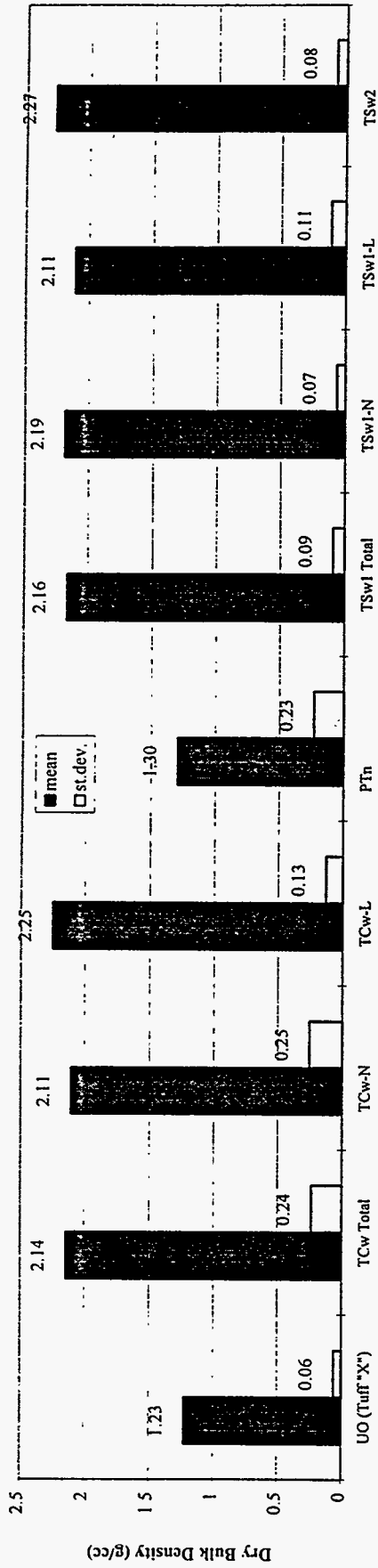
Table 6-6. Comparison of Mean and Standard Deviation of Average Grain Density (g/cc) — NRG Holes

CORE HOLE	UO (Tuff "X")			ALL TCw			TCw-NL			TCw-LR			PTn			ALL TSw1			TSw1-NL			TSw1-LR			TSw2		
	mean	sdev	N	mean	sdev	N	mean	sdev	N	mean	sdev	N	mean	sdev	N	mean	sdev	N	mean	sdev	N	mean	sdev	N	mean	sdev	N
UE25 NRG-2				2.52	0.02	37	2.52	0.02	37																		
UE25 NRG-2A	2.34	0.03	11	2.56	0.03	13	2.56	0.02	12	2.53	—	1															
UE25 NRG-2B																											
UE25 NRG-3				2.53	0.03	26	2.54	0.03	16	2.52	0.01	10															
UE25 NRG-4													2.41	0.09	14	2.56	0.04	27	2.56	0.04	23	2.54	0.00	4			
UE25 NRG-5																2.54	0.01	5	2.54	0.01	3	2.54	0.01	4	2.55	0.02	20
USW NRG-6				2.50	0.01	5	2.50	0.00	2	2.50	0.01	3	2.43	0.04	12	2.55	0.03	39	2.56	0.02	28	2.53	0.01	11	2.55	0.03	22
USW NRG-7/7A				2.50	0.01	7	2.50	0.01	7				2.35	0.06	28	2.55	0.02	31	2.55	0.02	24	2.52	0.00	3	2.55	0.06	44
ALL HOLES																											
— Range	2.30 – 2.39			2.44 – 2.61			2.44 – 2.61			2.49 – 2.55			2.24 – 2.65			2.40 – 2.60			2.40 – 2.60			2.50 – 2.55			2.37 – 2.61		
— Mean	2.34			2.53			2.53			2.51			2.38			2.58			2.56			2.53			2.55		
— Sdev	0.03			0.03			0.03			0.02			0.08			0.03			0.03			0.01			0.04		
— N	11			88			74			14			54			100			78			22			86		

sdev = standard deviation, N = number of samples

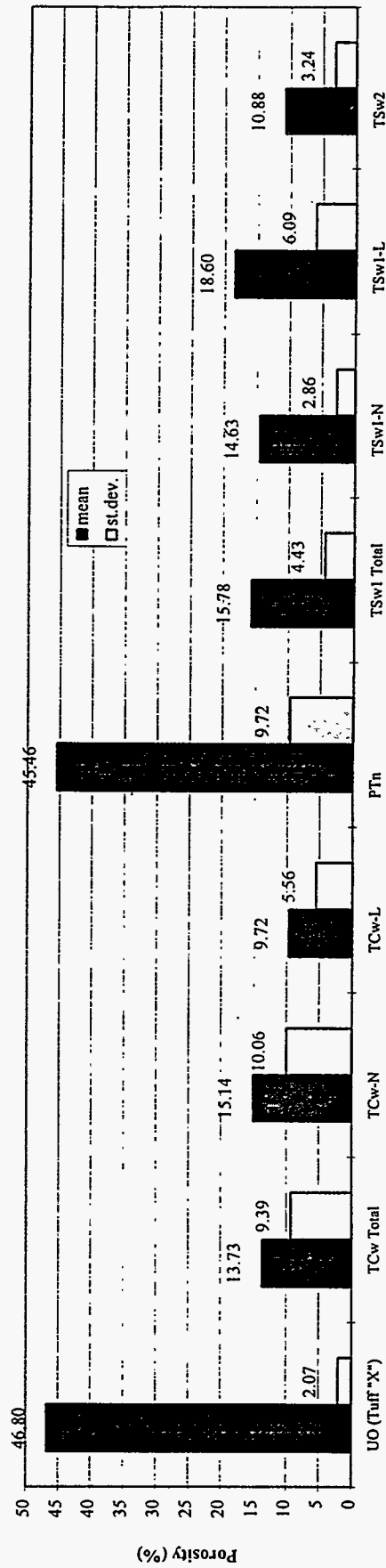
NL = Nonlithophysal, LR = Lithophysae Rich

Shaded area = No tests conducted, thermomechanical unit not sampled by borehole.



Thermomechanical (Thermal-Mechanical) Units

Figure 6-4. Summary of Dry Bulk Densities—NRG Holes



Thermomechanical (Thermal-Mechanical) Units

Figure 6-5. Summary of Porosities—NRG Holes

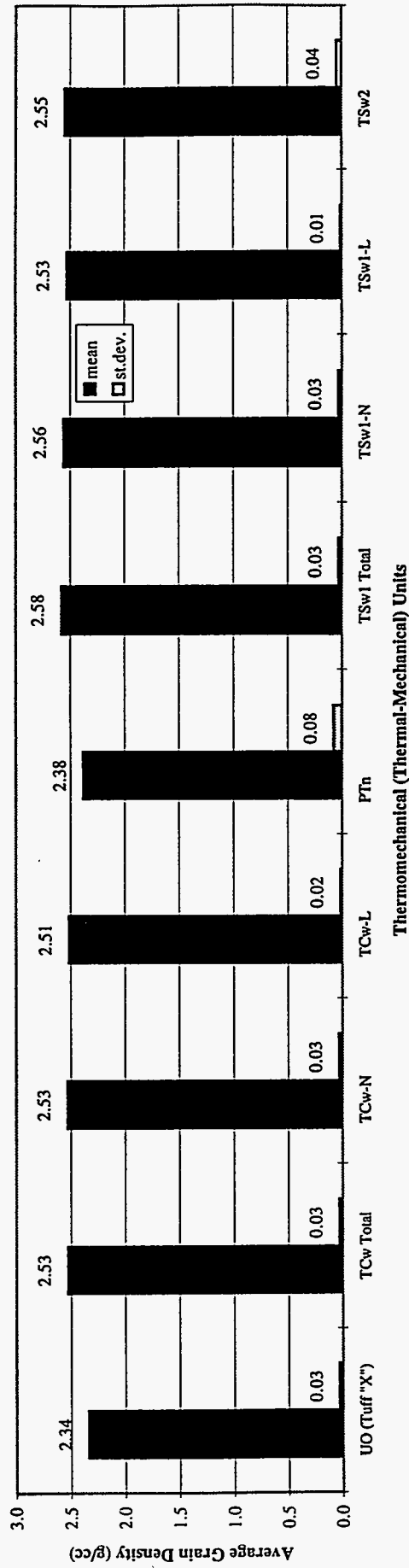


Figure 6-6. Summary of Average Grain Density—NRG Holes

6.5 Indirect Tensile Strength

Indirect tensile strengths were measured by conducting Brazilian tests. The results are summarized in Table 6-7 for each thermomechanical (thermal-mechanical) unit. The mean, standard deviation, and number of samples obtained in each NRG hole and for all NRG holes are included in the table. The mean and standard deviation are presented graphically in Figure 6-7. The trend of the indirect tensile strength results is similar to that of the unconfined compressive strength except that the highest average strength occurs in the TCw lithophysae-rich portion.

6.6 Confined Compressive Strength

The confined compressive strengths for intact rock were obtained in triaxial tests with confining pressures of 0, 5, and 10 MPa. In order to conduct tests on common samples at different levels of confining pressure, specimens were prepared with diameters of 25.4 mm by coring from the available samples. The results include six sets of confined compressive strengths from common depths and are listed in Table 6-8. No results have been generated for unit PTn. Results for TCw, TSw1, and TSw2 units are presented in Figures 6-8, 6-9, and 6-10, respectively, as plots of confined compressive strength versus confining pressure.

Least-square linear curve fits were performed on the data to develop estimates of the cohesion (C) and angle of internal friction (ϕ) for the data. The best-fit lines are plotted on the Figures 6-8, 6-9, and 6-10, the results of the curve fits are listed in Table 6-9. The relationship between the linear equations shown in the figure and the Mohr-Coulomb parameters C and ϕ are given in Section 8.2.4.

Table 6-7. Comparison of Means and Standard Deviations of Brazilian Tensile Strength (MPa) — NRG Holes

CORE HOLE	UO (Tuff "X")			ALL TCw			TCw-NL			TCw-LR			PTn			ALL TSw1			TSw1-NL			TSw1-LR			TSw2			
	mean	sdev	N	mean	sdev	N	mean	sdev	N	mean	sdev	N	mean	sdev	N	mean	sdev	N	mean	sdev	N	mean	sdev	N	mean	sdev	N	
UE25 NRG-2				10.7	1.9	9	10.7	1.9	9																			
UE25 NRG-2A	0.7	0.2	6	5.0	1.9	8	5.0	1.9	8																			
UE25 NRG-2B																												
UE25 NRG-3				7.7	3.7	15	7.1	4.2	11	9.2	1.4	4																
UE25 NRG-4													0.3	0.3	7	5.1	2.3	22	5.2	2.4	20	3.7	0.0	2				
UE25 NRG-5																4.3		1				4.3		1	11.8	4.9	5	
USW NRG-6				11.9	2.6	6	10.6	1.7	4	14.6	2.0	2	1.3	1.7	6	6.8	2.7	15	6.2	1.7	11	8.4	4.4	4	8.9	3.6	12	
USW NRG-7/7A				11.4	1.6	6	11.4	1.6	6				0.9	1.6	12	5.5	2.5	44	5.4	1.9	23	5.6	3.0	21	8.0	2.9	34	
ALL HOLES																												
— Range	0.4 - 1.0			2.6 - 16.0			2.6 - 14.8			7.4 - 16.0			0.02 - 5.10			1.6 - 14.5			1.6 - 10.5			1.9 - 14.5			3.2 - 16.8			
— Mean	0.7			8.9			8.5			11.0			0.8			5.6			5.5			5.8			8.6			
— Sdev	0.2			3.6			3.6			3.1			1.4			2.5			2.1			3.2			3.4			
— N	6			44			38			6			25			82			54			28			51			

sdev = standard deviation, N = number of samples

NL = Nonlithophysal, LR = Lithophysae Rich

Shaded area = No tests conducted, thermomechanical unit not sampled by borehole.

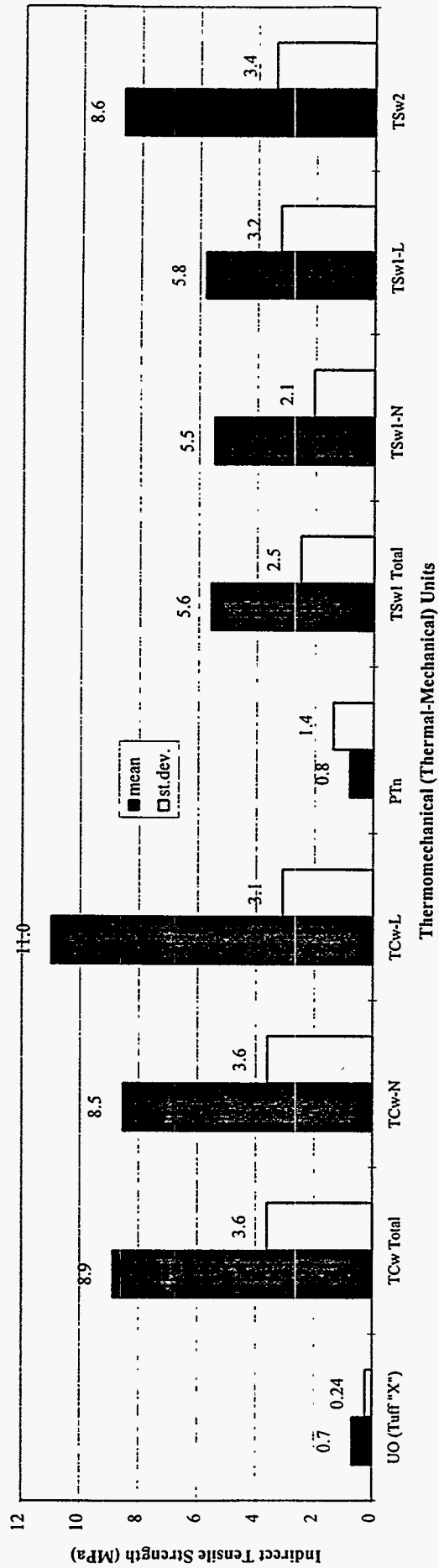


Figure 6-7. Summary of Indirect Tensile Strength—NRG Holes

Table 6-8. Confined Compressive Strength Test Results

Unit	Hole	ID	Confining Pressure (MPa)	Axial Stress (MPa)
TSW1	NRG-4	527.0-E	5	90.0
TSW1	NRG-4	527.0-G	5	67.5
TSW1	NRG-4	527.0-C	10	160.8
TSW1	NRG-4	527.0-F	10	142.1
TSW1	NRG-4	527.0-H	10	131.4
TSW1	NRG-4	527.0-I	10	133.0
TSW1	NRG-7/7A	344.4-A	10	185.0
TSW1	NRG-7/7A	344.4-B	10	139.1
TSW1	NRG-7/7A	344.4-D	10	208.3
TSW1	NRG-7/7A	344.4-E	5	56.5
TSW1	NRG-7/7A	344.4-F	5	163.9
TSW1	NRG-7/7A	344.4-G	5	75.9
TSW1	NRG-7/7A	344.4-H	5	110.2
TSW1	NRG-7/7A	344.4-I	0	106.2
TSW1	NRG-7/7A	344.4-J	0	89.5
TSW1	NRG-7/7A	344.4-K	0	97.3
TSW1	NRG-7/7A	344.4-L	0	88.7
TSW2	NRG-7	865.4-A	10	325.2
TSW2	NRG-7	865.4-B	10	354.0
TSW2	NRG-7	865.4-C	10	235.5
TSW2	NRG-7	865.4-D	10	316.7
TSW2	NRG-7	865.4-E	5	259.8
TSW2	NRG-7	865.4-F	5	322.3
TSW2	NRG-7	865.4-G	5	255.1
TSW2	NRG-7	865.4-H	5	231.6
TSW2	NRG-7	865.4-I	0	215.8
TSW2	NRG-7	865.4-J	0	232.0
TSW2	NRG-7	865.4-K	0	239.1
TSW2	NRG-7	865.4-L	0	248.5

Unit	Hole	ID	Confining Pressure (MPa)	Axial Stress (MPa)
TCW	NRG-6	22.2-B	10	439.7
TCW	NRG-6	22.2-C	10	434.6
TCW	NRG-6	22.2-D	10	343.4
TCW	NRG-6	22.2-E	10	417.3
TCW	NRG-6	22.2-F	5	395.5
TCW	NRG-6	22.2-G	5	391.2
TCW	NRG-6	22.2-H	5	396.8
TCW	NRG-6	22.2-I	5	307.1
TCW	NRG-6	22.2-J	0	315.8
TCW	NRG-6	22.2-K	0	284.2
TCW	NRG-6	22.2-L	0	313.8
TCW	NRG-6	22.2-M	0	332.4
TCW	NRG-3	263.3-E	5	158.2
TCW	NRG-3	263.3-D	10	291.4
TCW	NRG-3	265.7-B	5	295.9
TCW	NRG-3	265.7-D	5	275.1
TCW	NRG-3	265.7-F	5	180.3
TCW	NRG-3	265.7-C	10	369.0
TCW	NRG-3	265.7-E	10	339.1
TCW	NRG-3	265.7-G	10	309.9
TSW1	NRG-6	416.0-B	10	119.9
TSW1	NRG-6	416.0-C	10	147.9
TSW1	NRG-6	416.0-E	10	61.1
TSW1	NRG-6	416.0-F	5	77.1
TSW1	NRG-6	416.0-G	5	39.6
TSW1	NRG-6	416.0-H	5	84.7
TSW1	NRG-6	416.0-I	5	58.8
TSW1	NRG-4	527.0-A	5	76.5
TSW1	NRG-4	527.0-B	5	108.9
TSW1	NRG-4	527.0-D	5	113.6

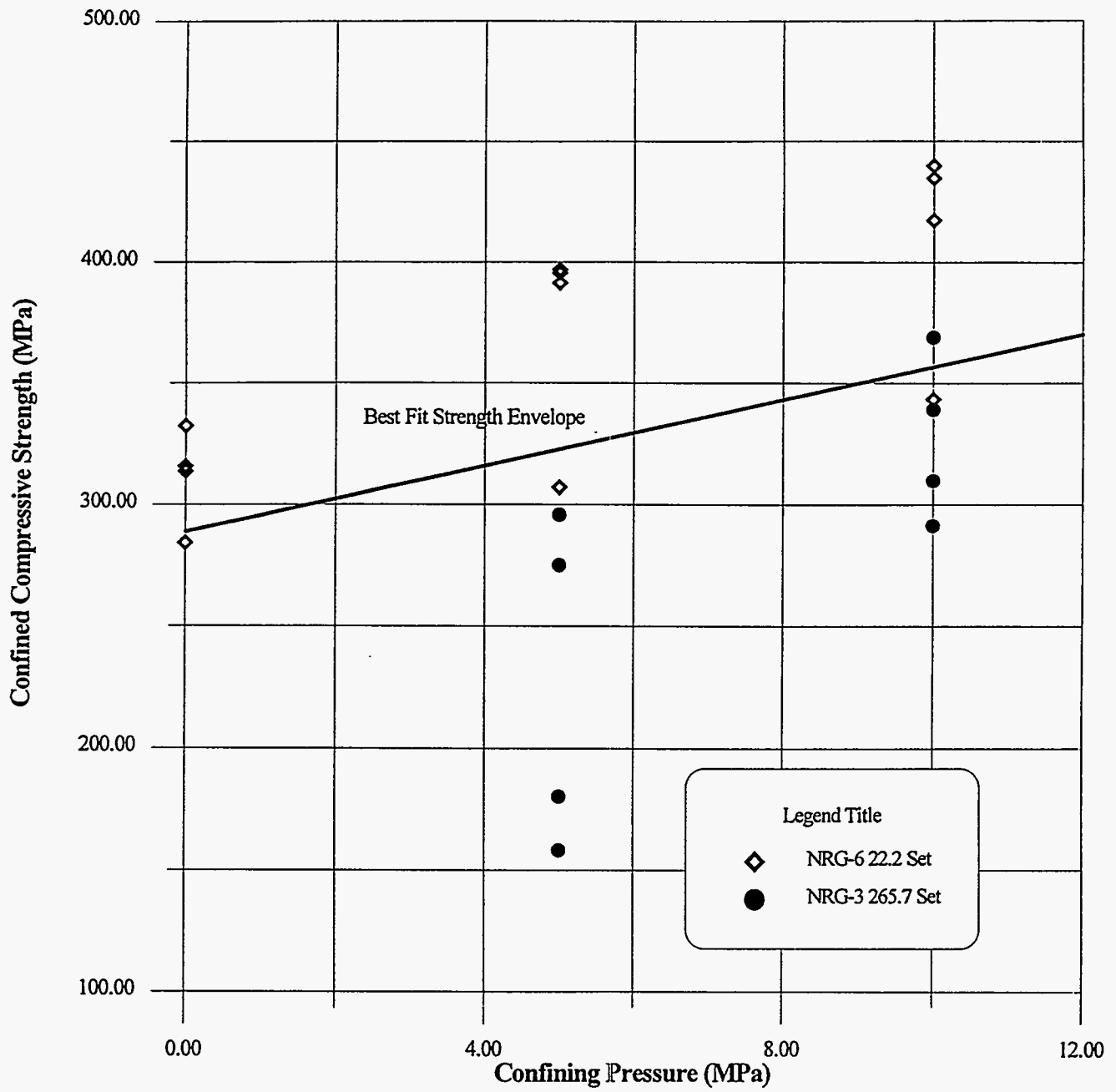


Figure 6-8. Confined Compressive Strength Results for TCw Unit — NRG Hole

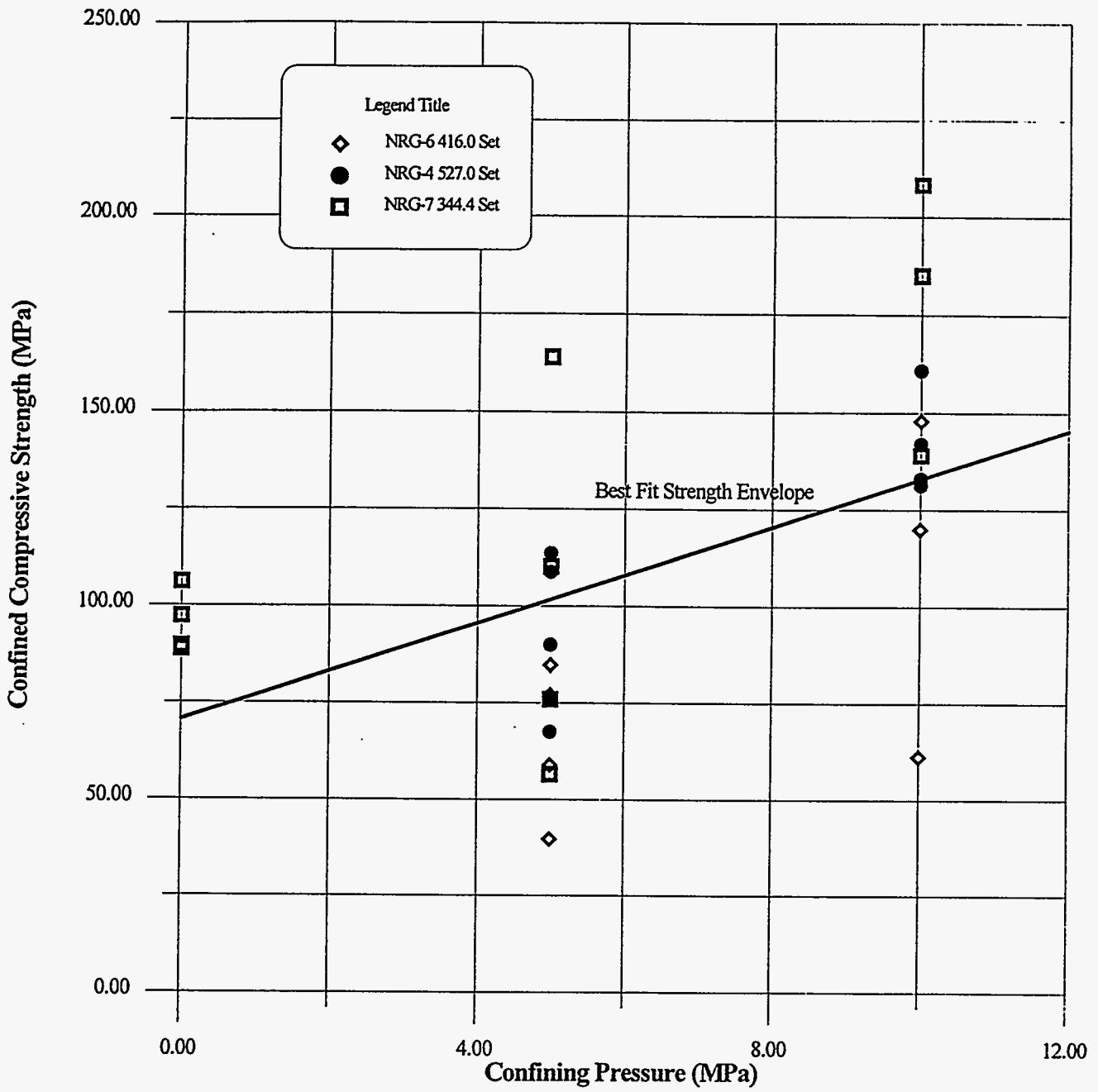


Figure 6-9. Confined Compressive Strength Results for TSw1 Unit — NRG Holes

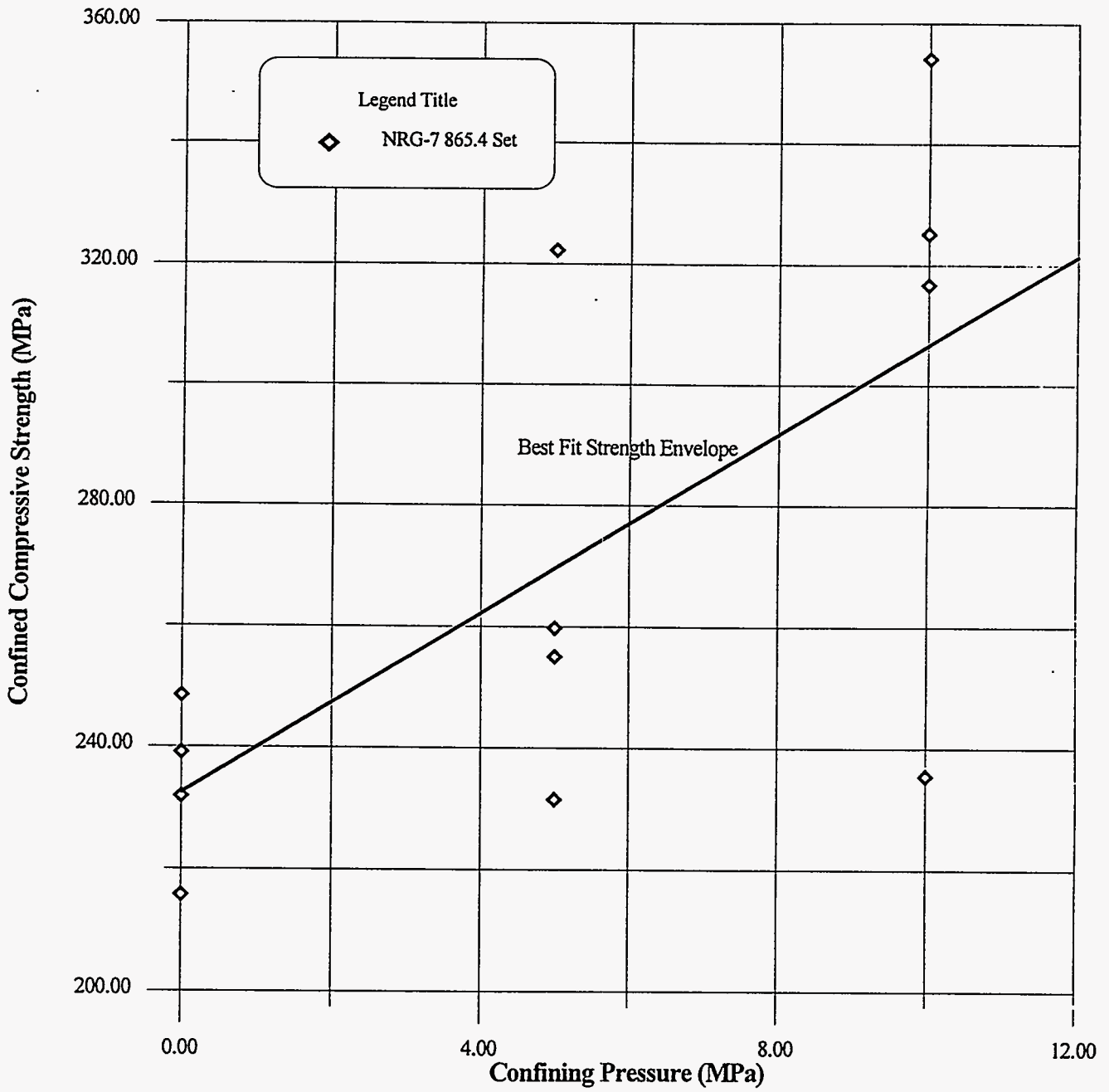


Figure 6-10. Confined Compressive Strength Results for TSw2 Unit — NRG Holes

Table 6-9. Best-Fit Linear Failure Criteria and Mohr-Coulomb Parameters for 25.4-mm Samples from NRG Holes

Thermomechanical (Thermal-Mechanical) Unit	Axial Strength σ_c (MPa)	N	Cohesion C (MPa)	Angle of Internal Friction ϕ (degrees)
TCw	288.8	6.79	55.4	48.0
TSw1	70.5	6.24	14.1	46.0
TSw2	232.6	7.40	42.8	50.0

6.7 Schmidt Hammer Rebound Hardness

The results of the Schmidt hammer measurements are summarized in Table 6-10 for each thermomechanical (thermal-mechanical) unit. The mean, standard deviation, and number of samples obtained in each core hole and for all NRG holes are presented in the table where outlying data points have been eliminated according to the methods suggested by Goktan and Ayday (1993). The standard deviations are presented graphically in Figure 6-11.

These tests were performed using the ISRM Suggested Method (Brown, 1981) on samples of core that had been left open to air dry conditions. This is in contrast to the rock mechanics lab samples which were tested at 100% saturation. Application of the Schmidt hammer to PTn samples was questionable because ISRM calls for limitation to “very soft” or “very hard” rocks. Subsequent application of the Schmidt hammer data to estimate compressive strength (page 7-5, Section 7.0) indicated that rocks in both PTn and TSw1 fall outside the range of application.

Table 6-10. Summary of Statistical Data for Schmidt Hammer Tests in Thermomechanical Units — NRG Holes

CORE HOLE	UO (Tuff "X")			ALL TCw			TCw-NL			TCw-LR			PTn			ALL TSw1			TSw1-NL			TSw1-LR			TSw2			
	mean	sdev	N	mean	sdev	N	mean	sdev	N	mean	sdev	N	mean	sdev	N	mean	sdev	N	mean	sdev	N	mean	sdev	N	mean	sdev	N	
UE25 NRG-2				45.94	3.11	13	47.68	1.92	4	45.16	3.31	9																
UE25 NRG-2A				44.09	2.60	10	44.09	2.60	10																			
UE25 NRG-2B				27.60	11.61	11	24.61	10.62	9	41.09	1.04	2																
UE25 NRG-3				39.76	9.17	21	34.67	11.98	10	44.39	3.49	11																
UE25 NRG-4													17.88	2.86	2	46.21	4.88	16	46.53	5.06	14	43.99	3.59	2				
UE25 NRG-5																11.83	—	1				11.83	—	1	42.70	9.25	5	
USW NRG-6				49.71	4.89	9	47.50	2.84	3	50.81	5.53	6	38.70	7.96	2	46.53	7.06	31	48.34	4.38	16	44.61	8.86	15	48.02	9.32	10	
USW NRG-7/7A				41.08	7.99	6	41.08	7.99	6				26.07	11.77	4	48.35	4.28	19	48.37	4.68	10	48.33	4.06	9	48.29	5.10	14	
ALL HOLES																												
— Range					11.48 – 56.95			11.48 – 50.15			36.33 – 56.95			15.85 – 44.33			11.83 – 56.58			35.75 – 56.58			11.83 – 54.70			23.65 – 56.45		
— Mean					41.01			37.82			45.78			27.18			46.45			47.71			44.59			47.23		
— Sdev					10.10			11.47			4.65			11.53			7.23			4.66			9.70			7.53		
— N					70			42			28			8			67			40			27			29		

sdev = standard deviation, N = number of samples

NL = Nonlithophysal, LR = Lithophysae Rich

Shaded area = No tests conducted, thermomechanical unit not sampled by borehole.

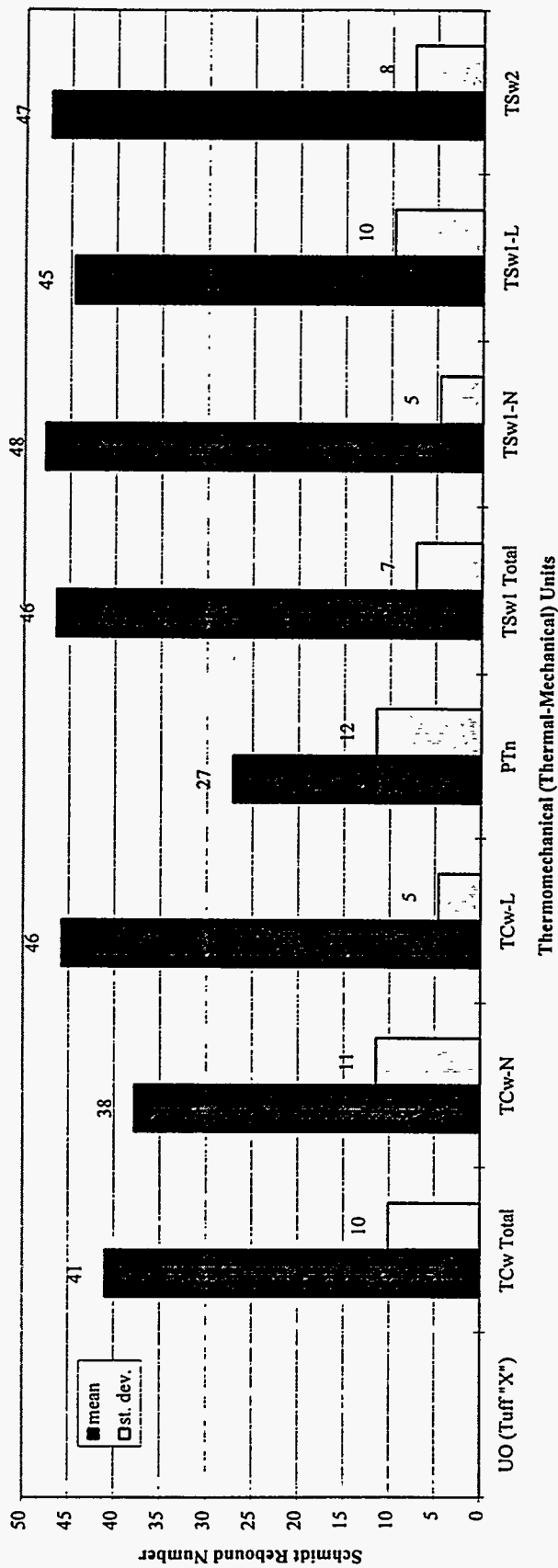


Figure 6-11. Summary of Schmidt Hammer Rebound Number — NRG Holes

This page left intentionally blank.

7.0 ROCK MASS QUALITY DATA

7.1 Introduction

This section of the report briefly discusses the methodology used to produce the estimates of rock mass quality indices RMR and Q from the core logging data and presents the resulting rock mass quality data. Each of the rock mass quality indices are calculated from parameters related to degree of jointing, interaction of joint orientations to form blocks, joint frictional strength, rock strength versus active stress, and hydrologic conditions. In this work, each parameter used to calculate Q or RMR has been assumed to be independent of the others. Parameters were determined directly from core log data for each 3-m (10-ft) interval or were determined by Monte Carlo simulation from data distributions considered representative of the site. The approach to estimation of each parameter is described and the distribution of each parameter within each thermomechanical (thermal-mechanical) unit is presented. A detailed discussion of the methodology for determination of the parameters is presented in Appendix B.

The rock mass quality variation described here represents the range of conditions of the rock mass between faults. There are up to 12 faults identified along the North Ramp. Most of the faults are normal faults with limited displacements and the extent of gouge zones is suspected to be small based upon the drilling of NRG-3 through a possible normal fault. The two exceptions are:

- ◆ Bow Ridge Fault—gouge zone sampled in NRG-2 and -2A and projected to be the 2-4 m (6.6-13.1 ft) thick; and
- ◆ Drill Hole Wash Fault—not sampled by NRG drilling, however, currently projected to have an extensive broken zone.

These two fault zones constitute known structures with the potential to produce off-normal conditions requiring site-specific ground support design.

Rock mass quality was not estimated for the nonlithified tuffs immediately west of the Bow Ridge Fault because their soil-like characteristics are outside of the range of the rock classification scheme. These materials were characterized in a separate study reported by Kessel et al.²⁸

The rock mass quality indices are estimated for each 3-m (10-ft) interval in the NRG holes and are presented in log form in Volume II of this report. All parameters in the RMR index can be estimated directly from the Rock Structural Summary Log and rock mechanics testing data. Simulation of data values was only performed if a rock strength test result or a rock strength estimate from a Schmidt hammer test was not available for a particular interval, and a compression strength was then determined by Monte Carlo simulation of the testing data for the particular thermomechanical (thermal-mechanical) unit.

Two of the six parameters required to calculate Q cannot be determined directly from the NRG core data—Joint Set Number (Jn) and Stress Reduction Factor (SRF). The values of these parameters were therefore estimated based on the results of surface mapping, preliminary (non-QA) mapping in the North Ramp Starter Tunnel (NRST), and oriented-core data from previous site drilling.

The Q estimate was based on Monte Carlo simulation of values of Jn and SRF for each interval based on the frequency distribution of surface mapping data or strength-stress ratio as appropriate. Any spatial association was destroyed by the simulation; however, the data was presented in a log format along with the RMR index. Subsequent revision of Q estimates have

²⁸ Kessel et al.

produced different local values of Jn and SRF because of the Monte Carlo simulation; however, the distribution of all the data were very similar.

Q and RMR estimates were grouped into thermomechanical (thermal-mechanical) units based on the Scott and Bonk (1984) nomenclature. The data were rank ordered and the cumulative frequency of occurrence was calculated for each ascending value. A range of rock mass quality classes, corresponding to frequency of occurrences of 5%, 20%, 40%, 70%, and 90%, are listed for each thermomechanical (thermal-mechanical) unit. This approach provided a basis for the North Ramp design at different levels of confidence as discussed in the Drift Design Methodology of Hardy and Bauer (1991).

7.2 Rock Mass Quality Indices for the Rock Mass Rating System

The calculation of RMR is defined by Bieniawski (1979) to consist of five parameters that consider the strength of the rock, the RQD, the joint spacing, the condition of joint surfaces and the groundwater environment. The calculation is shown in the following equation:

$$\text{RMR} = C + I_{\text{RQD}} + \text{JS} + \text{JC} + \text{Jw} \quad (7-1)$$

where RMR is a dimensionless number from 0 to 100

C = the strength parameter,

I_{RQD} = the RQD parameter,

JS = the joint spacing parameter,

JC = the joint surface parameter, and

Jw = the joint water parameter.

The calculation procedure for each individual parameter and the results are discussed in the following subsection. No adjustments for joint orientation or effects of mining approach have been made to the RMR because its application is limited to estimation of rock mass mechanical properties in the drift design methodology.

7.2.1 Strength Parameter (C)

Both laboratory unconfined compressive strength data and Schmidt hammer rebound hardness data from the NRG holes were used to determine the intact rock strength parameter. In this approach to the determination of RMR, a strength test result was used for every 3-m (10-ft) interval. The rock mechanics testing could not meet this requirement because of the large portion of lost core and rubble and the Schmidt hammer measurements were therefore performed to supplement the database. Schmidt hammer measurements were conducted on air dry samples of the core, while the laboratory rock mechanics test samples were 100% saturated. A correlation between the Schmidt hammer rebound hardness and intact strength suggested by Stacey and Page (1986) and Brown (1981) was used to estimate the intact strength. Table 7-1 compares the averaged uniaxial compressive strength data derived from both the laboratory tests and field Schmidt hammer rebound numbers. The comparison indicated that the average laboratory unconfined compressive strength for the PTn and TSw1 units were much lower than that obtained from the correlation of Schmidt hammer data. In the TCw and TSw2 units, the strength derived from the Schmidt hammer data were approximately 75% of the unconfined compressive strength results. A conservative approach was taken which used the laboratory unconfined compressive strength data for the PTn and TSw1 units and the Schmidt hammer data for the TCw and TSw2 units as the basis for estimating the strength parameter C. The

Table 7.1 Summary of Average Intact Strength Values (MPa)

TM Unit	TCw	PTn	TSw1	TSw2
Schmidt Hammer Data*	97.9	52.4	116.8	121.4
Unconfined Compressive Strength	125.1	8.0	56.9	178.5

*Strength estimate derived from a correlation in Stacey and Page (1986).

application of the Schmidt hammer data was further checked by using the available rock mechanics laboratory testing data. The two approaches produced virtually no difference in the distribution of RMR values; however, locally interval RMR values were different.

An alternative approach to strength estimation could be to use the correlation of strength with porosity proposed by Price (1986). However, this would require extensive porosity measurements or a high resolution geophysical log that was calibrated specifically against the site testing data. Point load testing could also be substituted for Schmidt hammer measurements.

The strength parameter for each 3-m (10-ft) interval was estimated from data in the interval or Monte Carlo simulation was used for intervals without the data. The intact rock strength data (laboratory UCS for PTn and TSw1; Schmidt hammer for TCw and TSw2) for each thermomechanical (thermal-mechanical) unit were compiled as the data pool for Monte Carlo simulation of the missing strength data by the boot-strap procedure.

The distributions of the strength parameter (C) are presented as histograms for each thermomechanical (thermal-mechanical) unit in Figure 7-1. As shown in the figure, the majority of the strength ratings for TCw and TSw2 units are 12 (strength between 100 to 250 MPa), approximately 50% of the ratings for TSw1 unit are 7 (strength between 50 to 100 MPa), and close to 95% of the ratings for PTn unit are less than 2 (strength less than 5 MPa).

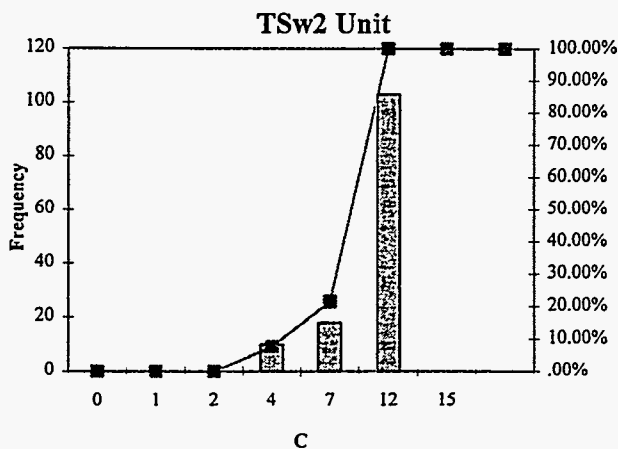
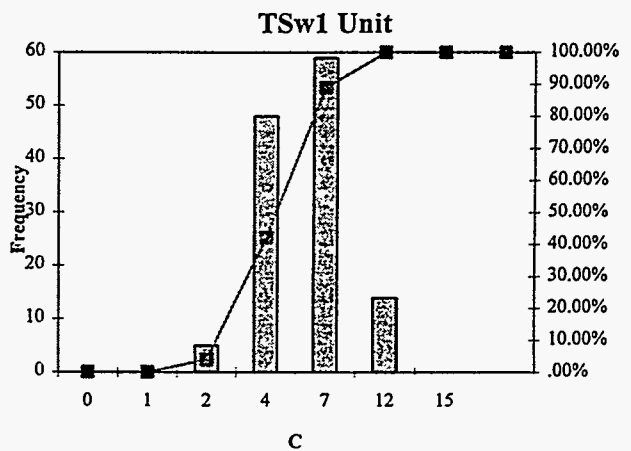
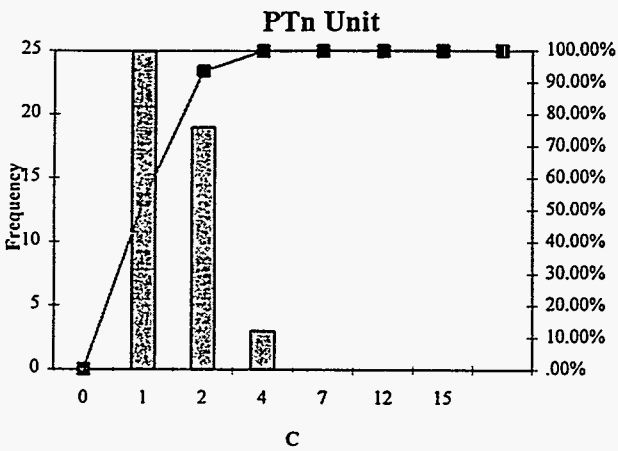
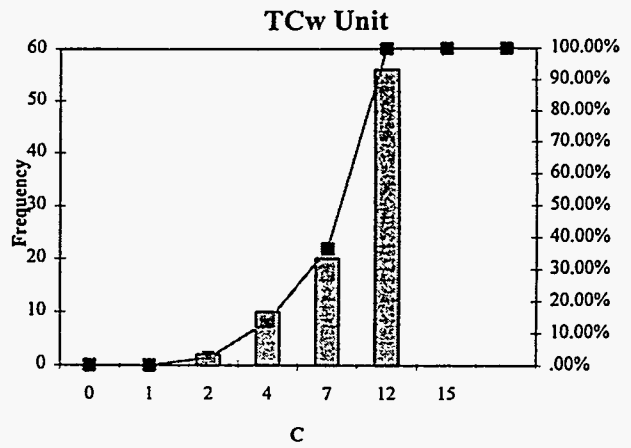
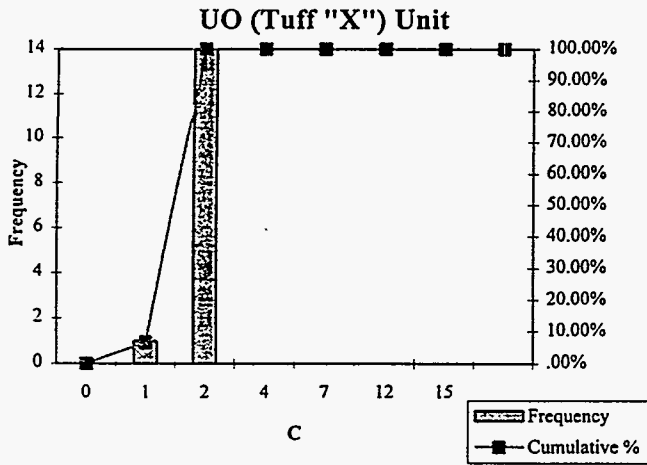


Figure 7-1. Histograms Showing the Distribution of the Strength Parameter (C) for the RMR System in the Thermomechanical (Thermal-Mechanical) Units—NRG Holes

7.2.2 Rock Quality Designation Rating (RQD)

RQD ratings were obtained using RQD values for each 3-m (10-ft) interval. Histograms showing the distribution of the RQD data were presented in Figure 5-2, Section 5.0. Histograms of the derived RQD ratings in RMR system are shown in Figure 7-2. The trend presented in RQD rating histograms is consistent with the RQD histograms in Section 5.0. The majority of intervals within the welded tuff units have RQD ratings of 3, whereas for the PTn unit, RQD ratings of 13 occurred most often.

7.2.3 Spacing of Discontinuity (JS)

The average spacings of discontinuities (fractures) were calculated directly by dividing the total number of fractures (types N, I, and C) identified in each 3-m (10-ft) interval by the interval length. The JS ratings determined from the average spacing were believed to be a conservative approach because all core-induced, indeterminate, and natural fractures were included in the calculation. Figure 7-3 presents the histograms of the JS ratings for each of the thermomechanical (thermal-mechanical) unit. The JS rating of 8 (joint spacing between 60 to 200 mm) appears to occur most frequently for all units.

The JS rating resulting from the corrected linear fracture frequencies presented in Section 5.6.3, were compared to the JS rating used in determination of RMR to check for any bias introduced by using vertical boreholes to sample the predominantly vertical structure. The joint spacings for the dominant vertical joint orientations were calculated by summing the fracture frequencies for 80° and 90° dips and are listed with their corresponding JS ratings in Table 7-2. The distribution of JS ratings shown in Figure 7-3 generally compares well with the

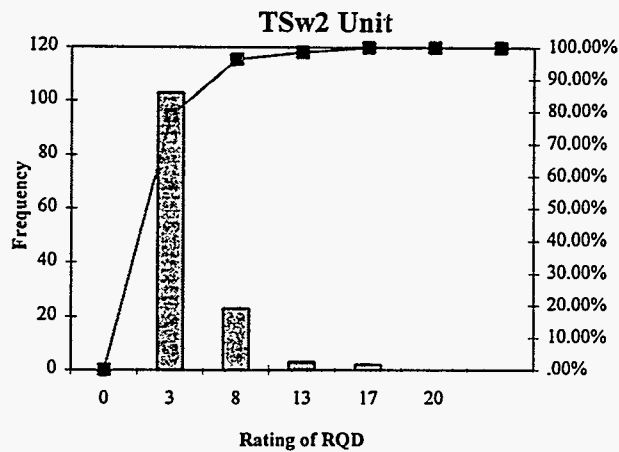
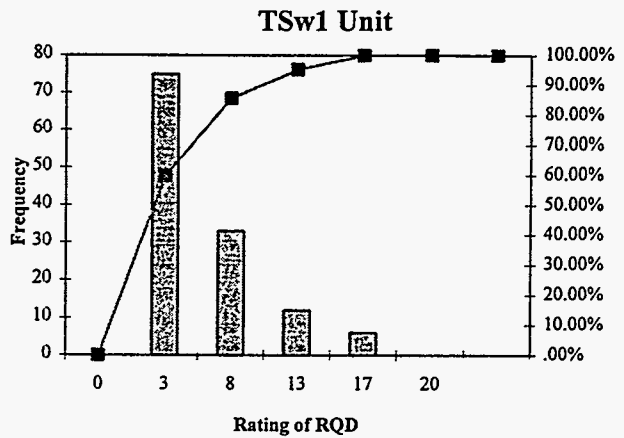
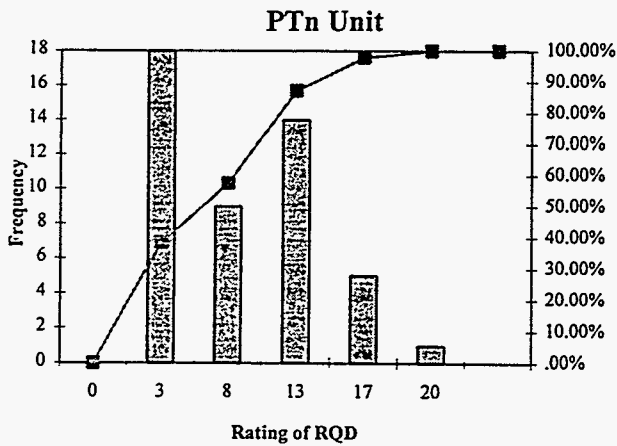
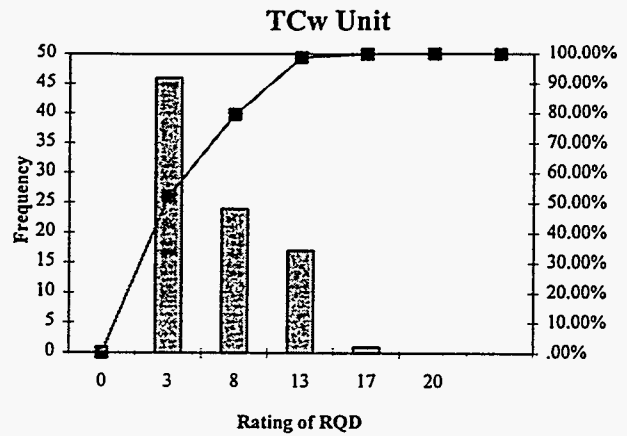
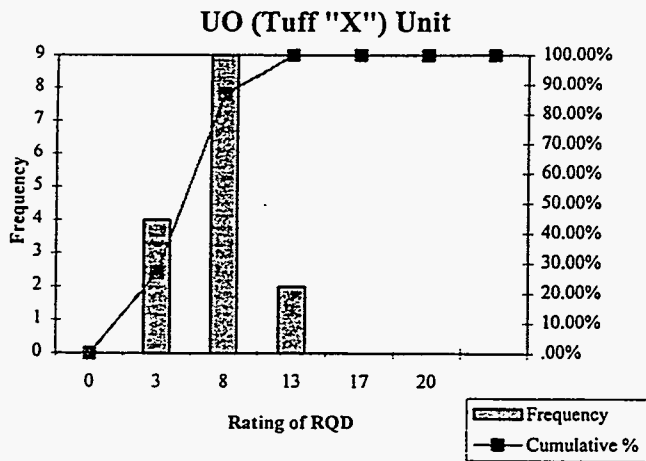


Figure 7-2. Histograms Showing the Distribution of RQD Rating for the RMR System in the Thermomechanical (Thermal-Mechanical) Units—NRG Holes

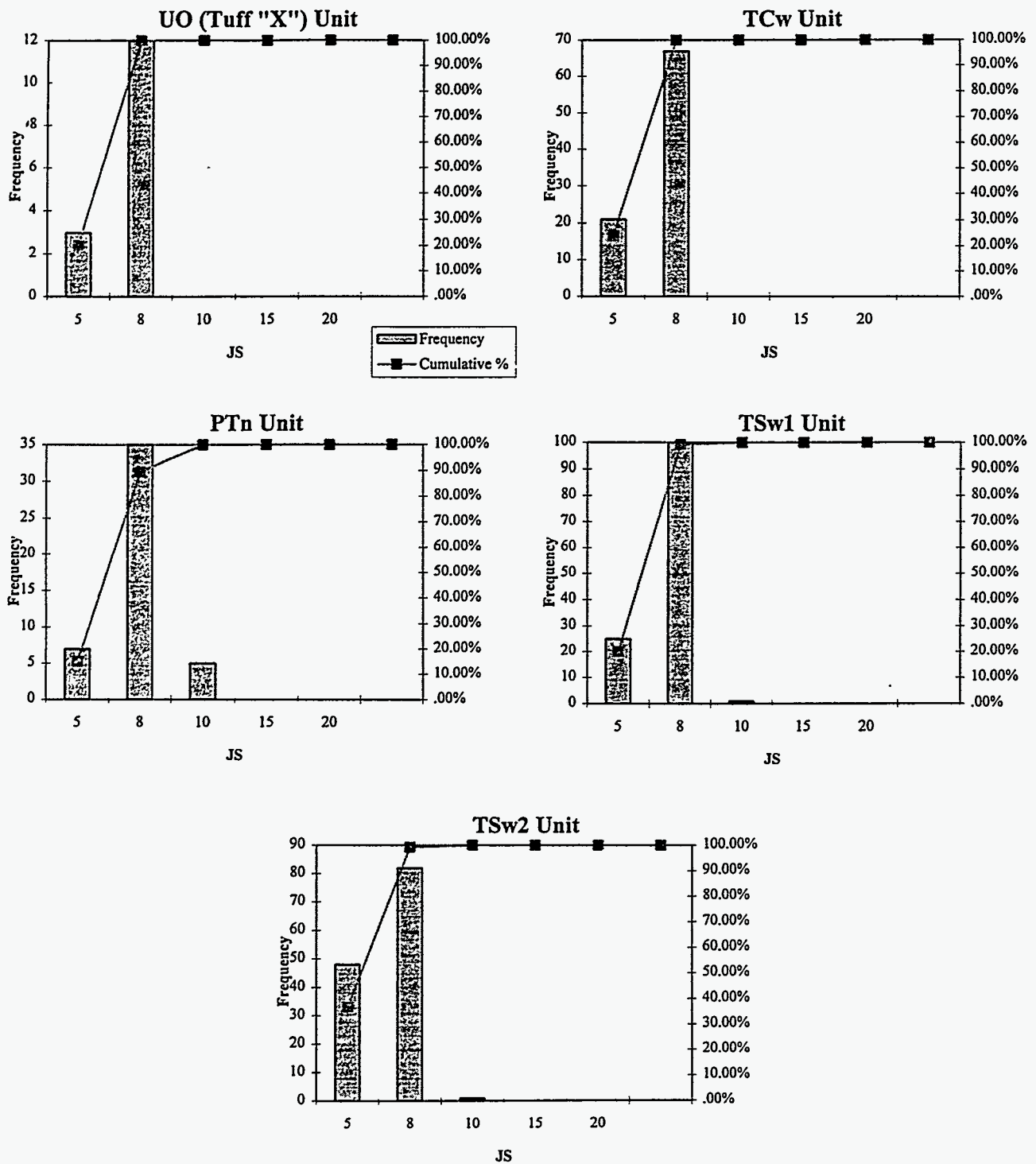


Figure 7-3. Histograms Showing the Distribution of the JS Rating for the RMR System in the Thermomechanical (Thermal-Mechanical) Units—NRG Holes

JS rating derived from the corrected vertical fracture spacings as shown in Table 7-2 which lists the median value from the distributions. The JS rating of 10 derived from corrected spacing data for PTn unit is slightly higher than the central tendency of the histograms in Figure 7-3 and the JS of 5 in TSw2 is slightly lower than the median value of the distribution used to determine RMR. The inclusion of core-induced and indeterminate fractures in the calculation of joint spacing rating produces spacing values similar to the corrected joint spacing.

Table 7-2. Comparison of Corrected Spacings of Vertical Joints and the Corresponding JS Rating to Median JS Ratings Used in RMR Calculation

TM Unit	TCw	PTn	TSw1	TSw2
Mean total joint spacing (mm)	58	149	61	37
Joint spacing 80°–90° dips (mm)	97	270	86	44
JS Rating based on spacing 80°–90° dips (mm)	8	10	8	5
Median value of JS Rating from Figure 7-3	7.3	7.8	7.4	6.9

7.2.4 Condition of Joint (JC)

The condition of joints was evaluated using the planarity and roughness of joint surface and joint infilling data from the core hole rock structure summaries for the NRG holes. A simple algorithm developed from a descriptive table by Laubscher (1990) was used to calculate the JC rating according to:

$$JC = 30 * a * b * c \quad (7-2)$$

where a is a factor related to planarity and roughness, b is a factor related to infilling mineral, and c is the factor related to infilling thickness. The values assigned for factors a, b, and c for different categories of fracture data are tabulated in Table 7-3. The value JC was calculated for each N and I type fracture in a 3-m (10-ft) interval and an average JC value was calculated for the interval by dividing by the number of fractures.

Table 7-3. Factors a, b, and c for JC Rating Calculation

Factor a (a = a1 + a2)											
a1 (Fracture Planarity)											
P	C	S	I								
0.20	0.35	0.50	0.50								
a2 (Fracture Roughness)											
V	R	M	S	P							
0.45	0.45	0.45	0.40	0.35							
Factor b (Infilling Mineral)											
C	WC	WN	BC	BD	TD	TC	CA	SI	MN	CL	TN
1	1	0.60	1	1	1	1	1	0.85	0.85	0.60	0.60
Factor b (Infilling Mineral)											
C	S	T	M	V	E						
1	1	1	0.05	0.30	0.30						

The histograms which present the distribution of JC ratings for all the 3-m (10-ft) intervals are shown in Figure 7-4. The JC rating of 25 occurs most frequently and corresponds to the descriptions for “slightly rough surfaces, separation <1 mm, slightly weathered walls,” in Bieniawski (1979). This is generally consistent with the fractures observed in the core.

7.2.5 Groundwater

The rock mass at or above the repository level is unsaturated and dry at Yucca Mountain site. A Jw rating of 15 was therefore assigned to all thermomechanical (thermal-mechanical) units.

7.2.6 Distribution of Rock Mass Rating (RMR) Values for the Thermomechanical (Thermal-Mechanical) Units

The RMR rating for each 3-m (10-ft) interval was calculated by summing the five parameters discussed in the preceding subsections. The values for the five parameters and the calculated RMR rating for every 3-m (10-ft) interval in each NRG-series core hole are presented

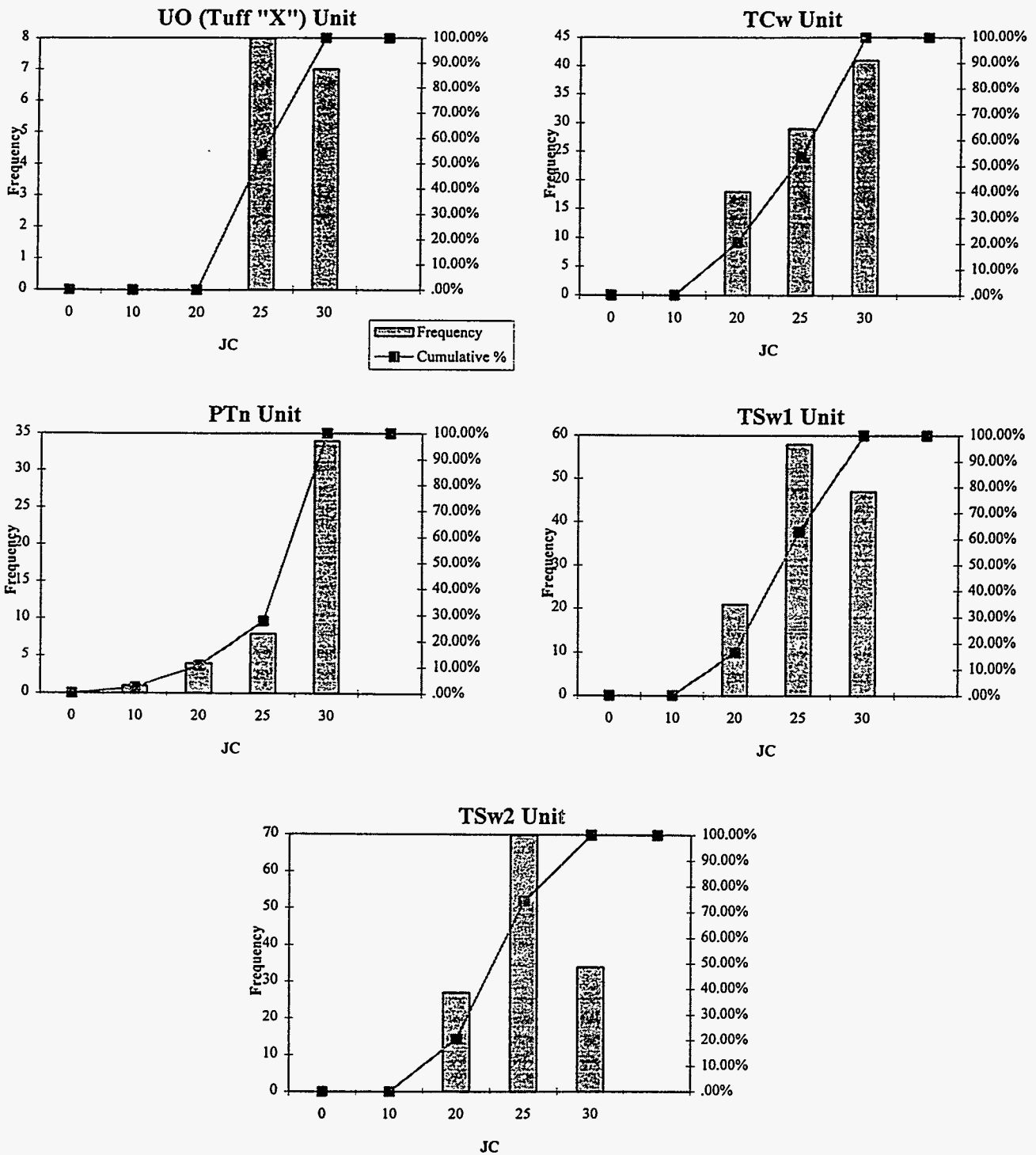


Figure 7-4. Histograms Showing the Distribution of the JC Rating for the RMR System in the Thermomechanical (Thermal-Mechanical) Units—NRG Holes

in Volume II. The distribution of the RMR in 3-m (10-ft) intervals is shown for each thermomechanical (thermal-mechanical) unit as histograms of the frequency of occurrence and cumulative percentage of occurrence in Figure 7-5. All the data were rank ordered and used to evaluate the cumulative frequency of occurrence to identify RMR ratings with different levels of confidence. Tables of the rank-ordered data are presented in Appendix C. The values of RMR for frequencies of occurrence of 5%, 20%, 40%, 70%, and 90% that define the five rock mass quality categories are listed in Table 7-4.

Table 7-4. RMR Ratings for the Five Rock Mass Quality Categories

Rock Mass Quality	Frequency of Occurrence (%)	UO (Tuff "X")	TCw	PTn	TSw1	TSw2	Relative Rating	
1	5	50	51	45	49	51	very good	81-100
2	20	53	56	52	53	56	good	61-80
3	40	56	59	55	57	58	fair	41-60
4	70	59	67	65	62	63	poor	21-40
5	90	60	72	70	70	67	very poor	<20

The RMR calculation system (Bieniawski, 1979) used in this study places heavy emphasis on the conditions of joints with 30 of the possible 100 points allocated to the JC parameter. The JC ratings of 25, calculated for most of the intervals in Section 7.2.4, combined with a Jw of 15 for the dry conditions, produces a minimum RMR rating for most of the intervals above 40 (fair rock category). In general, the RMR ranges from fair to good rock mass conditions throughout the five rock mass quality classes.

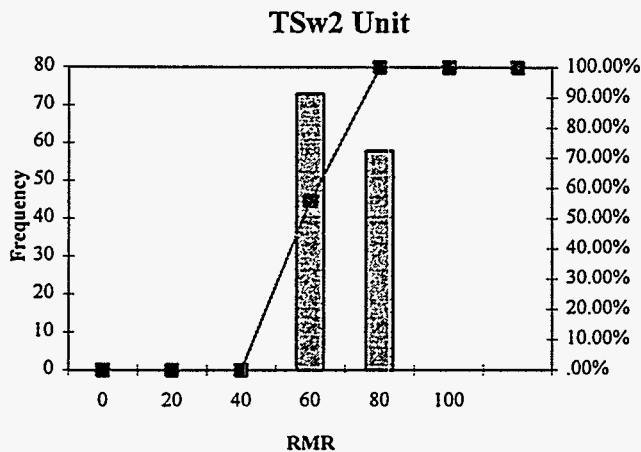
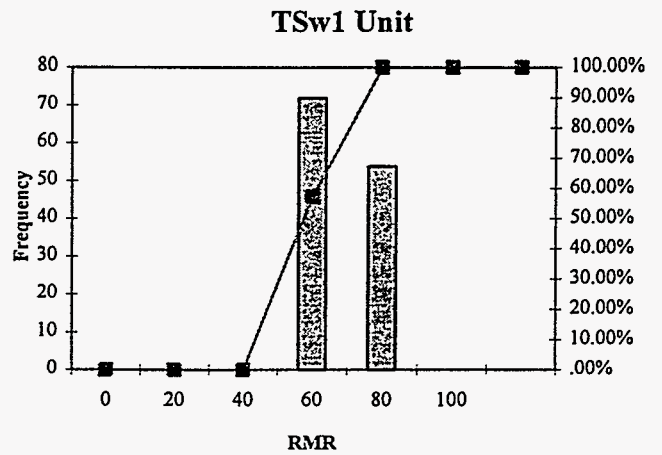
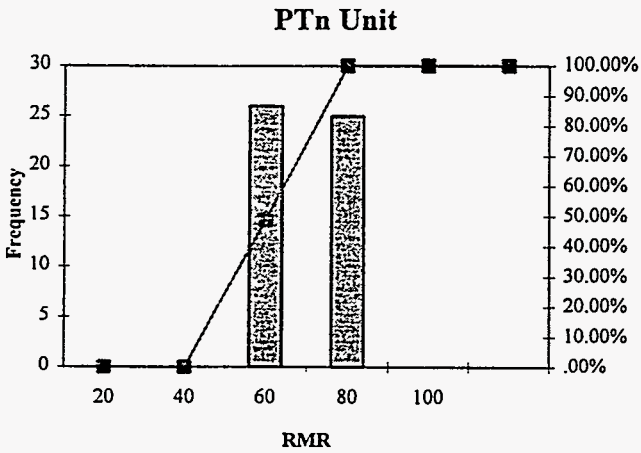
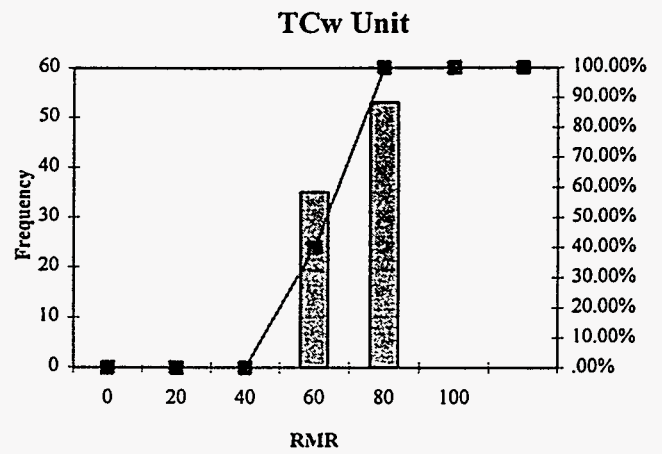
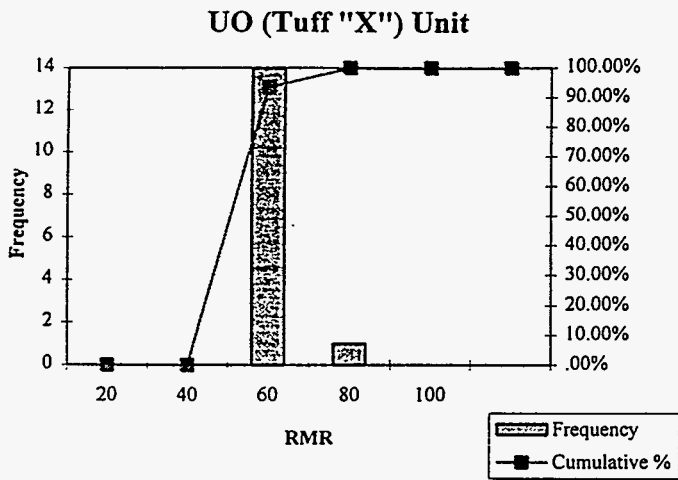


Figure 7-5. Distribution of Estimated RMR(79) in Each Thermomechanical (Thermal-Mechanical) Unit —NRG Holes

7.3 Rock Mass Quality Indices for the Q System

The Q index, as defined by Barton et al. (1974), is calculated from six parameters:

$$Q = \left(\frac{RQD}{J_n} \right) * \left(\frac{J_r}{J_a} \right) * \left(\frac{J_w}{SRF} \right) \quad (7-3)$$

where RQD = Rock Quality Designation (%)

J_n = Joint Set Number

J_r = Joint Roughness Number

J_a = Joint Alteration Number

SRF = Stress Reduction Factor

J_w = Joint water factor

The first term (RQD/J_n) describes the block size, the second term (J_r/J_a) describes interblock shear strength, and the third term describes the effect of the active stress.

In this work, the parameters RQD, J_r, and J_a were determined from each 3-m (10-ft) interval in the Rock Structure Summary Log. Because there is no direct way to determine the parameters J_n and SRF from core data, they were evaluated using Monte Carlo simulation based on surface mapping, mapping of the NRST by the U.S. Bureau of Reclamation, and oriented-core data from previous YMP drilling (Lin et al., 1993b). The determination of each parameter is described briefly in the following sections.

7.3.1 Rock Quality Designation (RQD)

RQD values described in Section 5.3 were used in the Q system. In the calculation of Q, RQD was set equal to 10% if it is less than 10% as per the procedures defined by Barton et al. (1974). The direct value was used in the calculation. Distributions of the RQD data were presented earlier in Figure 5-2, Section 5.0.

7.3.2 Joint Set Number (Jn)

Joint set number cannot be readily determined from the NRG core logs. Fracture orientations based on oriented core data and borehole television observations from USW core holes have been studied in Lin et al. (1993b), who identified one to three joint sets in the welded tuff units. Fracture orientations from mapping of the NRST indicated two to three joint sets in processed stereonets. Based upon the mapping data, two joint sets ($J_n = 4$) to three joint sets ($J_n = 9$), was selected as the range of the J_n parameter. Since the probability of two sets or three sets is not available at this time, a uniform distribution of J_n between 4 to 9 was assumed and Monte Carlo simulation was used to generate J_n values for each 3-m (10-ft) interval. The simulation was conditioned by setting J_n equal to 9 if the proportion of lost core and rubble in an interval was equal to or greater than 70% to be conservative. However, there was no indicated correlation between lost core and rubble and the number of joint sets.

The distribution of J_n values are presented in the histograms of Figure 7-6. As expected, the results are distributed in between 4 to 9 with the values of 9 (three joint sets) occurring most frequently because of the large number of intervals with high proportions of lost core and rubble. The distribution for the UO (Tuff "X") and PTn units are less uniform than the assumptions because of the limited number of trials due to relatively few 3-m (10-ft) intervals.

7.3.3 Joint Roughness Number (Jr)

Joint roughness number was related to the joint surface planarity and roughness described during logging of the fracture data. An additive process combining the planarity and roughness data was developed to match the descriptions for determining J_r (Barton et al., 1974). Table 7-5 lists the two component values of J_r , J_{r1} defined by planarity and J_{r2} by roughness. A J_r value was determined for each N or I type fracture as the sum of J_{r1} and J_{r2} . An average J_r was then calculated for the entire interval.

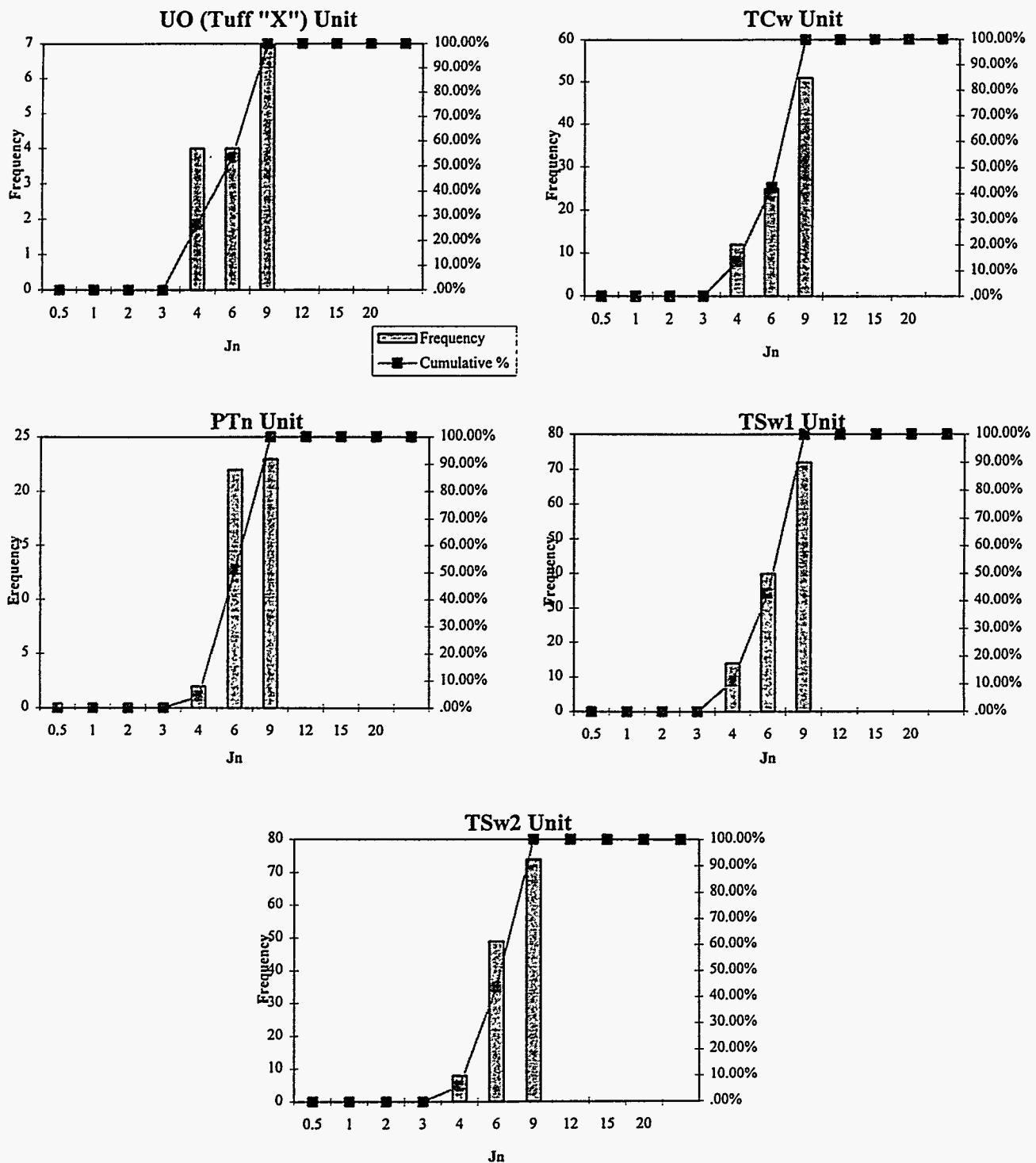


Figure 7-6. Histograms Showing the Distribution of Jn for the Q System in the Thermomechanical (Thermal-Mechanical) Units—NRG Holes

Table 7-5. Algorithm Relating Jr ($Jr = Jr1 + Jr2$) Values to Planarity and Roughness Described in the Geology and Rock Structure Log

Planarity Description	Jr1	Roughness Description	Jr2
I	1	V	2
S	1	R	2
P	0	M	2
C	0	S	1
		P	0.5

The distributions of Jr are presented as histograms in Figure 7-7. Most of the fractures have either planar (P) or irregular (I) surfaces with moderate (M) roughness (Section 5.6.5), which agrees well with the range of Jr between 2 and 3.

7.3.4 Joint Alteration (Ja)

Joint alteration number was determined in the Q system for three categories of surface contact:

- rock wall contact (tight, clean joints),
- rock wall contact before 10 cm shear (undulating joints, thin infilling), and
- no rock wall contact when sheared (thin infilling).

The log descriptions of both the infilling thickness and mineral infilling type were used for determining Ja. The infilling thickness from the fracture data was used to indicate the state of surface contact. For each of the three contact categories, four or five sub-categories were possible (Barton et al., 1974) based on the infill mineral type. For the NRG data, only two sub-categories, clay infilling or non-clay infilling, were used to determine Ja. Table 7-6 lists the algorithm to determine Ja for different combinations of infilling thickness and mineral type.

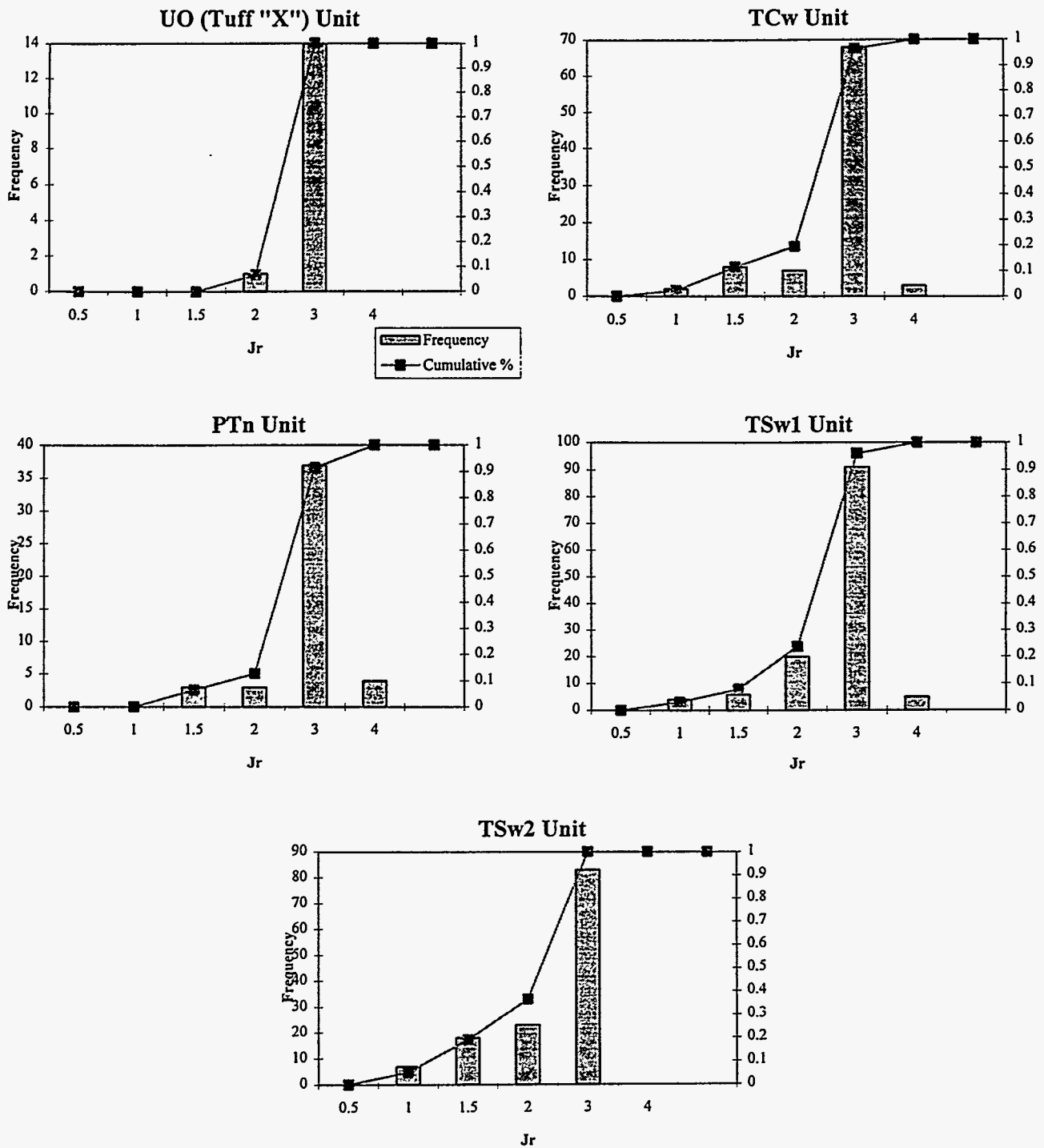


Figure 7-7. Histograms Showing the Distribution of Jr for the Q System in the Thermomechanical (Thermal-Mechanical) Units—NRG Holes

Table 7-6. Algorithm to Determine Ja Values from Log Data

Infilling Thickness Abbreviations	C		S		T		M		V		E	
Infilling Mineral	Non-Clay	Clay	Non-Clay	Clay	Non-Clay	Clay	Non-Clay	Clay	Non-Clay	Clay	Non-Clay	Clay
Ja Value	1	3	1	3	1	3	1	3	6	8	8	10

Histograms of the distribution of Ja are presented in Figure 7-8 for each thermomechanical (thermal-mechanical) unit. The majority of Ja values in all the thermomechanical (thermal-mechanical) units range between 1 and 2 corresponding to a description of rock wall contact with “unaltered joint walls, surface staining only” or “slightly altered joint walls, clay free.”

7.3.5 Joint Water Reduction Factor (Jw)

The joint water reduction factor Jw is set to a value of 1 for “dry excavations” in all thermomechanical (thermal-mechanical) units.

7.3.6 Stress Reduction Factor (SRF)

The stress reduction factor SRF is defined by Barton et al. (1974) as a measure of:

- ♦ weakness zones intersecting the excavation, which may cause loosening of the rock mass;
- ♦ competent rock, rock stress problems; and
- ♦ squeezing rock, plastic flow of incompetent rock.

SRF for the welded tuff units was determined by Monte Carlo simulation for each 3-m (10-ft) interval on the basis of conditions observed in the NRST. The distribution of SRF was derived from the U.S. Bureau of Reclamation’s Full Perimeter Geology Map²⁹ of the NRST. This map

²⁹ Non-QA data.

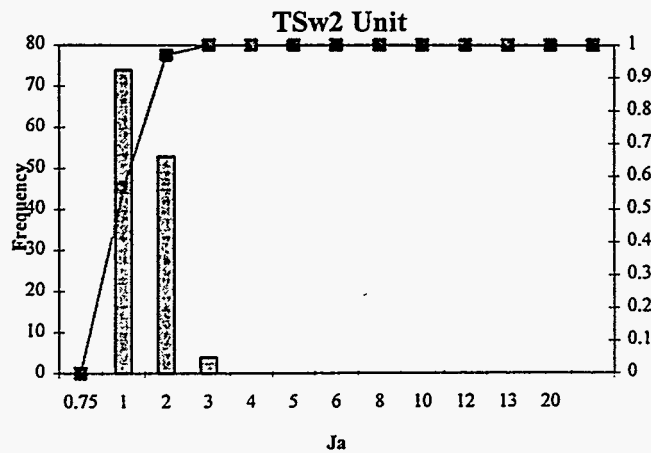
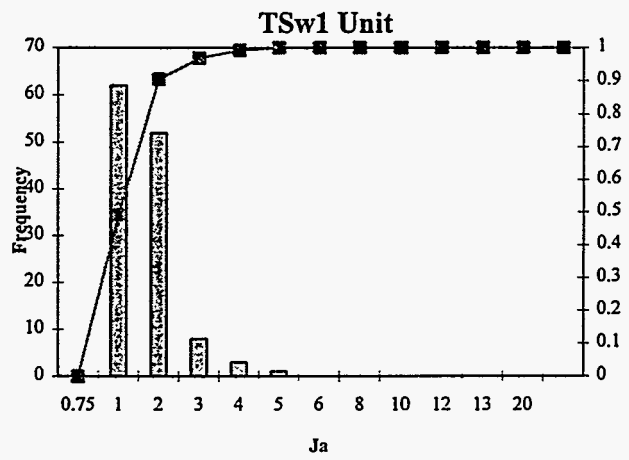
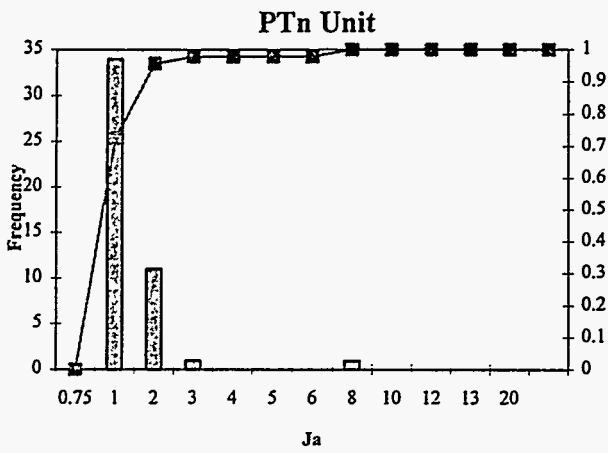
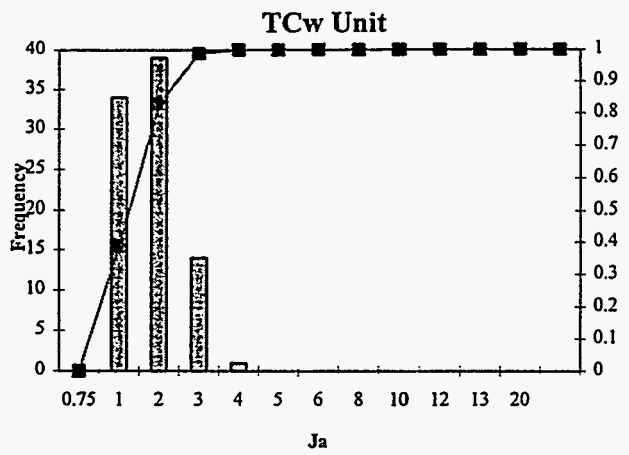
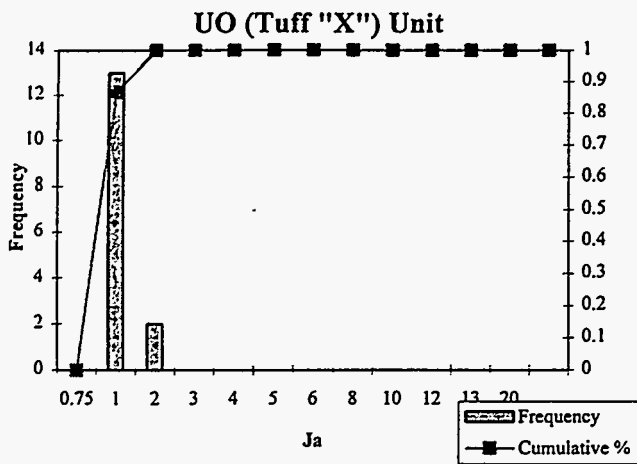


Figure 7-8. Histograms Showing the Distribution of Ja for the Q System in the Thermomechanical (Thermal-Mechanical) Units—NRG Holes

was subdivided into unit areas of 3 m (10 ft) in length along the tunnel axis. For each 3 m (10 ft) of tunnel length, 4 unit areas were examined consisting of each wall and 2 sections of roof from the tunnel centerline to each of the right and left spring line. The map was judged to contain unit areas with three types of conditions: unit areas that contained sheared zones of some thickness, unit areas that contained the notation of “intensely fractured,” and unit areas where joints were indicated, but the relatively density is judged to be consistent with competent rock conditions. The frequency distribution of these unit area types in the map and their corresponding description and SRF values are:

- ♦ Unit areas with shears, 9 out of 40 = 22.5%: use “multiple shear zones any depth”
SRF = 7.5;
- ♦ Unit areas “intensely fractured,” 8 out of 40 = 20%: use “single shear zone”
SRF = 5.0; and
- ♦ Unit areas with typical jointing: 23 out of 40 = 57.5%: use SRF = 1.0, competent rock, medium stress.

Selection of the value SRF = 1 for unit areas with typical jointing was based on photographs presented by Barton et al. (1974) which also lists the various parameters used to calculate Q for the outcrop in each photograph. A density of jointing exposed in outcrops of TSw1 and TSw2 at Fran Ridge also seemed consistent with a SRF value of 1.0 (ignoring the fact that the outcrop is exposed at the surface).

SRF in the PTn was initially set equal to 1 as suggested by Lin et al. (1993b) because fracture frequency (Section 5.6.3) in the PTn is less than 50% of that in the welded units and because the ratio of vertical stress to compressive strength estimated in the RIB (DOE, 1991) was

in the range of 9. Subsequent rock mechanics tests on PTn and UO samples from the NRG boreholes indicated much lower compressive strength than estimates in the RIB. SRF values for UO (Tuff Unit "X") remained at 1.0 because of the relatively shallow depth of the ramp (30 m) where it penetrates the Tuff "X." However, SRF values for the PTn were revised to reflect the lower compressive strength indicated by the testing.

The "competent rock, rock stress problems" definitions in the Q system were used to evaluate SRF in PTn based upon the ratio of vertical stress to compressive strength for each 3-m (10-ft) interval. Interval estimates of uniaxial compressive strength were based on rock mechanics test data from the 3-m (10-ft) interval, or a value was generated by Monte Carlo simulation from the distribution of all PTn test data. The maximum depth at which the North Ramp is projected to penetrate PTn was used as the vertical stress based on the mean dry bulk density of the TCw unit in Table 6-4 (2.14 g/cc).

The distribution of SRF values are presented in Figure 7-9 as frequency histograms. The Monte Carlo simulation results agree with the input distributions for the welded units (TCw, TSw1, TSw2). Relatively high values of SRF in the PTn reflect the fact that vertical stresses are high with respect to the rock strength, and stress-induced failure of the tunnel walls is expected.

The approach to estimating the SRF parameter produces an average value of 3.26 for the welded units, which may not be high enough given the corrected fracture density indicated for the TSw1 and TSw2 units. An average SRF value of 5.0 may be more appropriate which corresponds to the description of "Loose open joints, heavily jointed or 'sugar cube', etc." in the Barton et al. (1974) description. Because the SRF parameter is in the denominator of the equation to calculate Q, the impact of this difference would be to multiply by a factor of 0.31 for

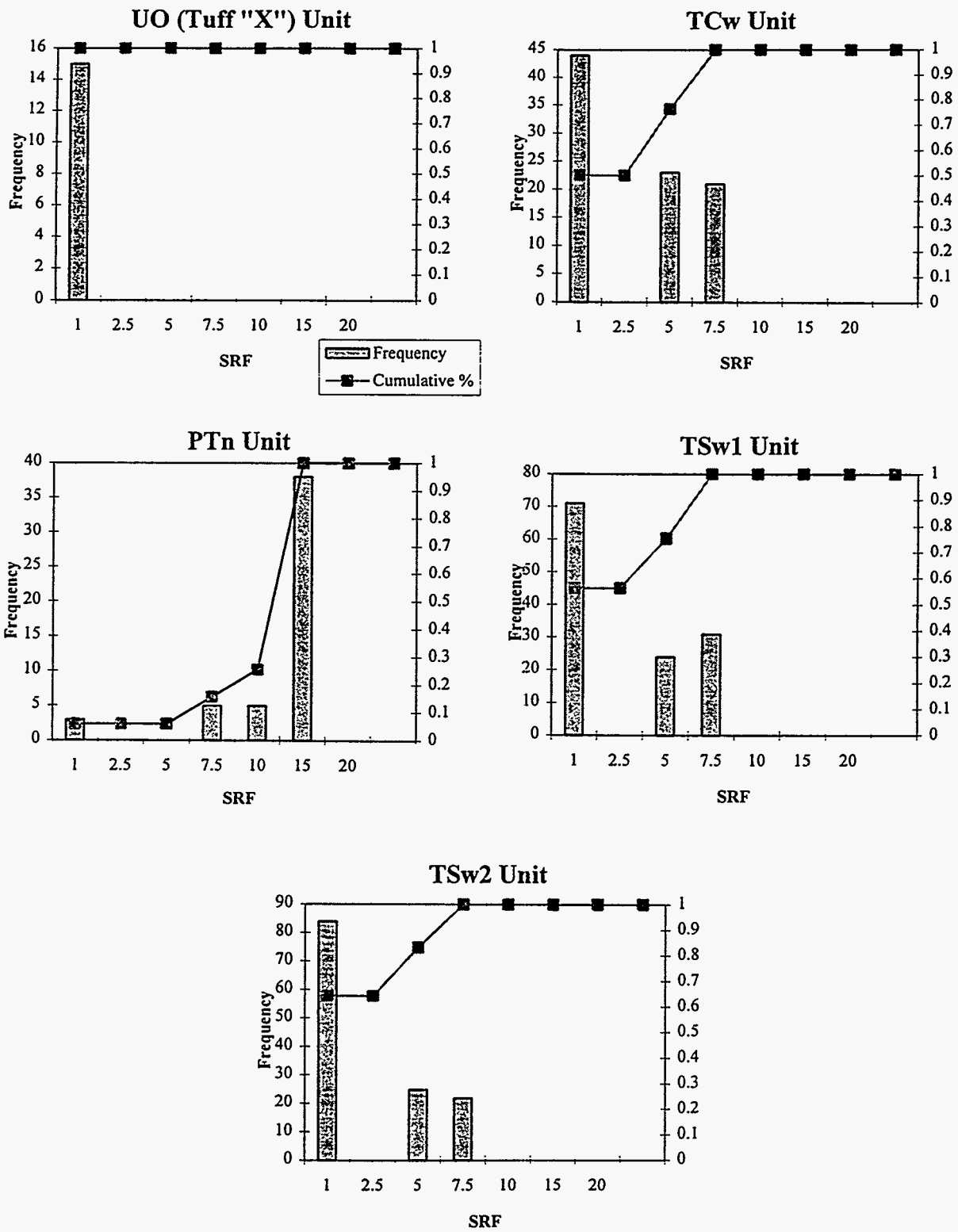


Figure 7-9. Histograms Showing the Distribution of SRF for the Q System in the Thermomechanical (Thermal-Mechanical) Units—NRG Holes

the distribution used, as opposed to 0.20 for an average value of $SRF = 5.0$. This difference (11%) has been compensated for by use of the conservative approach to RQD.

7.3.7 Distribution of Q Values for the Thermomechanical (Thermal-Mechanical) Units

The values for the six parameters and the resulting Q indices for every 3-m (10-ft) interval are tabulated in log form for each NRG hole in Volume II. The data from all holes were grouped by thermomechanical (thermal-mechanical) unit and histograms showing the frequency of occurrence and cumulative percentage are presented in Figure 7-10. Rank-ordered data tables with cumulative frequency of occurrence are presented in Appendix C. Table 7-7 lists the relative rock quality and percentage of the 3-m (10-ft) intervals that occur in each category for each thermomechanical (thermal-mechanical) unit. The welded units vary between very poor and good rock mass quality. The nonwelded units vary between extremely poor and good rock mass quality. The values of Q for the five levels of confidence (5%, 20%, 40%, 70%, and 90%) are listed in Table 7-8.

7.4 Evaluation of RMR and Q Results

The Q and RMR values determined based on the NRG core logging data have been evaluated with respect to a correlation between RMR and Q reported by Bieniawski (1974) and by comparing them to ranges of Q and RMR developed from observations made during excavation of the NRST.³⁰ This evaluation was performed to confirm that the rock mass quality estimated using the core logging data was consistent with the reported correlations between the two indices from other published work and that the core-based estimates were reasonable when compared to assessments made in the NRST exposures.

³⁰ C.E. Brechtel, S.C. Carlisle, and J. Pott, 1993. "Rock Mass Quality Estimation, North Ramp Starter Tunnel, Upper Bench," SLTR93-7001, DTN:SNF28021693001.001, Sandia National Laboratories, Albuquerque, New Mexico.

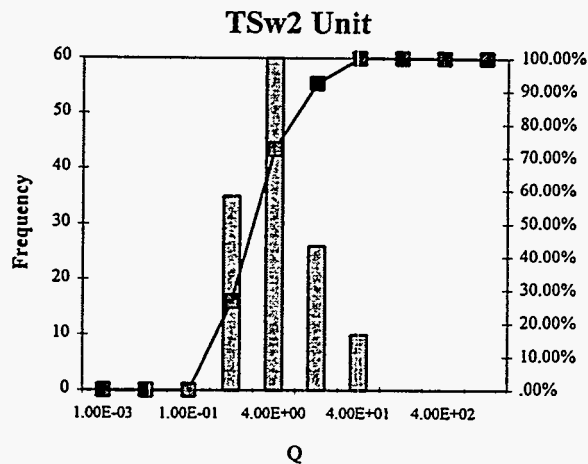
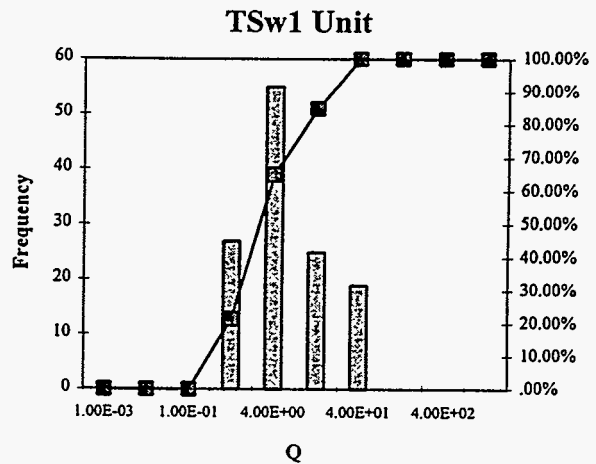
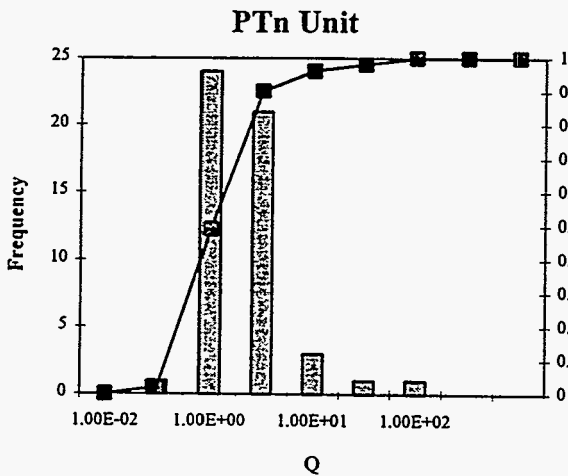
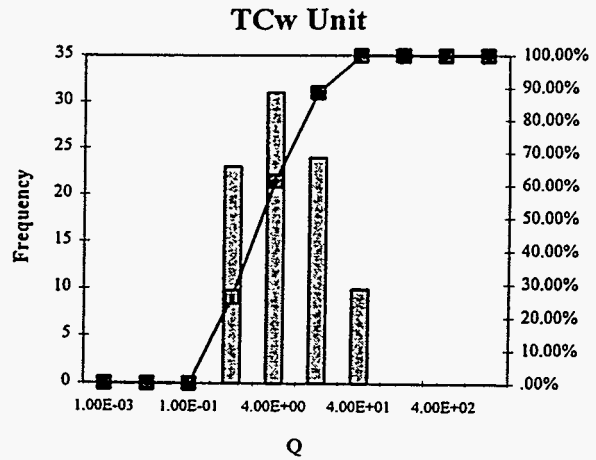
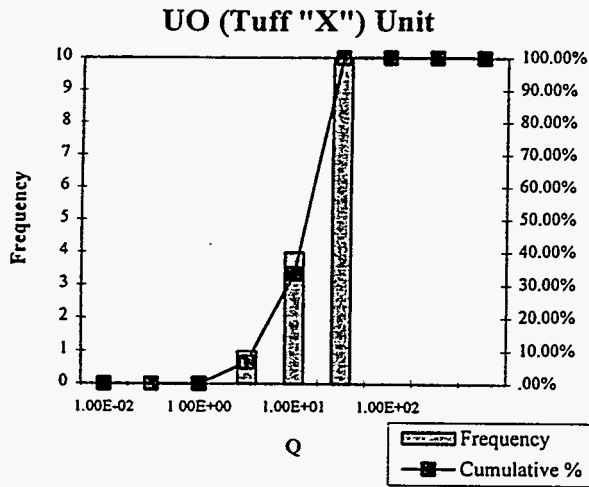


Figure 7-10. Distribution of Estimated Q in Each Thermomechanical (Thermal-Mechanical) Unit — NRG Holes

Table 7-7. Percentage of Occurrence for Relative Rock Mass Quality Estimated using the Q System — NRG Holes

Relative Rock Quality	Range of Q	UO (Tuff "X")	TCw	PTn	TSw1	TSw2
exc. poor	0.001–0.01	0%	0%	0%	0%	0%
ext. poor	0.01–0.1	0%	0%	2%	0%	0%
very poor	0.1–1	0%	26%	47%	21%	27%
poor	1–4	10%	35%	41%	44%	46%
fair	4–10	26%	28%	6%	20%	19%
good	10–40	64%	11%	2%	15%	8%
very good	40–100	0%	0%	2%	0%	0%
ext. good	100–400	0%	0%	0%	0%	0%
exc. good	400–1000	0%	0%	0%	0%	0%

Table 7-8. Q Values for the Five Rock Mass Quality Categories

Rock Mass Quality	Frequency of Occurrence (%)	Old UO (Tuff "X")	TCw	PTn	TSw1	TSw2
1	5	2.23	0.38	0.15	0.24	0.30
2	20	7.50	0.68	0.28	0.87	0.65
3	40	10.98	2.08	0.66	1.73	1.91
4	70	14.49	5.66	1.62	5.09	3.75
5	90	24.29	9.14	3.74	12.00	8.44

7.4.1 Correlation of RMR and Q Results

Bieniawski (1976) developed a correlation between the Q index and RMR with 90% confidence intervals bounding the relationship which was based on 111 case histories. Q and RMR values estimated for the NRG-series core holes are compared to the correlation equations in Figures 7-11 to 7-15 for each thermomechanical (thermal-mechanical) unit. For all the welded tuff units, most of the data points with Q indices greater than 1 appear to be in the median to upper 90% confidence limit of the correlation equations. However, for intervals with Q indices less than 1, RMR ratings tend to exceed the upper 90% confidence limit. In the UO unit, the rock quality indices are within the median and lower 90% confidence limit of the correlation equations.

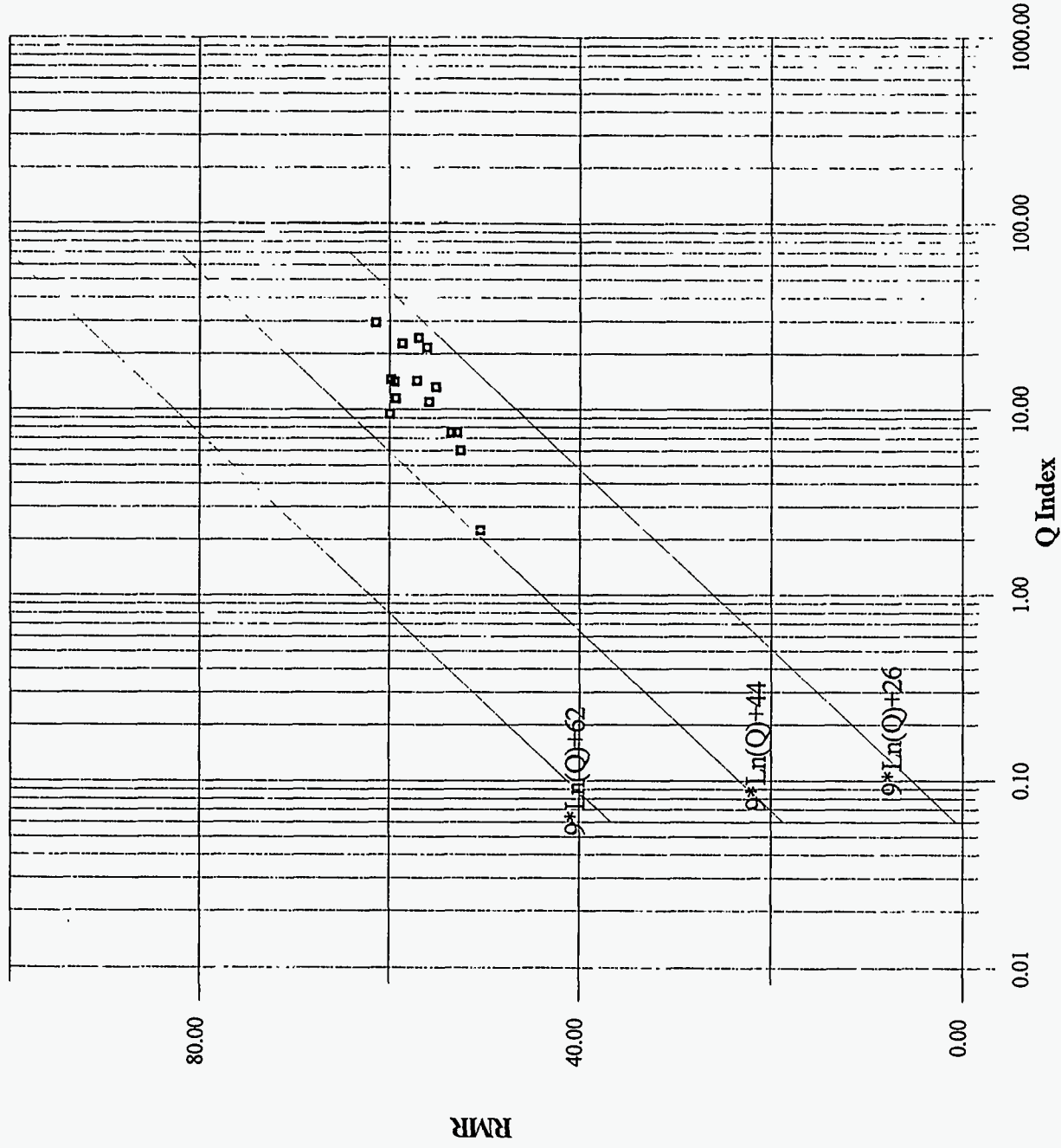


Figure 7-11. Correlation of Q and RMR Results for the UO (Tuff "X") Unit—NRG Holes

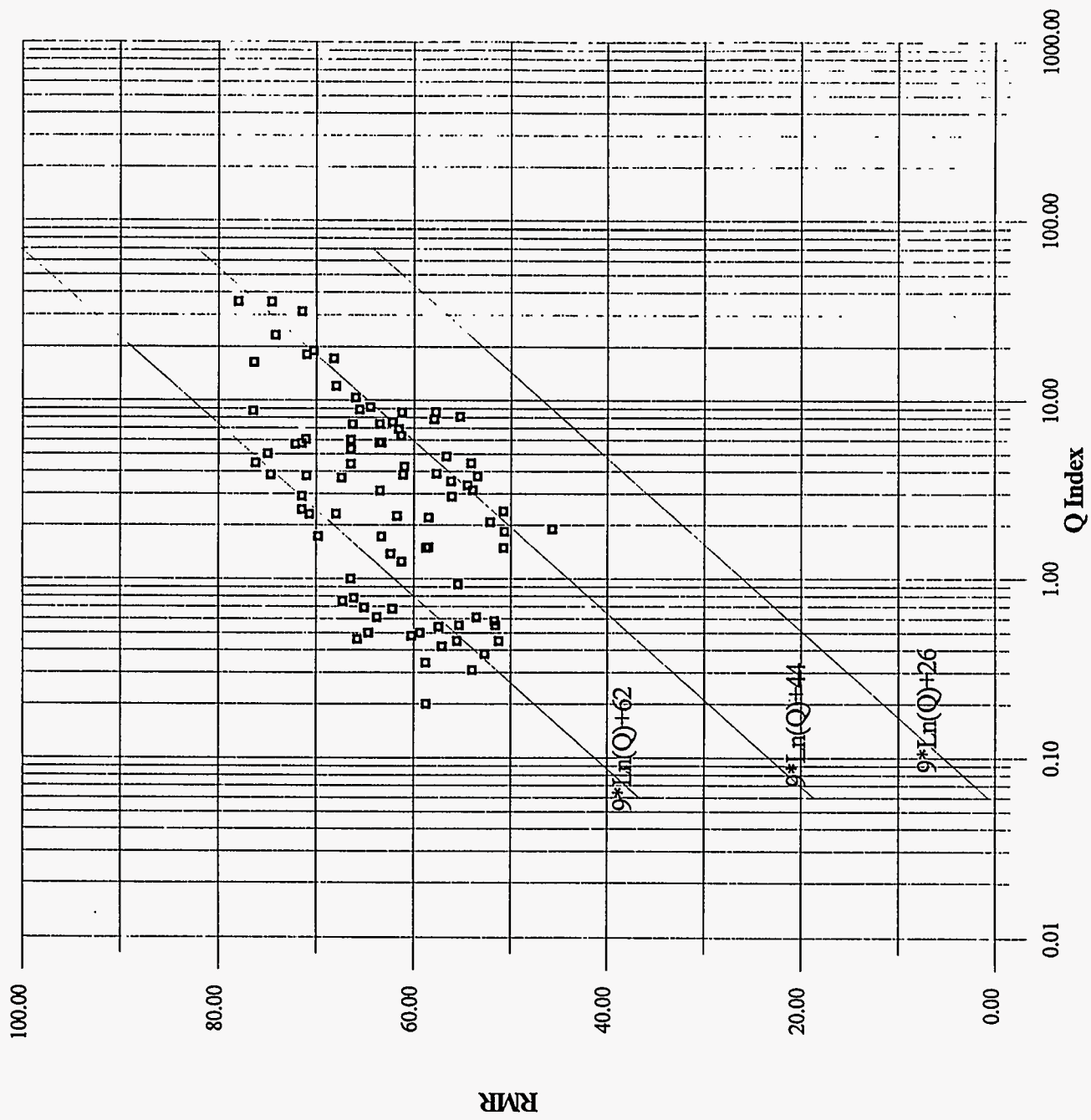


Figure 7-12. Correlation of Q and RMR Results for the TCw Unit—NRG Holes

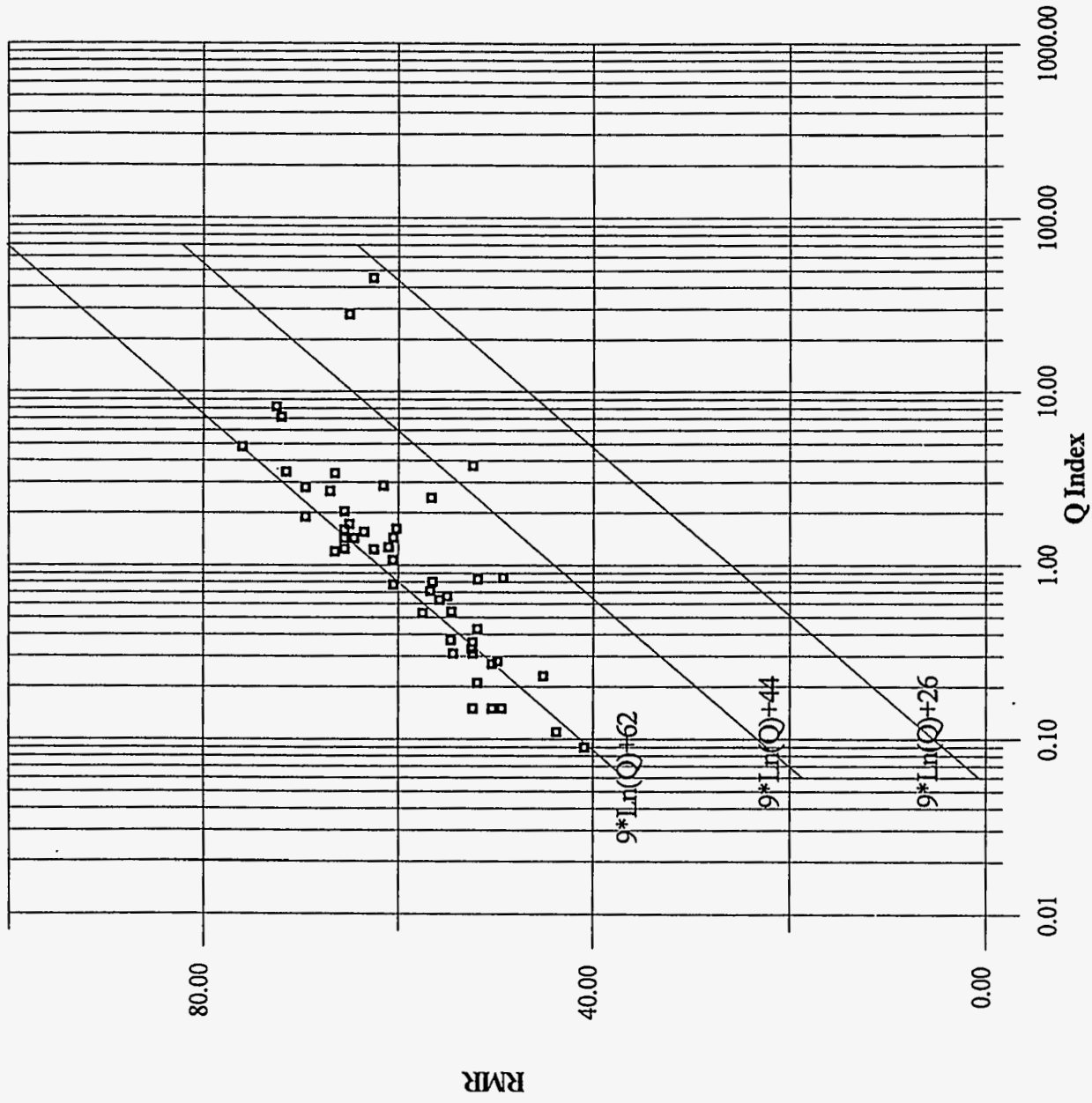


Figure 7-13. Correlation of Q and RMR Results for PTn Unit — NRG Holes

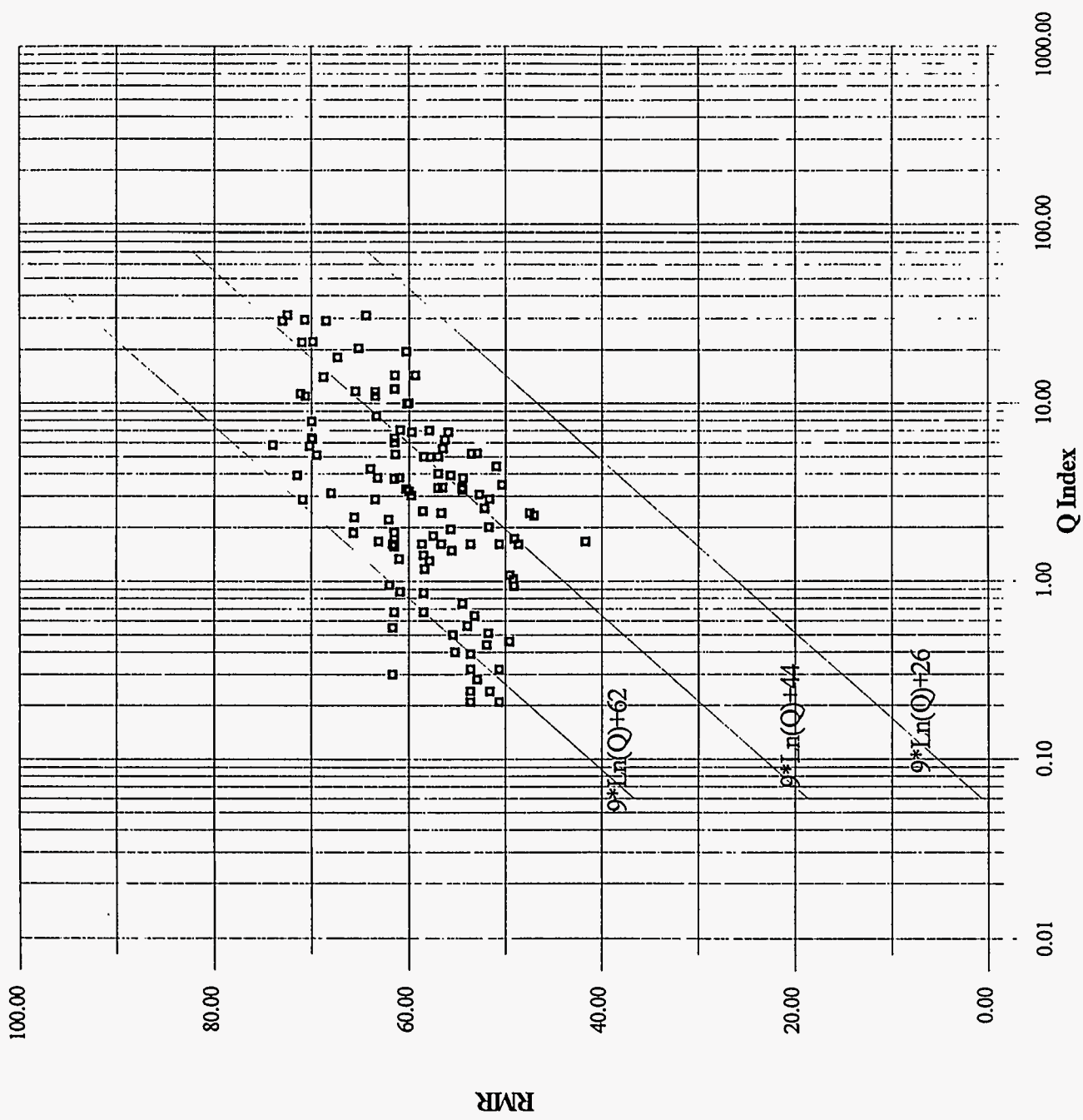


Figure 7-14. Correlation of Q and RMR Results for the TSsw1 Unit—NRG Holes

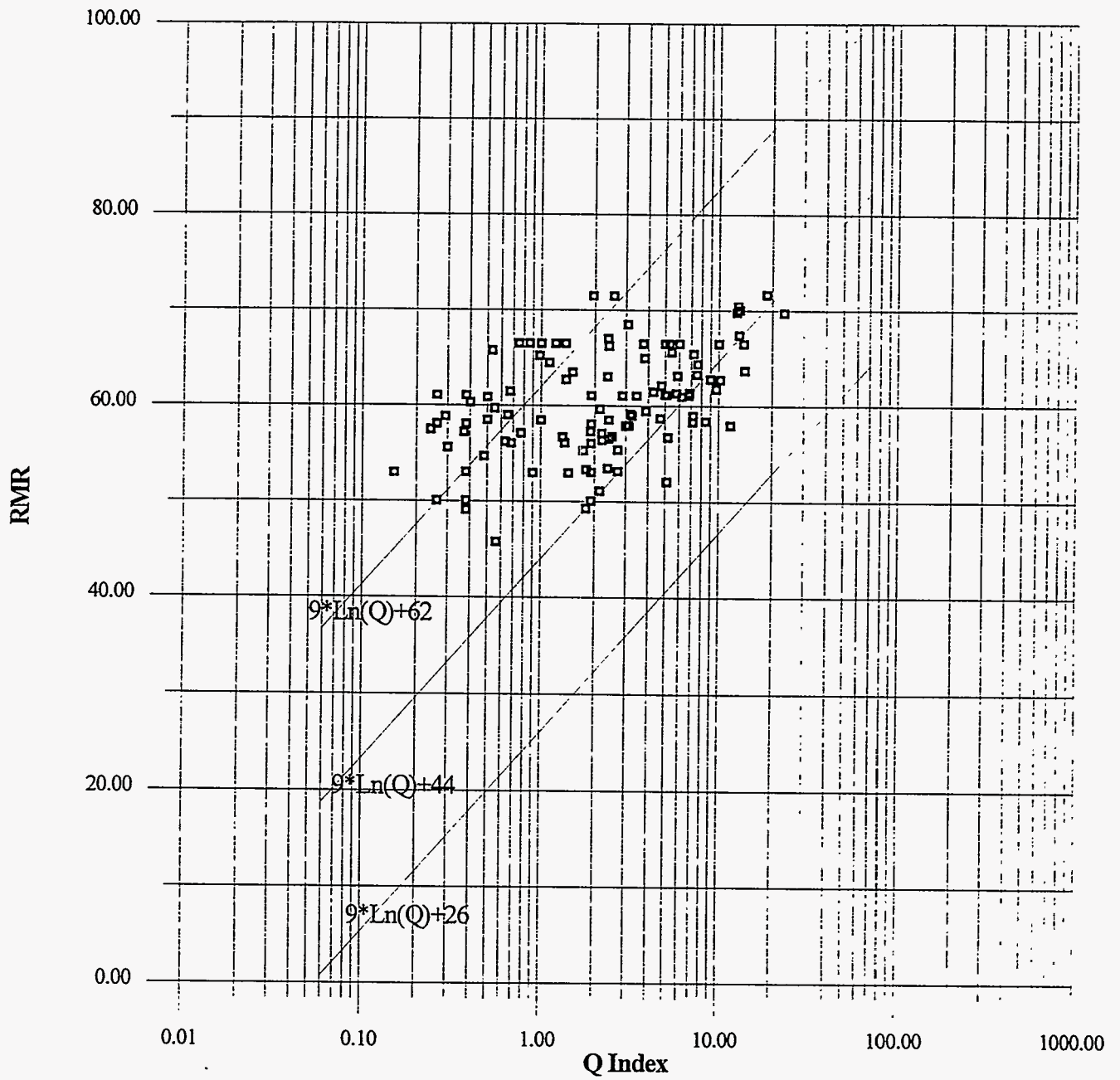


Figure 7-15. Correlation of Q and RMR Results for the TSw2 Unit—NRG Holes

The comparison of the Q-RMR correlations to the previously published correlations in Figures 7-11 through 7-15 indicates trends similar to those reported by others. The deviations at low values of Q may be due to the fact that the RMR in this work has not been adjusted for joint orientations with respect to tunnel access. The joint orientation adjustment is not made when RMR is used in correlation with rock mass mechanical properties.

7.4.2 Comparison of Q and RMR Determined in the NRST to NRG Core-Based Data

Observations of the tunnel walls during the excavation of the NRST were used to calculate Q and RMR for both the upper heading³¹ and lower bench. The rock mass quality indices were calculated based upon the observed range of individual parameters in sections of the tunnel that varied in length from 3.96 m (13 ft) to 16.76 m (55 ft). The data were then presented as a minimum and maximum value based upon the assessment of the observed range in the individual parameters.

The NRST data provide an opportunity to compare the core log derived Q and RMR to data from the tunnel exposures. The NRST was excavated in the Tiva Canyon Upper Lithophysal Zone (TCw thermomechanical (thermal-mechanical) unit) on the east face of Exile Hill. Borehole NRG-1 was drilled through the portal area of the NRST and provides a site-specific comparison to the NRST Q data in Table 7-9 and NRST RMR data in Table 7-10.

The range and mean values of each parameter used to calculate Q (Table 7-9) are compared to the borehole data from NRG-1 to evaluate how well the core-based approach estimated the exposed conditions. The mean of the core-based data from NRG-1 agrees well with the mean of the maximum value of the NRST data, and the range and mean of the individual parameters were comparable with the exception of the joint alteration number (Ja) and

³¹ Ibid.

Table 7-9. Comparison of the Range and Mean of Individual Parameters Used to Calculate Q at the NRST and in NRG-1

	NRST		NRG-1 Tiva Canyon Upper Lithophysal	
	Range	Mean	Range	Mean
Maximum Value				
RQD	44.0 – 91.0	78.4	10.0 – 58.0	36.5
Jn	3.0 – 9.0	6.0	4.0 – 9.0	7.3
Jr	1.0 – 3.0	2.3	1.0 – 4.0	2.5
Ja	1.0 – 8.0	4.4	1.0 – 1.9	1.3
Jw*	1.0	1.0	1.0	1.0
SRF	2.5 – 7.5	4.5	1.0 – 7.5	4.4
Q Mean		1.5	—	2.2
Minimum Value				
RQD	31.0 – 87.0	66.8	10.0 – 58.0	36.5
Jn	6.0 – 12.0	8.1	4.0 – 9.0	7.3
Jr	1.0 – 3.0	1.7	1.0 – 4.0	2.5
Ja	4.0 – 12.0	6.7	1.0 – 1.9	1.3
Jw*	1.0	1.0	1.0	1.0
SRF	4.0 – 10.0	7.2	1.0 – 7.5	4.4
Q Mean		0.29	—	2.2

*Dry conditions.

Table 7-10. Comparison of the Range and Mean of Individual Parameters Used to Calculate RMR at the NRST and in NRG-1

	NRST		NRG-1 Tiva Canyon Upper Lithophysal	
	Range	Mean	Range	Mean
Maximum Value				
C	9.0	9.0	7.0 – 12.0	10.8
I _{RQD}	16.0 – 18.0	17.2	3.0 – 13.0	8.6
JS	14.0 – 20.0	17.4	5.0 – 8.0	7.6
JC	10.0	10.0	20.8 – 30.0	26.3
Jw*	15.0	15.0	15.0	15.0
RMR		68.6	—	68.3
Minimum Value				
C	6.0	6.0	7.0 – 12.0	10.8
I _{RQD}	13.0 – 16.0	15.4	3.0 – 13.0	8.6
JS	8.0 – 13.0	10.4	5.0 – 8.0	7.6
JC	0	0	20.8 – 30.0	26.3
Jw*	15.0	15.0	15.0	15.0
RMR		46.8	—	68.3

*Dry conditions.

the RQD. The mean of the minimum values is one order of magnitude below the mean of the NRG-1 data, and the primary difference was in the joint alteration number (Ja), the stress reduction factor (SRF), and the RQD.

A similar trend was observed in the NRST RMR data which are compared to the NRG-1 data in Table 7-10. The NRG-1 mean RMR is very close to the mean value of the maximum RMRs determined in the tunnel. The NRG-1 data diverge from the mean of the minimum RMRs by 21.4. The major difference occurs in the joint condition parameter (JC), which is due to the fact that the vertical borehole did not sample the intermediate scale vertical faults or shears exposed in NRST.

The differences in the observations are attributed to the existence of intermediate scale, near-vertical faults or shears in the NRST that were not sampled by the borehole because it was drilled vertically. The structures were of varying widths (up to 1 m) containing crushed, broken rock with substantial clay/mud. Their presence is due to the horst-like structure of Exile Hill, a local topographic high between the Midway Valley and Bow Ridge faults and the extensional stress state associated with faulting. The surface proximity has allowed more extensive weathering of rock in the shear structures.

7.5 Comparison of Lithophysae-Rich and Nonlithophysal Portions of the Welded Units

Rock mass quality indices were estimated for the lithophysae-rich and nonlithophysal portions of the welded units TCw and TSw1. The results indicated little difference in rock mass quality as shown in Table 7-11. Further discussion is therefore focused only on thermomechanical (thermal-mechanical) units without further subdivision. The rock quality indices for lithophysae-rich and nonlithophysal portions of TCw and TSw1 units are included in Appendix D.

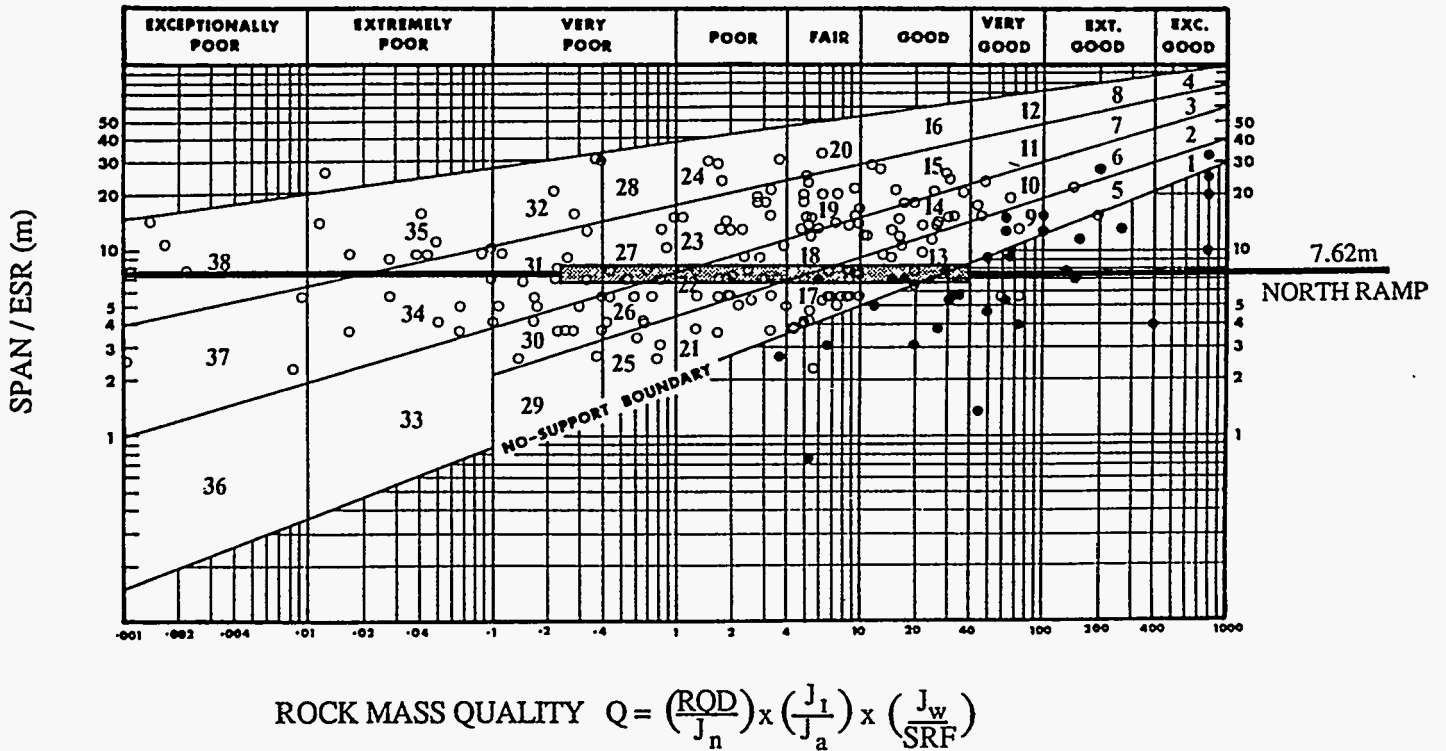
Table 7-11. Comparison of Rock Mass Quality for Lithophysae-Rich and Nonlithophysal Portions of the TCw and TSw1

Rock Mass Category		Frequency of Occurrence (%)	TCw			TSw1		
			All Data	TCw-LR	TCw-NL	All Data	TSw1-LR	TSw1-NL
Q	1	5	0.38	0.45	0.38	0.24	0.24	0.28
	2	20	0.68	0.78	0.55	0.87	0.67	0.95
	3	40	2.08	2.44	1.84	1.73	1.61	2.01
	4	70	5.66	6.00	4.84	5.09	4.00	5.80
	5	90	9.14	12.00	9.14	12.00	10.93	20.40
RMR	1	5	51	54	51	49	50	48
	2	20	56	59	54	53	52	53
	3	40	59	64	59	57	57	56
	4	70	67	68	65	62	61	63
	5	90	72	75	72	70	67	71

LR—Lithophysae Rich; NL—Nonlithophysal

7.6 Indicated Ground Conditions

The application of rock-mass-quality-based empirical design is appropriate for the North Ramp. An example of the design chart is shown in Figure 7-16. The case history data utilized to develop the design method is shown in the chart with a blocked-out area indicating the general range of Q data from the NRG drilling program. The case history data used to develop the Q-based empirical design method generally bracket a range in NRG Q values which indicates that conditions projected in the North Ramp are well bounded by the tunneling case history. The Q index data are correlated with ground conditions and ground support measures by Barton et al. (1974) using a log-log plot of Q versus a parameter “equivalent dimension.” Equivalent dimension is the span of the excavation (diameter) divided by a factor called “excavation support ratio” (ESR), which introduces a factor of safety. A value of 1.0 was used for the ESR in this work because a high factor of safety was required to meet project design goals and criteria.



Range of Q Values for the Five Rock Mass Quality Categories

Figure 7-16. Design Chart Used to Correlate Rock Mass Quality Q with Tunneling Case History Data (Barton et al., 1974)

The design chart is subdivided into ground support categories for use in empirical design of ground support. The distribution of Q data from the NRG drilling is correlated with the design charts in Figures 7-17 through 7-21 for each thermomechanical (thermal-mechanical) unit. The equivalent dimension for the North Ramp (7.62 m) is also plotted to identify the support categories that are indicated by the data.

The distribution of Q data is intended to identify the types of ground support required and the relative lengths of tunnel in each unit that will require the indicated support. Table 7-12 lists the thermomechanical (thermal-mechanical) units and the indicated ground support categories required. The cumulative frequency of occurrence at the maximum Q value for each support category is also listed. Ground support measures from the Q design tables (Barton et al., 1974) are also listed in the table. Table 7-12 was compiled to indicate the range of ground support measures that are consistent with the case history data used to develop the empirical design method. The specific support design will be developed by the M&O design team and will be based upon the many requirements of the Exploratory Studies Facility (ESF) and the construction technique. General guidelines for the North Ramp ground support can be derived from the data distributions and Table 7-12. Specific conclusions regarding the ground support are:

- ♦ Ground support requirements in the nonwelded UO (Tuff "X") units would be relatively light. A substantial portion (up to 64%) of the tunnel in the UO (Tuff "X") unit would be supported with spot bolting or pattern bolting on spacings up to 1.5 m (5 ft).

Rock Mass Quality (Q) in UO (Tuff "X") - NRG Holes

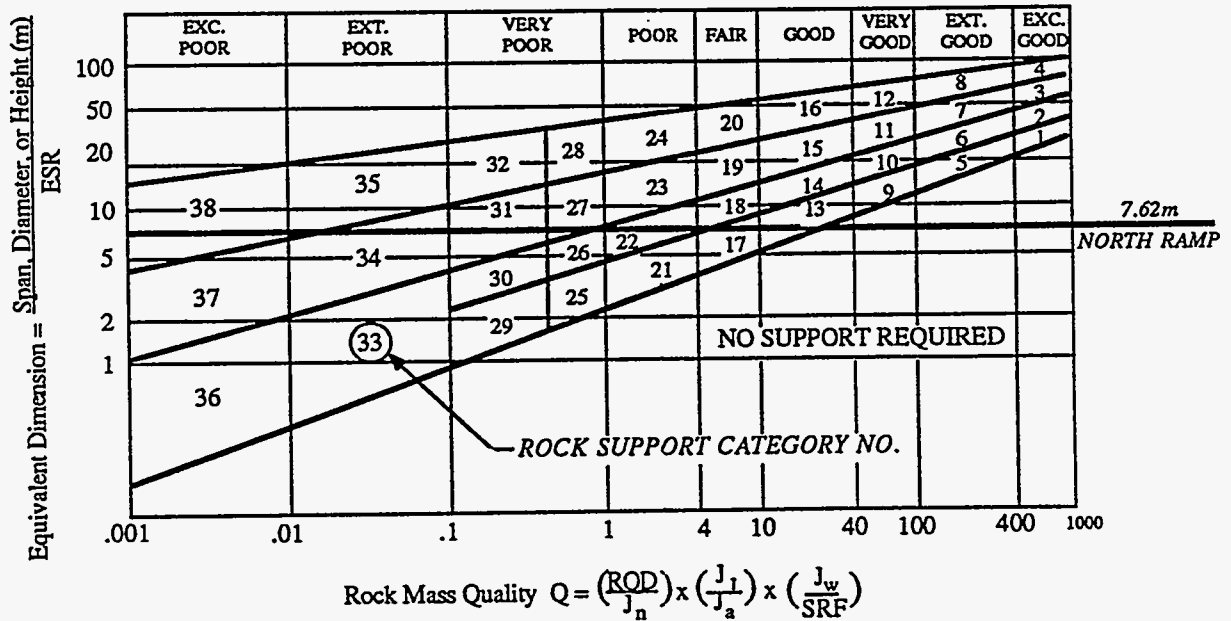
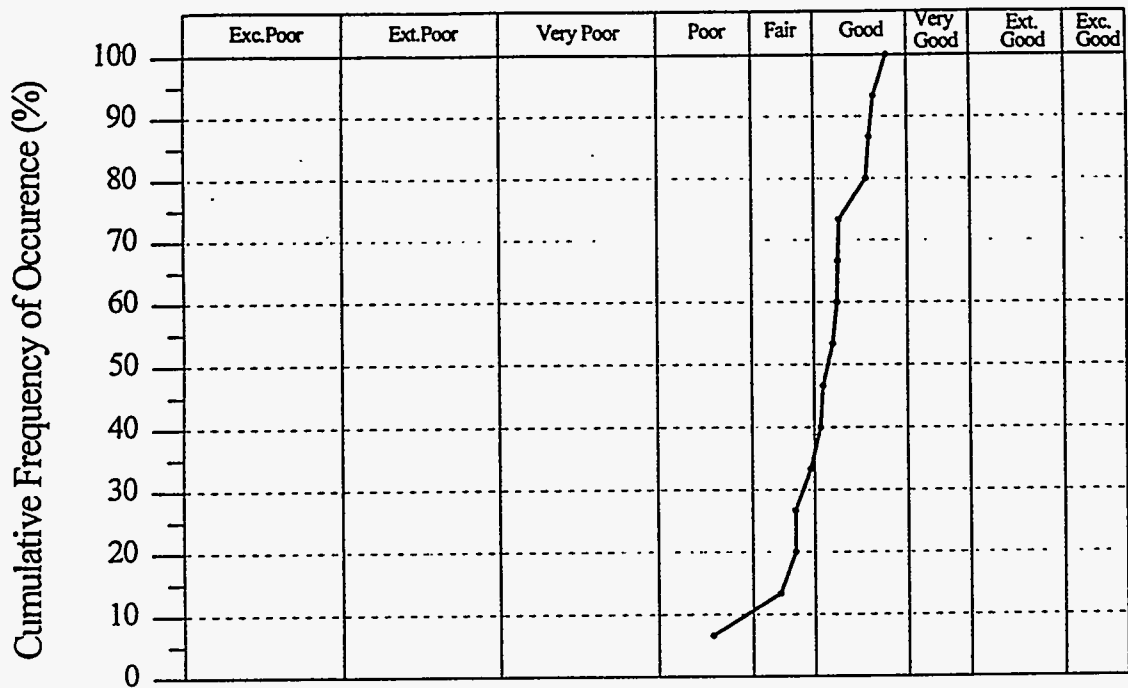


Figure 7-17. Cumulative Frequency of Occurrence of Q in UO (Tuff "X") Compared to Ground Support Design Chart (after Barton et al., 1974)

Rock Mass Quality (Q) in TCw Unit - NRG Holes

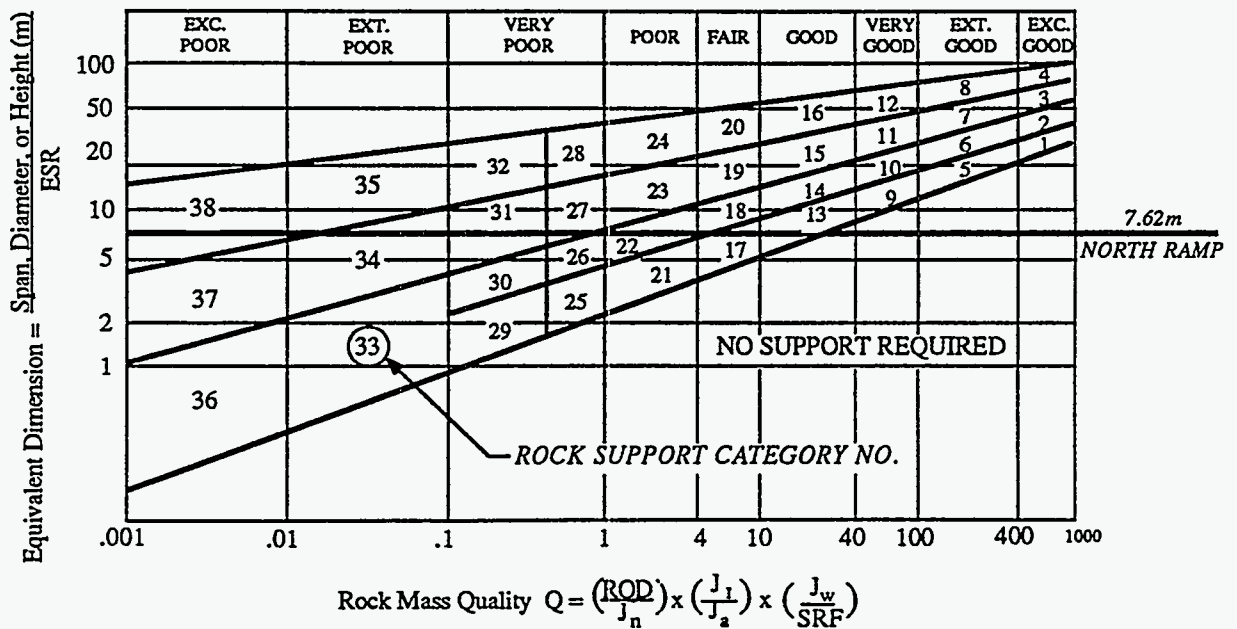
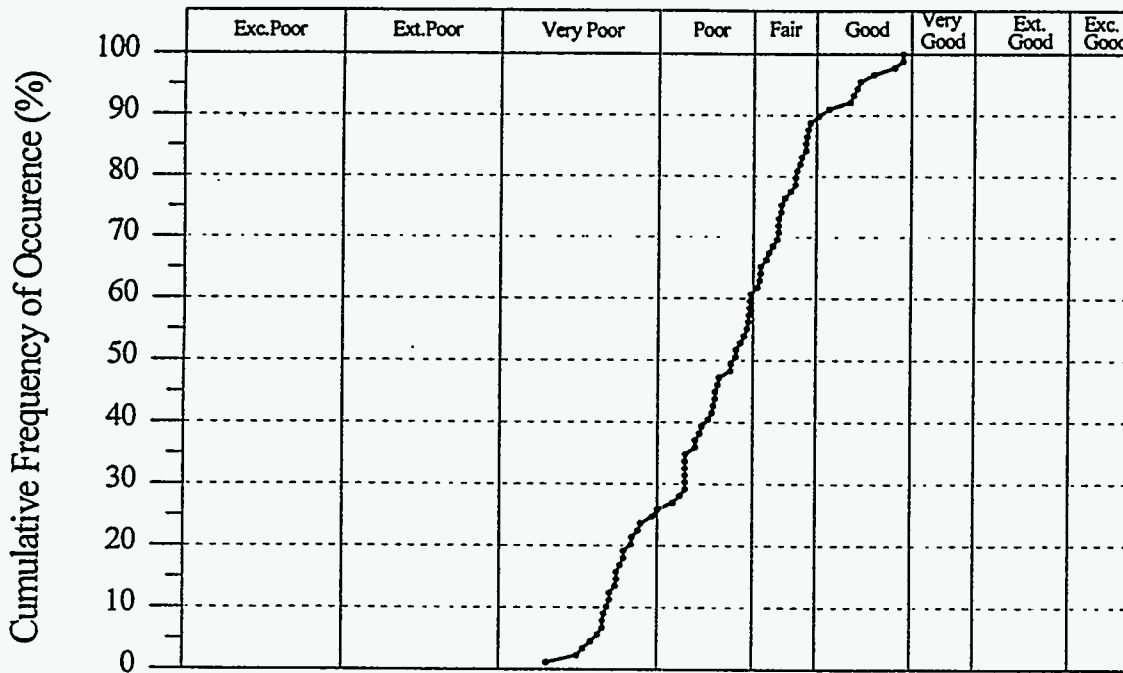


Figure 7-18. Cumulative Frequency of Occurrence of Q in TCw Compared to Ground Support Design Chart (after Barton et al., 1974)

Rock Mass Quality (Q) in PTn Unit - NRG Holes

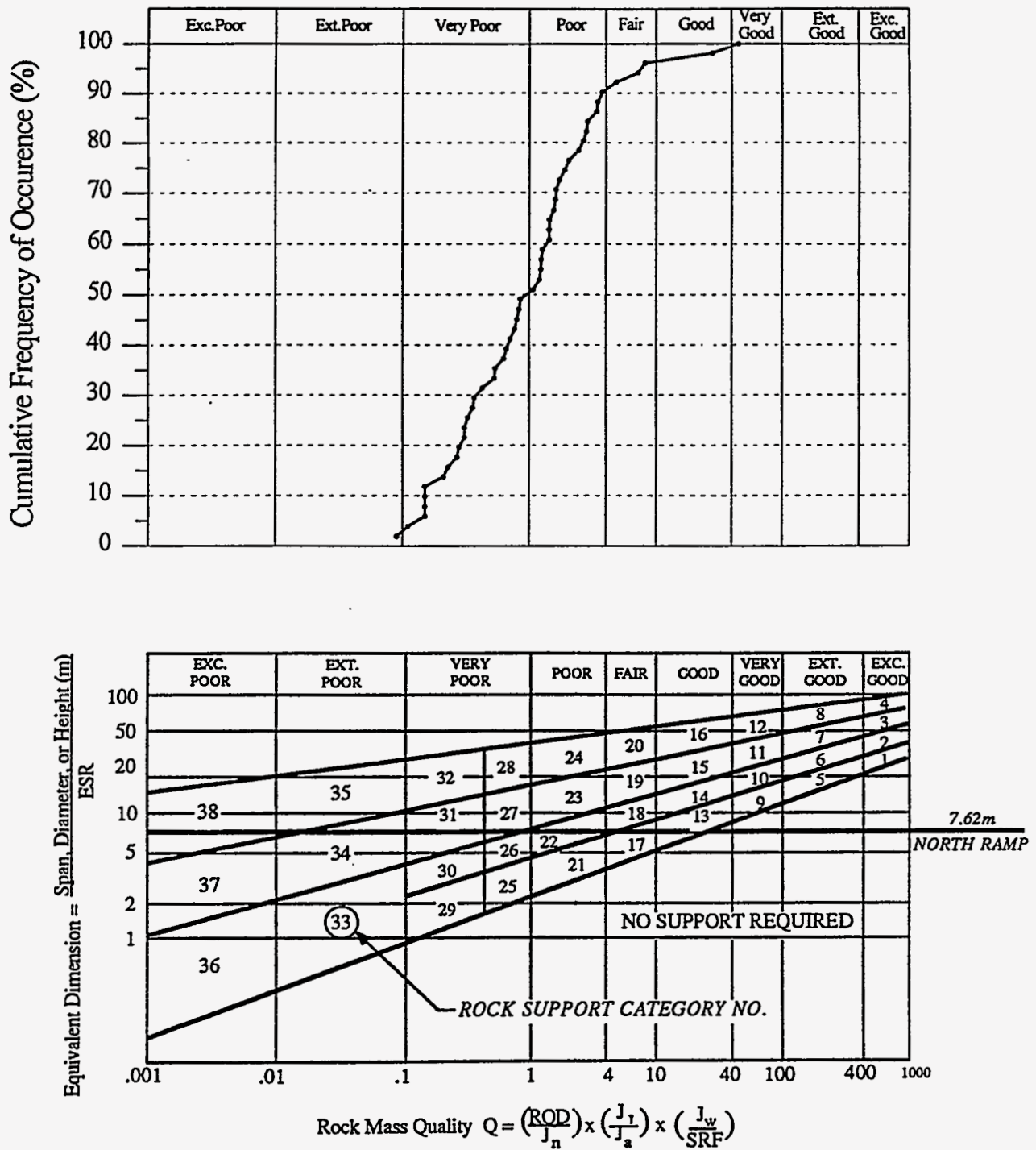


Figure 7-19. Cumulative Frequency of Occurrence of Q in PTn Compared to Ground Support Design Chart (after Barton et al., 1974)

Rock Mass Quality (Q) in TSw1 Unit - NRG Holes

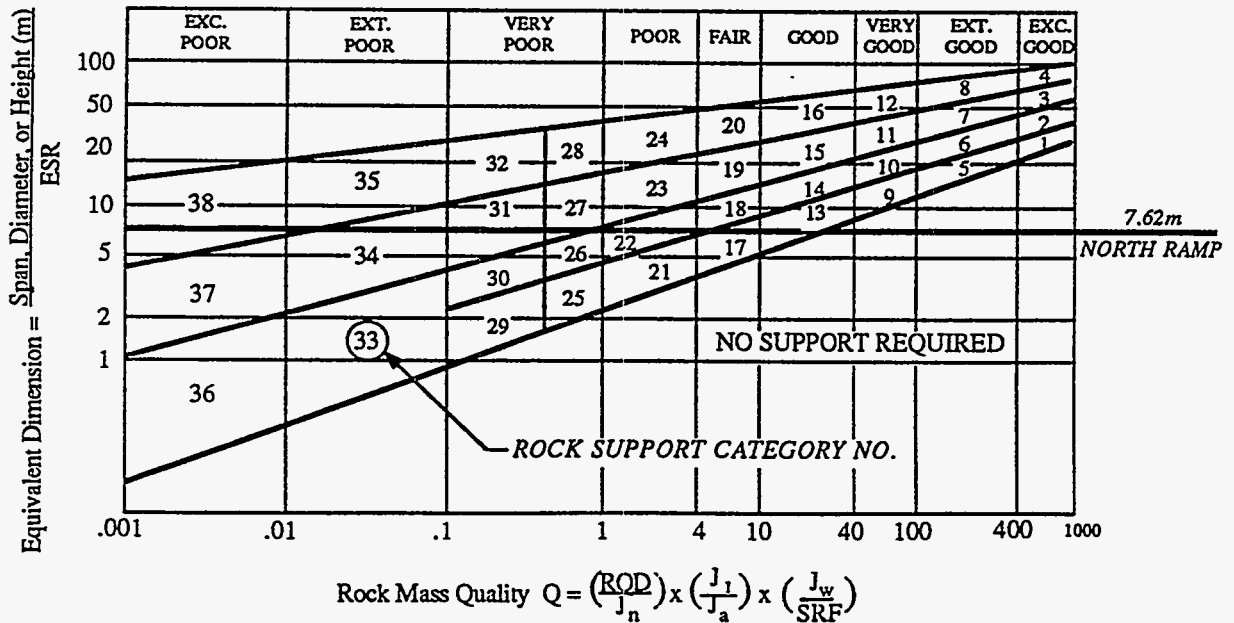
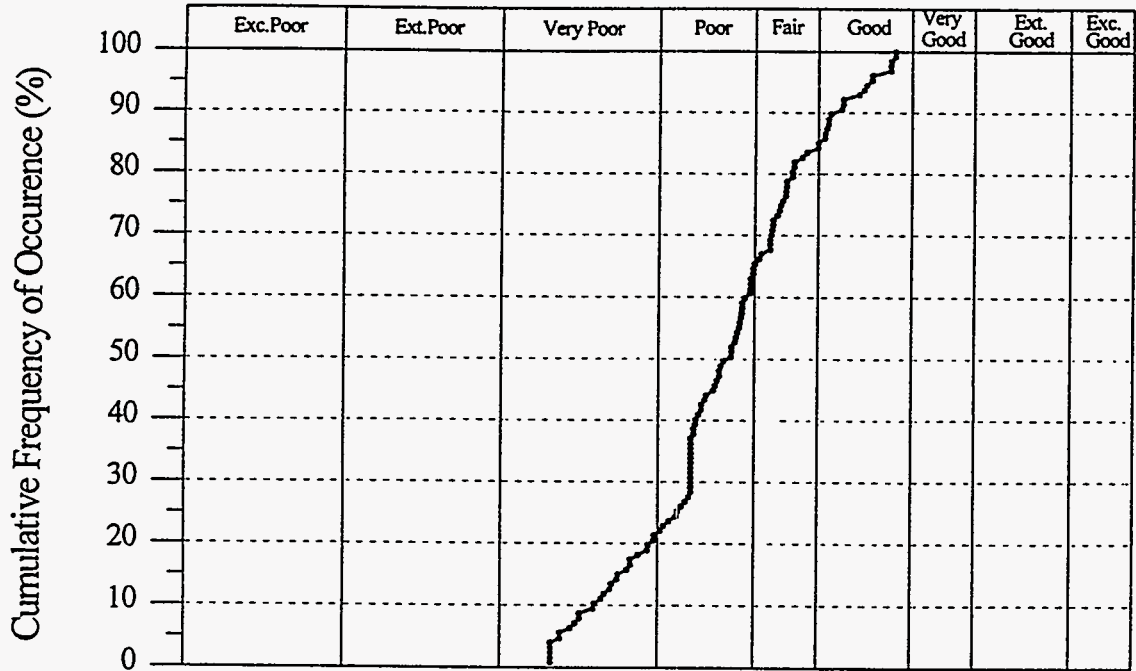


Figure 7-20. Cumulative Frequency of Occurrence of Q in TSw1 Compared to Ground Support Design Chart (after Barton et al., 1974)

Rock Mass Quality (Q) in TSw2 Unit - NRG Holes

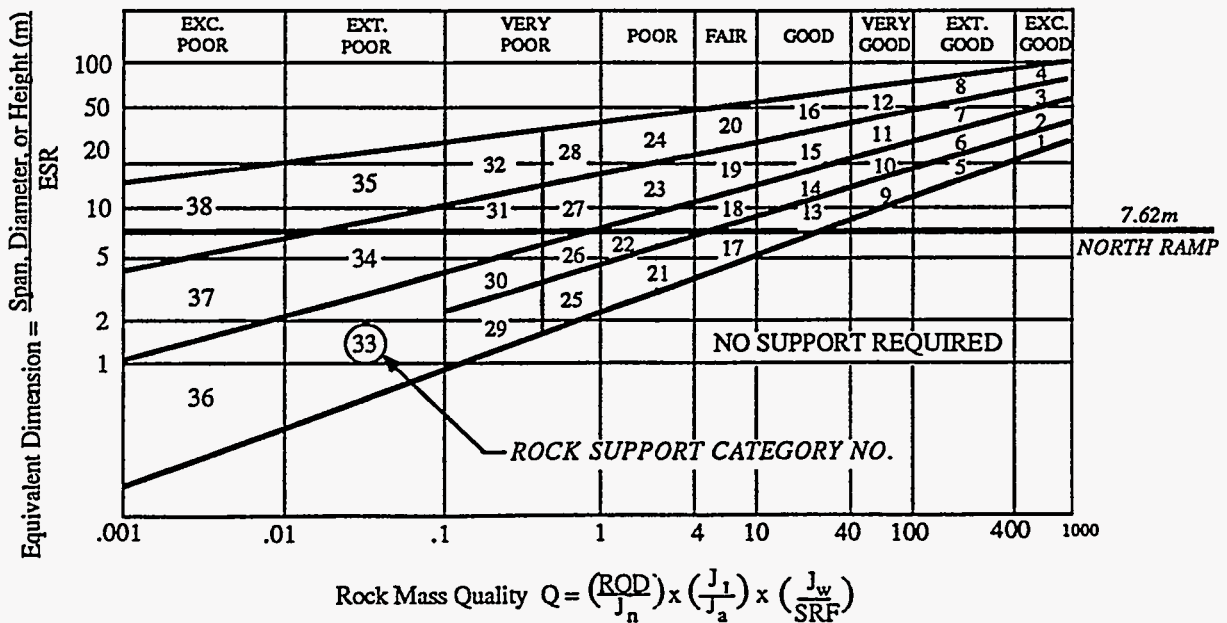
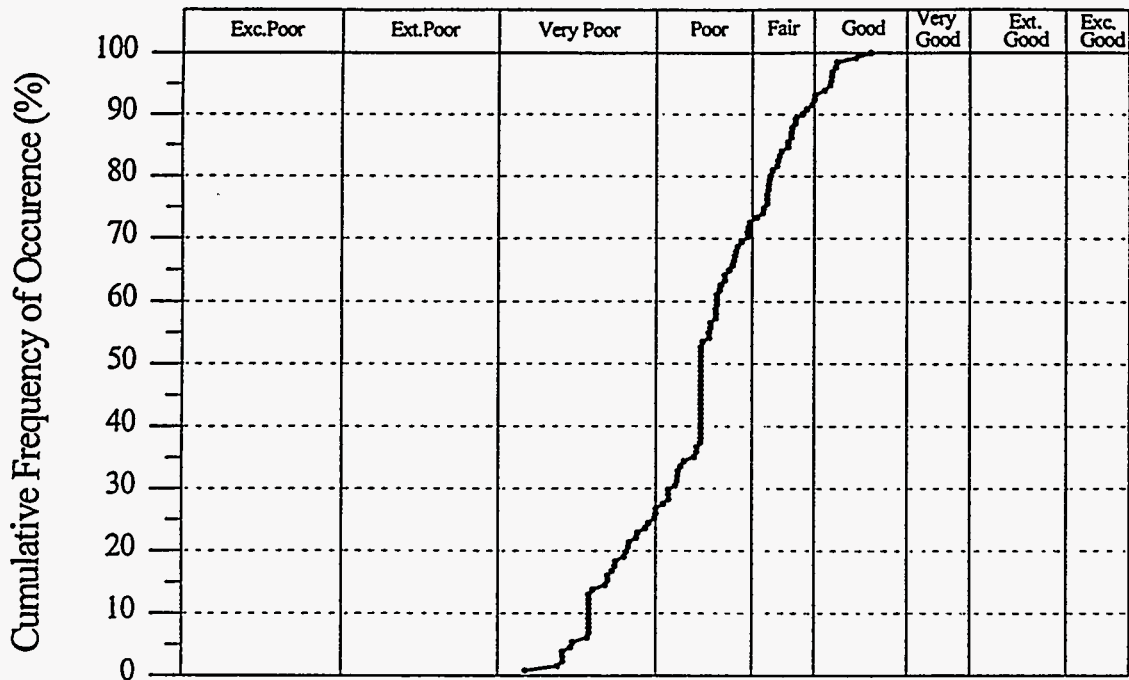


Figure 7-21. Cumulative Frequency of Occurrence of Q in TSw2 Compared to Ground Support Design Chart (after Barton et al., 1974)

Table 7-12. Range of Ground Support Indicated by Rock Support Categories in Each Thermomechanical (Thermal-Mechanical) Unit — NRG Holes

Thermo-Mechanical Unit	Ground Support Category	Range of Q for Ground Support Category		Proportion of Data Intervals in Support Category	Cumulative Frequency of Occurrence at Maximum Q	Range in Ground Support Measures*
UO (Tuff Unit "X")	22	1-4	Poor	10%	10%	B(utg) 1 m + CLM to B(utg) 1 m + 5 (Mr) 2.5- cm
	18	4-5.5	Fair	2%	12%	B(tg) 1-1.5 m + CLM to B(utg) 1-1.5 m + S 2-3 cm
	17	5.5-10	Fair	24%	36%	Sb(utg) to S 2-3 cm
	13	10-26	Good	59%	95%	Sb(utg) to B(utg) 1.5-2.0 m + S 2-3 cm
	—	>26	Good	5%	100%	No support required.
TCw	31	0.1-0.4	V. Poor	4%	4%	B(tg) 1 m + S(Mr) 5-12.5 cm to CCA(Sr) 30-50 cm + B(tg) 1 m
	27	0.4-1.0	V. Poor	22%	26%	B(tg) 1 m + S(Mr) 7.5-10 cm to CCA 20-40 cm + B(tg) 1 m
	22	1.0-4.0	Poor	35%	61%	B(utg) 1 m + CLM to B(utg) 1 m + S(Mr) 2.5-5 cm
	18	4.0-5.5	Fair	8%	69%	B(tg) 1-1.5 m + CLM to B(utg) 1-1.5 m + S 2-3 cm
	17	5.5-10.0	Fair	20%	89%	Sb(utg) to S 2-3 cm
	13	10-26	Good	8%	97%	Sb(utg) to B(utg) 1.5-2.0 m + S 2-3 cm
	—	>26	Good	3%	100%	No support required.
PTn	34	0.01-0.1	Ext. Poor	2%	2%	B(tg) 1 m + S(Mr) 5-7.5 cm to CCA(Sr) 20-60 cm + B(tg) 1 m
	31	0.1-0.4	V. Poor	27%	29%	B(tg) 1 m + S(Mr) 5-12.5 cm to CCA(Sr) 30-50 cm + B(tg) 1 m
	27	0.4-1.0	V. Poor	20%	49%	B(tg) 1 m + S(Mr) 7.5-10 cm to CCA(Sr) 20-40 cm + B(tg) 1 m
	22	1-4	Poor	41%	90%	B(utg) 1 m + CLM to B(utg) 1 m + S(Mr) 2.5-5 cm
	18	4-5.5	Fair	2%	92%	B(tg) 1-1.5 m + CLM to B(utg) 1-1.5 m + S 2-3 cm
	17	5.5-10	Fair	4%	96%	Sb(utg) to S 2-3 cm
	13	10-26	Good	0%	96%	Sb(utg) to B(utg) 1.5-2.0 m + S 2-3 cm
	—	>26	Good	4%	100%	No support required.
TSwl	31	0.1-0.4	V. Poor	10%	10%	B(tg) 1 m + S(Mr) 5-12.5 cm to CCA(Sr) 30-50 cm + B(tg) 1 m
	27	0.4-1.0	V. Poor	11%	21%	B(tg) 1 m + S(Mr) 7.5-10 cm to CCA 20-40 cm + B(tg) 1 m
	22	1.0-4.0	Poor	44%	65%	B(utg) 1 m + CLM to B(utg) 1 m + S(Mr) 2.5-5 cm
	18	4.0-5.5	Fair	7%	72%	B(tg) 1-1.5 m + CLM to B(utg) 1-1.5 m + S 2-3 cm
	17	5.5-10.0	Fair	13%	85%	Sb(utg) to S 2-3 cm
	13	10-26	Good	11%	96%	Sb(utg) to B(utg) 1.5-2.0 m + S 2-3 cm
	—	>26	Good	4%	100%	No support required.

Table 7-12. *continued*

Thermo-Mechanical Unit	Ground Support Category	Range of Q for Ground Support Category		Proportion of Data Intervals in Support Category	Cumulative Frequency of Occurrence at Maximum Q	Range in Ground Support Measures*
		Q Range	Support Category			
TSw2	31	0.1-0.4	V. Poor	14%	14%	B(tg) 1 m + S(Mr) 5-12.5 cm to CCA(Sr) 30-50 cm + B(tg) 1 m
	27	0.4-1.0	V. Poor	13%	27%	B(tg) 1 m + S(Mr) 7.5-10 cm to CCA 20-40 cm + B(tg) 1 m
	22	1.0-4.0	Poor	46%	73%	B(utg) 1 m + CLM to B(utg) 1 m + S(Mr) 2.5-5 cm
	18	4.0-5.5	Fair	8%	81%	B(tg) 1-1.5 m + CLM to B(utg) 1-1.5 m + S 2-3 cm
	17	5.5-10.0	Fair	11%	92%	Sb(utg) to S 2-3 cm
	13	10-26	Good	8%	100%	Sb(utg) to B(utg) 1.5-2.0 m + S 2-3 cm

*Based on Barton et al. (1974).

B—bolts; tg—tensioned, grouted; utg—untensioned, grouted; S—shotcrete; Mr—reinforced; CLM—chainlink, mesh; CCA—cast concrete arch; Sr—steel, reinforced; Sb—spot bolting

- ♦ Heavier ground support would be required in the welded units and the PTn unit. Spot bolting or pattern bolting on relatively large spacings (1.5 m) would be limited to 8%–15% of the length of the tunnel in each of the TCw, TSw1, TSw2, and PTn units.
- ♦ Regular pattern bolting with mesh or shotcrete to restrain loose material is the indicated support system for the majority of the tunnel within the welded and PTn units (up to 70%).
- ♦ Heavy support in the form of pattern bolting with significant thickness of shotcrete is indicated for 26%–30% of the tunnel within the welded units and PTn.

Although the support categories for the welded units and PTn unit for rock qualities below $Q = 1.0$ (support categories 27 and 31) do include cast concrete arches in the range of support measures, the conditions normally associated with their use are not projected to occur in the North Ramp outside of major fault zones. Cast concrete arches could be required in response

to squeezing ground conditions or swelling clays; however, these conditions are not indicated by any of the existing data. The low values of Q for the PTn are due to its low strength (8 MPa) which, when compared to the maximum depth where the North Ramp penetrates PTn (135 m), suggests rock failure may cause slabbing of the tunnel walls. The extent of the slabbing would be expected to be limited because PTn has low strength and high porosity and should not be prone to brittle-type failure. Existing excavations at NTS in nonwelded tuffs similar to PTn at similar and greater depths (for example, G tunnel) exhibited good stability.

It is possible that very heavy support could be required locally within a large zone of fault gouge. This type of occurrence would only be anticipated within the Drill Hole Wash fault because no drilling data is available. Support pressure capabilities with the tunnel boring machine (TBM) are very high because of its ability to install steel ring beams, and there is no indication in the NRG data that the existing capacity is not sufficient to meet the range of conditions. Drill sampling of the other major fault on the North Ramp alignment (Bow Ridge Fault) indicated a gouge zone limited to 2–4 m (13.1 ft) in thickness.

Comparison of the distribution of the core-derived Q data in the welded units to Q determined in the NRST indicated that the drilling-based estimates of Q cover the rock conditions associated with the minimum Q values (see Section 7.4) observed in the tunnel. The minimum Q values in the NRST were associated with intermediate scale, vertical fault or shear structures observed in the tunnel. These structures could not be characterized by vertical hole NRG-1 which raises the question whether the predominantly vertical drilling has overestimated the rock conditions along the North Ramp. The interpretation of all of the drilling-derived Q data as a statistical distribution extends the data to cover the range of rock conditions indicated

by the NRST observations. The drilling-based Q data suggests that up to 49% of the tunnel length in the welded units and PTn unit would require ground support consistent with categories 27 and 31. Ground support installed in the NRST was generally consistent with these categories and has been suitable for ambient conditions. The NRST support design³² called for 3 m (10 ft) untensioned fully grouted rockbolts on a 1.5 m (5 ft) nominal spacing, with 152 mm (6 in.) of shotcrete (102 mm minimum) reinforced with 152 mm × 152 mm (6 in. × 6 in.) welded-wire fabric. Seismic design requirements dictate that the NRST have much heavier permanent support in the form of cast concrete.

Although the vertical holes did not sample the intermediate-scale vertical structures effectively, it appears that the conservative approach to generation of the Q estimates has covered the likely variability outside of the major faults and known off-normal conditions. The rock conditions in the NRST may also be somewhat off-normal due to its close proximity to two major faults and its topographic relief and subsequent destressing and weathering.

The intermediate-scale structures cause the minimum NRST values of Q to diverge from the borehole estimates. The borehole Q values are representative of the general variability of the rock mass between the intermediate scale structures and agree well with the maximum Q values developed in the NRST.

³² Raytheon, 1994. "ESF Package 1A, Starter Tunnel Rock Support, Section and Details," YMP Site Characterization Project, Rev. 3, February 16, 1994, BABEAB000-01717-2100-10143-01.

This page left intentionally blank.

8.0 ROCK MASS MECHANICAL PROPERTIES

8.1 Introduction

Numerical analysis to support rock mechanics design of the North Ramp are required to address the impacts of seismic and thermomechanical (thermal-mechanical) loading. These analyses require mechanical properties at the rock mass scale which are known to be very different than laboratory mechanical properties, in strong, jointed rocks. These differences are termed “scale effects” and are attributed to the influence of size of the rock mass affected and jointing. Hardy and Bauer (1991) proposed a methodology to estimate rock mass mechanical properties based on empirical correlations with the rock mass quality index RMR.

Appropriate rock mass strength criteria and mechanical models for representing the mechanical rock mass response of the tuff at Yucca Mountain recommended in the Drift Design Methodology by Hardy and Bauer (1991) were utilized. Empirical relationships, based on rock mass quality index RMR, were used in conjunction with data from the rock structure summary logs and the rock mechanical properties.

The rock mass strengths in a form of power law relationship were derived based on both Hoek and Brown (1988) and Yudhbir et al. (1983) criteria. Design parameters for rock mass elastic modulus (Serafim and Periera, 1983), Poisson’s ratios, and Mohr-Coulomb strength were developed for each thermomechanical (thermal-mechanical) unit.

8.2 Rock Mass Strengths

Rock mass strengths based on the empirical strength criteria of Yudhbir et al. (1983) and Hoek and Brown (1988) for the thermomechanical (thermal-mechanical) units are developed in

this subsection. The required information for obtaining the rock mass strengths include rock mass quality indices, intact rock uniaxial compressive strengths, and the triaxial compressive strength data.

The procedures employed in these calculations follow the Drift Design Methodology (Hardy and Bauer, 1991) and utilize the RMR parameter calculated using the approach described in Bieniawski (1979). This is consistent with recommendations by Bieniawski (1979, p. 178). This index, RMR_{79} , is slightly different from the version utilized by Hoek and Brown (1988) and Yudhbir et al. (1983) which is based on the approach described by Bieniawski (1974). RMR_{74} has been estimated in this work to evaluate the impact of the difference in the two approaches. The resulting difference in the design RMR numbers is small and is discussed in the following sections.

The rock mass strength criteria are generated for the five classes of rock mass quality based on frequency of occurrence of 5%, 20%, 40%, 70% and 90%, which were presented in Section 7.2.6. Both the RMR_{79} and Q index are used to determine a composite or design value of RMR (RMR_D), by using the correlation developed by Bieniawski (1974) between RMR and Q (shown in Figure 7-11) with the calculation in equation 8-1.

$$RMR_{CAL} = 9 \ln Q + 44 \quad (8-1)$$

RMR_{CAL} is calculated, then the design RMR_D is determined as the average of RMR_{CAL} and RMR_{79} . Table 8-1 lists the values of Q and RMR_{79} and resulting design RMR_D for each thermomechanical (thermal-mechanical) unit.

Table 8-1. Tabulation of Q, RMR₇₉, and Design RMR_D Values for Rock Mass Classes 1-5 in Each Thermomechanical (Thermal-Mechanical) Unit

		Rock Mass Quality Class				
		1	2	3	4	5
UO (Tuff "X")	Q	2.23	7.5	10.98	14.49	24.29
	RMR _{CAL}	51	62	66	68	73
	RMR ₇₉	50	53	56	59	60
	Design RMR _D	51	58	61	64	66
TCw	Q	0.38	0.68	2.08	5.66	9.14
	RMR _{CAL} *	35	41	51	60	64
	RMR ₇₉	51	56	59	67	72
	Design RMR _D	43	48	55	63	68
PTn	Q	0.15	0.28	0.66	1.62	3.74
	RMR _{CAL}	27	33	40	48	56
	RMR ₇₉	45	52	55	65	70
	Design RMR _D	36	42	47	56	63
TSw1	Q	0.24	0.87	1.73	5.09	12
	RMR _{CAL}	31	43	49	59	66
	RMR ₇₉	49	53	57	62	70
	Design RMR _D	40	48	53	60	68
TSw2	Q	0.3	0.65	1.91	3.75	8.44
	RMR _{CAL}	33	40	50	56	63
	RMR ₇₉	51	56	58	63	67
	Design RMR _D	42	48	54	59	65

*RMR_{CAL} = 9 LNQ + 44; RMR_D = (RMR_{CAL} + RMR₇₉) ÷ 2

The design values of RMR_D used in the estimation of rock mass strength (Table 8-2) are compared to similar values produced using RMR₇₄ in Table 8-2. The differences are small, with the maximum difference being 4. This difference is smoothed by the procedure of considering the value of Q in determination of RMR_D.

Table 8-2. Comparison of RMR_p Values Determined Using RMR₇₉ and RMR₇₄ for Rock Mass Classes 1–5 in Each Thermomechanical (Thermal-Mechanical) Unit

		Rock Mass Class				
		1	2	3	4	5
UO (Tuff “X”)	RMR ₇₉	51	58	61	64	66
	RMR ₇₄	48	55	60	62	66
TCw	RMR ₇₉	43	48	55	63	68
	RMR ₇₄	41	45	52	59	65
PTn	RMR ₇₉	36	42	47	56	63
	RMR ₇₄	36	41	46	55	61
TSw1	RMR ₇₉	40	48	53	60	68
	RMR ₇₄	38	46	50	57	64
TSw2	RMR ₇₉	42	48	54	59	65
	RMR ₇₄	40	45	51	56	61

8.2.1 Yudhbir Criterion

The equation proposed by Yudhbir et al. (1983) for calculation of rock mass strength is:

$$\sigma_1 = A \sigma_c + B \sigma_c \left(\frac{\sigma_3}{\sigma_c}\right)^\alpha \quad (8-2)$$

where σ_c = intact rock uniaxial compressive strength,

σ_1 = the strength of the rock mass,

σ_3 = the confining stress,

A = a dimensionless parameter dependent on the RMR, and

α , B = rock material constants dependent on rock type.

The value of A for the rock mass is obtained from the RMR by equation 8-3 from Yudhbir et al. (1983).

$$A = e^{0.0765(\text{RMR}) - 7.65} \quad (8-3)$$

The material constants B and α are constants related to the rock type and are determined by curve fitting of the confined compressive strength test results.

The triaxial compression test data for NRG core were evaluated to develop the constants B and α for each of the thermomechanical (thermal-mechanical) units. The evaluation indicated

that sufficient triaxial test data from the NRG core were available for the TCw, TSw1, and TSw2 units; however, the data scatter in the results produced concave-shaped curve fits in the TSw1 and TSw2 rather than convex shapes. Existing nonqualified triaxial data from the TSw1 and TSw2 units were available to compare to the NRG data from TSw1 and TSw2. No triaxial test data were available from either the NRG core testing or existing data for the nonwelded UO or PTn units.

The following approach was used to develop the B and α parameters because of the data limitations:

- TCw Unit: NRG triaxial test data were used to determine B and α using the method outlined in Hardy and Bauer (1991) and Lin et al. (1993b).
- UO and PTn Units: NRG uniaxial compression and Brazilian tensile strength tests were used to determine B and α with modifications of the method suggested by Hardy and Bauer (1991) and Lin et al. (1993b).
- TSw1 and TSw2 Units: Values of B and α developed by Lin et al. (1993b) using existing but nonqualified test data were used. The existing data used by Lin et al. (1993b) were similar to the NRG testing data.

A modified method was used to produce the parameters B and α for the UO and PTn units. The data from uniaxial compressive strength and Brazilian tensile strength tests were used to develop a linear least-square curve fit of the form shown in equation 8-6. Using equation 8-6, data pairs were then calculated and a nonlinear curve fit used to estimate values of B and α . Examination of the data variability within the PTn unit indicated two distinct materials, the stronger Tiva Canyon nonwelded tuffs and Yucca Mountain tuffs (4–27 MPa) and the weaker

bedded tuffs and Pah Canyon tuff (0.8–9.8 MPa). B and α values were determined separately for these materials. Table 8-3 lists the value of the B and α for each unit.

Table 8-3. Intact Rock Constants for the Rock Mass Strength Criteria

Thermomechanical (Thermal-Mechanical) Unit		Yudhbir Criterion		Hoek & Brown Criterion m_i
		B	α	
UO (Tuff "X")		8.10	1.00	125.64
TCw		2.50	0.64	18.50
PTn	Tiva Canyon, Yucca Mountain	4.56	1.00	17.64
	Bedded Tuffs, Pah Canyon	6.10	1.00	150.97
TSw1*		2.00*	0.65*	8.00*
TSw2*		2.00*	0.65*	8.00*

*Based on nonqualified data, Lin et al. (1993b).

Predicted values of rock mass compressive strength for various levels of confining stress were then calculated using parameters A, B, and α and equation 8-2.

8.2.2 Hoek and Brown Criterion

The Hoek and Brown (1988) rock mass strength criterion is shown in equation 8-4:

$$\sigma_1 = \sigma_3 + \sqrt{m \sigma_c \sigma_3 + s \sigma_c^2} \quad (8-4)$$

where m = a constant that depends on the properties of the rock and

$$m = m_i e^{(RMR-100)/28}$$

s = a constant that depends on the extent to which the rock is fractured.

$$s = e^{(RMR - 100)/9}$$

The parameter m_i is the constant for intact rock determined by curve fitting of the confined compressive strength test data. The triaxial test data for NRG-6 at 6.76 m (22.2 ft) were utilized for the TCw unit. The values of m_i for TSw1 and TSw2 units were derived from Lin et al. (1993b). Values for m_i for PTn and UO (Tuff "X") were based on UCS and tensile strength data

from NRG boreholes, using the identical approach as described for the Yudhbir criterion. The m_i values used are listed in Table 8-3.

8.2.3 Design Rock Mass Strengths

The design rock mass strengths for each rock mass quality class were calculated by averaging the strengths determined from both Yudhbir et al. (1983) and Hoek and Brown (1988) criteria following the procedure of Hardy and Bauer (1991).

A power law relationship of the form

$$\sigma_1 = A + B\sigma_3^c \quad (8-5)$$

was employed to describe the nonlinear design rock mass strength. The parameters A, B, and C were determined by curve fitting the strength envelopes using a least-square method. Table 8-4 presents the results of the best fit.

Figures 8-1 to 8-5 present the design rock mass strengths for all five rock quality categories for confining stresses of 0 to 3 MPa for each thermomechanical (thermal-mechanical) unit, respectively. The power law relationship for PTn was generated by averaging the rock mass strength results predicted for the two groups of Tiva Canyon nonwelded/Yucca Mountain tuff and bedded tuffs/Pah Canyon tuff. The mean intact compressive strength is plotted on each figure to illustrate the magnitude of the reduction that occurs in the rock mass criteria.

8.2.4 Rock Mass Mohr-Coulomb Strength Parameters and Dilation Angles

The Mohr-Coulomb strength parameters, including cohesion and angle of internal friction, and the dilation angle are commonly used to describe rock mass strength in numerical analysis. The strength parameters were developed from the least-square curve fits of strength data pairs (σ_1, σ_3) produced using the power law criterion in Section 8.2.3, and are listed in Table 8-4. The linear relationship for strength (σ_1) and confining pressure (σ_3) in the form of equation 8-6:

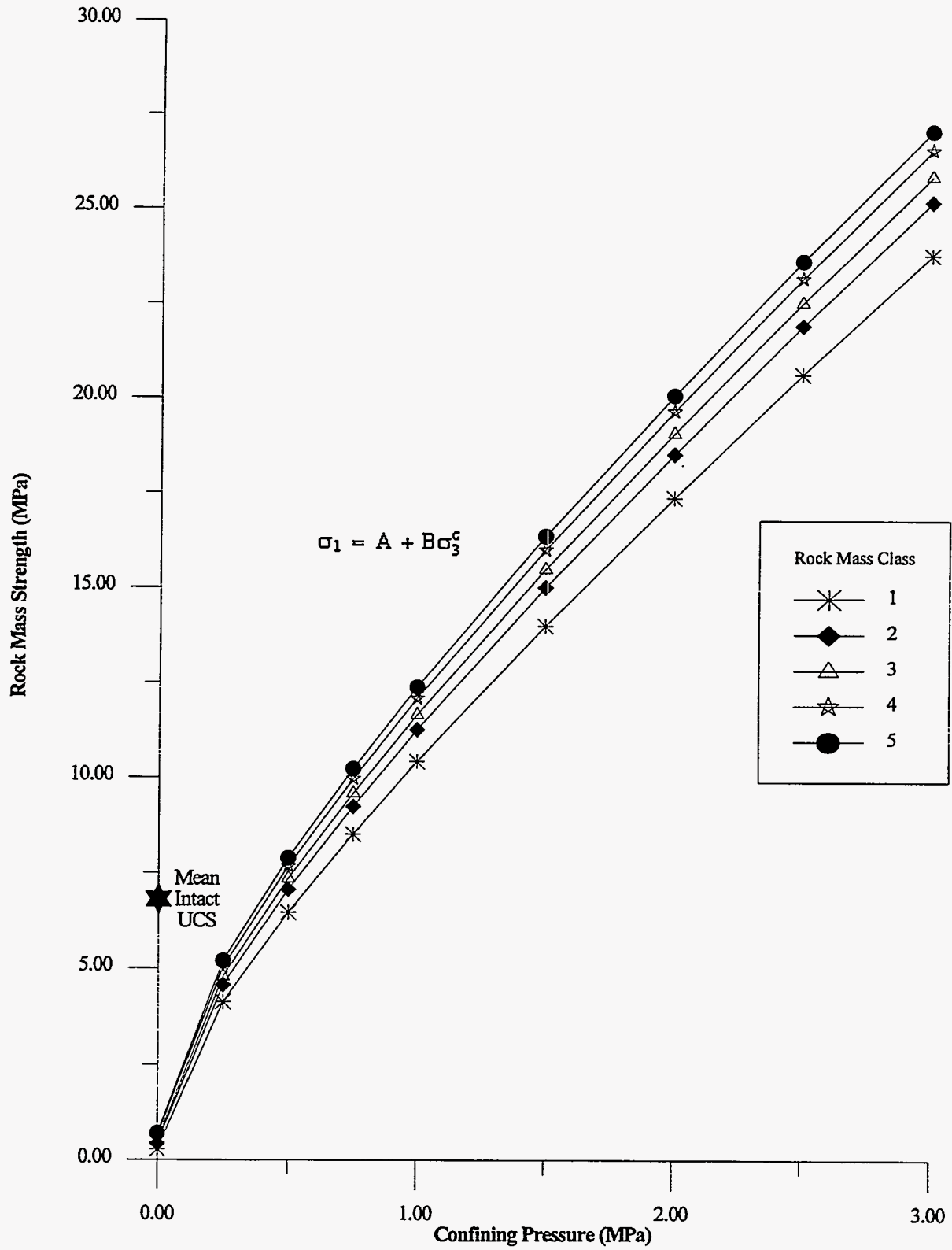


Figure 8-1. Design Rock Mass Strength Envelopes for Tuff X (UO) Unit--NRG Holes

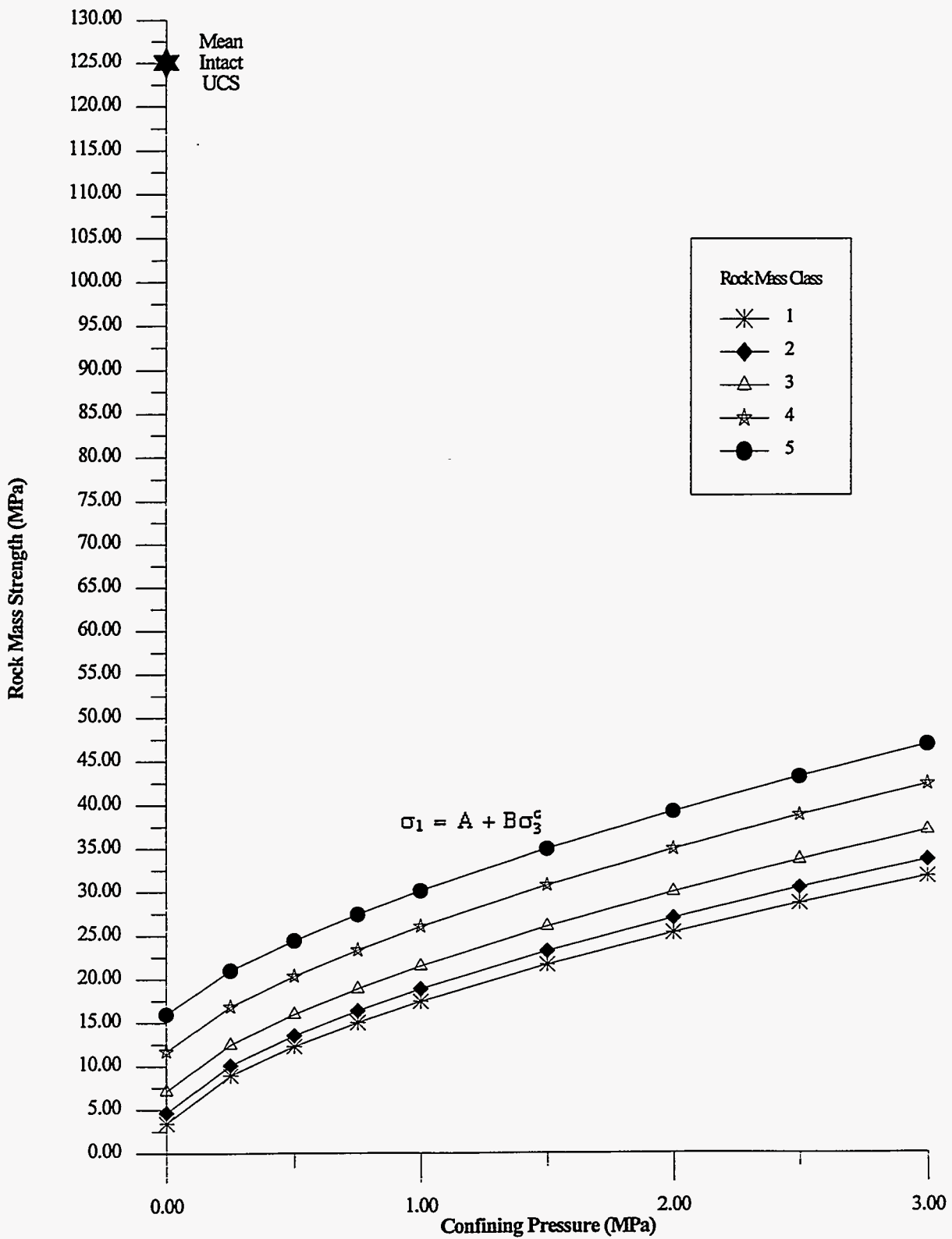


Figure 8-2. Design Rock Mass Strength Envelopes for TCw Unit--NRG Holes

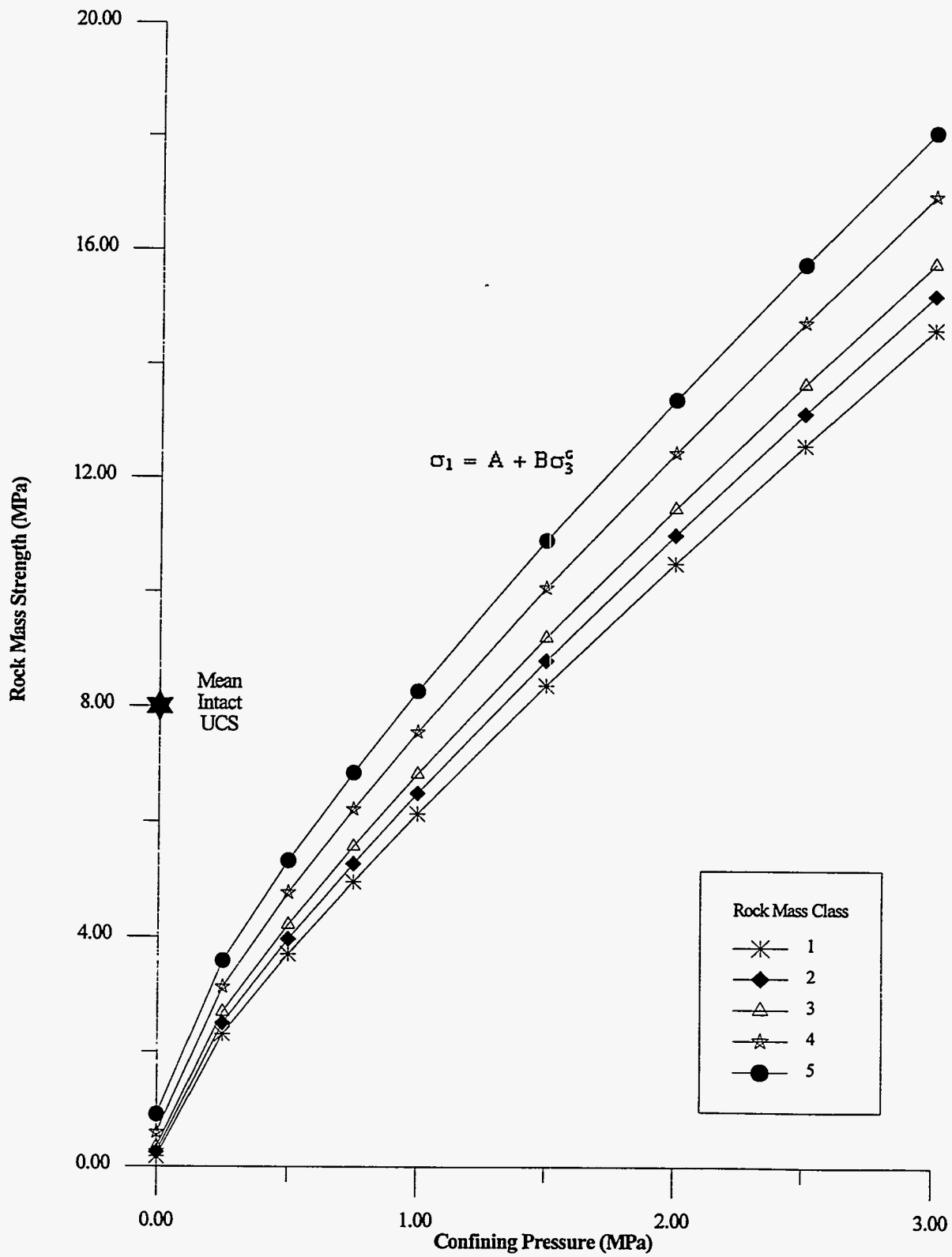


Figure 8-3. Design Rock Mass Strength Envelopes for PTn Unit-NRG Holes

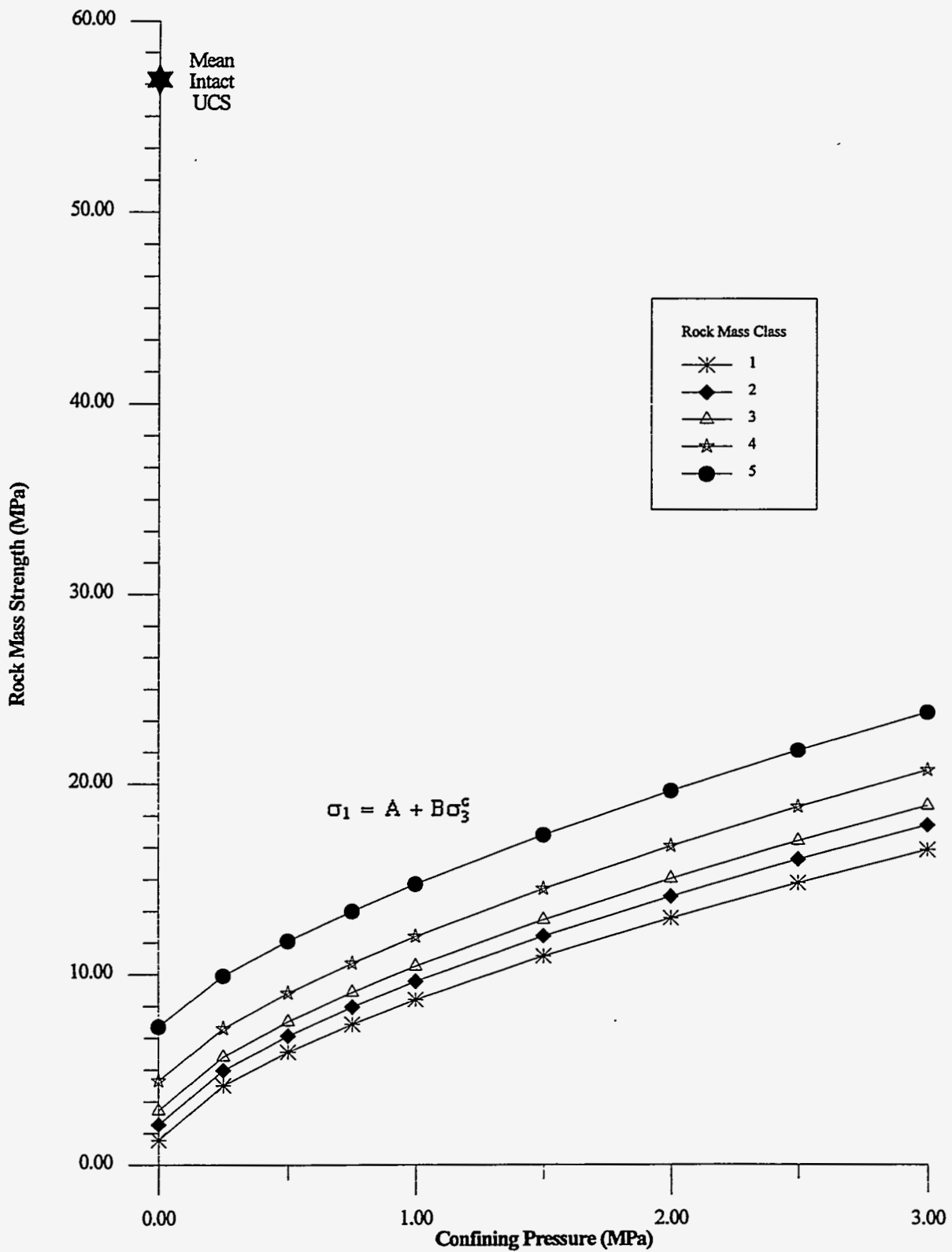


Figure 8-4. Design Rock Mass Strength Envelopes for TSw1 Unit—NRG Holes
(Based on Nonqualified Data—Lin et al., 1993b)

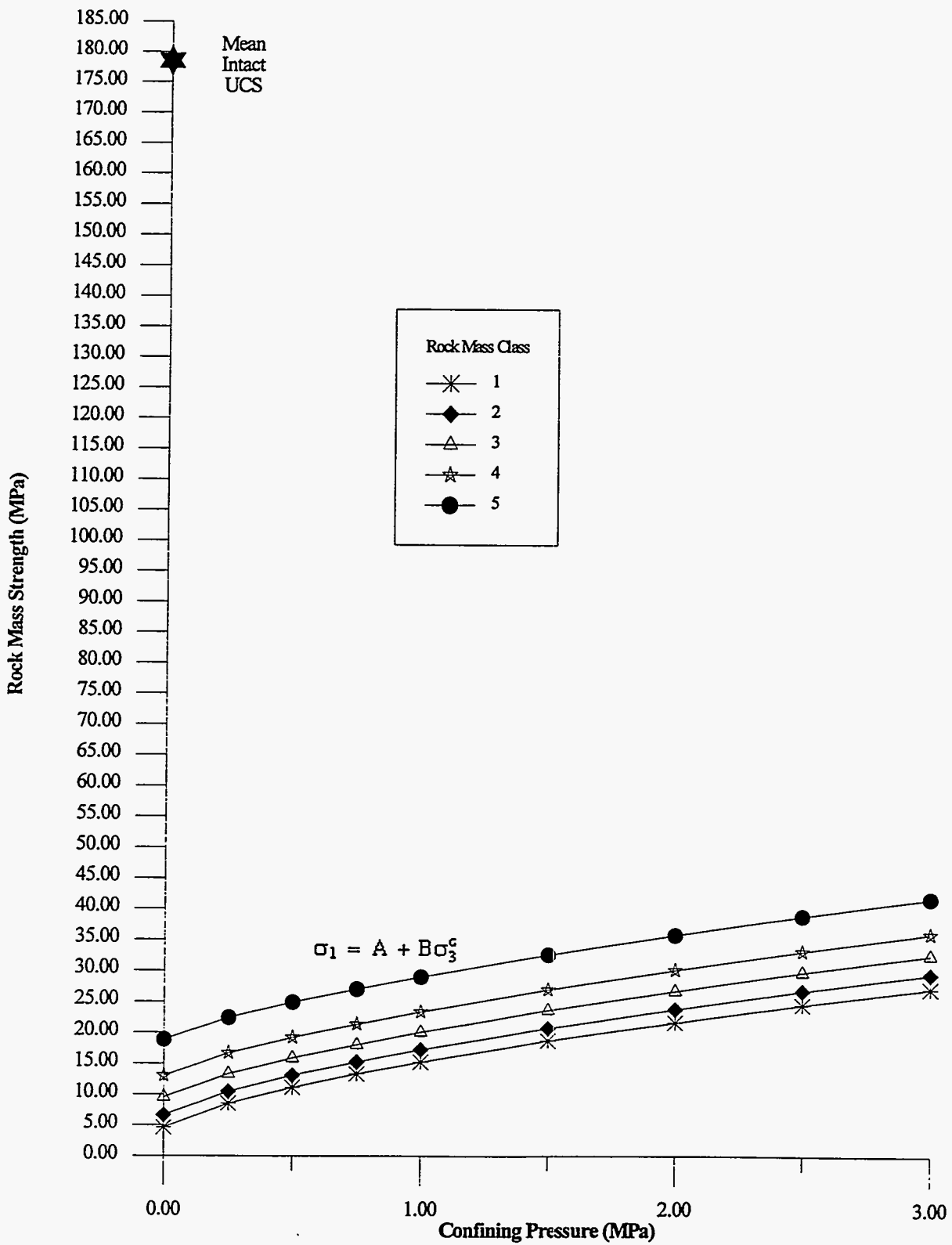


Figure 8-5. Design Rock Mass Strength Envelopes for TSw2 Unit—NRG Holes (Based on Nonqualified Data—Lin et al., 1993b)

Table 8-4. Power Law Constants* for Rock Mass Strength (MPa)

Thermomechanical (Thermal-Mechanical) Unit		Rock Mass Class				
		1	2	3	4	5
UO (Tuff "X")	A*	0.39	0.54	0.62	0.73	0.81
	B*	10.12	10.81	11.12	11.44	11.66
	C*	0.76	0.75	0.74	0.74	0.73
TCw	A	3.37	4.57	7.04	11.60	15.89
	B	14.05	14.25	14.41	14.40	14.27
	C	0.65	0.66	0.68	0.70	0.71
PTn	A	0.25	0.32	0.41	0.65	0.97
	B	5.93	6.22	6.47	6.95	7.34
	C	0.80	0.79	0.78	0.77	0.77
TSw1**	A	1.28	2.09	2.84	4.38	7.23
	B	7.39	7.54	7.59	7.60	7.53
	C	0.67	0.68	0.69	0.70	0.72
TSw2**	A	4.56	6.58	9.53	12.99	18.88
	B	10.68	10.65	10.55	10.40	10.17
	C	0.69	0.70	0.72	0.73	0.74

*Equation 8-5

** Based on nonqualified data assumptions.

$$\sigma_1 = \sigma_c + N\sigma_3 \quad (8-6)$$

is defined, where

σ_c = uniaxial compressive strength and

N = confinement factor.

The parameters σ_c and N were then used to generate a Mohr-Coulomb failure criterion relating the shear (τ) and normal stress (σ_n) on the plane of failure to cohesion and angle of internal friction:

$$t = C_o + \sigma_n \tan \phi \quad (8-7)$$

where C_o = cohesion and

$$C_o = \sigma_c / \sqrt{N}$$

ϕ = angle of internal friction

$$\phi = 2 \left(\tan^{-1} \sqrt{N} - 45^\circ \right)$$

The least-square best fit was performed over the range of confining pressures from 0 to 3 MPa, which is representative of the projected range in minimum principal stresses near the boundary of the excavations. Table 8-5 presents the resulting Mohr-Coulomb strength parameters. The non-associated flow rule, suggested by Michelis and Brown (1986), which uses a dilation angle equal to half the internal friction angle, was considered suitable for the tuff (Hardy and Bauer, 1991) and the resulting values for dilation angles are also listed in Table 8-5.

Table 8-5. Strength Parameters and Dilation Angles for the Mohr-Coulomb Failure Criterion for Rock Mass Classes 1–5 in Each Thermomechanical (Thermal-Mechanical) Unit

		Rock Mass Class				
		1	2	3	4	5
UO (Tuff "X")	cohesion (MPa)	0.4	0.5	0.5	0.5	0.5
	friction angle (degrees)	50	51	51	52	52
	dilation angle (degrees)	25	25	26	26	26
TCw	cohesion (MPa)	1.2	1.3	1.7	2.4	3.0
	friction angle (degrees)	53	53	54	55	55
	dilation angle (degrees)	26	27	27	27	27
PTn	cohesion (MPa)	0.3	0.3	0.3	0.4	0.5
	friction angle (degrees)	40	41	42	43	44
	dilation angle (degrees)	20	20	21	21	22
TSw1*	cohesion (MPa)	0.7	0.9	1.0	1.3	1.9
	friction angle (degrees)	41	42	42	43	43
	dilation angle (degrees)	20	21	21	21	22
TSw2*	cohesion (MPa)	1.3	1.6	2.2	2.8	3.8
	friction angle (degrees)	49	49	50	50	50
	dilation angle (degrees)	25	25	25	25	25

*Based on nonqualified data reported by Lin et al. (1993b).

The Mohr-Coulomb failure criteria for RMR_{79} versus RMR_{74} are compared in Table 8-6, which lists the cohesion term only because coefficient of internal friction and dilation angle are not affected.

The rock mass cohesion is compared to the value of intact material cohesion determined using the NRG test data listed in Table 6-9, Section 6.0. The comparison indicates that the difference between RMR_{79} and RMR_{74} produces maximum changes in cohesion of 0.7 MPa. These differences amount to a maximum difference of 24.1% of the rock mass cohesion; however, they are in the range of 2%–3% of the intact cohesion. Given the limited database for reducing intact strength to the rock mass scale, the indicated differences in Table 8-6 are judged to be well within the experimental uncertainty. Application of the Drift Methodology using RMR_{79} values is sufficiently accurate for design purposes.

Table 8-6. Comparison of Range of Rock Mass Cohesion (MPa) Using RMR_{79} and RMR_{74} Approaches

		Intact Sample Cohesion (MPa)	Rock Mass Class				
			1	2	3	4	5
UO ¹ (Tuff "X")	RMR_{79}	1.09	0.4	0.5	0.5	0.5	0.5
	RMR_{74}		NC ²	NC ²	NC ²	NC ²	NC ²
TCw	RMR_{79}	55.4	1.2	1.3	1.7	2.4	3.0
	RMR_{74}		1.1	1.2	1.5	2.0	2.6
PTn ¹	RMR_{79}	2.25	0.3	0.3	0.3	0.4	0.5
	RMR_{74}		NC ²	NC ²	NC ²	NC ²	NC ²
TSw1 ³	RMR_{79}	14.1	0.7	0.9	1.0	1.3	1.9
	RMR_{74}		0.7	0.8	0.9	1.2	1.6
TSw2 ³	RMR_{79}	42.8	1.3	1.6	2.2	2.8	3.8
	RMR_{74}		1.2	1.5	1.9	2.4	3.1

¹Based on uniaxial compressive strength (Table 6-1, Section 6.0) and Brazilian tensile strength.

²NC— not calculated

³Rock mass cohesion based on nonqualified data reported by Lin et al. (1993b).

8.3 Rock Mass Elastic Modulus

Serafim and Pereira (1983) developed a correlation between the RMR_{79} and rock mass elastic modulus that was recommended for use by Hardy and Bauer (1991) and is shown in equation 8-8:

$$E = 10^{\frac{(RMR - 10)}{40}} \quad (8-8)$$

where E is in GPa.

Since the equation does not incorporate the intact rock elastic modulus, the predicted rock mass elastic modulus can exceed the intact rock elastic modulus at high RMR_{79} values. An upper bound limit of the rock mass modulus was therefore set equal to the intact rock modulus data. The calculated rock mass moduli based on averaged RMR_{79} values presented in Section 7-4 are listed in Table 8-7.

Table 8-7. Estimated Rock Mass Elastic Modulus (GPa)

Thermomechanical (Thermal-Mechanical) Unit	Rock Mass Class				
	1	2	3	4	5
UO (Tuff "X")	4.30	4.30	4.30	4.30	4.30
TCw	6.70	8.92	13.33	21.20	27.71
PTn	2.50	2.50	2.50	2.50	2.50
TSw1	5.66	8.78	11.71	17.86	18.90
TSw2	6.37	8.96	12.55	17.11	23.51

8.4 Rock Mass Poisson's Ratios

Empirical relationships to estimate Poisson's ratio from rock mass quality are not available. The mean values for intact rock Poisson's ratios from the laboratory tests for each thermomechanical (thermal-mechanical) unit are listed in Table 6-3 were adopted as the rock mass Poisson's ratios. Table 8-8 lists the results. No adjustments for rock mass class are recommended.

Table 8-8. Estimated Rock Mass Poisson's Ratio

UO (Tuff "X")	TCw	PTn	TSw1	TSw2
0.14	0.21	0.20	0.26	0.21

9.0 REFERENCES

- Angell, M.M, 1994. "Bedrock Geology of Exile Hill," TDIF 303180, DTN: SNL9204199300210022, a report prepared by Geomatrix Consultants, Inc., San Francisco, California, for Sandia National Laboratories, Albuquerque, New Mexico. (MOL.19940718.0024)
- Barton, N.R., R. Lien, and J. Lunde, 1974. "Engineering Classification of Rock Masses for the Design of Tunnel Support," *Rock Mechanics*, 6:189-236, Springer Verlag. (NNA.8700406.0237)
- Bieniawski, Z.T., 1974. "Geomechanics Classification of Rock Masses and Its Application in Tunneling," *Proceedings of the 3rd Congress of the ISRM*, Denver, CO, International Society of Rock Mechanics, Lisbon Portugal. (HQS.880517.2256)
- Bieniawski, Z.T., 1976. "Rock Mass Classification in Rock Engineering," *Proceedings, Symposium on Exploration for Rock Engineering*, Johannesburg, South Africa, pp. 97-106, A.A. Balkema, Rotterdam. (NNA.870406.0217)
- Bieniawski, Z.T., 1979. *Engineering Rock Mass Classification*, Wiley-Interscience Publication, John Wiley & Sons, New York. (NNA.901005.0044)
- Brown, E.T., editor, 1981. *Rock Characterization Testing and Monitoring, ISRM Suggested Methods*, Published for the Commission on Testing Methods, International Society for Rock Mechanics, Pergamon Press, Elmsford, New York. (NNA.890713.0194)
- Byers, F.M. Jr., W.J. Carr, P.P. Orkild, W.D. Quinlivan, and K.A. Sargent, 1976. *Volcanic Suites and Related Cauldrons of Timber Mountain-Oasis Valley Caldera Complex of*

- Southern Nevada*, U.S. Geological Survey Professional Paper 919, U.S. Department of the Interior, 70 p. (NNA.870406.0239)
- Carr, W.J., 1984. *Regional Structural Setting of Yucca Mountain, Southwestern Nevada, and Late Cenozoic Rates of Tectonic Activity in Part of the Southwestern Great Basin, Nevada and California*, U.S. Geological Survey Open-File Report 84-854, U.S. Department of the Interior, 109 p. (NNA.870325.0475)
- Carr, W.J., 1992. *Structural Model for Western Midway Valley Based on RF Drillhole Data and Bedrock Outcrops: in Gibson, J.D., F.H. Swan, J.R. Wesling, T.F. Bullard, R.C. Perman, M.M. Angell, and L.A. DiSilvestro, Summary and Evaluation of Existing Geological and Geophysical Data near Prospective Surface Facilities in Midway Valley, Yucca Mountain Project, Nye County, Nevada*, SAND90-2491, Appendix A, Sandia National Laboratories, Albuquerque, New Mexico. (NNA.910709.0001)
- Cloos, E., 1968. "Experimental Analysis of Gulf Coast Fracture Patterns," *American Association of Petroleum Geologists Bulletin*, 52:420-444. (MOL.19950321.0066)
- Deere, D.U., 1963. "Technical Description of Rock Cores for Engineering Purposes," *Felsmechanik und Ingenieurgeologie* (Rock Mechanics and Engineering Geology), 1(1):16-22. (NNA.900827.0239)
- Deere, D.U., 1968. "Geological Considerations," *Rock Mechanics in Engineering Practice*, R.G. Staff and D.C. Zienkiewicz, eds., pp. 1-20, Wiley Publishing, New York, NY. (NNA.891222.0015)

Department of Energy (DOE), 1991. *The Yucca Mountain Site Characterization Project Reference Information Base*, Version 4, Revision 4, YMP/CC-0002, April (NNA.920131.0196).

Department of Energy (DOE), November 1991. *Yucca Mountain Site Characterization Project, Study Plan No. 8.3.1.14.2, Studies to Provide Soil and Rock Properties of Potential Locations of Surface and Subsurface Access Facilities*, U.S. Geological Survey. (NNA.911108.0238)

Department of Energy (DOE), February 1994a. *Site Characterization Progress Report: Yucca Mountain, Nevada*, DOE/RW-0434, U.S. Department of Energy, OCRWM. (NNA.940302.0052)

Department of Energy (DOE), December 1994b. *Exploratory Studies Facility Design Requirements*, Vol. 1, Rev. 01, YMP/CM-0019, U.S. Department of Energy. (NNA.920903.0087)

Diehl, S.F., and M.P. Chornack, 1990. *Stratigraphic Correlation and Petrography of the Bedded Tuffs, Yucca Mountain, Nye County, Nevada*, U.S. Geological Survey Open-File Report 89-3, U.S. Department of the Interior, 152 p. (NNA.901102.0006)

Fernandez, J.A., J.B. Case, C.A. Givens, and B.C. Carney, 1994. *A Strategy to Seal Exploratory Boreholes in Unsaturated Tuff*, SAND93-1184, Yucca Mountain Site Characterization Project, Sandia National Laboratories, Albuquerque, New Mexico. (NNA.940418.0005)

Gibson, J.D., F.H. Swan, J.R. Wesling, T.F. Bullard, R.C. Perman, M.M. Angell, and L.A. DiSilvestro, 1992. *Summary and Evaluation of Existing Geological and Geophysical Data Near Prospective Surface Facilities in Midway Valley, Yucca Mountain Project*,

- Nye County, Nevada, Yucca Mountain Site Characterization Project*, SAND90-2491, Sandia National Laboratories, Albuquerque, New Mexico. (NNA.910709.0001)
- Goktan, R.M., and C. Ayday (1993). "A Suggested Improvement to the Schmidt Rebound Hardness ISRM Suggested Method with Particular Reference to Rock Machineability," *International Journal of Rock Mechanics, Mining Sciences & Geomechanics Abstracts*, 30(3):321–322, Pergamon Press, New York. (MOL.19950321.0065)
- Hamblin, W.K., 1965. "Origin of 'Reverse Drag' on the Downthrown Side of Normal Faults," *Geological Society of America Bulletin*, 76:1145–1163. (NNA.920505.0073)
- Hardy, M.P., and S.J. Bauer, 1991. *Drift Design Methodology and Preliminary Application for the Yucca Mountain Site Characterization Project*, SAND89-0837, Sandia National Laboratories, Albuquerque, New Mexico. (NNA.910808.0105)
- Hoek, E., and E.T. Brown, 1988. "The Hoek-Brown Failure Criterion—A 1988 Update," *Canadian Rock Mechanics Symposium*, np. (NNA.900515.0018)
- Hudson, J.A., and S.D. Priest, 1979. "Discontinuities and Rock Mass Geometry," *International Journal of Rock Mechanics, Mining Sciences and Geomechanics Abstracts*, 16(6):339–362, Pergamon Press. (NNA.900403.0399)
- Kirkaldie, L. (editor), 1988. ASTM STP 984, "Rock Classification Systems for Engineering Purposes," American Society for Testing and Materials, Philadelphia, Pennsylvania. (MOL.19950505.029)
- Kirsten, H.A.D., 1988. ASTM STP 984, "Written Discussion — Rock Classification Systems for Engineering Purposes," L. Kirkaldie (editor), American Society for Testing and Materials, pg. 32. (MOL.19950505.029)

- Laubscher, D.H., 1990. "A Geomechanics Classification System for the Rating of Rock Mass in Mine Design," *Journal of the South African Institute of Mining and Metallurgy*, 90(10):257–271. (MOL.19950329.0282)
- Lin, M., M.P. Hardy, and S.J. Bauer, 1993a. *Fracture Analysis and Rock Quality Designation Estimation for the Yucca Mountain Site Characterization Project*, SAND92-0449, Sandia National Laboratories, Albuquerque, New Mexico. (NNA.921204.0012)
- Lin, M., M.P. Hardy, and S.J. Bauer, 1993b. *Rock Mass Mechanical Property Estimations for the Yucca Mountain Site Characterization Project*, SAND92-0450, Sandia National Laboratories, Albuquerque, New Mexico. (NNA.921204.0013)
- Lipman, P.W., R.L. Christiansen, and J.T. O'Connor, 1966. *A Compositionally Zoned Ash-Flow Sheet in Southern Nevada*, U.S. Geological Survey Professional Paper 524-F, U.S. Department of the Interior. (NNA.870519.0035)
- Martin III, R.J., R.H. Price, P.J. Boyd, and J.S. Noel, 1994. *Bulk and Mechanical Properties of the Paintbrush Tuff Recovered from Boreholes USW NRG-6; Data Report*, SAND93-4020, Sandia National Laboratories, Albuquerque, New Mexico. (MOL.19940811.0001)
- Martin III, R.J., R.H. Price, P.J. Boyd, and J.S. Noel, 1995. *Bulk and Mechanical Properties of the Paintbrush Tuff Recovered from Boreholes USW NRG-7/7A; Data Report*, SAND94-1996, Sandia National Laboratories, Albuquerque, New Mexico. (MOL.19950316.0087)
- Michelis, P., and E.T. Brown, 1986. "A Yield Equation for Rock," *Canadian Geotechnical Journal*, 23:9–17, np. (NNA.901005.0031)

Munsell Soil Color Charts, 1992. Kollmorgen Instruments Corporation, New York, New York.

(NNA.920207.0001)

Ortiz, T.S., R.L. Williams, F.B. Nimick, B.C. Whittet, and D.L. South, 1984. *A Three-Dimensional Model of Reference Thermal/Mechanical and Hydrological Stratigraphy at Yucca Mountain, Southern Nevada*, SAND84-1076, 76 p, Sandia National Laboratories, Albuquerque, New Mexico. (NNA.890315.0013)

Price, R.H., 1986. *Effects of Sample Size on the Mechanical Behavior of Topopah Spring Tuff*, SAND82-1315, Sandia National Laboratories, Albuquerque, New Mexico. (NNA.870406.0181)

Sawyer, D.A., R.J. Fleck, M.A. Lanphere, R.G. Warren, D.E. Broxton, and M.R. Hudson, 1994. "Episodic Caldera Volcanism in the Miocene Southwestern Nevada Volcanic Field: Revised Stratigraphic Framework, $^{40}\text{AR}/^{39}\text{AR}$ Geochronology, and Implications for Magmatism and Extension," *Geological Society of America Bulletin*, 106:1304-1318. (MOL.19950315.0276)

Scott, R.B., and J. Bonk, 1984. *Preliminary Geologic Map of Yucca Mountain, Nye County, Nevada, with Geologic Sections*, U.S. Geological Survey Open-File Report 84-494, scale 1:12,000, U.S. Department of Interior. (HQS.880517.1443)

Scott, R.B., G.D. Bath, V.J. Flanigan, D.B. Hoover, J.G. Rosenbaum, and R.W. Spengler, 1984. *Geological and Geophysical Evidence of Structures in Northwest-Trending Washes, Yucca Mountain, Southern Nevada, and Their Possible Significance to a Nuclear Waste Repository in the Unsaturated Zone*, U.S. Geological Survey Open-File Report-84-567, U.S. Department of Interior. (NNA.890715.0538)

- Scott, R.B., and J.R. Rosenbaum, 1986. "Evidence of Rotation about a Vertical Axis During Extension of Yucca Mountain, Southern Nevada," [abs.]: *Eos. American Geophysical Union Transactions*, 67:358. (NNA.910128.0135)
- Serafim, J.L., and J.P. Periera, 1983. "Consideration of the Geomechanical Classification of Bieniawski," *Proceedings, International Symposium on Engineering Geology and Underground Construction*, pp. 1133–1144, np. (NNA.910327.0063)
- Spengler, R.W., and K.F. Fox, Jr., 1989. "Stratigraphic and Structural Framework of Yucca Mountain, Nevada," *Radioactive Waste Management and the Nuclear Fuel Cycle*, 13:21–36. (NNA.900706.0343)
- Stacey, T.R., and C.H. Page, 1986. *Practical Handbook for Underground Rock Mechanics*, Trans Tech Publications, Zellerfeld, Federal Republic of Germany. (MOL.19950505.0228)
- Terzaghi, R.D., 1965. "Sources of Error in Joint Surveys," *Geotechnique*, 15:287–304. (NNA.900403.0402)
- Yudhbir, W. Lemonza, and F. Prinzl, 1983. "An Empirical Failure Criterion for Rock Masses," *5th International Congress on Rock Mechanics*, pp. B1–B8, International Society for Rock Mechanics, Melbourne, Australia. (NNA.900123.0087)

This page left intentionally blank.

APPENDIX A
TECHNICAL PROCEDURE
Geotechnical Logging of Core by Examination of Core and Video Records

The following technical instruction has been approved for implementation.

TP #	Title	Rev	Date
TP-233	Geotechnical Logging of Core by Examination of Core and Video Records	0	2/22/95
	SNL PI		Date
	AAI PI		Date
	Technical Review		Date
	QA Review		Date

TECHNICAL PROCEDURE

Geotechnical Logging of Core by Examination of Core and Video Records

1.0 Scope

This procedure applies to Yucca Mountain Project (YMP) Sandia National Laboratories' (SNL) personnel and contractors who are engaged in the generation and analysis of geotechnical core logging data for the holes being drilled for engineering characterization of rock mass conditions along the path of the Exploratory Studies Facility (ESF). Field rock structural logging of the core, excluding sections that are quickly removed and sealed to maintain in situ moisture content, is being conducted at the rig site by personnel from the YMP T&MSS Drilling Management Group using Procedure WI-DS-001 "Field Logging, Handling and Documenting Borehole Samples." The resulting log is a quality affecting (QA) record, however, it requires extensive checking and relogging.

The purpose of this procedure is to provide a technically credible methodology to prepare QA records of geology and rock structural core logging data for the ESF design.

2.0 Objective

A detailed geologic and rock structural (G&RS) core log will be generated for the ESF core holes to provide the basis for rock mass characterization. The G&RS log will include rock structural data, lithologic descriptions, and stratigraphic identifications based upon:

- copies of the T&MSS generated (QA) structural data,
- the core stored at the YMP Sample Management Facility (SMF),
- copies of video imagery of the core that are developed as QA records by the T&MSS personnel at the rig site, and

- lithologic and stratigraphic descriptions of the core generated by SNL or USGS geologic personnel.

3.0 Definitions

Defined below are terms for specific application to YMP core logging.

- Core—Continuous cylindrical samples of rock taken by drilling with diamond coring equipment.
- Fracture—Any through-going break in the rock core that cuts the core centerline or impacts the core for a distance greater than or equal to the core diameter.
- Rubble Zone—Sections of core where rock is fragmented to the point where logging individual fractures is not feasible. This applies to zones of broken rock that cannot be reassembled and to highly fractured zones where the core breaks into pieces of 0.20 ft or less upon removal from the core barrel.
- Lost Core—Gaps in the core record where the rock sample has been ground up during drilling or where an empty void/cavity exists.
- RQD—Rock Quality Designation: An index used to describe the integrity of the core, calculated by summing the length of intact pieces with length greater than or equal to 0.33 ft and dividing by an interval length.
- Core Run—An interval in the coring process representing the lowering of a core barrel into the hole, drilling, and then removing the core barrel and recovering the core at surface.
- Samples—Pieces of core removed for testing of rock characteristics. Tests may be either destructive or nondestructive, however, the core is no longer available to be logged.

4.0 Description of Activities

Logs of rock characteristics generated for core holes consist of quantitative measurements, semi-quantitative measurements, and qualitative descriptions. This procedure deals with collection of data being produced within the YMP Site Characterization and with compilation of the G&RS log to meet QA requirements. The data utilized for the log will include:

- lithologic and stratigraphic descriptions of the core (QA records developed under SNL TP-0162) and USGS lithologic logs transferred by TDIF,
- field rock structural and lithologic logging of the core by the T&MSS Drilling Management Group (QA records), and
- videotape records of the core by the T&MSS Drilling Management Group (QA records).

Procedure WI-DS-001 provides a methodology for field logging, handling, and documenting borehole samples and is being implemented by T&MSS personnel. Two constraints impact the field logging:

- a requirement to seal samples to prevent moisture loss within 5 minutes of removal from the core barrel prevents accurate description of some intervals of the core, and
- the quantity of core being generated may result in partial descriptions at the rig site.

Although the field data is QA and the structural logging being performed is a technically acceptable record of rock structural data required for engineering characterization for construction planning, the field data requires extensive checking and relogging. This procedure is designed to provide a methodology to produce the final QA record by relogging the core using the high-resolution Super VHS video imagery (a QA record generated at the rig site) and the core

stored at the SMF. The original T&MSS field structural logging data will be used as the basis for the relogging.

5.0 Equipment Requirements

Equipment required for the relogging using video imagery includes:

- a Super VHS video cassette recorder (VCR) and
- a television monitor.

Examination of the actual core at the SMF requires:

- a measuring tape graduated in 0.1 ft,
- a protractor,
- a circumferential compass for HQ and PQ core, and
- equipment for computer logging.

6.0 Procedures

All final records generated during the use of this procedure will be made using indelible black ink or will be photocopies. Field logging data will be in pencil on photocopies of the T&MSS field logs.

Copies of the T&MSS field rock structural log will be obtained as the basis of generation of the QA G&RS log according to the following detailed procedure. Lithologic logs and stratigraphic identifications are developed using SNL Technical Procedure 0162, "Geologic Description and Core Logging," or are supplied by USGS via TDIF.

6.1 General

The T&MSS field structural logging will be checked and relogged using both the remaining core at the SMF and a copy of the QA video record. In the relogging process, the following activities will be performed on a run basis:

- Check the run interval.
- Check the length of the core recovered and calculate the percentage recovery.
- Check the location and length of lost core, rubble, and fractured zones. The fractured zone coding may be used to describe intervals where coring-induced fracturing results in fracture frequencies greater than or equal to 8 per ft, but where core can still be reconstructed.
- Check the piece lengths and record the pieces with lengths greater than or equal to 0.33 ft.
- Calculate the run Rock Quality Designation (RQD). RQD is the summation of piece lengths greater or equal to 0.33 ft in a run interval, divided by the run interval length, and expressed as a percentage. In this calculation, all fractures are considered except those that are handling-induced by removal from the core barrel and are identified as such by the T&MSS personnel by marking the core.

$$\text{Run RQD} = \frac{\sum \text{Piece lengths} \geq 0.33 \text{ ft}}{\text{Run length (ft)}} \times 100\% \quad (1)$$

- Check all fractures noted in the SMF log and identify all natural fractures for inspection in the core.
- Confirm the log at the sampled intervals using the video imagery. The sampled intervals are identified in the log or video as WC (Whole Core removed). The sampling instructions generally require whole pieces of core for testing. It will

typically be the case that the half of the fracture that allowed selection of the sample will remain in the core box. These bounding surfaces will be identified for later examination.

- The estimated percent lithophysal and other cavities will be recorded on a per-run basis by comparing cavities on the visible face of the core with charts designed for estimating the percent composition of rock constituents, as described in Section A.7.

Direct observations of all natural fractures (remaining after sampling) in the core will also be performed. Fracture characteristics that will be recorded include:

- surface planarity, roughness, mineral infilling, infill thickness, healing, and moisture;
and
- relative orientation of the fracture within SMF-indicated intervals where core can be fit together.

The field structure log may be either completely regenerated or the existing T&MSS log may be checked and edited. Upon completion of the relogging process using a computerized format, field data files will be combined for each hole and will be identified as revision 0. Any succeeding modifications to these files will be noted by an ascending revision number.

6.2 Structural Logging Procedure

Structural relogging will follow procedures outlined below. This procedure is, in general, compatible with those outlined in WI-DS-001 and is presented here. The logging procedures provided herein include standardized descriptions of core features and minimize the need for subjective and interpretive descriptions.

6.2.1 Logging Format

Data will be recorded in the format of the logging form shown in Figure 1. Figure 2 shows short-form instructions which are reproduced on the back of the form. Not all spaces on the form will be completed, depending on the nature of the feature being described. The same format is used by the "Hard Core" logging program to create a data file suitable for further computer processing and plotting. A screen from "Hard Core" is shown in Figure 3. Data may be recorded by T&MSS personnel directly into a data file using "Hard Core" or may be recorded on the logging form. The field structural log may be checked by SNL personnel either by checking the data file using "Hard Core," checking and entering the data from the logging form into "Hard Core" or by checking and annotating a copy of the field logging form.

6.2.2 Structural Logging

The structural logging procedure is described here. Some of the descriptions recorded by the field loggers will be modified during the checking. Because time constraints on the rig site often prevent complete description, it is the intent of this procedure to both check the field log and complete the description where necessary.

Each major section of the logging form is discussed below.

6.2.2.1 Header Information—Header information is completed for each sheet of the log to assure association of the information generated with the proper core hole. The categories are self-explanatory. In the relogging process, the authors of the field log and the checker are identified. The individual performing the SNL relogging to generate the first QA records is identified in the "checked by" column. These forms must be completed on each sheet of the log data.

YUCCA MOUNTAIN SITE CHARACTERIZATION PROJECT
STRUCTURAL LOG

YMP-011-R4
10/18/93

Borehole ID U15W NX6-77A From 676.8 To 680.6 Core Size P & Page 95 of
DS Staff M. ENDEHALL Dates 12/1/93 Checked By B. A. Wilson Date 12/7/93

NON ORIENT BRACKET / X	DEPTH	BRACKET		FRAC ORIGIN	FRACURE ORIENTATION	DIP	CORE			FRACTURES					REMARKS						
		CODE	VALUE				HARDNESS	WEATHERING	FRAC FREQ	PIECE LENGTH	PLANARITY	TOUGHNESS	FILLING	HEALING		MOISTURE	MINERALIZ				
1	3																				
X	4																				
X	5																				
	6																				
X	7	RZ		C		0															
X	8	RZ		C		0															
	9																				
	10																				
	11																				
	12																				
	13																				
	14																				
	15																				
	16																				
	17																				
	18																				
	19																				
	20																				
	21																				
	22																				
	23																				
	24																				
	25																				
	26																				
	27																				
	28																				
	29																				
	30																				

NOTE: Blank spaces
Intentionally blank.

YLP-S11.2Q-SMF.3

INSTRUCTIONS ATTACHED

Figure 1. Structural Log Coding Form

INSTRUCTIONS FOR PREPARATION OF STRUCTURAL LOG

HEADER INFORMATION

Borehole ID	Unique designation given to borehole	Pagination	Numbers assigned to sequential sheets and total numbers of sheets at end of hole
From/To	Top and bottom depths on page from columns 3-7	Drilling Support Staff	Signature(s) of geologist(s) and date(s) sheet completed
Core Size	Core diameter (Begin new sheet if diameter changes)	Checked By/Date	Signed/dated by DS Staff member not directly responsible for completion of form

COLUMN INFORMATION [Note: Column number in ()]

(1) Nonorientation Marks	Depth below which relative orientation could not be carried.			
(2) Bracket /-X	Enter "/" at top depth and "X" at bottom depth of runs and intervals of loss or removal, or zones of similar structural features. Never enter "/" or "X" on separate pages.			
(3-7) Depth	Enter depth or feature to nearest 0.1 ft; locate most fractures at midpoint.			
(8-9) Bracket Code	Identity of features bracketed in column 2:			
	CR: Core run interval	UC: Unrecovered interval	WC: Whole core removed	VI: Void interval (lithophysal zone)
	FL: Fracture length (> 0.5 ft)	RZ: Rubble zone	FZ: Interval of similar fractures	
(10-13) Bracket Value	Each bracket has a numeric value:			
	CR: Length of interval to the nearest 0.1 ft	VI: Percent lithophysal cavities by linear measurement	FL: Length that the fracture impacts the core (parallel to core axis)	FZ: Number of fractures in the interval excluding the starting and ending fractures.
	WC:			RZ: Average maximum diameter of rubble pieces to nearest 0.01 ft
(14) Fracture Origin	Following codes indicate origin of break or fracture:			
	N: Natural—indicated by mineral coating or evidence of weathering, slickensides, lack of fit between sides.		C: Coring induced—fresh, clean, tightly fitting breaks.	
	I: Indeterminate—origin questionable, rotates so that coatings possibly removed.		H: Handling induced—description not necessary.	
	V: Vug or large void.		P: Foliation plane due to gravity flattening upon deposition.	
(15-17) Orientation	Relation of feature to orientation stripes			
(18-19) Dip	Angle between plane normal to core axis and plane of fracture, axis assumed vertical except in deviated hole.			
(20) Rock Hardness	Subjective evaluation of resistance to breakage:			
	1: Extremely hard	2: Very hard	3: Hard	4: Moderately hard
	6: Soft	7: Very soft	8: Soil-like, cohesive	9: Soil-like, non-cohesive
(21) Rock Weathering	Subjective evaluation of rock degradation by mechanical/chemical agents:			
	F: Fresh	S: Slightly weathered	M: Moderately weathered	I: Intensely weathered
				D: Decomposed
(22) Fracture Frequency	Fracture frequency will not be logged since it will be calculated in the final structural and lithologic log.			
(23-28) Characteristics	Description of core run and description of individual features according to criteria outlines			
(23) Planarity	Describes the overall shape of the feature:			
	P: Planar	C: Curved	S: Stepped	I: Irregular
(24) Roughness	Describes the local relief of the surface:			
	V: Very rough—stepped, near-normal steps and ridges occur.		R: Rough—large angular asperities can be seen.	
	M: Moderately rough—asperities clearly visible, surface has abrasive feel.		S: Smooth—no asperities, smooth to the touch.	
	P: Polished—slickensided, extremely smooth and shiny.			
(25) Filing	Describes the thickness of mineral infillings on the fracture surface:			
	C: Clean, no filling	S: Very thin, surface sheen	T: Thin (up to 0.1 inches)	M: Moderately thick (0.1-0.4 inches)
	V: Very thick (0.4 - 1.0 inches)	E: Extremely thick, greater than 1.0 inches		
(26) Healing	Describes the degree to which fractures have been cemented by mineral infilling:			
	T: Total—Completely healed or cemented at least as hard as the rock matrix.		M: Moderate—More than 50% healed or cemented and the cementing mineral is less hard than the whole rock.	
	P: Partial—Less than 50% healed or cemented.			
(27) Moisture	Used with CR bracket to describe moisture in core run interval or used to describe individual fracture:			
	D: Fracture is tight or densely filled and core dry.	P: Dry but water flow appears possible.	F: Dry but evidence of previous flow.	S: Fracture filling or core damp but no free water.
				W: Fracture shows evidence of free water or core saturated.
(28) Mineralization	Describes the infilling on fracture surfaces:			
	C: Clean	WC: White, crystalline	WN: White, non-crystalline	BC: Black crystalline
	BD: Black dendritic	TD: Brown dendritic	TC: Tan crystalline	
(29) Piece Length	Record lengths of core 0.33 ft and longer (to nearest 0.01 ft) between natural and/or indeterminate breaks, in same row as bottom break. Length measured between midpoints of fractures.			
(30) Remarks	General observations or notes of special occurrences.			

A-10

Figure 2. Instructions for Preparation of Structural Log Coding Form

Files Edit Help Hard Core - C:\WPLOG\EX:STR

1	2	3	4	5	6	7	8	9	10	11	12	13	14	15	16	17	18	19	20	21	22	23	24	25	26	27	28	29	30	31
NON-ORIENT	BRACKET	DEPTH	CODE	VALUE	FRAC ORIGIN	FRACURE ORIENTATION	DIP	CORE						FRACTURE						RAW	ADJ.	REMARKS								
								HARDNESS	WEATHERING	FRAC FREQ	PLANARITY	ROUGHNESS	FILLING	HEALING	MOISTURE	MINERALIZ	PIECE LENGTH	PIECE LENGTH												
*	/			50CR	350			4F3																						Core Run#1
	X			85																										
				52																										
				58																										

60

General

Non Oriented

Bracket Start

Bracket End

Depth

Bracket

Bracket Codes

Bracket Values

Fracture Orig.

Coreing Induced

Fracture Orientation

Dip

Core

Hardness

Weathering

Frac. Freq.

Fracture

Planarity

Roughness

Filling

Raw Piece Length

Adj. Piece Length

Remarks

Commands

Next Line

Save File

Save File As

New File

Exit

Figure 3. Sample Screen from "Hard Core" Logging Program Showing Menu and Data Format

6.2.2.2 Column Information—The structural logging data is discussed using a column format.

- Non-Oriented Marks (Column 1): An “*” is placed in Column 1 to indicate points at which the relative orientation of the core can no longer be continued due to rubble that prevents reconstruction of the core, lost core, or fracture surfaces that cannot be fit together.
- Bracket (Column 2): Brackets identify intervals in the core record with a common feature (i.e., core run interval, lost core zone, rubble zone, sample zone, etc.). A forward slash (“/”) is entered at the beginning depth and “X” is entered at the bottom depth. Bracket codes are described in Columns 8–9.
- Depth (Columns 3–7): The downhole depth is entered to the nearest 0.1 ft. Fracture locations are measured to the vertical midpoint at the center of the core.
- Bracket Code (Columns 8–9): Intervals to be identified using a depth bracket and the alphanumeric descriptors are listed below.

CR — Core Run interval.

UC — Unrecovered Core or lost core zone. Note that lost core is always placed at the bottom of the core run to allow depth adjustment if part of the “lost core” is recovered in the next core run.

WC — Whole Core removed as a sample.

VI — Void Interval (lithophysal and other cavities zone).

FL — Fracture Length, used to note the length over which a fracture parallel to the core axis impacts the core. Note only if FL > 0.5 ft.

RZ — Rubble Zone, sections of core where rock is fragmented to the point where logging individual fractures is not feasible. This applies to zones of broken rock that cannot be reassembled and to highly fractured zones where the core breaks into pieces of 0.20 ft or less upon removal from core barrel.

FZ — Fracture Zone, an interval of similar fractures at relatively high density (8 per ft).

- Bracket Value (Columns 10–13): Each bracket interval has an associated numerical value as listed below.
 - CR — Run RQD as an integer number, right-justified in Columns 11 through 13.
 - UC — Length of the interval to the nearest 0.01 ft.
 - WC — Length of the interval to the nearest 0.01 ft.
 - VI — Estimated percentage lithophysal cavities as an integer number, right-justified in Columns 11 through 13.
 - FL — Length that the fracture impacts the core (parallel to core axis).
 - FZ — Number of fractures in the interval, excluding the starting and ending fractures, as an integer number, right-justified in Columns 11 through 13.
 - RZ — Estimated average diameter of rubble pieces to the nearest 0.01 ft.
- Fracture Origin or Type (Column 14): Alphanumeric codes are used to identify the type of fracture according to four categories:
 - N — Natural fractures are indicated by mineral coatings, evidence of weathering, slickensides, lack of rematch/fit between sides or by surfaces that form an ellipse in the core.
 - C — Coring-induced fractures are generally normal to the axis of the core or may indicate some torquing of the core. They are typically clean, fresh, and fit tightly back together.
 - I — Indeterminate fractures cannot clearly be identified as “N” or “C.” This includes fracture surfaces that have been shaped by drilling rotation.
 - H — Handling-induced fractures are formed in the core by removal from the core barrel or placement in the core box. These fractures are witnessed and, according to YLP-SII.2Q-SMF, are marked by the site personnel with lines parallel to the fracture on both sides of the core. “H” fractures are typically not recorded in the log unless there is a specific reason.
 - V — Vug or large void.
 - P — Foliation plane due to gravity flattening upon deposition.
- Orientation (Column 15–17): Dip direction of “N” or “I” type fractures or “P” foliation planes with respect to the up-down orientation lines (red and blue inked lines) on the core. This orientation is reported as the down-dip azimuth measured

clockwise from the midpoint between the red and blue lines (to the nearest 10°), as shown in Figure 4.

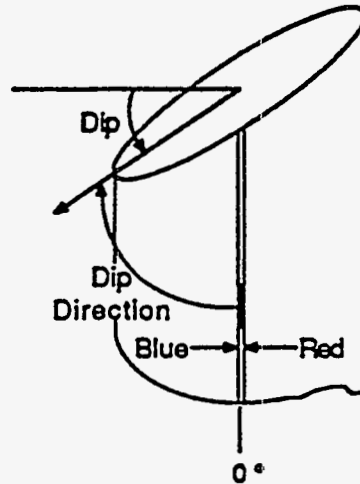


Figure 4. Illustration of Dip Direction Orientation Conventions Utilized in Structural Logging

- Dip (Columns 18–19): In the log, the dip angle is defined as the angle between the plane normal to the core axis and the fracture plane.
- Rock Hardness (Column 20): Subjectively evaluated using the criteria and numeric codes presented below. YMP procedures do not allow scratching or breaking of the core as suggested by the criteria, hence the criteria can only be subjectively assessed using the numerical criteria.
 - 1 — Extremely hard: Cannot be scratched, chipped only with repeated heavy hammer blows.
 - 2 — Very hard: Cannot be scratched, broken only with repeated heavy hammer blows.
 - 3 — Hard: Scratched with heavy pressure, breaks with heavy hammer blow.
 - 4 — Moderately hard: Scratched with light–moderate pressure, breaks with moderate hammer blow.
 - 5 — Moderately soft: Grooved (16th inch) with moderate heavy pressure, breaks with light hammer blow.

- 6 — Soft: Grooved easily with light pressure, scratched with fingernail, breaks with light–moderate manual pressure.
 - 7 — Very soft: Readily gouged with fingernail, breaks with light manual pressure.
 - 8 — Soil-like, cohesive.
 - 9 — Soil-like, non-cohesive.
- Weathering (Column 21): Describes the character of rock weathering and is described using the alphanumeric codes described as follows:
 - F — Fresh: Rock and fractures not oxidized or discolored, no separation of grains, change of texture or solutioning.
 - S — Slightly weathered: Oxidized or discolored fractures and nearby rock, some dull feldspars, no separation of grains, minor leaching.
 - M — Moderately weathered: Fractures and most of rock oxidized or discolored, partial separation of grains, crystals rusty or cloudy, moderate leaching of soluble minerals.
 - I — Intensely weathered: Fractures and rock totally oxidized or discolored, extensive clay alteration, leaching complete, grain separation extensive, rock is friable.
 - D — Decomposed: Grain separation and clay alteration complete.
 - Fracture Frequency (Column 22): This will not be utilized since the graphics program that creates the G&RS log will calculate it.
 - Piece Length (Column 23): Core pieces whose length is greater than or equal to 0.33 ft is recorded on the line associated with the bottom break/fracture. All fractures (type N, I, and C) in the core are considered to interrupt the piece length, except handling-induced fractures (H) that are clearly identified by black ink marks on both sides of the fracture. Piece length is measured from the midpoints of fractures. Fractures parallel to the core axis (dip = 90°) are interpreted to have broken the core along the length of the fracture and therefore cannot have a piece length.

- Fracture Characteristics (Columns 24–29): Consists of planarity, roughness, filling, healing, moisture, and mineral infilling. Each of these characteristics is discussed below.

Planarity (Column 24): Describes the overall shape of the feature and is subdivided into the four descriptions illustrated in Figure 5 which are:

P — Planar

C — Curved

S — Stepped

I — Irregular

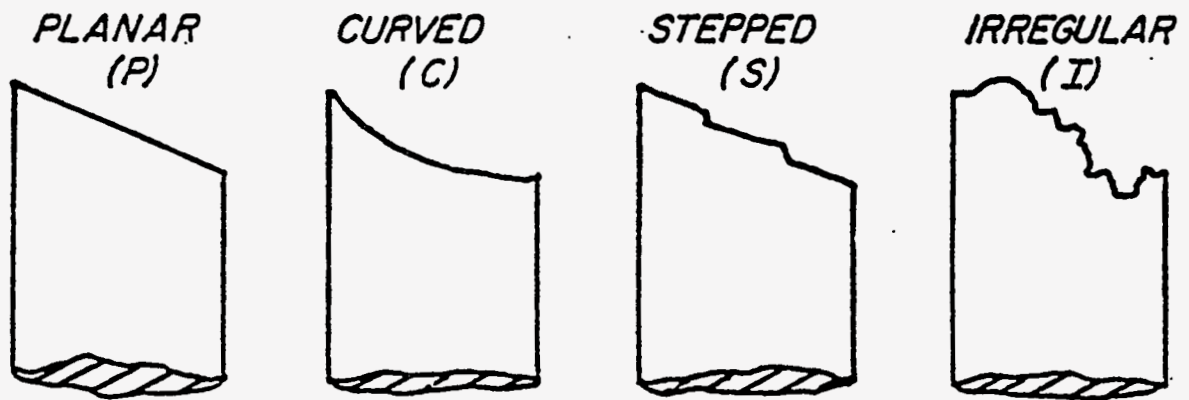


Figure 5. Illustration of Planarity Classifications

- Roughness (Column 25): Describes the local relief of the surface and is subdivided into the six descriptions listed below and are illustrated in Figure 6.

V — Very Rough: Stepped, near-normal steps, and ridges occur.

R — Rough: Large angular asperities can be seen.

M — Moderately Rough: Asperities clearly visible, surface has an abrasive feel to slightly rough; small asperities are visible and can be felt.

S — Smooth: No asperities, smooth to the touch.

P — Polished: Slickensides, extremely smooth and shiny.

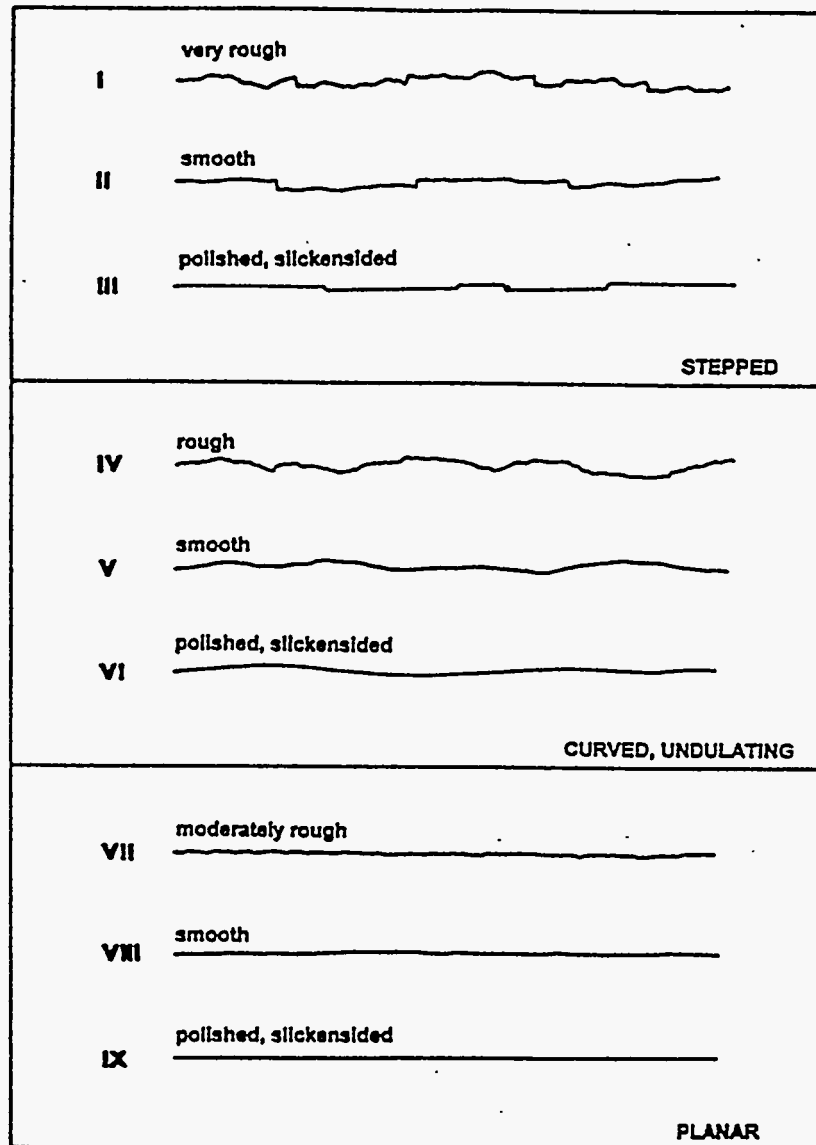


Figure 6. Illustration of Roughness Profiles and Nomenclature

- Infill Thickness (Column 26): Describes the thickness of mineral infillings on the fracture surface. Codes used in the description are listed below:
 - C — clean, no filling;
 - S — very thin, surface sheen;
 - T — thin (up to 0.1 inch);
 - M — moderately thick (0.1–0.4 inch);
 - V — very thick (0.4–1.0 inch); and
 - E — extremely thick (greater than 1.0 inch).

- Healing (Column 27): Describes the degree to which fractures have been healed or recemented by mineral infilling and is subdivided into three categories:

T — total, completely healed or cemented, at least as hard as the rock matrix.

M — moderate, more than 50% healed or cemented and the cementing material is less hard than the whole rock.

P — partial, less than 50% healed or cemented.

If the fracture is totally separated, not healed or cemented, this descriptor is not entered in the log.

- Moisture (Column 28): Used with core run (CR) bracket either to describe moisture in a core run interval or used to describe individual fractures. The moisture column describes any indication of moisture presence or potential of water flow and is subdivided into five categories:

D — fracture is tight or densely filled and core dry,

P — dry, but water flow appears possible,

F — dry, but evidence of previous flow,

S — fracture filling or core damp, but no free water, and

W — fracture shows evidence of free water or core saturated.

- Mineralization (Column 29): Describes infilling on fracture surfaces. Generic descriptors may be used or specific mineral infill codes:

C or blank — clean;

WC — white or clear, crystalline, includes calcite, zeolites or quartz;

WN — white or clear, non-crystalline, includes opal and minerals too fine grained to identify;

BC — black crystalline, includes specular hematite;

BD — black dendritic, includes manganese oxides;

RD — red-brown stains or rounded dendrites, includes iron oxides;

TC — tan crystalline;

SI — silica;

MN — manganese;

CA — calcite;

CL — clay; and
TN — tan, non-crystalline.

New infill codes may be added as required.

- Remarks (Column 30): Remarks and notes about general observations or special occurrences are recorded at the extreme right of the form.
- Run RQD: Run RQD is calculated using Equation A-1. The calculation should be entered in the remarks column at the base of the run in the record sheet, and the percent RQD for each row is entered as the bracket value in Columns 11–13.

6.3 Lithologic Logging

The lithologic and stratigraphic descriptions will be developed separately using SNL Technical Procedure 0162, “Geologic Description and Core Logging,” or will be supplied by USGS via TDIF.

6.4 Data Processing and Presentation

The field structural and lithologic logs will be digitized for development of a unified graphical presentation of the data called the Geology and Rock Structural (G&RS) log. An example of the final log product is shown in Figures 7a, 7b, and 7c, which includes:

- the log cover sheet containing the hole number, location, elevation, core size, and personnel involved in development of the various parts of the data;
- the legend explaining the alphanumeric characters presented in the log; and
- the graphical representation of the collected data.

The graphical log contains the data that are pertinent to engineering characterization of design of the ESF. Some of the data collected are not contained in the graphical log, but are available in the digital record for further analysis as required.

**YUCCA MOUNTAIN SITE CHARACTERIZATION PROJECT
GEOLOGY AND ROCK STRUCTURE LOG**

Sandia National Laboratories
Print Date: 8/5/94
WBS 1.2.3.2.6.2
QA: QA
Revision 1

REVISION HISTORY

Revision 1 Change in method for calculating % lithophysae.

BOREHOLE ID:	<u>UE25 NRG-5</u>	TOTAL DEPTH:	<u>1350.0 ft</u>
STUDY PLAN NO:	<u>8.3.1.2.2.1</u>	ANGLE FROM VERT:	<u>0°</u>
CORE SIZE:	<u>HQ</u>	AZIMUTH:	<u>NA</u>
DRILL DATES:	<u>4/20/93 - 6/9/93</u>		
GROUND ELEV:	<u>4106.66 ft</u>		
COORDINATES:	N: 767,889.61 ft		
	E: 564,769.87 ft		

Field Rock Structure

Field Log by:

Pitterlee
Edwards Drilling Support Division, Drilling
Wilcoxon Support and Sample Management
Hattler Department, T&MSS
Myers
Henson

Relogged by:

Richard Lippoth J. F. T. Agapito & Associates, Inc.

Lithology and Stratigraphy

Logged by:

Chris Rautman Sandia National Laboratories

Checked by:

Carl Brechtel J. F. T. Agapito & Associates, Inc.
Eric Martin J.F.T. Agapito & Associates, Inc.

Log prepared by J. F. T. Agapito & Associates, Inc. for Sandia National Laboratories

EXPLANATION GEOLOGY AND ROCK STRUCTURE

 NONWELDED

 WELDED


 BEDDED TUFF

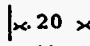
 ASH-FLOW TUFF

FRACTURE TYPE

- N Natural fractures are indicated by mineral coatings, evidence of weathering, slickensides, lack of rematch/fit between sides or by surfaces that form an ellipse in the core.
- C Coring-induced fractures are generally normal to the axis of the core or indicate some torquing of the core. They are typically clean, fresh and fit tightly back together.
- I Indeterminate fractures are those not clearly described as "N" or "C." This includes fracture surfaces that have been shaped by drilling rotation.
- H Handling-induced fractures are formed in the core by removal from the core barrel or placement in the core box. These fractures are witnessed and, according to BTP-SMF-008, are marked by the SMF personnel by lines parallel to the fracture on both sides of the core. "H" fractures are typically not recorded in the log unless there is a specific reason.
- V Vug or large void.
- P Foliation plane due to gravity flattening upon deposition.

LOST CORE AND RUBBLE

 LOST CORE

 RUBBLE ZONE
(with average maximum diameter of rubble pieces to nearest 0.01 ft; NM = not measured)

HARDNESS (Subjective estimate, YMP procedures do not allow core to be broken or scratched etc.)

- 1 Extremely Hard—Cannot be scratched, chipped only with repeated heavy hammer blows.
- 2 Very Hard—Cannot be scratched, broken only with repeated heavy hammer blows.
- 3 Hard—Scratched with heavy pressure, breaks with heavy hammer blow.
- 4 Moderately Hard—Scratched with light-moderate pressure, breaks with moderate hammer blow.
- 5 Moderately Soft—Grooved (16th in.) with moderate heavy pressure, breaks with light hammer blow.
- 6 Soft—Grooved easily with light pressure, scratched with fingernail, breaks with light-moderate manual pressure.
- 7 Very Soft—Readily gouged with fingernail, breaks with light manual pressure.

WEATHERING

- F Fresh—Rock and fractures not oxidized or discolored, no separation of grains, change of texture or solutioning.
- S Slightly Weathered—Oxidized or discolored fractures and nearby rock, some dull feldspars, no separation of grains, minor leaching.
- M Moderately Weathered—Fractures and most of rock oxidized or discolored, partial separation of grains, crystals rusty or cloudy, moderate leaching of soluble minerals.
- I Intensely Weathered—Fractures and rock totally oxidized or discolored, extensive clay alteration, leaching complete, grain separation extensive, rock is friable.
- D Decomposed—Grain separation and clay alteration complete.

PLANARITY

- P Planar
 - C Curved
 - S Stepped
 - I Irregular
- V Very rough, stepped, near-normal steps and ridges occur.
R Rough, large angular asperities can be seen.
M Moderately rough, asperities clearly visible, surface has an abrasive feel; to slightly rough, small asperities are visible and can be felt.
S Smooth, no asperities, smooth to the touch.
P Polished, slickensided, extremely smooth and shiny.

ROUGHNESS

INFILLING THICKNESS AND MINERALIZATION

- | | | |
|---|---------------------------|----------------------|
| C Clean, no filling. | C Clean | CA Calcite |
| S Very thin, surface sheen | WC White, crystalline | SI Silica |
| T Thin (up to 0.1 inches) | WN White, non-crystalline | MN Manganese |
| M Moderately thick (0.1 - 0.4 inches) | TD Brown dendritic | CL Clay |
| V Very thick (0.4 - 1.0 inches) | TC Tan crystalline | BC Black crystalline |
| E Extremely thick, greater than 1.0 inches) | TN Tan, non-crystalline | BD Black dendritic |

UE25 NRG-5, Revision 1

Date: 8/12/94

Figure 7b. Legend Explaining Alphanumeric Abbreviations Used in Geology and Rock Structure Log

A-21

Processing of the structural log data from the field data includes various steps to ensure accuracy of the record and consistency of the data:

- The field log data is entered into the computer.
- The computerized data is checked against the field log.
- Run RQDs are calculated and entered into the CR brackets.
- The percent lithophysal and other cavities are estimated and checked, then entered into the log as VI brackets.
- Data entered using “Hard Core” and checked by SNL personnel can proceed directly to the next step.
- Checking programs are run on the data to detect logging errors and ensure consistency with the plotting program. These include comparisons of recorded piece lengths, closure of bracket codes, recording of individual features with incompatible bracket codes, and calculation of run RQDs, fracture frequency, 10-ft RQD, and estimated percent lithophysals.

7.0 Procedure for Determining Percentage of Lithophysal Cavities in Drill Core

7.1 Method

The percent volume of core occupied by open lithophysal cavities or other voids is estimated with the aid of charts. The charts are held side-by-side with either photographs or video of the core or the core itself and the estimated value recorded. The values are then spot checked by graphically quantifying the percent area occupied by the lithophysal cavities in regard to the total area of the core segment in question.

7.2 Procedure

View the entire core run in question. Concentrate on the sections of intact core and disregard rubble. Hold the charts side-by-side with the video and the core, and find the best match between the charts and the area occupied by cavities on the core. The chart used for this purpose is "Charts for estimating proportions of mottles and coarse fragments," *Munsell Soil Color Charts* (Kollmorgen Instruments Corporation, 1992).

Where the percent lithophysae lie between the range covered by the charts, estimate the value (for instance, where a core run shows a greater percentage than the 10% chart, but less than the 15% chart).

Use the entire core run to estimate the value, if possible, but do not take into consideration any voids associated with fractures or zones of rubble. View the core run on the video, one-screen width at a time, and estimate the percentage, advancing through the entire core run in this manner. Then examine the core, if available, to confirm the estimates. Next, subjectively estimate the average percent lithophysae value for the entire core run and record this value.

Estimates will be done on each core run and will be entered into the log as a bracketed void interval with the following bracket values.

- For runs with a measurable percentage of lithophysal voids greater than or equal to 1%, the percentage will be entered as the bracket value.
- For runs with no observable lithophysal cavities or lithophysal-related vapor- phase alteration, "0" shall be entered.
- For runs with observable lithophysal cavities, but composed of excessively broken or rubblized core, or for runs with no recovery or broken beyond recognition, no void

interval entry will be made. These intervals will be denoted by "Not Measured" on the final log.

- For core with vapor-phase alteration, but very small or no cavities, enter "-1" to denote <1%. This designation may be applied to zones of rubble if enough intact rock exists to identify the alteration.

7.3 Checking Procedure

About 5% of the core runs will need to be checked by a quantitative graphical method using either core photographs or video as follows.

- First, the structural log will be compared to either the USGS or SNL lithologic log and examined for any inconsistencies in zones identified as lithophysal or nonlithophysal.
- Next, select a core run at random and locate several segments of core from the videotape or photographs that appear to have representative lithophysal content for that run. Overlay the video screen or photograph with transparent graph paper. Outline both the core segment and the lithophysal cavities. Add up the total nodes (graph line intersections) contained within the area of the core segment. Then determine the number of nodes contained within the lithophysae outlines.

The percent of area occupied by the lithophysal cavities can then be calculated by dividing the nodes contained within the lithophysal outlines by the total nodes contained within the core segment. This percentage is then compared to the estimated percentage and any significant deviations are noted.

This page left intentionally blank.

APPENDIX B

DEVELOPMENT OF ROCK MASS QUALITY ESTIMATES FROM CORE DATA

B.1 Introduction

This appendix presents a brief explanation of the methodology used to develop rock mass quality estimates from core data generated for the North Ramp Geotechnical drilling program. Rock mass quality estimates are being generated from the core data to provide a basis for empirical design of the North Ramp excavations and to begin the process of establishing a database to support the design of the potential repository excavations. The collection of rock structural core logging data from the NRG holes was designed to support implementation of the Drift Design Methodology proposed by Hardy and Bauer (1991). In that methodology, rock mass classification data provides the basis for both empirical design of drifts and estimation of rock mass mechanical properties required for thermomechanical (thermal-mechanical) analysis of the effects of waste emplacement.

The approach to rock mass quality estimation presented here has been applied to holes NRG-1, -2, -2A, -3, -4, -5, -6, and -7/7A, and used to develop estimates of rock mass mechanical properties to support thermal and seismic analysis of the North Ramp by Sandia National Laboratories.

Section B-2 of this report discusses the detailed rock structural core logging that is performed to provide the base data used for the estimates. Section B-3 presents the methodology used to calculate estimates of Q (Barton et al., 1974) and RMR (Bieniawski, 1979).

B.2 Data Used in Rock Mass Quality Estimation

This section of the report describes the process of detailed rock structural logging of the NRG core and the summarization of the data into even 3-m (10-ft) intervals. In addition to the core data, rock mechanics testing data and Schmidt Hammer logs are used to develop strength indices.

B.2.1 Detailed Rock Structural Logging Data

Aspects of the rock structural logging that are used in the estimation of rock mass quality are discussed here. Detailed instructions have been developed to control the logging of rock structural features in the NRG core holes and are presented in Appendix A of this report. The logging is used to produce a computer generated graphical presentation of the information (Geologic and Rock Structural Log), an example of which is shown in Figure B-1. Structural features are labeled according to whether they are judged to be:

- ♦ Natural fractures/joints (type N);
- ♦ Uncertain in origin, could be natural joints or drilling breaks (type I);
- ♦ Drilling-induced breaks (type C); or
- ♦ Vugs, natural cavities, large lithophysal voids (type V).

In addition, for each feature the depth, inclination, surface roughness, infill thickness and mineral infill type are recorded. To facilitate the recording of this information, data is recorded according to a structured descriptive code to insure consistency from hole to hole and between individuals logging the core. An explanation of the descriptive codes is presented in Appendix A.

GEOLOGY AND ROCK STRUCTURE LOG

Sandia National Labs
by J.F.T. Agapito & Assoc., Inc.

B-3

DEPTH (FT)	CORE		FRACTURES							ROCK QUALITY DESIGNATION-RQD(%)					FRACTURES (PER 10 FT)			HARDNESS	WEATHERING	ESTIMATED % LITHOLOGIC AND OTHER CAVITIES	LITHOLOGY	LITHOLOGIC DESCRIPTION AND STRATIGRAPHY			
	INTERVAL	% RECOVERY (RUN RQD-%)	LOST CORE & RUBBLE	FRACTURE TYPE	PLANARITY/ROUGHNESS	INFILL THICKNESS AND MINERALS	DIP	INDUCED	PIECE LENGTH	VERY POOR	POOR	FAIR	GOOD	EXCELLENT	10	20	30						10	20	30
		(29)								25	50	75	90												
885	RUN 25	100		N	PH	SBD	90							0%	22	(44)		3	F	0%	W W W W				
890				N	PH	SBD	70														W W W W				
895	RUN 26	100	<.07>	I	PH	C	15														W W W W				
			<.08>	I	PH	SWI	45														W W W W				
			<.03>	N	I	PH	SWI	70													W W W W				
			<.05>	N	I	PH	SWI	70							42%	27	(39)					W W W W	USGS LOG IDENTIFIES THE INTERVAL 889.0-901.5 AS THE CONTINUATION OF THE CRYSTAL-POOR MIDDLE NONLITHOPHYSAE ZONE. [DTH: GS931108314211.043]		
900				N	PH	SBD	80														W W W W				
				I	PH	SWI	90														W W W W				
				N	PH	SWI	90														W W W W				
905	RUN 27	61	<.04>	N	PH	SBD	85														W W W W				
			<.06>	I	PH	SWI	90								0%	12	(37)					W W W W	DISTINCT CHANGE IN CHARACTER OF ROCK		
				N	PH	SBD	85														W W W W	901.3 "HOTLED" SUBUNIT ASH-FLOW TUFF, DENSELY WELDED, DEVITRIFIED, VIRTUALLY APHYRIC. DISTINGUISHING CHARACTER IS PRESENCE OF 1-3 CM SUBANGULAR LITHIC CLASTS, WHITE TO LIGHT GRAY IN COLOR AND PROBABLY OF COGNATE ORIGIN, BUT COOL ENOUGH TO RETAIN SHAPE (EQUANT), VERY SPARSE FLATTENED LITHOPHYSAE CAVITIES TO 3 CM LONG BY 1-2 MM. ALSO MORE EQUANT ILL-DEFINED PATCHY ALTERATION OF LITHOPHYSAE.			

Structure file: nrg5rv4.str Lithology file: nrg5rv5.lth Date: 11/15/93

PLLOG v 4.51

Figure B-1. Example of Geology and Rock Structure Log

The RQD is an index parameter, first introduced by Deere (1963) used in both rock mass quality systems. RQD is determined by the following calculation.

$$\text{RQD}(\%) = \frac{\sum \text{Piece length} \geq 4.0 \text{ inches}}{\text{Interval length}} \times 100 \quad (\text{B-1})$$

In the Geologic and Rock Structure Log, a parameter called Core RQD is calculated based on piece lengths as seen by the core logger without concern for the origin of the breaks or structural features. Hence, piece length could be bounded by one or other features listed previously (Types N, I, C and V). This approach was adopted to be conservative. The welded tuff rocks contain a foliation similar to bedding. Procedural discussions of RQD determination (Kirkaldie, 1988, and Brown, 1978) suggest that uncertainty in identification of coring breaks under these circumstances is justification of such a conservative approach.

Another RQD parameter, called enhanced RQD, is also calculated where the effects of fractures that are identified as coring-induced breaks are filtered out of the piece lengths. The enhanced RQD is always greater in value than Core RQD.

B.2.2 Rock Structural Summary Log

The Rock Structural Summary Log forms the basis for calculation of the Q and RMR estimates for each 3-m (10-ft) interval. Detailed data in the Geology and Rock Structure Summary Log is summarized on the 3-m (10-ft) intervals and presented graphically in the summary log as shown in Figure B-2. Data used in the rock mass quality calculation consists of Core RQD, fracture spacing, and the fracture characteristics which include surface roughness, planarity, infill type and infill thickness.

YUCCA MOUNTAIN SITE CHARACTERIZATION PROJECT
 Core Hole Structural Data Summary
 Hole UES1 NRG-3
 Zone 0 - 330 ft, Tiva Canyon

C-8

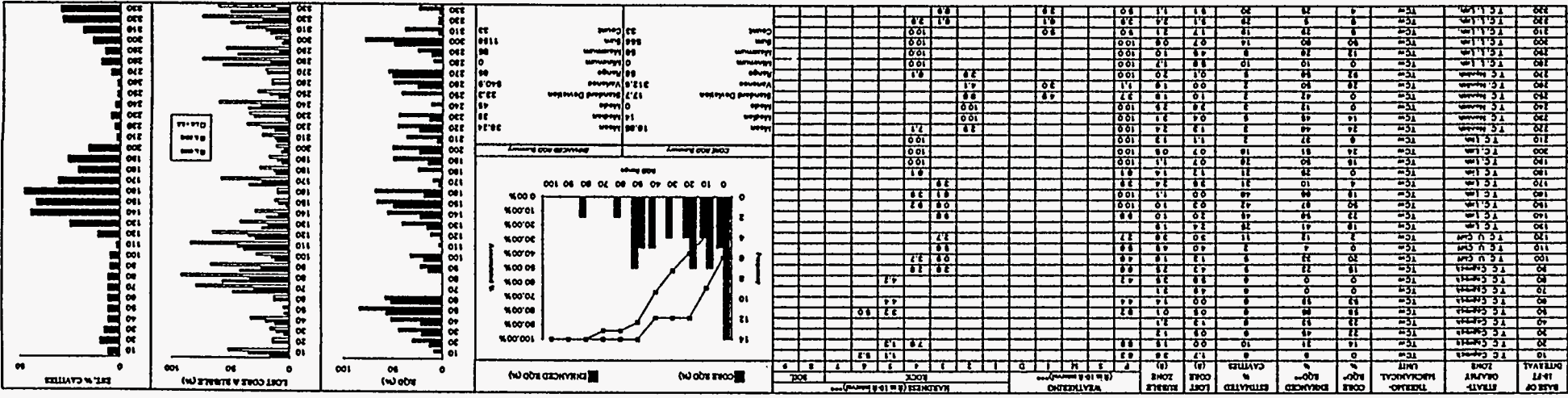


Figure B-2a. Example of Rock Structural Summary Log (page 3)

B.2.3 Rock Strength Testing and Schmidt Hammer Logs

Rock mechanics testing was conducted on core samples from the NRG boreholes where possible. However, the generally broken condition of the core made it difficult to collect samples on a systematic basis. Schmidt Hammer rebound hardness logs were therefore generated to supplement the laboratory testing. Figure B-3 is an example of the Schmidt Hammer Log of rebound hardness.

B.3 Calculation of Rock Mass Quality

The methodology used to calculate Q and RMR is presented in this section. Not all of the parameters used in the rock mass quality calculations are available from the core logs. These parameters are estimated from observations of surface outcrop and Monte Carlo techniques.

The density of drilling along the North Ramp is too low for local estimation of rock mass conditions, and therefore the purpose of the Monte Carlo simulation of parameters is to attempt to develop overall distributions of the variability of rock mass quality within strata or thermomechanical (thermal-mechanical) units. The rock mass quality estimates are expected to reflect the global variability to be encountered by the North Ramp, not local conditions associated with the position of the NRG boreholes. Since the North Ramp cuts each thermomechanical (thermal-mechanical) unit at a shallow grade, the distribution of the rock mass quality predicted for each thermomechanical (thermal-mechanical) unit should indicate the range of conditions to be encountered, and the proportional lengths of the ramp requiring various types of ground support.

SCHMIDT HAMMER TESTS																									
Initial Calibration <u>66.5 66.5 67.0 67.5 69.5 70.0 70.5 71.0 72.0 73.5</u>												Average Calibration Reading: <u>69.1</u>						Correction Factor: <u>1.07</u>		Test Date: <u>8/24/93</u>					
Final Calibration <u>65.0 68.0 68.0 68.0 68.5 68.5 68.5 70.5 70.5 72.0</u>												Anvil Standard Value: <u>74.0</u>						SMF Staff: <u>R. Henson</u>							
T. Warburton																									
Borehole	Depth Interval	Hammer Readings (20)																				Mean	Standard Deviation	Schmidt Value	Adjusted Std. Dev.
		1	2	3	4	5	6	7	8	9	10	11	12	13	14	15	16	17	18	19	20				
UE25 NRG-3	18.1 - 18.2	12.0	13.5	13.5	15.0	17.0	17.0	17.5	17.5	18.0	18.5	18.5	19.0	20.0	20.0	20.5	20.5	20.5	22.0	24.0	18.2	3.002	19.5	3.0	
	28.3 - 28.4	12.0	14.5	15.5	16.0	17.0	19.0	20.0	20.5	21.0	22.0	22.0	22.0	22.5	23.0	23.0	24.0	24.5	24.5	26.0	26.5	20.8	3.978	22.3	4.0
	38.0 - 38.1	10.0	10.0	10.0	12.0	13.0	14.0	14.0	15.5	16.0	16.5	17.0	17.0	18.0	18.0	18.0	20.0	20.0	20.5	22.5	16.0	34.1	5.254	36.6	5.3
	48.7 - 48.8	24.0	25.0	26.5	27.0	30.0	32.5	33.0	33.0	33.5	33.5	36.0	36.5	37.0	38.5	39.0	39.0	39.0	39.0	40.0	40.5	45.3	6.488	48.5	6.5
	90.6 - 90.7	33.0	33.0	34.0	35.0	43.0	44.5	46.0	46.5	46.5	46.5	47.0	47.5	47.5	50.0	50.0	50.5	51.0	53.0	54.0	45.3	40.4	4.791	43.8	4.2
	141.35 - 141.45	29.5	32.5	33.0	37.0	38.5	38.5	38.5	39.0	40.0	40.0	41.0	41.0	43.0	43.0	44.0	44.0	44.5	46.0	47.0	47.0	45.7	3.504	49.8	1.4
	152.0 - 154.1	32.0	44.5	44.5	44.5	45.0	45.0	45.0	46.0	46.5	46.5	46.5	46.5	47.0	47.0	47.5	47.5	48.0	48.5	49.0	45.3	42.4	2.657	45.8	2.2
	172.6 - 172.7	36.0	38.0	39.0	39.5	41.0	41.5	42.0	42.0	42.5	43.0	43.5	43.5	44.0	44.0	44.0	44.0	44.5	45.5	47.0	42.4	---	---	---	---
	185.6 - 185.7	30.5	31.0	33.5	CORE BROKEN																	---	---	---	---
	195.3 - 195.7	36.5	37.0	41.5	44.0	44.5	49.0	50.0	50.0	51.0	51.0	51.0	51.0	51.5	52.0	52.0	52.0	52.5	52.5	57.5	48.9	5.409	53.1	4.7	
	211.4 - 211.5	36.5	39.0	39.0	39.0	40.0	40.5	42.0	45.0	45.0	45.0	46.0	46.0	46.5	47.5	48.0	48.0	48.0	49.0	50.0	50.5	44.5	4.222	47.7	4.2
	221.2 - 221.4	SAMPLE DOES NOT EXIST AS A RECOVERABLE UNIT																							
	221.15 - 222.25	36.0	37.5	41.5	44.0	44.0	44.5	44.5	45.0	45.0	46.0	46.0	46.5	46.5	46.5	46.5	47.0	47.0	50.0	50.0	51.0	45.3	3.669	49.0	3.0
	245.2 - 245.3	32.0	33.5	34.0	34.5	34.5	35.0	35.5	36.0	36.0	36.5	37.0	37.0	37.5	37.5	38.0	38.0	38.0	38.5	38.5	39.0	36.3	1.921	39.2	1.7
	258.7 - 258.8	43.5	44.0	44.0	44.5	45.0	45.5	45.5	45.5	45.5	46.0	46.0	46.0	46.0	46.5	46.5	46.5	46.5	46.5	46.5	46.5	45.6	0.958	48.9	1.0
	268.0 - 268.1	38.5	38.5	39.0	39.0	39.0	39.5	40.0	40.0	40.0	40.5	40.5	41.0	41.0	41.5	42.0	42.0	42.0	42.0	42.5	42.5	40.6	1.356	43.4	1.4
	284.4 - 286.3	42.5	44.0	44.5	44.5	44.5	45.0	45.0	45.0	45.0	45.0	45.0	45.5	45.5	46.0	46.0	46.0	46.5	46.5	47.0	47.0	45.3	1.081	48.7	0.9
	286.3 - 286.5	SAMPLE DOES NOT EXIST AS A RECOVERABLE UNIT																							
	291.85 - 291.95	40.0	40.0	40.5	40.5	40.5	43.0	43.0	43.0	43.5	44.0	45.0	45.0	45.5	46.0	46.0	46.0	46.5	47.0	47.5	49.0	46.0	2.721	47.2	2.7
	302.4 - 302.5	45.0	46.0	46.5	47.0	47.0	47.0	47.5	47.5	48.0	48.0	48.0	48.0	48.0	48.0	48.0	48.5	48.5	48.5	49.0	49.0	47.7	1.001	51.2	0.8

Indicates outlying values excluded in calculating the final Schmidt Hardness Value.

Figure B-3. Example of Schmidt Rebound Hardness Log

The rock mass quality estimates produced by this methodology are representative of the range of general rock qualities and not representative of the conditions through and near faults. Surface mapping has identified 10 fault zones that may be intersected along the North Ramp alignment.

B.3.1 Calculation of Rock Mass Quality Q

The Index Q, as is defined by Barton et al. (1974), is based on six parameters as follows. The first two parameters RQD/Jn describe the block size, the second two Jr and Ja describe surface characteristics of the fractures, and the last two describe the stress (SRF) and hydrologic conditions (Jw), respectively.

$$Q = \left(\frac{RQD}{J_n} \right) \times \left(\frac{J_r}{J_a} \right) \times \left(\frac{SRF}{J_w} \right) \quad (B-2)$$

where Q is a dimensionless rock mass quality ranging from 0.001 to 1000

RQD = Rock Quality Designation (%)

Jn = Joint Set Number

Jr = Joint Roughness Number

Ja = Joint Alteration Number

SRF = Stress Reduction Factor

Jw = Joint Water Factor.

In this approach, the parameters RQD, Jr and Ja are determined for each 3-m (10 ft) interval in the Rock Structure Summary Log. The parameters Jn and SRF are evaluated using Monte Carlo simulation based on surface mapping and mapping of the North Ramp Starter Tunnel by the US Bureau of Reclamation. The tables proposed by Barton et al. (1974) to select the value of the parameters are presented in this appendix. The determination of each parameter is described in the following sections.

B.3.1.1 RQD:

The Core RQD listed for the 3-m (10-ft) interval in the Rock Structure Summary Log is used directly. If the Core RQD is less than 10%, it is set equal to 10% as per Barton et al. (1974).

B.3.1.2 J_n:

The range of the Joint Set Number was derived from stereonets of fractures mapped in outcrop and underground excavations at the North Ramp Starter Tunnel by the US Bureau of Reclamation. The stereonets were judged to indicate two predominant sets of joints with steep dips. Periodically, a third set with near-horizontal inclination was observed to occur. The joint set number was therefore assumed to be uniformly distributed between two joint sets ($J_n = 4$) and three joint sets ($J_n = 9$). Monte Carlo simulation was then performed using this distribution for each interval.

B.3.1.3 J_r:

The Joint Roughness parameter is defined by relating the planarity and roughness descriptors in the log to the numerical values defined in Barton et al. (1974). Here, we have combined a roughness parameter, J_{r1} , with planarity, J_{r2} , to get J_r , where $J_r = J_{r1} + J_{r2}$. The logic is defined below:

where	J_{r1}	=	2 for roughness	V, R, M	very rough, rough, moderately rough
	J_{r1}	=	1 for roughness	S	smooth
	J_{r1}	=	0.5 for roughness	P	planar
and	J_{r2}	=	1 for planarity code	I, S	irregular, stepped
	J_{r2}	=	0 for planarity code	P, C	planar or curved

The descriptor codes are presented in Appendix A. The total J_r for the interval is the average of the J_r numbers for all the fractures in the interval.

B.3.1.4 Ja:

The joint alteration parameter combines two joint core descriptors from the geology and rock structure log, the infill thickness and infill type. The joint alteration parameter, as presented by Barton et al. (1974), is calculated based on three categories: rock wall contact, rock wall contact before 10 cm of shear movement, and no rock wall contact when sheared. The infill thickness in the rock structure summary log is used as an indicator of these categories. Infill type is subdivided on the basis of clay infill and nonclay infill. The procedure used to set the Ja is:

if infill thickness = C, S, or T	then rock wall contact assumed
if infill thickness = M	then rock wall contact before 10 cm
if infill thickness = V or E	then no rock wall contact
if rock wall contact and no clay infill	Ja = 1
if rock wall contact with clay infill	Ja = 3
if rock wall contact <10 cm w/o clay	Ja = 6
if rock wall contact <10 cm w/clay	Ja = 8
if no rock wall contact w/o clay	Ja = 8
if no rock wall contact w/clay	Ja =10

A Ja is calculated for each fracture and the average Ja determined for the entire interval. The averaging is performed because the infills are not associated with fracture inclination, therefore there is no way to identify the fracture most likely to be unstable. In general, fractures observed in the core are clean or have minor nonclay infills.

B.3.1.5 Jw:

The North Ramp is to be excavated above the water table in the unsaturated zone. J_w was therefore set equal to 1.0, representative of dry conditions.

B.3.1.6 SRF:

The parameter SRF is a measure of: (1) loosening load if the excavation is developed through shear zones or clay bearing rock, (2) magnitude of rock stress to rock strength if the excavation is developed through competent rock, or (3) squeezing or swelling load if the excavation is developed through plastic incompetent rock. For most of the North Ramp (with the exception of the nonlithified tuff section in the Ranier Mesa), cases (1) and (2) apply.

Stress Reduction Factor in the welded units was determined by Monte Carlo simulation for each 3-m (10-ft) interval on the basis of conditions observed in the North Ramp Starter Tunnel. The distribution of SRF was derived from the preliminary copy of the U.S. Bureau of Reclamation's Full Perimeter Geology Map of the Top Cut of the tunnel. This map was subdivided into unit areas of 3-m (10-ft) length along the tunnel axis. For each 3-m (10-ft) of tunnel length, 4 unit areas were examined consisting of each wall and 2 sections of roof from the tunnel centerline to each of the right and left spring line. The map was judged to contain unit areas with three types of conditions; unit areas that contained sheared zones of some thickness, unit areas that contained the notation of "intensely fractured," and unit areas where joints were indicated but the relative density is judged to be consistent with competent rock conditions. The distribution of these unit area types in the map was the basis of the statistical distribution used to Monte Carlo the SRF parameter and consisted of:

Unit areas with shears: 9 out of 40 = 22.5 % frequency

Unit areas “intensely fractured:” 8 out of 40 = 20%

Unit areas with jointing: 23 out of 40 = 57.5%

For Unit areas w/shears use “multiple shear zones any depth” SRF = 7.5

For Unit areas w/intense fracturing use “single shear zone” SRF = 5.0

For Unit areas with typical jointing use SRF = 1.0

The magnitude of rock strength to vertical stress was used to estimate SRF in the nonwelded units because of the indicated low fracture density. The strength was estimated for each 3-m (10-ft) interval by Monte Carlo simulation using the existing rock mechanics laboratory testing data. For the UO (Tuff Unit “X”) unit, strength:stress ratio were such that SFR = 1.0 because of the shallow depth of the North Ramp (30 m) where it penetrates the Tuff “X” below Daylight Valley. Values of SRF in the PTn were calculated using the maximum depth that the unit was penetrated by the North Ramp (135 m), with the average dry bulk density for the TCw (2.14 g/cc) used to estimate the vertical stress at that depth.

SRF was then set using the ratio of rock strength to vertical stress with the following values according to the table presented by Barton et al. (1974):

♦ low stress, near surface	$\sigma_c/\sigma_1 > 200$	SRF = 2.5
♦ medium stress	$\sigma_c/\sigma_1 = 200-10$	SRF = 1.0
♦ high stress	$\sigma_c/\sigma_1 = 10-5$	SRF = 0.5-2
• mild rock burst	$\sigma_c/\sigma_1 = 5-2.5$	SRF = 5-10
• heavy rock burst	$\sigma_c/\sigma_1 = < 2.5$	SRF = 10-20

Values of SRF were linearly interpolated based on the strength:vertical stress ratio, with the exception that values of $\sigma_c/\sigma_1 < 2.5$ were assigned SRF = 15.0.

B.3.2 Calculation of RMR

The calculation of RMR is defined by Bieniawski (1979) to consist of five parameters that consider the strength of the rock, the RQD, the joint spacing, the condition of the joint surfaces and the hydrologic regime. The calculation is shown in Equation B-3.

$$\text{RMR} = C + I_{\text{RQD}} + \text{JS} + \text{JC} + \text{Jw} \quad (\text{B-3})$$

where RMR is a dimensionless number from 0 to 100;

C	= the strength parameter;
I_{RQD}	= the RQD parameter;
JS	= the joint spacing parameter;
JC	= the joint surface condition parameter;
Jw	= the joint water parameter.

The table used to determine the value of the index parameters is presented in Appendix D. The individual parameter values are calculated using the following procedures:

B.3.2.1 C:

The strength parameter was generated using both the laboratory rock mechanics test data from the NRG holes and the Schmidt Rebound Hardness data. A comparison of the compressive strength predicted by Schmidt Rebound Hardness and the rock mechanics test data indicated that the Schmidt Rebound Hardness correlation with strength would provide a more conservative value of C for the TCw and the TSw2 units. The comparison indicated that the rock strength testing data would be the more conservative value for the PTn and TSw1 units. For each 3-m (10-ft) interval, the data base was searched for a direct measurement (Schmidt Hammer for TCw and TSw1, Compressive Strength for PTn and TSw1). If a direct measurement was available for

the interval, it was used to determine the C parameter. If no direct measurement was available, a value was developed using Monte Carlo simulation and the distribution of the available measurements (Schmidt Hammer or Compressive Strength) within the particular thermo-mechanical (thermal-mechanical) unit. The correlation between Schmidt Rebound Hardness and compressive strength was obtained from Stacey and Page (1986) and is presented in Equation B-4.

$$\text{Log (UCS)} = 0.021165 (\text{RN}) + 1.0414 \quad (\text{B-4})$$

where UCS = Unconfined Compressive Strength (MPa)

RN = Schmidt Rebound Number.

The value of the C parameter for the derived strength was developed from the tables in Appendix D.

B.3.2.2 I_{RQD} :

The Core RQD was used for each 3-m (10-ft) interval. The value of the parameter I_{RQD} was then derived for the table in Appendix D.

B.3.2.3. JS:

Joint spacing was calculated for each 3-m (10-ft) interval using Equation B-5.

$$\text{JS} = \frac{1}{(\text{Number of joints of } N, I, C) / (3\text{m}(10') - \text{LC} - \text{Rubble})} \quad (\text{B-5})$$

where JS = Joint Spacing (ft)

LC = length of lost core in 3-m (10-ft) interval

Rubble = length of rubble zones in 3-m (10-ft) interval.

The parameter JS was then determined based on the fracture spacing (m) from the rock structure summary log and the table in Appendix D.

B.3.2.4. JC:

Joint condition was evaluated based on the planarity and roughness, infill type, and infill thickness using Equation B-6.

$$JC = 30 \times a \times b \times c \quad (B-6)$$

where a = planarity and roughness factor

b = infill mineral factor

c = infill thickness factor

The planarity and roughness factor (a) was determined using the separate planarity (a1) and roughness (a2) codes from the core logging.

Factor a = a1 + a2, where

a1 = 0.2 if planarity = p (planar)

a1 = 0.35 = c (curved)

a1 = 0.5 = s (stepped)

a1 = 0.5 = I (irregular)

and

a2 = 0.45 if roughness = V (very rough)

a2 = 0.45 = R (rough)

a2 = 0.45 = M (moderately rough)

a2 = 0.4 = S (smooth)

a2 = 0.35 = P (slickensides)

The mineral infill factor (b) was determined using the following logic where,

b = 1.0 if infill = C, WC, BC, BC, BD, TD, TC, or CA (see Appendix A)

b = 0.85 if infill = SI or MN (silica or manganese)

b = 0.6 if infill = WN, TN, CL (clay)

The infill thickness factor (c) was determined using the following logic where,

c = 1 if thickness C, S, or T (clean, very thin or thin)

c = 0.45 if thickness M (moderately thick)

c = 0.30 if thickness V or E (very thick, extremely thick)

A JC was then calculated for each fracture in the 3-m (10-ft) interval and the average JC assigned to the interval. Appendix D lists the description of these parameters.

B.3.2.5 Jw:

The Jw factor was set equal to 15 for all intervals assuming dry conditions due to the unsaturated state of the site.

B.3.3 Computer Calculation of Q and RMR

A FORTRAN subroutine was developed to list the interval parameter values derived using the approach outlined in Sections B.3.1 and B.3.2 and calculate the indices Q and RMR. The subroutine in WPLOG produces an ASCII file of the individual parameters and the resulting calculated values of Q and RMR. This ASCII data is read into an EXCEL spreadsheet, an example of which is presented as Figure B-4.

The resulting Q and RMR data were submitted to the Data Records Center in Technical Data Information Form No. (TDIF) 302271.

APPENDIX C

**Table C-1. Rank-Ordered Rock Mass Quality Data for UO (Tuff "X")
Total of 15 Sets of Results — Sorted Indices**

Percentage	Q	RMR	RQD
7%	2.23	50.40	0
13%	6.00	52.50	4
20%	7.50	52.90	5
27%	7.50	53.50	21
33%	9.44	55.16	29
40%	10.98	55.88	29
47%	11.42	56.10	30
53%	13.21	57.00	33
60%	14.07	57.15	36
67%	14.24	58.69	36
73%	14.49	59.42	37
80%	21.60	59.50	40
87%	22.67	59.86	49
93%	24.29	60.00	60
100%	29.40	61.50	68

**Table C-2. Rank-Ordered Rock Mass Quality Data for TCw
Total of 89 Sets of Results — Sorted Indices**

Percentage	Q	RMR	RQD
1%	0.20	45.71	0
2%	0.31	50.66	0
3%	0.34	50.74	0
4%	0.38	50.77	0
6%	0.42	51.25	0
7%	0.45	51.61	0
8%	0.45	51.73	0
9%	0.46	52.18	0
10%	0.48	52.71	0
11%	0.50	53.50	0

Table C-2. *continued*

Percentage	Q	RMR	RQD
12%	0.50	53.59	2
13%	0.54	54.00	4
15%	0.55	54.03	4
16%	0.55	54.17	4
17%	0.58	54.53	5
18%	0.61	55.35	5
19%	0.61	55.39	6
20%	0.68	55.50	8
21%	0.69	55.61	9
22%	0.75	56.18	10
24%	0.78	56.26	10
25%	0.93	56.71	12
26%	1.00	57.14	12
27%	1.25	57.46	14
28%	1.38	57.71	14
29%	1.49	57.80	14
30%	1.49	57.98	14
31%	1.49	58.50	15
33%	1.49	58.50	15
34%	1.49	58.74	15
35%	1.50	58.74	15
36%	1.72	58.74	16
37%	1.73	58.74	16
38%	1.84	58.74	16
39%	1.90	58.81	19
40%	2.08	59.39	20
42%	2.20	60.25	21
43%	2.24	61.00	22
44%	2.30	61.12	22
45%	2.31	61.27	22
46%	2.39	61.28	23
47%	2.44	61.33	23
48%	2.88	61.59	23
49%	2.90	61.74	24
51%	3.11	62.19	24

Table C-2. *continued*

Percentage	Q	RMR	RQD
52%	3.13	62.22	24
53%	3.34	62.38	26
54%	3.52	63.33	26
55%	3.68	63.33	26
56%	3.75	63.50	27
57%	3.78	63.53	28
58%	3.82	63.60	29
60%	3.82	63.81	30
61%	3.88	64.53	32
62%	4.25	64.70	32
63%	4.40	65.09	34
64%	4.44	65.59	35
65%	4.46	65.80	37
66%	4.84	65.99	38
67%	5.02	66.15	39
69%	5.33	66.31	39
70%	5.66	66.50	41
71%	5.76	66.50	43
72%	5.78	66.50	44
73%	5.79	66.50	44
74%	6.00	67.30	44
75%	6.05	67.45	45
76%	6.32	68.00	45
78%	6.89	68.00	48
79%	7.35	68.25	48
80%	7.37	69.81	50
81%	7.56	70.31	50
82%	7.84	70.69	51
83%	8.10	71.00	52
84%	8.58	71.02	52
85%	8.59	71.10	52
87%	8.70	71.50	53
88%	8.86	71.50	58
89%	9.14	71.50	58
90%	10.33	71.50	60

Table C-2. *continued*

Percentage	Q	RMR	RQD
91%	12.00	72.20	61
92%	16.30	74.22	62
93%	17.14	74.57	62
94%	18.06	74.70	62
96%	18.98	75.00	63
97%	23.14	76.25	70
98%	31.20	76.40	72
99%	35.29	76.50	74
100%	35.43	78.00	75

Table C-3. Rank-Ordered Rock Mass Quality Data for PTn
Total of 51 Sets of Results — Sorted Indices

Percentage	Q	RMR	RQD
2%	0.09	40.86	0
4%	0.11	43.76	0
6%	0.15	45.13	0
8%	0.15	49.25	0
10%	0.15	49.40	0
12%	0.15	49.40	0
14%	0.21	49.83	2
16%	0.23	50.40	4
18%	0.27	50.40	4
20%	0.28	51.90	6
22%	0.31	51.92	9
24%	0.31	51.92	12
25%	0.33	52.40	14
27%	0.36	52.40	16
29%	0.37	52.40	16
31%	0.43	52.43	16
33%	0.53	52.50	20
35%	0.54	54.42	21
37%	0.63	54.59	24
39%	0.66	54.64	25
41%	0.71	55.02	26

Table C-3. *continued*

Percentage	Q	RMR	RQD
43%	0.77	55.81	27
45%	0.80	56.50	31
47%	0.83	56.63	32
49%	0.85	56.75	36
51%	1.07	57.50	39
53%	1.20	60.20	48
55%	1.23	60.50	48
57%	1.24	60.50	49
59%	1.27	60.54	50
61%	1.43	61.00	50
63%	1.43	61.50	50
65%	1.44	62.50	51
67%	1.55	62.55	53
69%	1.60	63.50	54
71%	1.62	64.50	56
73%	1.72	65.00	58
75%	1.90	65.00	58
76%	2.04	65.50	58
78%	2.44	65.50	59
80%	2.67	65.50	61
82%	2.80	65.50	61
84%	2.87	66.50	66
86%	3.38	66.50	67
88%	3.44	67.00	72
90%	3.74	69.50	76
92%	4.80	69.50	84
94%	7.15	71.50	86
96%	8.18	72.00	87
98%	27.91	72.50	88
100%	45.31	76.00	90

Table C-4. Rank-Ordered Rock Mass Quality Data for TSw1
Total of 127 Sets of Results — Sorted Indices

Percentage	Q	RMR	RQD
1%	0.21	41.70	0
2%	0.21	47.06	0
2%	0.21	47.50	0
3%	0.21	48.67	0
4%	0.21	48.67	0
5%	0.24	49.09	0
6%	0.24	49.12	0
6%	0.28	49.21	0
7%	0.30	49.59	0
8%	0.32	49.61	0
9%	0.32	50.38	0
9%	0.39	50.67	0
10%	0.40	50.67	0
11%	0.44	50.67	0
12%	0.46	50.67	0
13%	0.50	50.67	0
13%	0.51	50.67	0
14%	0.55	51.00	0
15%	0.56	51.67	0
16%	0.64	51.71	0
17%	0.67	51.77	0
17%	0.67	51.85	0
18%	0.75	52.00	2
19%	0.86	52.20	4
20%	0.87	52.75	4
20%	0.94	52.95	4
21%	0.95	53.00	4
22%	1.03	53.25	4
23%	1.08	53.58	4
24%	1.17	53.67	4
24%	1.30	53.67	5
25%	1.33	53.67	5
26%	1.40	53.67	5

Table C-4. *continued*

Percentage	Q	RMR	RQD
27%	1.48	53.67	5
28%	1.56	53.67	5
28%	1.61	53.67	7
29%	1.61	53.67	7
30%	1.61	53.67	7
31%	1.61	54.00	8
31%	1.61	54.47	8
32%	1.61	54.49	9
33%	1.61	54.50	9
34%	1.61	54.55	9
35%	1.61	55.28	11
35%	1.61	55.50	11
36%	1.61	55.61	11
37%	1.61	55.73	12
38%	1.67	55.75	12
39%	1.67	56.00	12
39%	1.71	56.32	12
40%	1.73	56.54	13
41%	1.79	56.60	13
42%	1.86	56.67	13
43%	1.87	56.67	13
43%	1.95	56.67	14
44%	2.01	57.00	14
45%	2.22	57.00	14
46%	2.28	57.00	15
46%	2.33	57.51	15
47%	2.41	57.82	15
48%	2.41	57.88	15
49%	2.47	57.94	15
50%	2.57	58.38	16
50%	2.86	58.50	17
51%	2.88	58.50	17
52%	2.89	58.50	19
53%	3.03	58.50	20
54%	3.07	58.60	20

Table C-4. *continued*

Percentage	Q	RMR	RQD
54%	3.12	58.67	21
55%	3.20	59.39	21
56%	3.25	59.75	21
57%	3.30	59.75	22
57%	3.33	60.00	22
58%	3.35	60.07	22
59%	3.36	60.21	24
60%	3.47	60.29	24
61%	3.75	60.29	25
61%	3.79	60.90	26
62%	3.80	60.90	27
63%	3.80	61.00	27
64%	3.92	61.00	28
65%	3.93	61.43	29
65%	4.00	61.48	30
66%	4.26	61.50	30
67%	4.40	61.50	31
68%	4.98	61.50	31
69%	5.00	61.50	33
69%	5.00	61.50	33
70%	5.09	61.50	33
71%	5.14	61.50	33
72%	5.19	61.50	34
72%	5.22	61.67	34
73%	5.54	61.67	35
74%	5.71	61.67	36
75%	5.80	62.01	37
76%	6.00	62.07	37
76%	6.23	63.13	38
77%	6.25	63.25	38
78%	6.33	63.37	40
79%	6.34	63.50	40
80%	6.86	63.50	41
80%	6.86	63.50	42
81%	7.00	64.00	42

Table C-4. *continued*

Percentage	Q	RMR	RQD
82%	7.05	64.43	43
83%	7.89	65.16	45
83%	8.44	65.50	45
84%	9.92	65.58	47
85%	10.00	65.69	48
86%	10.93	67.33	49
87%	11.00	68.00	55
87%	11.30	68.50	57
88%	11.57	68.77	58
89%	11.63	69.46	58
90%	12.00	69.86	59
91%	14.03	69.93	63
91%	14.38	70.00	69
92%	14.39	70.00	70
93%	18.12	70.22	71
94%	19.54	70.62	73
94%	20.40	70.70	73
95%	22.00	70.93	74
96%	22.14	71.00	77
97%	29.00	71.14	78
98%	29.00	71.50	80
98%	29.33	72.50	80
99%	31.06	73.00	83
100%	31.13	74.00	87

Table C-5. Rank-Ordered Rock Mass Quality Data for TSw2
Total of 131 Sets of Results — Sorted Indices

Percentage	Q	RMR	RQD
1%	0.15	45.80	0
2%	0.24	49.12	0
2%	0.26	49.31	0
3%	0.26	50.07	0
4%	0.26	50.07	0
5%	0.29	50.07	0

Table C-5. *continued*

Percentage	Q	RMR	RQD
5%	0.30	51.14	0
6%	0.37	52.11	0
7%	0.38	53.00	0
8%	0.38	53.00	0
8%	0.38	53.00	0
9%	0.38	53.07	0
10%	0.38	53.07	0
11%	0.38	53.07	0
11%	0.38	53.07	0
12%	0.38	53.07	0
13%	0.38	53.19	0
14%	0.40	53.36	0
15%	0.48	53.50	0
15%	0.50	54.72	0
16%	0.50	55.33	0
17%	0.53	55.40	0
18%	0.55	55.64	0
18%	0.56	56.07	0
19%	0.63	56.07	0
20%	0.65	56.07	0
21%	0.67	56.14	0
21%	0.68	56.24	0
22%	0.75	56.43	0
23%	0.77	56.56	0
24%	0.86	56.75	0
24%	0.90	56.75	0
25%	0.98	56.81	0
26%	1.00	57.13	0
27%	1.00	57.13	0
27%	1.11	57.26	0
28%	1.20	57.35	0
29%	1.20	57.50	0
30%	1.20	57.91	0
31%	1.32	57.97	0
31%	1.36	58.00	0

Table C-5. *continued*

Percentage	Q	RMR	RQD
32%	1.37	58.07	0
33%	1.38	58.07	0
34%	1.43	58.07	0
34%	1.50	58.07	2
35%	1.73	58.07	3
36%	1.79	58.07	3
37%	1.80	58.07	3
37%	1.90	58.07	3
38%	1.91	58.07	4
39%	1.91	58.07	4
40%	1.91	58.07	4
40%	1.91	58.07	4
41%	1.91	58.07	4
42%	1.91	58.07	5
43%	1.91	58.07	5
44%	1.91	58.07	5
44%	1.91	58.07	5
45%	1.91	58.07	5
46%	1.91	58.33	5
47%	1.91	58.43	5
47%	1.91	58.50	6
48%	1.91	58.50	6
49%	1.91	58.53	6
50%	1.91	58.73	7
50%	1.91	58.86	8
51%	1.91	58.99	8
52%	1.91	59.01	8
53%	1.91	59.03	8
53%	1.95	59.17	8
54%	2.14	59.50	8
55%	2.14	59.66	9
56%	2.19	59.73	9
56%	2.20	60.33	9
57%	2.36	60.88	10
58%	2.37	61.00	10

Table C-5. *continued*

Percentage	Q	RMR	RQD
59%	2.37	61.07	10
60%	2.40	61.07	10
60%	2.40	61.07	11
61%	2.40	61.07	11
62%	2.50	61.07	11
63%	2.55	61.11	12
63%	2.70	61.18	12
64%	2.70	61.19	12
65%	2.87	61.36	13
66%	3.00	61.42	13
66%	3.07	61.50	14
67%	3.12	61.50	15
68%	3.18	61.79	15
69%	3.24	62.13	15
69%	3.44	62.71	16
70%	3.75	62.76	16
71%	3.75	62.80	17
72%	3.81	63.04	18
73%	3.89	63.15	18
73%	4.29	63.31	19
74%	4.68	63.50	20
75%	4.76	63.72	20
76%	4.98	64.38	20
76%	5.00	64.50	21
77%	5.00	65.00	21
78%	5.08	65.23	23
79%	5.10	65.44	24
79%	5.17	65.62	25
80%	5.25	65.75	25
81%	5.41	66.25	26
82%	5.76	66.50	27
82%	5.85	66.50	27
83%	6.00	66.50	28
84%	6.17	66.50	29
85%	6.79	66.50	30

Table C-5. *continued*

Percentage	Q	RMR	RQD
85%	6.82	66.50	30
86%	7.11	66.50	31
87%	7.14	66.50	32
88%	7.20	66.50	33
89%	7.54	66.50	33
89%	7.59	66.50	36
90%	8.44	66.50	37
91%	8.96	66.50	38
92%	9.67	66.50	39
92%	10.00	66.50	41
93%	10.16	67.03	42
94%	11.67	67.43	44
95%	12.60	68.50	46
95%	12.80	69.75	48
96%	12.97	69.79	48
97%	13.07	70.04	50
98%	13.80	70.45	58
98%	14.00	71.50	70
99%	18.58	71.50	76
100%	23.20	71.67	83

This page left intentionally blank.

APPENDIX D

ROCK MASS QUALITY INDICES FOR THE LITHOPHYSAE AND NONLITHOPHYSAL TUFF ROCK IN TCw AND TSw1 UNITS

Further subdivision was introduced with the TCw and TSw1 units because both these units contain portions of lithophysae-rich and nonlithophysal tuff rock. The rock mass quality for both these portions has been estimated and investigated to determine if there is a need for subdivision in design.

The process of obtaining the rock mass quality indices are described in Section 7. The estimated rock quality indices for lithophysae-rich and nonlithophysal tuff rock in TCw and TSw1 units are tabulated in Tables D-1 to D-4 with five rock mass quality classes for frequencies of occurrence of 5%, 20%, 40%, 70%, and 90%. Comparison of these indices with the total grouping of the units presented in Section 7 shows minor difference for the subdivision and the combined total. Tables D-5 and D-6 are constructed to illustrate the comparison by listing the indices of the most probable rock mass class (class 3). Rock mass quality calculated in TCw lithophysae-rich rock appear to be slightly better than other sections, but still rank in the same rock quality category according to both Bieniawski's and Barton's classification. As for TSw1 unit, the rock quality are almost identical for the subdivision and the combined total.

Table D-1. Rock Quality Indices for TCw Nonlithophysal Tuff

	Rock Mass Quality Category				
	1	2	3	4	5
Q	0.38	0.55	1.84	4.84	9.14
RMR _{CAL}	35	39	49	58	64
RMR ₇₉	51	54	59	65	72
Design RMR	43	46	54	61	68

Table D-2. Rock Quality Indices for TCw Lithophysae-Rich Tuff

	Rock Mass Quality Category				
	1	2	3	4	5
Q	0.45	0.78	2.44	6.0	12.0
RMR _{CAL}	37	42	52	60	66
RMR ₇₉	54	59	64	68	75
Design RMR	45	50	58	64	70

Table D-3. Rock Quality Indices for TSw1 Nonlithophysal Tuff

	Rock Mass Quality Category				
	1	2	3	4	5
Q	0.28	0.95	2.01	5.8	20.4
RMR _{CAL}	33	44	50	60	71
RMR ₇₉	48	53	56	63	71
Design RMR	40	48	53	62	71

Table D-4. Rock Quality Indices for TSw1 Lithophysae-Rich Tuff

	Rock Mass Quality Category				
	1	2	3	4	5
Q	0.24	0.67	1.61	4.0	10.93
RMR _{CAL}	31	40	48	56	66
RMR ₇₉	50	52	57	61	69
Design RMR	41	46	52	59	67

Table D-5. Comparison of Rock Quality Indices for Rock Mass Quality Classes 3 of TCw Unit

	TCw Total	TCw-NL	TCw-LR
Q	1.84	2.44	2.08
RMR ₇₉	59	64	59
Design RMR	54	58	55

Table D-6. Comparison of Rock Quality Indices for Rock Mass Quality Classes 3 of TSw1 Unit

	TSw1 Total	TSw1-NL	TSw1-LR
Q	2.01	1.61	1.73
RMR ₇₉	56	57	57
Design RMR	53	52	53

YUCCA MOUNTAIN SITE CHARACTERIZATION PROJECT

UC814 - DISTRIBUTION LIST

1	D. A. Dreyfus (RW-1) Director OCRWM US Department of Energy 1000 Independence Avenue SW Washington, DC 20585	1	R. M. Nelson (RW-20) Office of Geologic Disposal OCRWM US Department of Energy 1000 Independence Avenue SW Washington, DC 20585
1	L. H. Barrett (RW-2) Acting Deputy Director OCRWM US Department of Energy 1000 Independence Avenue SW Washington, DC 20585	1	S. J. Brocoum (RW-22) Analysis and Verification Division OCRWM US Department of Energy 1000 Independence Avenue SW Washington, DC 20585
1	J. D. Saltzman (RW-4) Office of Strategic Planning and International Programs OCRWM US Department of Energy 1000 Independence Avenue SW Washington, DC 20585	1	D. Shelor (RW-30) Office of Systems and Compliance OCRWM US Department of Energy 1000 Independence Avenue SW Washington, DC 20585
1	J. D. Saltzman (RW-5) Office of External Relations OCRWM US Department of Energy 1000 Independence Avenue SW Washington, DC 20585	1	J. Roberts (RW-33) Director, Regulatory Compliance Division OCRWM US Department of Energy 1000 Independence Avenue SW Washington, DC 20585
1	Samuel Rousso (RW-10) Office of Program and Resource Mgt. OCRWM US Department of Energy 1000 Independence Avenue SW Washington, DC 20585	1	G. J. Parker (RW-332) Reg. Policy/Requirements Branch OCRWM US Department of Energy 1000 Independence Avenue SW Washington, DC 20585
1	J. C. Bresee (RW-10) OCRWM US Department of Energy 1000 Independence Avenue SW Washington, DC 20585	1	R. A. Milner (RW-40) Office of Storage and Transportation OCRWM US Department of Energy 1000 Independence Avenue SW Washington, DC 20585
1	S. Rousso (RW-50) Office of Contract Business Management OCRWM US Department of Energy 1000 Independence Avenue SW Washington, DC 20585	1	D. R. Elle, Director Environmental Protection Division DOE Nevada Field Office US Department of Energy P.O. Box 98518 Las Vegas, NV 89193-8518

1	T. Wood (RW-52) Director, M&O Management Division OCRWM US Department of Energy 1000 Independence Avenue SW Washington, DC 20585	1	Repository Licensing & Quality Assurance Project Directorate Division of Waste Management US NRC Washington, DC 20555
4	Victoria F. Reich, Librarian Nuclear Waste Technical Review Board 1100 Wilson Blvd., Suite 910 Arlington, VA 22209	1	Senior Project Manager for Yucca Mountain Repository Project Branch Division of Waste Management US NRC Washington, DC 20555
5	Wesley Barnes, Project Manager Yucca Mountain Site Characterization Office US Department of Energy P.O. Box 98608—MS 523 Las Vegas, NV 89193-8608	1	NRC Document Control Desk Division of Waste Management US NRC Washington, DC 20555
1	C. L. West, Director Office of External Affairs DOE Nevada Field Office US Department of Energy P.O. Box 98518 Las Vegas, NV 89193-8518	1	Chad Glenn NRC Site Representative 301 E Stewart Avenue, Room 203 Las Vegas, NV 89101
8	Technical Information Officer DOE Nevada Field Office US Department of Energy P.O. Box 98518 Las Vegas, NV 89193-8518	1	E. P. Binnall Field Systems Group Leader Building 50B/4235 Lawrence Berkeley Laboratory Berkeley, CA 94720
1	P. K. Fitzsimmons, Technical Advisor Office of Assistant Manager for Environmental Safety and Health DOE Nevada Field Office US Department of Energy P.O. Box 98518 Las Vegas, NV 89193-8518	1	Center for Nuclear Waste Regulatory Analyses 6220 Culebra Road Drawer 28510 San Antonio, TX 78284
1	J. A. Blink Deputy Project Leader Lawrence Livermore National Lab. 101 Convention Center Drive Suite 820, MS 527 Las Vegas, NV 89109	3	W. L. Clarke Technical Project Officer - YMP Attn: YMP/LRC Lawrence Livermore National Laboratory P.O. Box 5514 Livermore, CA 94551
4	J. A. Canepa Technical Project Officer - YMP N-5, Mail Stop J521 Los Alamos National Laboratory P.O. Box 1663 Los Alamos, NM 87545	1	V. R. Schneider Asst. Chief Hydrologist—MS 414 Office of Program Coordination and Technical Support US Geological Survey 12201 Sunrise Valley Drive Reston, VA 22092
1	H. N. Kalia Exploratory Shaft Test Manager Los Alamos National Laboratory Mail Stop 527 101 Convention Center Dr., #820 Las Vegas, NV 89109	1	J. S. Stuckless Geologic Division Coordinator MS 913 Yucca Mountain Project US Geological Survey P.O. Box 25046 Denver, CO 80225

1	N. Z. Elkins Deputy Technical Project Officer Los Alamos National Laboratory Mail Stop 527 101 Convention Center Drive, #820 Las Vegas, NV 89109	1	D. H. Appel, Chief Hydrologic Investigations Program MS 421 US Geological Survey P.O. Box 25046 Denver, CO 80225
5	L. S. Costin, Acting Technical Project Officer - YMP Sandia National Laboratories Organization 6313, MS 1325 P.O. Box 5800 Albuquerque, NM 87185	1	E. J. Helley Branch of Western Regional Geology MS 427 US Geological Survey 345 Middlefield Road Menlo Park, CA 94025
1	J. F. Devine Asst Director of Engineering Geology US Geological Survey 106 National Center 12201 Sunrise Valley Drive Reston, VA 22092	1	R. W. Craig, Chief Nevada Operations Office US Geological Survey 101 Convention Center Drive Suite 860, MS 509 Las Vegas, NV 89109
1	L. R. Hayes Technical Project Officer Yucca Mountain Project Branch MS 425 US Geological Survey P.O. Box 25046 Denver, CO 80225	1	D. Zesiger US Geological Survey 101 Convention Center Drive Suite 860, MS 509 Las Vegas, NV 89109
1	A. L. Flint US Geological Survey MS 721 P.O. Box 327 Mercury, NV 89023	1	G. L. Ducret, Associate Chief Yucca Mountain Project Division US Geological Survey P.O. Box 25046 421 Federal Center Denver, CO 80225
1	D. A. Beck Water Resources Division, USGS 6770 S. Paradise Road Las Vegas, NV 89119	2	L. D. Foust Nevada Site Manager TRW Environmental Safety Systems 101 Convention Center Drive Suite 540, MS 423 Las Vegas, NV 89109
1	P. A. Glancy US Geological Survey Federal Building, Room 224 Carson City, NV 89701	1	C. E. Ezra YMP Support Office Manager EG&G Energy Measurements Inc. MS V-02 P.O. Box 1912 Las Vegas, NV 89125
1	Sherman S. C. Wu US Geological Survey 2255 N. Gemini Drive Flagstaff, AZ 86001	1	Jan Docka Roy F. Weston, Inc. 955 L'Enfant Plaza SW Washington, DC 20024
1	J. H. Sass - USGS Branch of Tectonophysics 2255 N. Gemini Drive Flagstaff, AZ 86001	1	Technical Information Center Roy F. Weston, Inc. 955 L'Enfant Plaza SW Washington, DC 20024

1	<p>DeWayne Campbell Technical Project Officer - YMP US Bureau of Reclamation Code D-3790 P.O. Box 25007 Denver, CO 80225</p>	1	<p>D. Hedges, Vice President, QA Roy F. Weston, Inc. 4425 Spring Mountain Road Suite 300 Las Vegas, NV 89102</p>
1	<p>J. M. LaMonaca Records Specialist US Geological Survey 421 Federal Center P.O. Box 25046 Denver, CO 80225</p>	1	<p>D. L. Fraser, General Manager Reynolds Electrical & Engineering Company, Inc. MS 555 P.O. Box 98521 Las Vegas, NV 89193-8521</p>
1	<p>W. R. Keefer - USGS 913 Federal Center P.O. Box 25046 Denver, CO 80225</p>	1	<p>B. W. Colston, President & Gen. Mgr. Las Vegas Branch Raytheon Services Nevada MS 416 P.O. Box 95487 Las Vegas, NV 89193-5487</p>
1	<p>M. D. Voegelé Technical Project Officer - YMP SAIC 101 Convention Center Drive Suite 407 Las Vegas, NV 89109</p>	1	<p>R. L. Bullock Technical Project Officer - YMP Raytheon Services Nevada Suite P-250, MS 403 101 Convention Center Drive Las Vegas, NV 89109</p>
1	<p>Paul Eslinger, Manager PASS Program Pacific Northwest Laboratories P.O. Box 999 Richland, WA 99352</p>	1	<p>C. H. Johnson Technical Program Manager Agency for Nuclear Projects State of Nevada Evergreen Center, Suite 252 1802 N. Carson Street Carson City, NV 89710</p>
1	<p>A. T. Tamura Science and Technology Division OSTI US Department of Energy P.O. Box 62 Oak Ridge, TN 37831</p>	1	<p>John Fordham Water Resources Center Desert Research Institute P.O. Box 60220 Reno, NV 89506</p>
1	<p>Carlos G. Bell, Jr. Professor of Civil Engineering Civil and Mechanical Engineering Dept. University of Nevada, Las Vegas 4505 S. Maryland Parkway Las Vegas, NV 89154</p>	1	<p>David Rhode Desert Research Institute P.O. Box 60220 Reno, NV 89506</p>
1	<p>P. J. Weeden, Acting Director Nuclear Radiation Assessment Div. US EPA Environmental Monitoring Sys. Lab P.O. Box 93478 Las Vegas, NV 89193-3478</p>	1	<p>Eric Anderson Mountain West Research Southwest Inc. 2901 N. Central Avenue, #1000 Phoenix, AZ 85012-2730</p>
1	<p>ONWI Library Battelle Columbus Laboratory Office of Nuclear Waste Isolation 505 King Avenue Columbus, OH 43201</p>	1	<p>The Honorable Cyril Schank Chairman Churchill County Board of Commissioners 190 W. First Street Fallon, NV 89406</p>

1	T. Hay, Executive Assistant Office of the Governor State of Nevada Capitol Complex Carson City, NV 89710	1	Dennis Bechtel, Coordinator Nuclear Waste Division Clark County Department of Comprehensive Planning 301 E. Clark Avenue, Suite 570 Las Vegas, NV 89101
3	R. R. Loux Executive Director Agency for Nuclear Projects State of Nevada Evergreen Center, Suite 252 1802 N. Carson Street Carson City, NV 89710	1	Juanita D. Hoffman Nuclear Waste Repository Oversight Program Esmeralda County P.O. Box 490 Goldfield, NV 89013
1	Brad Mettam Inyo County Yucca Mountain Repository Assessment Office Drawer L Independence, CA 93526	1	Eureka County Board of Commissioners Yucca Mountain Information Office P.O. Box 714 Eureka, NV 89316
1	Lander County Board of Commissioners 315 South Humbolt Battle Mountain, NV 89820	1	Economic Development Dept. City of Las Vegas 400 E. Stewart Avenue Las Vegas, NV 89101
1	Vernon E. Poe Office of Nuclear Projects Mineral County P.O. Box 1026 Hawthorne, NV 89415	1	Community Planning & Development City of North Las Vegas P.O. Box 4086 North Las Vegas, NV 89030
1	Les W. Bradshaw Program Manager Nye County Repository P.O. Box 429 Tonopah, NV 89049	1	Community Development & Planning City of Boulder City P.O. Box 61350 Boulder City, NV 89006
1	Florindo Mariani White Pine County Nuclear Waste Project Office 457 Fifth Street Ely, NV 89301	1	Commission of European Communities 200 Rue de la Loi B-1049 Brussels BELGIUM
1	Judy Foremaster City of Caliente Nuclear Waste Project Office P.O. Box 158 Caliente, NV 89008	2	M. J. Dorsey, Librarian YMP Research & Study Center Reynolds Electrical & Engineering Company, Inc. MS 407 P.O. Box 98521 Las Vegas, NV 89193-8521
1	Philip A. Niedzielski-Eichner Nye County Nuclear Waste Repository Project Office P.O. Box 221274 Chantilly, VA 22022-1274	1	Amy Anderson Argonne National Laboratory Building 362 9700 S. Cass Avenue Argonne, IL 60439
		1	Steve Bradhurst P.O. Box 1510 Reno, NV 89505

1	Michael L. Baughman 35 Clark Road Fiskdale, MA 01518	1	A. M. Segrest M&O/Duke 101 Convention Center Drive TESS/423 Las Vegas, NV 89109
1	Glenn Van Roekel Director of Community Development City of Caliente P.O. Box 158 Caliente, NV 89008	1	J. H. Pye M&O/MK 101 Convention Center Drive MS423 Las Vegas, NV 89109
1	Jason Pitts Lincoln County Nuclear Waste Project Office Lincoln County Courthouse Pioche, NV 89043	1	S. B. Jones, AMSP U. S. Department of Energy YMSCO MS 423 P. O. Box 98608 Las Vegas, NV 89193-8608
1	Ray Williams, Jr. P.O. Box 10 Austin, NV 89310	1	J. T. Sullivan U. S. Department of Energy YMSCO MS 423 P. O. Box 98608 Las Vegas, NV 89193-8608
1	Nye County District Attorney P.O. Box 593 Tonopah, NV 89049	1	D. R. Williams U. S. Department of Energy YMSCO MS 423 P. O. Box 98608 Las Vegas, NV 89193-8608
1	William Offutt Nye County Manager Tonopah, NV 89049	1	W. H. Hansmire Kewitt/PB 4460 S. Arville Street, Suite 6 Las Vegas, NV 89103
1	Charles Thistlethwaite, AICP Associate Planner Inyo County Planning Department Drawer L Independence, CA 93526	1	MS
1	R. F. Pritchett Technical Project Officer - YMP Reynolds Electrical & Engineering Company, Inc. MS 408 P.O. Box 98521 Las Vegas, NV 89193-8521	2	1330 C. B. Michaels, 6352 100/1232621/SAND95-0488-1/QA
1	Dr. Moses Karakouzian 1751 E. Reno, #125 Las Vegas, NV 89119	20	1330 WMT Library, 6352
1	C. E. Brechtel Agapito Associates, Inc. 3841 W. Charleston, Suite 203 Las Vegas, NV 89102	1	1399 D. S. Kessel, 6314
1	M. P. Hardy Agapito Associates, Inc. 715 Horizon Drive, Suite 340 Grand Junction, CO 81506	1	1324 C. A. Rautman, 6115
		1	1325 J. Pott, 6313
		1	1325 R. H. Price, 6313
		1	9018 Central Technical Files, 8523-2
		5	0899 Technical Library, 13414
		1	0619 Print Media, 12615
		2	0100 Document Processing, 7613-2 for DOE/OSTI